The Thermophilic Route to Succinic Acid

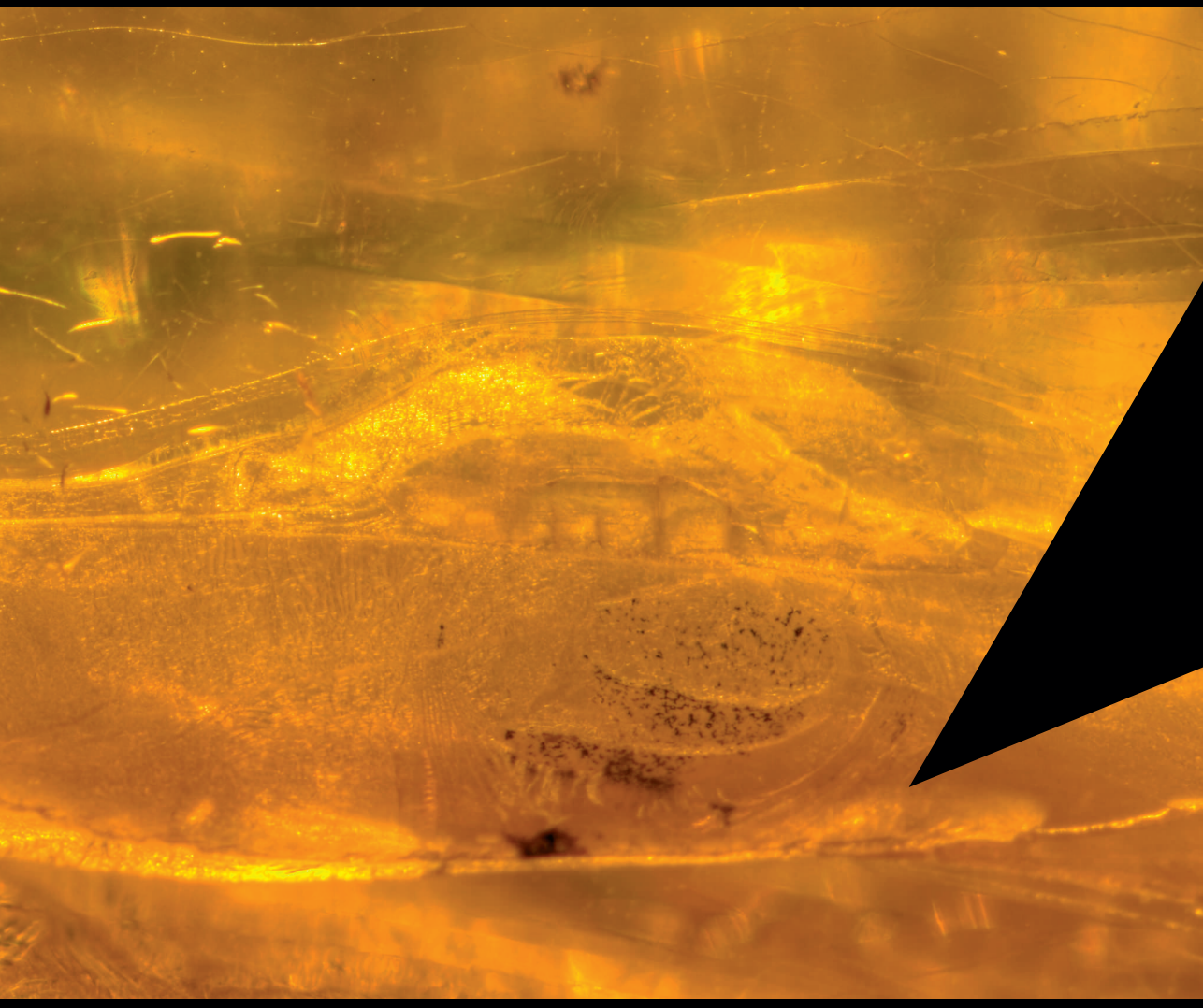

Jeroen G. Koendjbiharie

The Thermophilic Route to Succinic Acid

Jeroen G. Koendjbiharie

Thesis committee

Promotor
Prof. Dr Richard van Kranenburg
Special Professor Bacterial Cell Factories
Wageningen University & Research
Head of Regulatory and Biotechnology Innovation
Corbion, Gorinchem

Other members
Prof. Dr M.J. Barbosa, Wageningen University & Research
Prof. Dr D.J. Leak, University of Bath, UK
Prof. Dr B. Teusink, VU Amsterdam
Dr A.J. Else, Corbion, Gorinchem

This research was conducted under the auspices of the Graduate School VLAG (Advanced studies in Food Technology, Agrotechnology, Nutrition and Health Sciences)

The Thermophilic Route to Succinic Acid

Jeroen G. Koendjbiharie

Thesis

submitted in fulfillment of the requirements for the degree of doctor
at Wageningen University
by the authority of the Rector Magnificus,
Prof. Dr A.P.J. Mol,
In the presence of the Academic Board
to be defended in public
on Wednesday 4 March 2020
at 4 p.m. in the Aula.

Jeroen G. Koendjbiharie
The Thermophilic Route to Succinic Acid,
186 pages.

PhD thesis, Wageningen University, Wageningen, The Netherlands (2020)
With references, with summary in English

ISBN 978-94-6395-268-2
DOI https://doi.org/10.18174/510683

Voor mijn moeder

Table of Contents

Chapter 1 – General introduction and thesis outline 9

Chapter 2 - Investigating the central metabolism of *Clostridium thermosuccinogenes*..... 27

Chapter 3 - Assessing cofactor usage in *Pseudoclostridium thermosuccinogenes* via heterologous expression of central metabolic enzymes 47

Chapter 4 - Identification of a Novel Fumarate Reductase Potentially Involved in Electron Bifurcation 67

Chapter 5 – Effects of CO_2 limitation on the metabolism of *Pseudoclostridium thermosuccinogenes* 87

Chapter 6 - The pentose phosphate pathway of cellulolytic clostridia relies on 6-phosphofructokinase instead of transaldolase..... 113

Chapter 7 – Thesis summary 141

Chapter 8 – General Discussion..... 145

Appendices..... 159

References
Acknowledgments
List of publications
Overview of completed training activities
About the author

Chapter 1 – General introduction and thesis outline

Biotechnology and the biobased economy

Many nuanced definitions exist for *biotechnology* that generally describe the use of living systems, organisms, or parts thereof in order to alter or generate products, systems, or environments to benefit people. As such, biotechnology is a very broad, and broadly used term that covers a plethora of different fields and technologies, ranging from ancient beer brewing and winemaking processes to the production of modern therapeutics using engineered eukaryotic cell-lines. Agriculture itself, however, is generally not considered biotechnology, even though it would fit the definition. Since about fifteen years ago, it has become common to distinguish between different types of biotechnology using colors: white (industrial) biotechnology, red (pharmaceutical) biotechnology, green (agro) biotechnology, and blue (marine) biotechnology are the most common distinctions that are used, but many more exist and they are not always used consistently.

White, or industrial biotechnology is the central theme in this thesis, and revolves around the production of fuels, chemical building blocks, and industrial enzymes using microorganisms. It has gained a lot of momentum in the last few decades as an alternative to a petroleum based chemical industry. The most prominent reasons for shifting away from a petroleum based chemical industry, or a fossil fuel based economy in general, are climate change fuelled by the emission of greenhouse gasses, the heavy reliance on a small number of "oil states", and the depletion of known fossil fuel reserves. Climate change in particular is a problem that could pose an existential risk (to humanity), if not properly addressed. Many independent reports exist stating that, in order to avoid a catastrophic climate break-down, the net emission of CO_2, i.e. the use of fossil fuels, has to be reduced to zero within a time-frame of mere decades [119,189]. The situation in which biotechnology replaces fossil fuels is often referred to as the *biobased economy*, where renewable feedstocks, such as biomass – either as agricultural or forestry waste, or from dedicated crops or organisms – is converted in *biorefineries* into biofuels and platform chemicals, from which the majority of our goods and chemicals can be derived [41,57]. The main challenge in industrial biotechnology is simply the ability to compete with petrochemistry, which has had many more decades to mature, and (arguably) is unjustly cheap, due to the fact that in our current economic system, sustainability – or lack thereof – is not meaningfully included in the intrinsic value of a commodity [108,277].

In the USA, the majority of petroleum (87%), and fossil fuels in general (93%) are used for combustion (i.e. energy) [86]. The rest is consumed as chemicals, construction materials, and a variety of other products. Following these numbers, finding alternative energy sources that are renewable will be the most impactful way to reduce the reliance on fossil fuels. There are, of course, many alternative sources for the generation renewable energy (in the form of electricity) that do not include biotechnology. Some prominent examples

include, wind power, hydropower, solar energy, and geothermal energy. Nuclear power, either via fission or via fusion is *sensu stricto* non-renewable. Yet, the virtually unlimited availability of nuclear fuel renders nuclear power renewable in the practical sense [171,221]. Many challenges exist, however, regarding the storage of electrical energy, in particular for transportation. In the absence of technological breakthroughs, it is improbable that battery electricity will play a major role for ships and aircrafts [89]. As such, there will remain a demand for high-density chemical fuels, and therefore, an important niche for biofuels will likely exist, regardless of renewable electricity production.

Albeit being a much smaller fraction of fossil fuel uses, the non-combustion uses are much harder to replace. Biotechnology is particularly suited for this, as many microorganisms naturally produce a variety of chemicals that can replace petrochemically derived chemical building blocks, as well as fuels [25]. Succinic acid – the envisioned building block in this thesis – is a prime example, and will be thoroughly discussed further down. Moreover, microorganisms can be engineered to be more productive, and to produce completely novel molecules.

An aspect of biotechnology that is often not addressed directly is land use. For example, it was calculated that in order to fully replace oil consumption (in 2008), which accounts for around a third of the total fossil fuel consumption, an area of at least 100 million hectare of high yielding crops is required, an area the size of Eqypt, or 25 times The Netherlands [110,272]. At lower, more likely yields, the required area is many times that. Land that could either be used for food production, or that can be designated for nature conservation, raising the 'Food, Energy, and Environment Trilemma' [299].

To reflect the status of biofuels with respect to the food, energy, and environment trilemma, they are often designated as first-, second-, or third-generation biofuels, which essentially refers to the used feedstock:

- **First-generation** biofuels rely on easily degradable (i.e. edible) biomass, and therefore compete with food production. Current biofuels (e.g. bioethanol) are almost exclusively first-generation [85].
- **Second-generation** biofuels refer to use of non-food biomass, such as agricultural or forestry waste, and dedicated crops grown on land that is unsuitable for food production. The price for second-generation feed-stocks is significantly lower than those for the first generation, however, the process is much more complex, making second-generation biofuels currently often prohibitively expensive [162,281]. Soil erosion is another potential issue that has emerged regarding the use of crop residues as feedstock. Conventionally, crop residues are left on the field, protecting it to a substantial extend from erosion. In the case of maize, CO_2 emissions from soil erosion can result in cellulosic ethanol having a total CO_2 footprint that is equal to

that of gasoline [174,235]. Proper land management, to prevent the decrease of soil organic carbon is therefore of paramount importance for second generation biofuels to contribute to a reduction of net CO_2 emissions [234].

- **Third-generation** biofuels refer to the use of algae biomass (typically rich in fatty acids), or more broadly to the use of CO_2 in general. Algae do not rely on any form of biomass as a feedstock, and have an areal productivity that is orders of magnitude larger compared to typically used crops [187]. However, the use of algae is currently held back by the expensive nature of the required reactors [105]. The use of CO_2, in a mixture with H_2 and CO (i.e. synthesis gas or syngas), or reduced to formic acid or methanol, as a substrate for biotechnology (e.g. with acetogenic bacteria or methylotrophic microorganisms) has gained a lot of interest in recent years. It has the advantage that the reducing power of hydrogen, formic acid, and methanol can come from electricity, virtually decoupling the process from land use [7].

Thermophiles in industry

Microbial fermentation processes in industrial biotechnology almost exclusively rely on microorganisms that optimally grow at moderate temperatures around 25 – 37 °C. Microbiologists term such organisms mesophiles, to distinguish them – perhaps somewhat arbitrarily – from psychrophiles, growing at lower temperatures, and thermophiles, growing at higher temperatures. Yet, in industry it can have many advantages to have a process operate at higher-than-moderate temperatures, and thus use thermophilic organisms, to have a more economic process. The following advantages are typically acknowledged for the use of thermophilic organisms:

- **Efficient cooling**
  At industrial scale, the heat generated by the metabolic activity of the microorganisms is greater than the heat loss through the fermenter wall and via evaporation. Active cooling is therefore a necessity to maintain the required temperature. Energy requirements for cooling are a significant part of the operating costs, and in some cases, the heat generation and concomitant cooling duty can be so high that it becomes the limiting factor of the entire process. The larger the difference between the required fermentation temperature and the cooling water – i.e. the ambient temperature if not refrigerated – the more efficient the cooling, due the larger thermal driving force. For mesophilic organisms, active refrigeration is often required to increase the thermal driving force. Using a thermophilic organism will therefore reduce the cooling costs significantly. Additionally, cooling time between sterilization of fermentation medium (at 121 °C) and start of the fermentation is reduced with higher fermentation temperatures, reducing the total process time [195,328].

- **Lower risk of contaminations**

The lower risk of contamination is possibly the most often mentioned advantage, but at the same time it is also the hardest to verify, due to limited availability of information regarding contamination frequencies [328]. The most likely sources of contaminants are the feedstock and the human operators, both predominantly carrying mesophiles that should not be able to contaminate a thermophilic process. Nevertheless, once a contamination (with a thermophilic contaminant or a phage) has occurred at any site, it seems unlikely that there is a very big difference in terms of contamination risk between a thermophilic process and a mesophilic process, in particular when non-wild type strains are used. And since the losses of having to abort a fermentation due to a contamination are so high, maximum precautions will be taken in either case. Other strategies exist to have a production organism with a reduced risk of contamination, for example, by adapting or engineering the strain to use xenobiotic or ecologically rare chemicals as nutrients, such as melamine, cyanamide, or phosphite [267].

- **Increased solubility of products and substrates**
  Generally speaking, the solubility of solids increases with increasing temperature. For most medium components, the difference will not have any relevance. However, lignocellulosic biomass components typically have a poor solubility. Increased fermentation temperatures can therefore increase the bioavailability of second-generation feedstock, as well as decrease the viscosity of the medium, improving the process.

  Gasses, on the other hand, have a decreased solubility at higher temperatures. This is in particularly relevant for oxygen transfer, which is proportional to the solubility, as well as the diffusion rate. Since the diffusion rate increases with increasing temperature, the effects completely offset each other, leaving no significant impact of temperature on the oxygen transfer rate [158,312]. In the case of CO_2, the increased diffusion is not enough to compensate the overall gas transfer rate of CO_2, which decreases for increasing temperatures [36].

- **Higher reaction rates**
  Chemical reaction rates increase with increasing temperatures, as described by the Eyring equation as well as empirically by the Arrhenius equation. As a rule of thumb, the rate doubles for every 10 °C rise in temperature [165]. As such, thermophiles have the potential for much higher production rates, as is also somewhat reflected by their generally higher growth rates, and the relatively lower growth rates of psychrophiles [199,243,317].

  It has recently been proposed that cellular metabolism – and thus growth and production – might be constrained by an upper limit on the cellular Gibbs energy

dissipation rate [212]. Possibly explained by dissipated Gibbs energy being translated into work (non-thermal motion), which could be detrimental to vital cellular functions. If indeed true, the upper limit could still be higher for thermophiles, but the benefit might not necessarily be as high as would be expected from the Arrhenius equation.

Besides impacting reaction rates, temperature can also change the reaction equilibrium, by affecting change in entropy ($\Delta G = \Delta H - T\Delta S$). Reactions that are thermodynamically unfeasible or barely feasible at mesophilic temperatures might become more feasible at higher – thermophilic – temperatures, for example the formation of hydrogen [328].

- ***In situ* removal of volatiles**
  Downstream processing – the isolation of a pure product – often comprises a majority of the entire process costs [195]. Volatile products, such as alcohols, ketones, and esters are generally separated from the water phase via distillation, for which a significant input of heat is required. Firstly, a thermophilic process can therefore lower the downstream costs simply because less heat is required to heat the broth downstream of the fermentation. But secondly, it can enable the *in situ* removal of volatile products, during the fermentation process. The main advantage of such a set-up is the relief of toxicity effects of accumulated products, resulting in increased and prolonged productivity. The removal of the volatiles is accomplished via gas stripping, where a gas is sparged through the medium to capture the volatiles that are subsequently condensed in a cooling unit. Challenges connected to this include excessive foaming, high costs for equipment, and high energy requirement [313]. No examples of industrial fermentations using gas-stripping are currently known.

- **Simultaneous saccharification and fermentation**
  The use of second-generation feedstock, comprised of lignocellulosic material, requires the pre-treatment of that material, to allow it to be used efficiently by the microorganisms. The pre-treatment consists of two parts. First, the lignocellulosic fibres need to be opened up to increase the accessibility for added enzymes to break down the fibres into monomeric sugar molecules, which represents the second part (i.e. saccharification). Many methods exist to open up the fibres, but the most widely used process to date is steam explosion, where the rapid release of pressure causes the fibres to fracture [54]. The commercial hydrolysing enzymes used for the saccharification, typically a complex mixture, function optimally in the temperature range of 40–50 °C. Having a thermophilic process allows the saccharification and fermentation processes to be conducted simultaneously, in the same reactor, making for a simpler – more economic – process. This is referred to as *simultaneous*

saccharification and fermentation (SSF). Furthermore, the need to cool the substrate between pre-treatment and fermentation is also eliminated.

Aside from conducting fermentation at elevated temperatures, thermophiles have had a lot of interest as a source of proteins and enzymes [47]. Enzymes have an impressive range of industrial applications on their own, ranging from laundry and dishware detergents to food processing, but also the very enzymes used in the pre-treatment of lignocellulosic biomass, often subjected to very harsh conditions, including high temperatures. Thermophiles, but also other extremophilic organisms might have versions of the required enzymes that are more stable at such harsh conditions, making them an excellent source.

As explained above, the growth temperature can impact the process in many different ways. Nevertheless, it is just one of many aspects to take into account when selecting the optimal organism for a specific process. The most important parameters are the titer, rate, and yield of the product that should be optimized while minimizing the formation of side-products [213]. These parameters are predominantly determined by the biology of the production strain. Often, the organism will still need to be improved in those aspects, for which the strain needs to be genetically accessible. Furthermore, the organism needs to be able to tolerate both high substrate concentrations and high product concentration, as well as the harsh, often quickly fluctuating conditions of bioreactors in general. If the nature of the product allows it, a (facultative) anaerobic organism is preferred, since aeration, to supply the organism with oxygen is extremely expensive in large scale [115]. The medium requirements need to be cheap and simple. Finally, each process and product come with their own specific requirements. For example, when producing an organic acid, having the pH of the culture well below the pK_a of the product allows the recovery of the product directly in the acid form, simplifying the downstream recovery. It also diminishes the need for base titration during the fermentation. Having an organism that tolerates low pH might therefore improve the process economics of organic acid production, including succinic acid [3].

Succinic acid as a sustainable platform chemical

Succinic acid is the common name used for butanedioic acid, a four-carbon dicarboxylic acid. The name is derived from *succinum*, the Latin word for amber, as it was first isolated from Baltic amber, which contains around 5% succinic acid. It is a very common cellular metabolite since it is an intermediate in the tricarboxylic acid (TCA) cycle and the glyoxylate cycle (Figure 1). Some microorganisms produce succinic acid as a fermentation product via the reductive branch of the TCA cycle (in reverse). In humans, succinic acid is also known to act as a signal molecule in a variety of cell types [305].

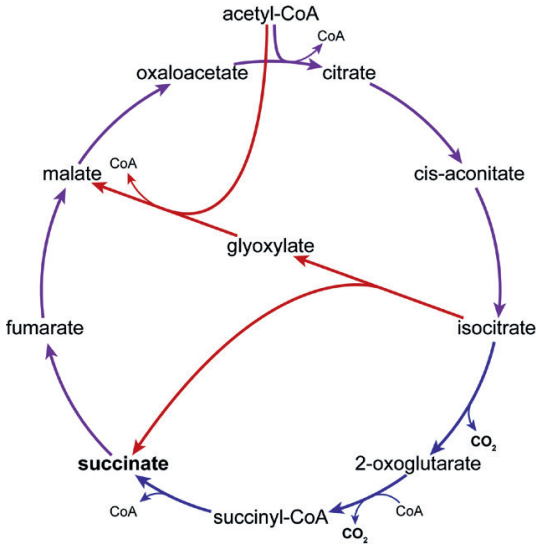

Figure 1: Simplified diagram of the tricarboxylic acid cycle (TCA; in blue) and the glyoxylate cycle (in red). Reactions with purple arrows are part of both.

Industrial applications of succinic acid

Succinic acid is relevant in industry as well. Traditionally, succinic acid was a niche product with a modest market size of around 50 kilotons per year (in 2016) [122] – mostly produced chemically via the conversion of fossil fuel-derived maleic anhydride – with four major markets: First and foremost as a surfactant; secondly, as an ion chelator used primarily for metal plating; thirdly, as a pH regulator and antimicrobial in food and beverages; and fourthly, as an additive in pharmaceutical formulations [327].

Mainly due to its relatively high price, it has never been an important intermediate in the chemical industry, despite the capability to function as a precursor of a variety of prominent polymers, resins, and solvents [229]. However, with the need to find alternatives to fossil fuel based chemicals, succinic acid produced via biological fermentation has the potential to replace a sizable portion of fossil fuel derived bulk chemicals and products, creating a potential demand in the order of megatons, rather than kilotons [41].

This outstanding biotechnological potential was already recognized as early as the 1990s, and in the last decade several different parties have started operating the first industrial plants, placing succinic acid amongst the first economically feasible bio-based platform chemicals [23,122].

An overview of the most important solvents, monomers, and chemical intermediates that can be derived from succinic acid is given in Figure 2. Most prominent of all derivatives is probably polybutylene succinate (PBS; Figure 3), a biodegradable polyester of succinic acid

and 1,4-butanediol – a succinic acid derivative – with properties similar to polypropylene, the second-most widely produced synthetic plastic, with a marked size of around 56 megatons (in 2018) [48].

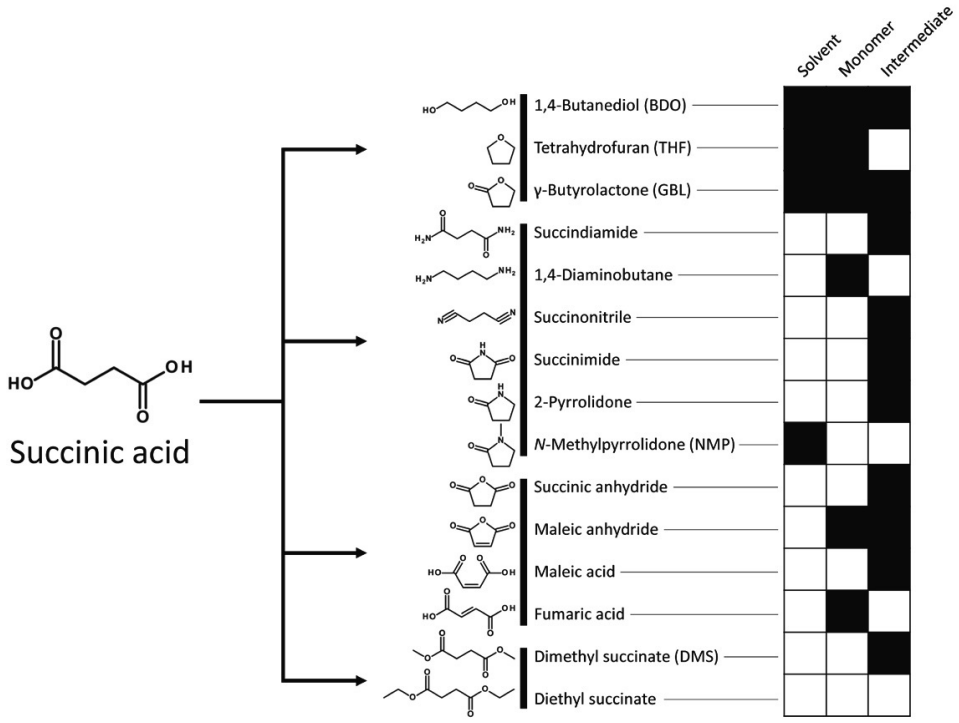

Figure 2: Important solvents, monomers, and chemical intermediates that can be derived from succinic acid. The different compounds are grouped according to a common synthesis route; something that is not strictly defined, since many possible synthesis routes exist. The black boxes indicate whether the major – but not exclusive – application is either as a solvent, monomer, and/or chemical intermediate.

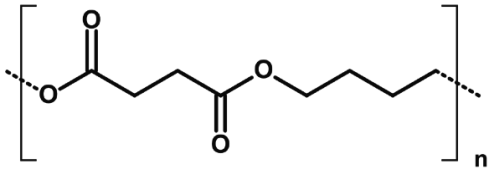

Figure 3: The repeating unit of polybutylene succinate (PBS)

Production of bio-based succinic acid

Over the last years four entities have started with the industrial production of succinic acid via fermentations (on pilot scale), each using a distinctive process; an overview is given in Table 1. Between the four of them, a production capacity of more than 400 kiloton per year

is currently being built [62]. Two main types of processes are used, either a eukaryotic (yeast)-based fermentation at low pH, or a bacterial-based process at neutral pH. Low pH fermentation allow the direct recovery of crystalized succinic acid, owing to (I) the acid dissociation constants (pK_a) of succinic acid of 4.2 and 5.6, such that at pH 3, the majority of succinic acid is in the associated form [122], and (II) the fact that the solubility of succinic acid is in the associated form is relatively low compared to other organic acids that are typically present as by-products [169]. Another main advantage is the fact that no excessive titration with slaked lime is needed for maintaining near-neutral pH, which traditionally leads to the formation of large amounts of gypsum (calcium sulfate) as by-product without added value. Succinity, however, has access to proprietary technology that allows the recycling of its titrant, thus circumventing gypsum formation as well [106]. GC Innovation America uses ammonia for titration instead, generating ammonium succinate. Ion exchange subsequently results in the formation of succinic acid as well as ammonium sulfate, which can be valorized as a fertilizer [92]. BioAmber has proprietary technology for electrodialysis, which allows the membrane assisted splitting of sodium succinate in succinic acid and sodium hydroxide [75], as well as proprietary technology for ammonia recycling via steam cracking [217]. However, after BioAmber switched to a low pH yeast production strain, licensed from Cargill, they were able to recover the succinic acid directly, similar to the process operated by Roquette.

The four processes have in common that they are all sugar-based, albeit from different sources. Yet, bacteria are generally more flexible in their substrate specificity. *B. succiniciproducens* – used by Succinity – for example, has the possibility to use glycerol as a feedstock. Glycerol is a cheap substrate, as it is formed as a byproduct during biodiesel production. Furthermore, per carbon, glycerol is more reduced than glucose, allowing theoretically higher carbon yields, through the fixation of 1 mol of CO_2 per mol of succinic acid produced, compared to 0.5 for glucose.

Table 1: The four entities currently operating pilot-scale succinic acid fermentation plants [23,122].

Producer	Capacity (kiloton)	Start-up in	Location	Production organism	Substrate	Downstream technology	Other details
BioAmber	30	2013	Ontario, Canada	Yeast, possibly *Candida krusei* (low pH)	Glucose	Electrodialysis / Ammonia recycling / Direct crystallization	Originally designed for a bacterial-based process. Yeast strain licensed from Cargill
GC Innovation America	14	2014	Louisiana, USA	*Escherichia coli*	Sorghum hydrolysate	Ammonia precipitation	Until August 2018 known as Myriant
Roquette	10	2013	Italy	*Saccharomyces cerevisiae* (low pH)	Starch	Direct crystallization	Originally as a joint venture of DSM & Roquette, known as Reverdia.
Succinity	10	2012	Spain	*Basfia succiniciproducens*	Sugars, glycerol (flexible)	Titrant recycling	Joint venture BASF & Corbion

(Un)sustainability of succinic acid

Chemicals produced from fossil fuels are per definition not sustainable. Of course, this does not automatically mean that bio-based chemicals are, even though sustainability is usually the main force behind the shift away from fossil fuel use. In order to quantify the degree at which a process is unsustainable a definition of a sustainable process needs to be established.

In an environmental context, *sustainability* could be defined as *"a condition of balance, resilience, and interconnectedness that allows human society to satisfy its needs while neither exceeding the capacity of its supporting ecosystems to continue to regenerate the services necessary to meet those needs nor by our actions diminishing biological diversity"* [201]. Net anthropogenic CO_2 emissions need to be zero, that much is clear, as well as all other forms of waste. But land use, soil quality, water use; every aspect of our supporting ecosystems needs to be balanced to be truly sustainable. How this balance is embodied is in the end very much an ethical as well as a political question.

For succinic acid, a number of studies exists trying to assess the sustainability of the biobased process compared to the petroleum-based equivalent, as well as different biobased processes compared with each other. Often the comparison is made between biobased succinic acid and petroleum-derived adipic acid, rather than petroleum-derived succinic acid, as this is thought to the most similar bulk-chemical in terms of the potential applications of succinic acid. Table 2 lists an overview of several different studies looking into CO_2 emissions or non-renewable energy use.

What is clear is that biobased succinic acid performs a lot better compared to petroleum-derived adipic acid. Compared to petroleum-derived succinic acid, the difference does not seem as big. However, the non-renewable cumulative energy demands (i.e. CED, a commonly used metric) for petroleum-based succinic acid is largely due to the inherent material requirements, whereas that of biobased succinic acid is largely down to the energy demands of the process [200], which should allow for significant future improvements. In particular the feedstock production and steam generation demand a lot of energy [60].

Table 2: Overview of several cradle-to-gate studies for biobased succinic acid, in terms of CO_2-equivalents emissions or non-renewable energy use (NREU).

[205]			
Chemical	**DSP**	**CO2-eq**	**Comments**
Petr. succinic acid	-	385 %	* Based on data from Myriant
Bio succinic acid	Ammonium sulphate	100 %*	
[60]			
Chemical	**DSP**	**kg CO2-eq / kg**	**Comments**
Adipic acid	-	8.8	
Malic anhydride	-	1.9	
Petr. succinic acid	-	1.8	
Bio succinic acid	Direct crystallization	0.9	
	Electro dialysis	1.7	
	Ammonium sulphate	1.5	
[2]			
Chemical	**DSP**	**kg CO2-eq / kg**	**Comments**
Adipic acid	-	13.6	
Bio succinic acid	Liquid-liquid extraction	1.9	
[111]			
Chemical	**DSP**	**kg CO2-eq / kg**	**Comments**
Adipic acid		5.8	Cradle-to-grave
Malic anhydride		6.8	
Bio succinic acid	Today	1.3-3.6 / 2.3-4.6*	* Sugar cane/ Maize
	Future	0.9-2.1 / 1.8-2.9*	
[226]			
Chemical	**DSP**	**GJ/t (NREU)**	**Comments**
Malic anhydride	-	67.7	* Sugar cane / Maize
Petr. succinic acid	-	96.3	
Bio succinic acid	Direct crystallization	44.9 / 66.5*	

Natural and engineered succinic acid producers

A large variety of organisms have been studied for their capacity to naturally produce succinic acid, and several natural and non-natural producers – both bacteria and eukaryotes – have been engineered to produce (more) succinic acid. The most-studied species are briefly described below.

Bacteria

Actinobacillus succinogenes

A. succinogenes is a facultative anaerobic, pleomorphic, Gram-negative rod, first isolated from bovine rumen [103]. It is capnophilic (CO_2-"loving") and can grow on a broad range of pentose and hexose sugars. It naturally produces succinic acid, up to 70 g/l with yields of

around 0.75 g/g sugar [178,249]. Succinic acid is formed via the reductive branch of the TCA cycle, which is bifurcated, with succinic acid as one of the end-points [102].

Anaerobiospirillum succiniciproducens

A. succiniproducens is an anaerobic, Gram-negative, spiral shaped bacterium. It was first isolated from a dog, but is also present in humans and can – in rare cases – be the cause of bacteraemia or other types of opportunistic infections [67,131]. Similar to *A. succinogenes*, *A. succiniproducens* is a capnophile able to grow on a large range of substrates. The available CO_2 concentration strongly influences the succinic acid production [250]. Yields of around 1.4 g/g glycerol have been reported [43,160].

Corynebacterium glutamicum

C. glutamicum is a facultative anaerobic, Gram-positive rod. It has a long history for industrial-scale production of a variety of amino acids [310]. It is unable to grow under oxygen deprived conditions, but retains the possibility to ferment sugars allowing a process to shift easily from a biomass formation phase and a high-density production phase, leading to high volumetric productivities [216]. *C. glutamicum* does not naturally excrete succinic acid, but a large number of studies exist where they have engineered the metabolism to create efficient succinate producing strains, reaching yields up to 1.67 mol/mol glucose, close to the theoretical maximum [3,175,216].

Escherichia coli

E. coli is a facultative anaerobic, Gram-negative rod that is commonly found in guts of warm-blooded animals. Most strains are harmless, but some serotypes are known to cause food poisoning. It is the most widely studied (prokaryotic) model organism, and is used extensively in laboratories as a host for propagating recombinant DNA. Furthermore, engineered *E. coli* strains are extensively used as industrial production platform, which includes the commercial production of succinic acid by GC Innovation America, as mentioned above, as well as a 1,3-propanediol by DuPont, a variety of amino acids, and a variety of protein therapeutics, most notably insulin [295].

The strain used by GC Innovation America has likely been engineering to have reduced pyruvate kinase activity and increased phosphoenolpyruvate carboxykinase activity, as well as eliminated activity for the PEP-dependent phosphotransferase system while having increased activity for a galactose-proton symporter. It is further likely that pathways for competing products have been eliminated [99,101].

Fibrobacter succinogenes

F. succinogenes is an strictly anaerobic, Gram-negative rod, found in the rumen of bovine animals, where it is able to ferment cellulose into succinate, acetate, and formate [282,284]. Its ability to naturally produce succinic acid from cellulose – potentially derived from agricultural waste – makes it interesting for industrial applications. However, the limited

studies that have been conducted report yields and productivities far below those from the other natural producers described here [98,168].

***Basfia succiniciproducens* (& *Mannheimia succiniciproducens*)**
B. succiniciproducens, which includes a strain that is usually called *Mannheimia succiniciproducens*, is a facultative anaerobic, Gram-negative coccoid, and is probably the most widely studied natural succinic acid producer [152]. It is able to grow in a variety of sugars and sugar alcohols, and (engineered) strains have been reported to convert their substrate almost exclusively to succinate [156,159,261]. A proprietary *B. succiniciproducens* strain of BASF is used for commercial succinic acid production by Succinity – a joint venture of BASF and Corbion, as described earlier.

B. succiniciproducens has been engineered to have reduced pyruvate kinase activity, as well as reduced or abolished lactate dehydrogenase and pyruvate formate lyase activity [24,146].

***Pseudoclostridium thermosuccinogenes* (originally *Clostridium thermosuccinogenes*)**
P. thermosuccinogenes is the only known thermophile to naturally produce succinic acid as a main fermentation product. It is a strict anaerobic, Gram-positive rod, growing optimally at 55 – 60 °C; first isolated on inulin as a substrate [74]. Research into the organisms has been limited, with succinate yields up to 0.54 g/g inulin reported, strongly depending on pH [278–280]. Its metabolism is the central topic of this thesis.

Eukaryotes

Saccharomyces cerevisiae
S. cerevisiae, also known as baker's yeast or budding yeast, is perhaps the most intensively studied eukaryotic model organism, much like *E. coli* is for bacteria. And like *E. coli*, it is also widely used in biotechnology. Historically for the production of bread, beer, and wine, but more recently for the production of ethanol as a biofuel, or a broad variety of non-native products – the latter owing largely to the ease of it genetic engineering [222]. The succinic acid process of Roquette (originally as a joint venture with DSM, named Reverdia) uses an engineered *S. cerevisiae* strain for the production of succinic acid.

The proprietary *S. cerevisiae* strain of DSM has most likely been modified via the introduction of the following heterologous genes: Phosphoenolpyruvate carboxykinase from *Actinobacillus succinogenes*, NAD(H)-dependent fumarate reductase from *Trypanosoma brucei*, fumarate hydratase from *Rhizopus oryzae*, and a dicarboxylic acid transporter from *Schizosaccharomyces pombe*. Finally, the native peroxisomal malate dehydrogenase lacking the peroxisomal targeting sequence is overexpressed [123].

***Pichia kudriavzevii* (or *Issatchenkia orientalis*; anamorph of *Candida krusei*)**
P. kudriavzevii is a yeast that is commonly isolated from (fermented) food sources that is able to tolerate very low pH and temperatures up to 45 °C [301]. Like *S. cerevisiae*, it naturally produces ethanol at high yields and is therefore being studied for its potential in the production of biofuels [215]. BioAmber has switched from an *E. coli* based process to a low-pH process for succinic acid production using an engineered *P. kudriavzevii* strain licenced from Cargill, which has patents for two different succinic acid producing *P. kudriavzevii* strains. Both have been extensively engineered (see references) [3,83,246].

Pseudoclostridium thermosuccinogenes and other *Hungateiclostridiaceae*

Pseudoclostridium thermosuccinogenes is a Gram-positive bacterium that belongs to the *Firmicutes* phylum, the *Clostridia* class, and the *Clostridiales* order. It was recently renamed from *Clostridium thermosuccinogenes* to *Pseudoclostridium thermosuccinogenes* and simultaneously placed within the newly designated *Hungateiclostridiaceae* family [330]. Both names will be used in this thesis. To make things even more confusing, the now *Hungateiclostridiaceae* family was for a short period of time (wrongly) designated by some as the genus *Ruminiclostridium* within the *Ruminococcaceae* family [141,326], and recently the *Hungateiclostridiaceae* family name (and corresponding genus names) were suggested to be illegitimate and placement within the genus *Acetivibrio* was proposed [300].

Four strains of *P. thermosuccinogenes* were first isolated in 1991 by researchers from the University of Groningen via enrichments at 58 °C using inulin as the sole carbon and energy source [74]. The name *Clostridium thermosuccinogenes* was chosen due to its thermophilic nature and the formation of succinic acid as a major fermentation product. At that time, the main interest was to find a thermophilic inulinase; an enzyme able to degrade the polysaccharide inulin into fructose (and traces of glucose) that could aid in the production of high-fructose syrup [311].

Later, at the turn of the century, researchers from the University of Georgia started to work on *P. thermosuccinogenes* for its ability to produce succinic acid, as the biotechnological potential of succinic acid was being recognized. They studied the effect of pH and redox potential on the distribution of the different fermentation products, which – besides succinate – include acetate, formate, lactate, and ethanol [278,279]. Of the four strains (DSM 5806 – DSM 5809), they showed that DSM 5809 was able to produce the most succinic acid. Via enzyme assays, they were able to elucidate the metabolic pathways leading to those different fermentation products [280]. However, no further studies had been published into *P. thermosuccinogenes* since then.

Many closely related *Hungateiclostridiaceae*, in particular the thermophilic *Hungateiclostridium* (*Clostridium*) *thermocellum* and mesophilic *Ruminiclostridium*

(*Clostridium*) *cellulolyticum* have been studied intensively for a long period of time. Mainly for their ability to degrade (hemi)cellulose, a defining feature of the *Hungateiclostridiaceae* that *P. thermosuccinogenes* seems to lack. Consequently, the work in this thesis builds greatly and gratefully on the research that was done into the metabolism of *H. thermocellum*.

Thesis outline

In **Chapter 2** we provide the sequenced genomes of the four available *P. thermosuccinogenes* strains and we present an updated characterization of the organism's metabolism. The characterization is based on genomics, transcriptomics, and enzyme assays with cell-free extract. Features such as the glycolysis relying on ATP, as well as GTP and PP_i as cofactors; the lack of an annotated transaldolase; and the 'malate shunt' for PEP to pyruvate conversion, that were previously described for *H. thermocellum* are now also shown to be present in *P. thermosuccinogenes*. Furthermore, xylulokinase – absent in *H. thermocellum* – was also shown to use GTP.

The unusual cofactor usage was further studied in **Chapter 3**. Thirteen enzymes from the central metabolism of *P. thermosuccinogenes* were heterologously expressed in *E. coli* to assess their cofactor usage *in vitro*. The use of PP_i and GTP as phosphoryl carriers are extensively discussed, and we hypothesize that the use of GTP allows for different (or more flexible) reaction thermodynamics compared to reactions relying on ATP.

Chapter 4 deals with the pathway to succinic acid. In particular with fumarate reductase, responsible for the conversion of fumarate to succinic acid. Based on genomic context and comparative genomics, we propose two hypothetical mechanisms through which the fumarate reductase associates with the electron bifurcating NADH-reductase-heterodisulfide reductase complex, coupling the reduction of fumarate to that of ferredoxin (using NADH). Some preliminary, inconclusive experimental data is presented as well.

In **Chapter 5** the effect of CO_2 limitation on the metabolism of *P. thermosuccinogenes* is studied via bioreactor cultivations. Succinate production is connected to net fixation of CO_2, by PEP carboxykinase, and was therefore expected to be impacted significantly. However, the effect on succinate yield was relatively small. Significant effects on formate and ethanol yields were observed. Endogenous CO_2, formed by pyruvate:ferredoxin oxidoreductase, was able to sustain the CO_2 required for succinic acid formation. Transcriptional changes following CO_2 limitation have been investigated through RNA-sequencing.

In **Chapter 6** the pentose phosphate pathway of *Hungateiclostridiaceae* is investigated in order to find out how they are able to interconvert C_5 and C_3/C_6 metabolites in the absence of a transaldolase. By means of metabolomics and *in vitro* enzyme assays we were able to confirm the existence of the – previously proposed – sedoheptulose 1,7-bisphosphate (SBP) pathway. In this pathway, sedoheptulose 7-phosphate is converted to SBP by a PP_i-dependent phosphofructokinase, followed by the cleavage of SBP into erythrose 4-phosphate and dihydroxyacetone phosphate that are compatible with the rest of glycolysis.

Chapter 2 - Investigating the central metabolism of *Clostridium thermosuccinogenes*

Jeroen G. Koendjbiharie[1], Kilian Wiersma[2], Richard van Kranenburg[1,2]

[1] Corbion, Gorinchem, Netherlands
[2] Laboratory of Microbiology, Wageningen University & Research, Netherlands

Chapter has been published as:

J.G. Koendjbiharie, K. Wiersma, R. van Kranenburg, Investigating the Central Metabolism of *Clostridium thermosuccinogenes*, Appl. Environ. Microbiol. 84 (2018) e00363-18.

Abstract

Clostridium thermosuccinogenes is a thermophilic anaerobic bacterium able to convert various carbohydrates to succinate and acetate as main fermentation products. Genomes of the four publicly available strains have been sequenced and the genome of the type-strain has been closed. The annotated genomes were used to reconstruct the central metabolism, and enzyme assays were used to validate annotations and to determine co-factor specificity. Genes for the pathways to all fermentation products were identified, as well as for the Embden-Meyerhof-Parnas pathway, and the pentose phosphate pathway. Notably, a candidate transaldolase was lacking and also transcriptomics during growth on glucose versus xylose did not provide any leads to potential transaldolase genes or alternative pathways connecting the C5 with the C3/C6 metabolism. Enzyme assays showed xylulokinase to prefer GTP over ATP, which could be of importance for engineering xylose utilization in related, thermophilic species of industrial relevance. Furthermore, the gene responsible for malate dehydrogenase was identified via heterologous expression in *E. coli* and subsequent assays with the cell-free extract, which has proven to be a simple and powerful method for basal characterization of thermophilic enzymes.

Importance

Running industrial fermentation processes at elevated temperatures has several advantages, including reduced cooling requirements, increased reaction rates and solubilities, and a possibility to perform simultaneous saccharification and fermentation of pretreated biomass. Most studies with thermophiles so far have focussed on bioethanol production. *C. thermosuccinogenes* seems an attractive production organism for organic acids, succinic acid in particular, from lignocellulosic biomass-derived sugars. This study provides valuable insights in its central metabolism and GTP and PPi co-factor utilization.

Introduction

Conversion of lignocellulosic biomass, which is typically a complex mixture of sugar polymers, into useful green chemicals, such as building blocks for polymers, is seen as an important step in the transition to a biobased economy. The United States' Department of Energy has published several well-known papers dealing with a top twelve of promising bio-based building blocks [41,320]. Several organic acids and dicarboxylic acids including succinic acid (SA) have been identified as such building block chemicals that can be produced from biomass. SA is currently mainly used as a food ingredient or as an additive and precursor for pharmaceuticals. However, it has a range of potential large scale industrial applications, which are ultimately dependent on their ability to economically compete with petroleum-based alternatives. Current commercial processes exclusively use mesophilic organisms, at temperatures around 30 to 37 °C. The use of thermophiles for an industrial fermentation process running at 50 to 60 °C has several advantages. Such processes (I) require less cooling, (II) generally have higher reaction rates and solubilities, and (III) have

the possibility to carry out simultaneous saccharification and fermentation of pretreated biomass, making a more economic process [1,128].

Clostridium thermosuccinogenes is the only known thermophile that naturally produces SA as one of its main fermentation products. It was first isolated in 1990, for its ability to grow on inulin at elevated temperatures, but like many Clostridia it grows well on a range of C5 and C6 sugars [74]. Although it belongs to a group of (hemi)cellulolytic organisms and it is a close relative of the industrially relevant thermophilic *C. thermocellum* and mesophilic *C. cellulolyticum*, it is incapable of degrading (hemi)cellulose. Physiological characterization of the only four strains of the species that have been described (DSM 5806, DSM 5807^T, DSM 5808 and DSM 5809) includes evaluation of the effect of pH and redox potential on the distribution of its fermentation products, SA, acetic acid, formic acid, lactic acid, ethanol and hydrogen [278–280]. Furthermore, enzyme assays have been used to shed light on the fermentation pathways towards these products. A pathway from phosphoenolpyruvate (PEP) to succinate was proposed via (I) PEP carboxylase (PEPC), (II) malate dehydrogenase (MDH), (III) fumarate hydratase (FH), and (IV) fumarate reductase (FR). For close relatives of *C. thermosuccinogenes* and most natural SA producers it is now well established that conversion from PEP to oxaloacetate is done by PEP carboxykinase (PEPCK), rather than PEPC [163,253,331]. A genome sequence should clarify whether there is a PEPC or PEPCK present. Likewise, ATP-linked phosphofructokinase (PFK) activity was detected, whereas for *C. thermocellum* only PPi-linked activity was detected [280,331].

In this paper we present an updated characterization of *C. thermosuccinogenes* metabolism by means of genomics, transcriptomics and enzyme assays, and provide evidence of a GTP dependent xylulokinase (XK).

Results

Genome sequences of *C. thermosuccinogenes*

Genomes of the four *C. thermosuccinogenes* strains were sequenced using Illumina HiSeq technology. From the initial assemblies it was clear that DSM 5806, DSM 5807^T, and DSM 5808 were quite similar, while DSM 5809 was more different from the others (see below). In an attempt to reduce the number of contigs, DSM 5807^T was selected for PacBio sequencing as type strain and representative for DSM 5806 and DSM 5808, together with DSM 5809, which appears to produce the most succinic acid [74,278]. The data from both Illumina and PacBio were combined in a hybrid assembly, which resulted in a closed genome for DSM 5807^T and an assembly of 8 scaffolds for DSM 5809. General features of the four genomes are presented in Table 1.

Table 1: General features of genome sequences of *C. thermosuccinogenes*. It should be noted that DSM 5806 and DSM 5808 were assembled with illumina data only, whereas the numbers for DSM 5807T and DSM 5809 represent the hybrid assembly with illumina and PacBio data. Therefore, the numbers of these different assembly methods cannot directly be compared to each other.

Attribute	DSM 5806 (illumina)	DSM 5807^T (hybrid)	DSM 5808 (illumina)	DSM 5809 (hybrid)
Genome size	4,519,012	4,731,216	4,509,994	4,665,658
GC content	41.5%	41.5%	41.5%	41.5%
DNA scaffolds	266	1	240	8
Total genes	3930	4086	3888	4035
Protein encoding genes	3783	3940	3751	3885
RNA genes	70	75	69	75
Pseudo genes	77	71	68	75
Hypothetical	1724 (43.9%)	1783 (45.3%)	1699 (43.7%)	1808 (44.8%)

As indicated, the four strains are very similar. Using the Genome-to-Genome Distance Calculator (GGDC) to estimate the DNA-DNA hybridization (DDH) [14], DSM 5806, DSM 5807^T and DSM 5808 were found to have 100% hybridization with each other and 92.3% with DSM 5809, which falls well within the 70% and 79% thresholds used to delineate species and subspecies, respectively [191].

Orthologous and paralogous proteins in the four assembled genomes were defined using OrthoMCL to further quantify their similarity. 22 Orthologous groups (OGs) were found that had only one or two paralogs in DSM 5806 and DSM 5808, while these had up to 15 paralogs in DSM 5807^T and DSM 5809. These 22 OGs consisted almost exclusively of transposases and hypothetical proteins. The difference in number of paralogs for the strains reflects the different assemblies used, as the short reads of Illumina do not allow the differentiation between repeated sequences, without a larger scaffold sequence provided by PacBio sequence analysis. From the OrthoMCL analysis it was also evident that DSM 5809 was more different from the other three strains; 369 OGs were uniquely absent from DSM 5809, whereas this was the case for only 1, 4, and 2 OGs for DSM 5806, DSM 5807^T, and DSM 5808, respectively. Conversely, 180, 154, 149, and 527 genes and/or OGs were unique for DSM 5806, DSM 5807^T, DSM 5808, and DSM 5809, respectively. A list of these unique genes can be found in the supplementary data, together with the rest of the results from the OrthMCL analysis (Table S1). The majority of the genes that are not shared between the four strains encode hypothetical proteins, and none encode apparent metabolic functions.

Many clostridia are being studied for their potential in biotechnology, including several close relatives of *C. thermosuccinogenes*: *C. thermocellum* and *C. cellulolyticum*. A 16S rRNA-based phylogenetic tree was constructed to place *C. thermosuccinogenes* in context with

those biotechnologically relevant species, as well as other natural succinic acid producers and species with a known GTP-dependent glucokinase (GK) (Fig. 1).

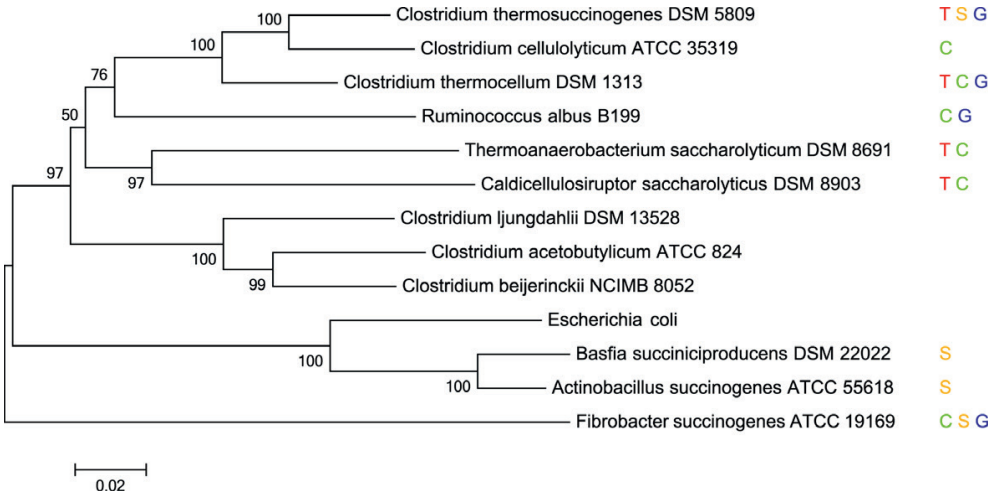

Figure. 1: Neighbor-joining tree based on 16S rRNA sequences of a selection of industrially relevant clostridia and other species related to *C. thermosuccinogenes*, as well natural succinic acid producers and species with a known GTP-dependent glucokinase. **T**, thermophile; **C**, cellulose degrader; **S**, succinate producer; **G**, known to have a GTP-dependent glucokinase. The percentages next to branching points represent the results of bootstrapping with 1000 replicates.

Central metabolism

The central metabolism of *C. thermosuccinogenes* was reconstructed based on the genome annotation of DSM 5809, which should be representative for the other three strains, according to the OrthoMCL analysis (see above), although in some cases they can have more or fewer isozymes for a certain reaction. The reconstruction was made by combining different annotations (NCBI pipeline, RAST, Prokka), which appeared to be significantly different in certain cases. Previous results from Sridhar *et al*. (2000) were also considered in the reconstruction [280]. All genes for the Embden-Meyerhof-Parnas pathway, and apart from the transaldolase (TAL) gene all genes for the pentose phosphate pathway (PPP) were annotated. Around the PEP–pyruvate–oxaloacetate node [253] four different pathways for the conversion from PEP to pyruvate seem to be present: Pyruvate kinase (PYK); Pyruvate, phosphate dikinase (PPdK); the 'malate shunt'; and one via oxaloacetate decarboxylase (OAD). The latter two involve a GTP-dependent PEPCK, rather than PEPC. As with most anaerobes, the TCA cycle is bifurcated, because no succinyl-CoA synthetase or succinyl-CoA ligase is present, which coincides with succinate being one of the end-products. Routes to the other products (lactate, acetate, formate, ethanol, and hydrogen) are annotated as well. Formation of acetyl-CoA can go either via pyruvate:ferredoxin oxidoreductase or via pyruvate formate lyase. Sugar transport seems to occur mainly via ABC transporters, as no

phosphotransferase systems were retrieved from the annotation, while many ABC transporters were found. The schematic reconstruction is shown in Fig. 2.

In order to get a clue about the missing TAL, an RNAseq analysis was performed on RNA isolated from cells growing on glucose versus xylose. Table S2 shows the genes with the highest differential expression. As expected, genes responsible for the uptake of xylose and the subsequent conversion to xylulose-5-phosphate (X5P) showed the most differential expression. CDQ83_14310 and CDQ83_08695 are annotated by RAST as (xylose) transport proteins. CDQ83_14315 is the xylulokinase and CDQ83_14305 is almost certainly a xylose isomerase, rather than a fucose isomerase, and is also annotated as such by RAST. The rest of the differentially expressed genes are mostly hypothetical and are either very short peptides, or still have a very low coverage. Since all carbon that enters the C3/C6 metabolism during growth on xylose has to be channelled through the non-oxidative PPP, it is not unlikely that the genes responsible for this conversion are upregulated as well, and would include an unknown TAL or an alternative pathway. However, no leads for candidate genes were derived from the differentially expressed genes (Table S2).

Many reactions in the central metabolism have several isoforms annotated. The transcriptomics data can in some cases already indicate which of the isoforms are the dominant ones during (exponential) growth on glucose and/or xylose. The transcriptomics data for all the annotated genes that potentially fulfil the roles of the reactions presented in Fig. 2 are listed in Table S3.

The annotation has no candidate MDH, but has three candidate lactate dehydrogenases (LDHs), one of which (CDQ83_05915) is very ambiguously annotated. As it is difficult to differentiate between MDH and LDH based on their sequence, it is likely that one of the genes annotated as LDH is really an MDH, which has not been annotated [322,325]. CDQ83_08825 has the highest homology with the isoform from *Clostridium thermocellum* that was found to be an MDH [224,289] and seems therefore the most likely candidate. To test this, the two unambiguous isoforms were overexpressed in *E. coli* and the cell-free extract of *E. coli* was subsequently used to determine the MDH and LDH activities (Table 2). SDS-PAGE analysis clearly showed protein overproduction of a protein of the expected size in both strains (Fig. S1). Background activities in *E. coli* extract with an empty vector control were negligible under the tested conditions. As expected, CDQ83_08825 is an MDH, and shows activity with both NADH and NADPH. The other isoform, CDQ83_04860 is an LDH, but also showed substantial NADH-dependent MDH activity.

Several genes are ambiguously annotated as potential oxaloacetate decarboxylases (OAD), including CDQ83_05940 which is part of a highly expressed operon containing three genes. Because none of those genes are predicted to be membrane proteins, which OAD is known to be [73,150], and because they have orthologous genes in *C. thermocellum*, for which no

OAD activity has currently been detected, it seems unlikely that they encode an OAD. Indeed, assays with (crude) cell-free extract of *C. thermosuccinogenes* did not show any OAD activity, therefore, the OAD reaction is denoted with a dashed arrow in Fig. 2.

Cofactor specificities are difficult to derive from annotations. For *C. thermocellum* it was demonstrated that it prefers GTP and PPi for several glycolytic reactions instead of the 'typical' ATP [331]. Therefore, enzyme assays were carried out to evaluate cofactor specificities in *C. thermosuccinogenes*. As summarized in Table 3, GK activity depends on GTP and PFK activity on PP_i. Phosphoglycerate kinase activity is highest with ATP, but is also detected with GTP. For XK, the highest activity was found with GTP, but ATP dependent activity was also detected. The activity for malic enzyme (ME) was dependent on $NADP^+$. Except for XK, the difference in enzyme activities measured with extracts from cells grown on glucose or xylose appeared to be minimal.

Table 2: Enzyme assay with *E. coli* cell-free extract containing the two malate dehydrogenase (MDH) candidates from *C. thermosuccinogenes*, which were initially annotated as lactate dehydrogenases (LDH). Reaction velocities are given in µmol per mg cell-free extract protein per minute (± the standard deviations).

Enzyme	Assay			
	MDH		LDH	
	NADH	NADPH	NADH	NADPH
CDQ83_08825	5.35 ± 0.04	6.27 ± 0.86	ND	ND
CDQ83_04860	1.34 ± 0.42	ND[a]	0.96 ± 0.13	ND

[a] ND, not detected.

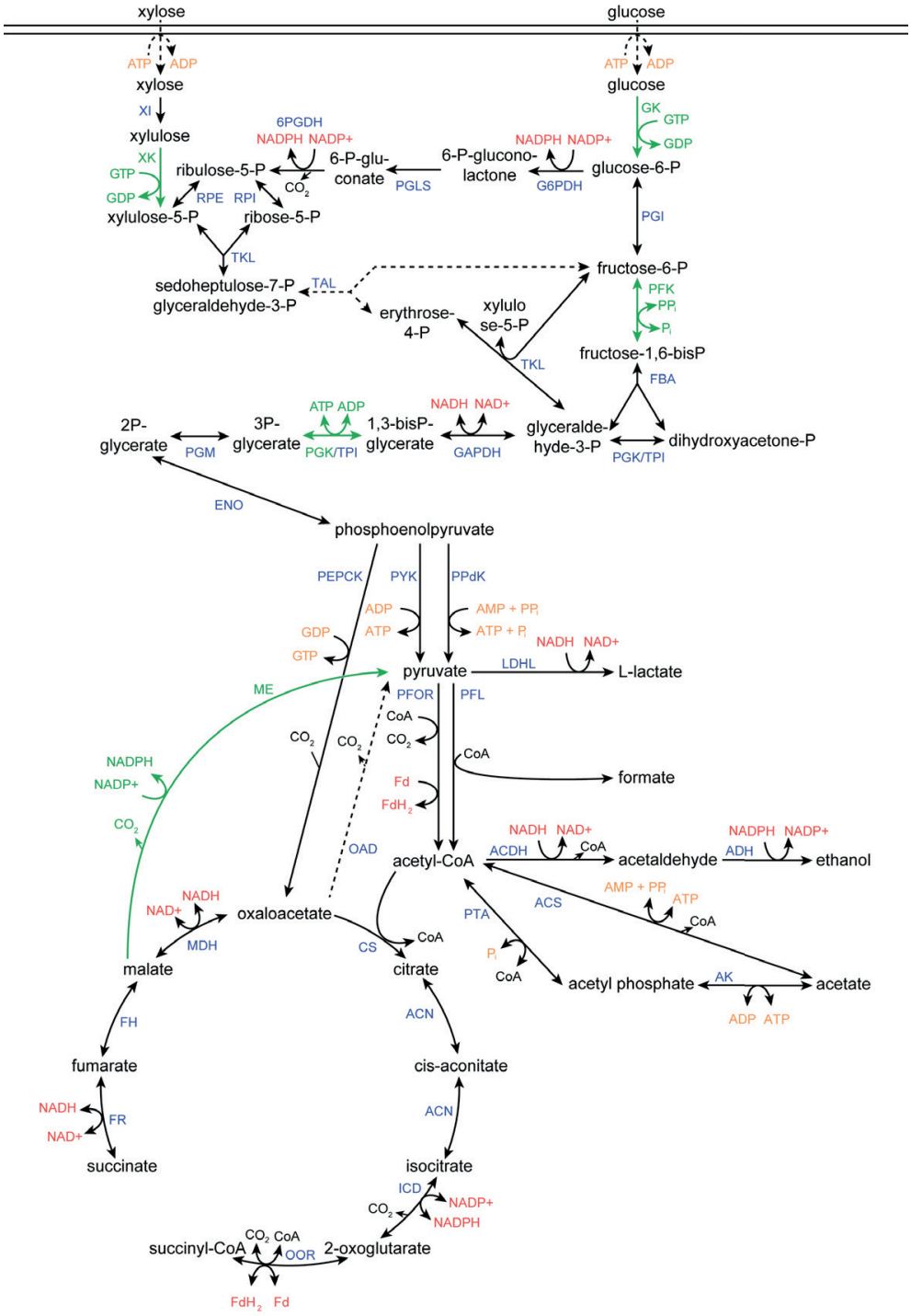

Figure 2: Reconstruction of the central metabolism of *C. thermosuccinogenes*. Green arrows denote reactions verified in enzyme assays with *C. thermosuccinogenes* cell-free extract. 6PGDH: 6-Phosphogluconate

dehydrogenase; ACDH: Acetaldehyde dehydrogenase; ACN: Aconitase; ACS: Acetyl-CoA synthetase; ADH: Alcohol dehydrogenase; AK: Acetate kinase; CS: Citrate synthase; ENO: Enolase; FBA: Fructose-bisphosphate aldolase; FH: Fumarate hydratase; FR: Fumarate Reductase; G6PDH: Glucose-6-phosphate dehydrogenase; GAPDH: Glyceraldehyde 3-phosphate dehydrogenase; GK: Glucokinase; ICD: Isocitrate dehydrogenase; LDHL: l-lactate dehydrogenase; MDH: Malate dehydrogenase; ME: Malic enzyme; OAD: Oxaloacetate; decarboxylase; OOR: 2-Oxoglutarate:ferredoxin oxidoreductase; PEPCK: Phosphoenolpyruvate carboxykinase; PFK: Phosphofructokinase; PFL: Pyruvate formate lyase; PFOR: pyruvate:ferredoxin oxidoreductase; PGI: Phosphoglucose isomerase; PGK: Phosphoglycerate kinase; PGLS: 6-phosphogluconolactonase; PPdK: Pyruvate, phosphate dikinase; PTA: Phosphate acetyltransferase; PYK: Pyruvate kinase; RPE: Ribulose-phosphate 3-epimerase; RPI: Ribose-5-phosphate isomerase; TAL: Transaldolase; TKL: Transketolase; TPI: Triosephosphate isomerase; XI: Xylose isomerase; XK: Xylulokinase.

Table 3: Enzyme assay with *C. thermosuccinogenes* cell-free extract, to determine cofactor specificities for several glycolytic reactions. Reaction velocities are given in µmol per mg cell-free extract protein per minute (± the standard deviations). Cell-free extract of cells grown on glucose and on xylose was tested.

Reaction	Cofactor	Cell-free extract	
		Glucose	Xylose
Glucokinase	ATP	ND[a]	ND
	GTP	0.90 ± 0.10	0.68 ± 0.12
	PP_i	ND	-
Xylulokinase	ATP	0.01 ± 0.01	0.60 ± 0.01
	GTP	0.02 ± 0.00	0.83 ± 0.05
Malic enzyme	$NADP^+$	2.5 ± 0.3	2.3 ± 0.3
	NAD^+	ND	ND
6-Phosphofructokinase[b]	ATP	ND	-
	GTP	ND	-
	PP_i	2.8 ± 0.2	4.0 ± 0.2
Phosphoglycerate kinase[b]	ATP	2.8 ± 0.3	2.9 ± 0.2
	GTP	1.2 ± 0.1	1.1 ± 0.1
	PP_i	-	-

[a] ND, not detected

[b] Cell-free extract prepared with Tris-HCl buffer instead of potassium phosphate buffer.

Discussion

Genome assembly

The hybrid assemblies of DSM 5807^T and DSM 5809 are approximately 200kb, and 150 – 200 genes larger than their SPAdes assemblies that are based on Illumina data. This difference presumably consists mostly of repeated sequences that cannot be assembled correctly based on the shorter reads from Illumina. This was also evident from the fact that a striking difference between the assemblies of DSM 5807^T and DSM 5809 compared to DSM 5806 and DSM 5808 was the much larger number of replicates of transposable elements.

With 4.7 Mb, the overall size of the genome is significantly larger than those of *C. thermocellum* and *C. cellulolyticum* of 3.6 Mb and 4.1 Mb, respectively.

Link between C5 and C3/C6 metabolism

The absence of an annotated TAL has already been discussed for several of the cellulolytic clostridia [208,247,258], and according to Schellenberg *et al*. [258] 18% of clostridia genomes do not have a TAL annotated, of which at least a few, including *C. thermosuccinogenes* can grow well on pentose sugars. From the transcriptomics data no candidate genes were found, and none of the annotated genes from the non-oxidative PPP appeared to be differentially expressed during growth on xylose versus glucose, apart from the genes responsible for the formation of X5P (Table S2). In many bacteria, including *E. coli*, none of the genes of the non-oxidative pathway are differentially expressed during growth on xylose versus glucose [100]. For *Clostridium termitidis*, an organism related to *C. thermosuccinogenes* that also lacks a transaldolase, the transketolase was found significantly upregulated during growth on xylose [208]. However, we did not observe this in *C. thermosuccinogenes*. Assuming that this is indeed the case, the PPP enzymes are either already present in amounts high enough to channel all X5P to the C3/C6 metabolism, or there is an alternative, unknown pathway being expressed during growth on xylose. No indication for any such highly and differentially expressed pathway seems to be apparent from our results. The presence of an alternative unknown pathway that is not differentially expressed on xylose versus glucose would not appear in these results.

One alternative pathway proposed for *C. thermocellum* runs via sedoheptulose-1,7-bisphosphate formed from sedoheptulose-7-phosphate by a PFK that is subsequently cleaved to dihydroxyacetone-phosphate (DHAP) and erythrose-4-phosphate (E4P) by a fructose-bisphosphate aldolase, thereby replacing the missing TAL activity [247]. This pathway has been demonstrated to exist in parasitic protists that also rely on PP_i-dependent PFK (PPi-PFK) [285]. As one of the hallmarks of the PPi-PFK is its reversibility, in contrast to the ATP-dependent one [193], it is not unlikely that the PPi-PFK of *C. thermosuccinogenes* could also play a role in the non-oxidative PPP. PPi-PFK does appear roughly 40% more active in cell extract from cells grown on xylose, but this is insignificant as long as it has not been tested with sedoheptulose-7-phosphate. However, due to the limited availability of PPP intermediates that could be used for enzyme assays, it is not trivial to search for an unknown alternative pathway. Moreover, the recursive nature of the PPP and the high reverse fluxes, due to low thermodynamic driving force of anaerobic metabolism in general, complicate stable-isotope-labelling studies, which would otherwise be a very powerful method.

PEP–pyruvate–oxaloacetate node

The PEP-pyruvate-oxaloacetate (PPO) node forms the junction between the glycolysis and the TCA cycle and can compromise a large set of reactions [253]. In *C. thermosuccinogenes*,

genes are annotated for PEPCK, PPdK, PYK, OAD, MDH, and ME. Taken together, these reactions would enable four different pathways from PEP to pyruvate, each involving different cofactors: (I) PPdK: AMP, PP_i → ATP + P_i; (II) PYK: ADP → ATP; (III) malate shunt: GDP, NADH → GTP, NADPH; and (IV) via PEPCK and OAD: GDP → GTP.

In contrast to what was found earlier by Sridhar *et al*. [280], *C. thermosuccinogenes* appears to rely on PEPCK for the formation of oxaloacetate, rather than PEPC. One explanation for their conclusion could be the fact that they only tested activity with ADP, whereas it is a GTP-dependent PEPCK. Furthermore, it is probable that the activity they measured, using MDH as a reporter enzyme, was in fact that of PYK, via non-specific activity of MDH with pyruvate.

From the transcriptomics, it seems that during exponential growth on glucose and xylose, the malate shunt and OAD are expressed the highest (Table S3). However, the annotation of OAD is ambiguous and activity could not be detected in enzyme assays. In *C. thermocellum*, no OAD activity has been detected either, and is said to be absent [219], which is the most likely explanation. Furthermore, *C. thermocellum* also does not contain a PYK and both the malate shunt and PPdK are shown to contribute substantially to pyruvate formation [219]. Much effort has been put into engineering the PPO node in *C. thermocellum*, mostly in order to decrease the transhydrogenase effect of the malate shunt to increase the ethanol yield, which requires NADH [70,219,289,331]. For *C. thermosuccinogenes*, the PPO node will likely also be an important target for improving succinate yield, since FH & FR directly compete with ME for malate.

CDQ83_08825, annotated as an LDH was shown to be responsible for the formation of malate from oxaloacetate, as was already shown for its homolog in *C. thermocellum*, which also utilized both NADH and NADPH, albeit with a 12-fold lower catalytic activity for the latter [289]. In *C. thermocellum*, the then putative MDH gene is located next to the ME gene, which made it the obvious MDH candidate to test. In *C. thermosuccinogenes*, however, the two genes are not adjacent to each other.

The other gene annotated as an LDH (CDQ83_04860) did indeed show LDH activity. However, it also appeared to exhibit significant NADH-dependent MDH activity. The relatively low LDH activity compared to MDH activity could be due to suboptimal assay conditions resulting for example from the *E. coli* cell extract or an inadequate fructose 1,6-bisphosphate concentration, which is typically required for LDH activity. Nevertheless, the heterologous expression of proteins in *E. coli* without further purification, save for an optional heating step, has proven to be a simple and powerful method for the basic characterization of enzymes with a thermophilic origin.

GTP-dependent xylulokinase

Our study provides evidence for a XK that prefers GTP over ATP. Although significant, the difference between the two nucleotides is not as big as for GK, where no ATP-dependent activity was detected at all. For cells grown on glucose, the XK activity is negligible compared to cells grown on xylose, which corresponds to the large difference in expression observed in the transcriptomics results. In only very few studies GTP has been tested as a cofactor for XK, and if any GTP activity is observed, it is much lower than ATP-dependent activity [27,64,72,186,188]. Nevertheless, GTP-dependent XKs could be widespread, similar to GTP-GKs, as it is increasingly apparent that a "typical" glycolysis does not exist [290]. Furthermore, it is possible that other sugar kinases in *C. thermosuccinogenes*, such as fructokinase and galactokinase, are also GTP-dependent, and perhaps other kinases such as acetate kinase as well.

C. thermocellum is not able to grow on xylose, as it lacks the genes for xylose isomerase and XK. By expressing those missing genes from *Thermoanaerobacterium saccharolyticum*, *C. thermocellum* was previously engineered to grow on xylose [9], with the goal to increase its efficiency of ethanol production from hemicellulosic biomass. However, it is not known whether *T. saccharolyticum* XK uses GTP or ATP, which could be of importance. The XK from *C. thermosuccinogenes* might therefore, besides being from a closer relative, also be an interesting candidate to test in *C. thermocellum*, to potentially further improve its ability to grow on xylose.

There is no clear explanation for the reliance of the central energy metabolism on GTP. The fact that the GTP-dependent GK appears throughout a range of distantly related bacteria, e.g. *C. thermocellum* and *Fibrobacter succinogenes* indicates that it is not simply an artefact of evolution, but instead is driven by a certain underlying mechanism. Too few have been characterized to form a meaningful theory, but it could be related to cellulolytic (rumen) bacteria, since *F. succinogenes*, *Ruminococcus albus*, *C. thermocellum* and *C. thermosuccinogenes*, the only organisms known to use an GTP-dependent GK [97,180,331], can all be associated to this group. The underlying mechanism can only be speculated upon. Perhaps GTP enables the existence of an additional energy charge, next to ATP, similar to NADH and NADPH having different oxidation states, enabling them to fulfil different roles in the metabolism. It could also be a primitive regulatory mechanism due to the direct link of GTP with anabolism, via protein synthesis.

Conclusions

We have sequenced and annotated the genomes of four strains of the thermophilic succinate producer *C. thermosuccinoges*, and with this reconstructed its central metabolism. All enzymes for glycolysis and the fermentation pathways to its main products, including succinate, were identified, with the exception of the transaldolase in the PPP. A transcriptomics study for growth on glucose versus xylose did not hint at any transaldolase

candidate genes or alternative pathways. Furthermore, we showed that *C. thermosuccinogenes*, similar to its close relative *C. thermocellum,* uses GTP and PP_i for several of the glycolytic reactions. Xylulokinase, which is not present in *C. thermocellum*, was found to be GTP dependent as well, and could therefore potentially aid in engineering xylose utilization in *C. thermocellum*. The malate dehydrogenase and the lactate dehydrogenase genes were identified via heterologous expression of the two candidate genes in *E. coli*. Unpurified cell-free *E.coli* extracts were used for the assays, which was found to be an efficient way to characterize thermophilic enzymes.

Materials and methods

Anaerobic cultivation

C. thermosuccinogenes DSM 5806, DSM 5807^T, DSM 5808 and DSM 5809 were acquired from DSMZ (Braunschweig, Germany). The strains were routinely cultivated anaerobically in 120 ml serum bottles containing 50 ml bicarbonate buffered liquid medium and a N_2/CO_2 (80%/20%) atmosphere. Cultures were incubated at 60 °C.

-80˚C Glycerol stocks were prepared by adding 2 ml of exponentially growing culture (OD_{600} 0.2 – 0.6) into previously prepared anaerobic vials containing 2 ml of 50% glycerol in phosphate buffered saline (pH 7.3) and 0.5 mg/L resazurin. The vials were reduced with a few drops of titanium citrate (100mM) directly before addition of the culture.

Over-night pre-cultures were typically grown with 2 g/L of substrate (i.e. glucose or xylose), as they were found to have a shorter lag phase upon transfer compared to over-night cultures grown in 5 g/L substrate, presumably because there is less to no acidification.

Medium composition and preparation

C. thermosuccinogenes was grown in adapted CP medium [231], which contained per liter 0.408 g KH_2PO_4, 0.534 g $Na_2HPO_4 \cdot 2\ H_2O$, 0.3 g NH_4Cl, 0.3 g NaCl, 0.1 g $MgCl_2 \cdot 6\ H_2O$, 0.11 $CaCl_2 \cdot 2\ H_2O$, 4.0 g $NaHCO_3$, 0.1 g Na_2SO_4, 1.0 g l-cysteine, 1.0 g yeast extract (BD Bacto), 0.5 mg resazurin, 1 ml vitamin solution, 1 ml trace elements solution I, and 1 ml trace elements solution II. The medium was autoclaved in serum bottles under 80/20 N_2/CO_2 atmosphere with ~0.7 bar overpressure, containing a final volume of 50 ml medium. A solution containing the $NaHCO_3$ and l-cysteine was autoclaved separately and added later as well as a solution containing the $CaCl_2 \cdot 2\ H_2O$ to which the vitamin solution was added after it was autoclaved. The substrate (glucose or xylose) was also autoclaved separately and added later to a final concentration of 2 g/l or 5 g/l.

The vitamin solution, which was 1000x concentrated, contained per liter 20 mg biotin, 20 mg folic acid, 100 mg pyridoxine-HCl, 50 mg thiamine-HCl, 50 mg riboflavin, 50 mg nicotinic acid, 50 mg Ca-d-pantothenate, 1 mg vitamin B12, 50 mg 4-aminobenzoid acid, 50 mg lipoic acid.

Trace elements solution I, which was 1000x concentrated, contained per liter 50 mM HCl, 61.8 mg H_3BO_4, 99.0 mg $MnCl_2 \cdot 4\ H_2O$, 1.49 g $FeCl_2 \cdot 4\ H_2O$, 119 mg $CoCl_2 \cdot 6\ H_2O$, 23.8 mg $NiCl_2 \cdot 6\ H_2O$, 68.2 mg $ZnCl_2$, 17.0 mg $CuCl_2 \cdot 2\ H_2O$.

Trace elements solution II, which was 1000x concentrated, contained per liter 10 mM NaOH, 17.3 mg Na_2SeO_3, 33.0 mg $Na_2WO_4 \cdot 2\ H_2O$, 24.2 mg $Na_2MoO_4 \cdot 2\ H_2O$.

Genome sequencing and annotation

10 – 20 ml of exponentially growing cells were harvested for DNA extraction, using the Gram Positive DNA Purification Kit (Epicentre, Madison, Wisconsin) for the extraction according to the manufacturer's instructions.

Library preparation and sequencing was carried out by BaseClear (Leiden, The Netherlands) both for Illumina and PacBio. Illumina sequencing was done with HiSeq2500 system, using paired-end chemistry and run lengths of 125 base pairs. FASTQ sequence files were generated using the Illumina Casava pipeline version 1.8.3. Initial quality assessment was based on data passing the Illumina Chastity filtering. Subsequently, reads containing adapters and/or PhiX control signal were removed using an in-house filtering protocol. The second quality assessment was based on the remaining reads using the FASTQC quality control tool version 0.10.0 [8]. This resulted in 4,159,110; 5,143,445; 4,483,080 and 3,992,113 reads for DSM 5806, DSM 5807, DSM 5808 and DSM 5809, respectively. The data collected from the PacBio RS instrument were processed and filtered using the SMRT Analysis software suite. The Continuous Long Read data were filtered by Read-length (>35), Subread-length (>35) and Read quality (>0.75). This resulted in 216,616 and 91,998 reads for DSM 5807, and DSM 5809, respectively, with average read lengths of 3,577 and 5,794, and maximum read lengths of 41,645 and 36,236.

Illumina sequence data from the four strains were assembled using SPAdes genome assembler [17]. For DSM 5807 and DSM 5809, the additional sequence data from PacBio sequencing were used in combination with the Illumina data for a hybrid assembly. The hybrid assembly was carried out by BaseClear (Leiden, The Netherlands), using ABySS assembler version 1.5.1, SSPACE-LongRead scaffolder version 1.0 [35], and GapFiller version 1.10 [34].

The final assemblies of the four strains, i.e. SPAdes assemblies for DSM 5806 and DSM 5808, and hybrid assemblies for DSM 5807 and DSM 5809 have been have been submitted to the NCBI database and were annotated by their in house annotation pipeline [293]. Accession numbers are NIOJ00000000, CP021850, NIOK00000000, NIOI00000000 for DSM 5806, DSM 5807, DSM 5808, and DSM 5809, respectively. Additionally, the different assemblies have also been annotated with RAST and with Prokka, aiding the manual reconstruction of the central metabolism [15,265].

In silico DNA-DNA hybridization

The Genome-to-Genome Distance Calculator (GGDC) version 2.1 from the DSMZ website was used to calculate the DNA-DNA hybridization of the four *C. thermosuccinogenes* strains [14]. For all four strains the SPAdes assembly of Illumina HiSeq sequence data was used as input. The results of formula 2 were used, as is recommended, but results from formula 1 and formula 3 led to an identical conclusion.

OrthoMCL analysis

The OrthoMCL algorithm was used to identify orthologous proteins in the four *C. thermosuccinogenes* genomes, using the default settings [167]. Protein FASTA files were used, derived from the genomes that were annotated by the NCBI pipeline, meaning that for DSM 5806 and DSM 5808 these were based the SPAdes assemblies, whereas these were based on the hybrid assembly for DSM 5807^T and DSM 5809. The output of the program was used to compile a list with unique genes, i.e. a list of genes that didn't appear in any of the orthologous (and paralogous) groups, including all the RNA genes, as these are not part of the OrthMCL analysis. Additionally, lists were made with orthologous groups that were present in all but one of the strains. The output of the OrthoMCL analysis found in Table S1.

Construction of phylogenetic tree

For construction of the phylogenetic tree, 16S-RNA sequences were aligned using ClustalW with the standard settings in MEGA6 [291]. Aligned sequences were trimmed to a length of 1324 base pairs, and were used for the construction of a phylogenetic tree using the Neighbor joining methods, in MEGA6. A bootstrap test with 1000 replicates was performed.

Transcriptomics

10 ml of exponentially growing cells at OD600 ~0.3 were harvested for RNA extraction by centrifugation at 4°C, 4800 x *g* for 15 minutes. Pellet was suspended in 0.5 ml ice cold TE buffer (pH 8.0). Samples were divided into two 2 ml screw capped tubes containing 0.5 g zirconium beads, 30 µL 10% SDS, 30 µL 3 M sodium acetate (pH 5.2), 500 µL in water saturated phenol, chloroform and isoamyl alcohol at a ratio of 25:24:1 (pH 4,5-5), Roti®-Aqua-P/C/I (Carl Roth, Karlsruhe, Germany). Cells were disrupted in a Precellys 24 tissue homogenizer (Bertin Instruments, Montigny-le-Bretonneux, France) at speed 6 for 40s. After centrifugation for 5 minutes at 9300 x *g* and 4 °C, the water phase (top) was transferred to a new tube containing 400 µL chloroform. After centrifugation for 3 minutes at max speed, the water phase was again transferred to a new tube and mixed with the lysis buffer from the High Pure RNA Isolation Kit from Roche. From there on the protocol of the kit was followed. The integrity of the RNA was checked using Experion RNA StdSens Chips from BioRad.

Library preparation and sequencing was performed by BaseClear (Leiden, The Netherlands), using Illumina HiSeq platform, yielding 50-bp single reads. The samples from cells growing

on glucose and xylose resulted in 25 and 67 million reads, respectively. Transcript reads were aligned on the coding sequences from the RAST annotation using the Burrows-Wheeler Aligner (BWA, version 0.7.12-r1039). From this, the reads per kilobase per million mapped reads (RPKM) were calculated for every coding sequence.

Preparation of cell-free extract of *C. thermosuccinogenes*

Cell-free extracts were made using 150 ml (3 x 50 mL) of exponentially growing cultures at OD600 0.3 – 0.4, according to a protocol adapted from Zhou *et al*. [331]. Cells were harvested by centrifugation at 4°C, 4800 x *g* for 10 minutes, and washed twice with 50 mM Tris-HCl buffer (pH 8.0) containing 5 mM freshly added dithioerythritol (DTT). Cells were finally suspended in 5 ml of either the wash buffer, or 50 mM potassium phosphate buffer (pH 7.0) containing 5 mM DTT. Cell suspensions were homogenized in a French press at ~1.2 bar. Lysate was centrifuged for 10 minutes at max speed in a micro centrifuge tubes, and supernatant was used as the cell-free extract. For the oxaloacetate decarboxylase assay, crude extract that was not centrifuged was also used, to test if any activity was present in the solid fraction. The total protein concentration in the cell-free extracts was determined using the Bradford assay, with bovine serum albumin as a standard. Protein concentrations were in all cases above 1 mg/ml. All steps were done aerobically.

Heterologous expression of malate dehydrogenase candidates in *E. coli*

The two malate dehydrogenase gene candidates from *C. thermosuccinogenes* investigated in this study were heterologously overexpressed in *E. coli*. CDQ83_08825 was amplified via PCR using the forward primer TACTTCCAATCCAATGCAGTAAAATCCAAATCAAAAGTTGCAATAATC and the reverse primer TTATCCACTTCCAATGTTATATATCCTTCACCTGATCGATTATAGCCTTTAC. CDQ83_04860 was amplified via PCR using the forward primer TACTTCCAATCCAATGCAATGCATGAAATTACACCAAAAAAGATC and the reverse primer TTATCCACTTCCAATGCTACAATTTAAGTTTGCCGGC. Via ligase independent cloning, the cloned enzymes were inserted in a pET-28b(+) (Novagen, Madison, Wisconsin) derived backbone that was generated using the primers ATTGGATTGGAAGTACAGGTTTTCATGGTGATGGTGATGGTGAGAAGAACCCATGGTATATCTCC TTCTTAAAG and ATTGGAAGTGGATAACGGATCCGAATTCGAGCGCCGTCGACAAGCTTGCGG. The ligase independent cloning protocol is described elsewhere, and takes advantage of the exonuclease activity of T4 polymerase to create compatible ends [11]. In the final construct, the enzyme has a N-terminal His-tag with a TEV protease site in between. Constructs containing CDQ83_08825 and CDQ83_04860 were transformed to *E. coli* DH5α and subsequently verified via sequencing.

CDQ83_08825 and CDQ83_04860 were heterologously overexpressed in *E. coli* Rosetta™ (Novagen), which is an *E. coli* BL21 derivative containing a plasmid encoding tRNAs of rare codons and a chloramphenicol resistance marker. Cells carrying the expression plasmids

were grown in LB containing 50 µg/ml kanamycin and 20 µg/ml chloramphenicol to OD_{600} 0.6-0.8 and, subsequently, placed on ice for 20 min. 50 ml culture was used for making *E. coli* cell-free extracts. Heterologous gene expression was then induced by addition of 0.2 mM IPTG and growing the cultures for an additional 3-4 hrs at 37 °C. From here, cell-free extract of *E. coli* was prepared identical to *C. thermosuccinogenes* cell-free extract, except for that no DTT was used in the buffers. Additionally, the *E. coli* cell extract was also subjected to a heating step of 30 minutes at 60 °C, followed by a centrifugation step to remove precipitated proteins. This heating step was included to decrease the background activity of the *E. coli* extract, although the assays were found to work very well even without this last step.

Enzyme assays

Activities in all assays were determined either directly or indirectly via one or more auxiliary enzymes by measuring the change in absorbance at 340 nm, which corresponds to $NAD(P)^+$ reduction or NAD(P)H oxidation. A Shimadzu U-2010 spectrophotometer in combination with a thermoelectric cell holder was used for the measurements, performed at 55 °C. Crystal cuvettes were used with 1.0 cm path length containing 1 ml of reaction mixture. Activities are expressed in µmol of product per minute per mg of cell-free extract protein. Enzymes and biochemicals were obtained from Sigma. Tris-HCl buffer used was set at pH 8.0 at room temperature, which corresponds to ~pH 7.0 at 55°C. All enzyme assays contained 50 mM Tris-HCl. 10 – 60 µL cell-free extract was used in the assays, and in all cases at least three different concentrations were tested to verify that the extract was the limiting factor in the assay. Water was added to a final volume of 1 ml. In the case of glucokinase and phosphofructokinase, a significant background activity was present without the addition of phosphoryl donor, which was subtracted from the final values.

The glucokinase (EC 2.7.1.2) assay was adapted from Zhou *et al*. [331], and contained 5 mM $MgCl_2$, 60 mM KCl, 2 mM glucose, 0.15 mM $NADP^+$, and 2 U/ml glucose-6-phosphate dehydrogenase. 2 mM ATP, GTP or PP_i was added to start the reaction.

The xylulokinase (EC 2.7.1.17) assay was adapted from Dills *et al*. [72], and contained 5 mM $MgCl_2$, 2 mM xylulose, 2 mM phosphoenolpyruvate, 0.15 mM NADH, 4 U/ml pyruvate kinase, and 4 U/ml lactate dehydrogenase. 2 mM ATP, GTP or PP_i was added to start the reaction.

The phosphofructokinase (EC 2.7.1.11/EC 2.7.1.90) assay was adapted from Zhou *et al*. [331], and contained 5 mM $MgCl_2$, 1 mM fructose-6-phosphate, 0.15 mM NADH, 4 U/ml aldolase, 4 U/ml triosephosphate isomerase, and 4 U/ml α-Glycerophosphate dehydrogenase. 2 mM ATP, GTP or PP_i was added to start the reaction.

The phosphoglycerate kinase (EC 2.7.2.3) assay was adapted from Zhou *et al*. [331], and contained 5 mM $MgCl_2$, 2 mM EDTA, 2 mM 3-phosphoglycerate, 0.15 mM NADH, and 2 U/ml glyceraldehyde-3-phosphate dehydrogenase. 2 mM ATP, GTP or PP_i was added to start the reaction.

The malic enzyme (EC 1.1.1.40) assay was adapted from Zhou *et al*. [331], and contained 5 mM $MgCl_2$, 5 mM NH_4Cl, 5 mM dithiothreitol, and 0.15 mM $NADP^+$. 2 mM malic acid was added to start the reaction.

The malate dehydrogenase (EC 1.1.1.37) assay was adapted from Taillefer *et al*. [289], and contained 0.3 mM NADH. 10 mM oxaloacetate was added to start the reaction.

The lactate dehydrogenase (EC 1.1.1.27) assay was adapted from Taillefer *et al*. [289], and contained 0.005 mM fructose 1,6-bisphosphate and 0.15 mM NADH. 10 mM pyruvate was added to start the reaction.

The oxaloacetate decarboxylase (EC 4.1.1.3) assay was adapted from Olson *et al.* [219], and contained 0 – 2 mM $MgCl_2$, 0 – 2 mM NaCl and 1 – 1.6 mM oxaloacetic acid. The (crude) cell extract was added to start the reaction, after the rate of spontaneous oxaloacetic acid degradation was determined. The reaction was monitored at 265 nm, which is the absorbance peak for oxaloacetic acid.

Acknowledgements

This research received funding from the European Union Marie Skłodowska-Curie Innovative Training Networks (ITN) contract number 642068.

We thank Bastienne Vriesendorp for her help with the bioinformatics analyses.

Supplementary data

Supplementary data for this chapter can be found at: https://doi.org/10.1128/AEM.00363-18.

Chapter 3 - Assessing cofactor usage in *Pseudoclostridium thermosuccinogenes* via heterologous expression of central metabolic enzymes

Jeroen G. Koendjbiharie[1], Kimberly Wevers[2], Richard van Kranenburg[1,2]

[1] Corbion, Gorinchem, Netherlands
[2] Laboratory of Microbiology, Wageningen University & Research, Netherlands

Chapter has been published as:

J.G. Koendjbiharie, K. Wevers, R. van Kranenburg, Assessing Cofactor usage in *Pseudoclostridium thermosuccinogenes* via Heterologous Expression of Central Metabolic Enzymes, Front. Microbiol. 10 (2019) 1162.

Abstract

Pseudoclostridium thermosuccinogenes and *Hungateiclostridium thermocellum* are being studied for their potential to contribute to a more sustainable bio-based economy. Both species were shown previously to rely on GTP or pyrophosphate instead of ATP as cofactors in specific reactions of central energy metabolism for reasons that are not well understood yet. Since it is often impossible to predict cofactor specificity from the primary protein structure, thirteen enzymes from *P. thermosuccinogenes* were cloned and heterologous expressed in *Escherichia coli* to assess the cofactor usage *in vitro* and paint a more complete picture of the cofactor usage in the central metabolism of *P. thermosuccinogenes*. The assays were conducted with heat-treated *E. coli* cell-free extract devoid of background activity to allow the quick assessment of a relatively large number of (thermophilic) enzymes. Selected enzymes were also purified to allow the determination of the enzyme kinetics for competing cofactors. Following the results of the glucokinase, galactokinase, xylulokinase, and ribokinase assays, it seems that phosphorylation of monosaccharides by and large is mainly GTP-dependent. Some possible implications of this relating to the adenylate/guanylate energy charge are discussed here. Besides the highly expressed pyrophosphate-dependent 6-phosphofructokinase, another 6-phosphofructokinase was found to be equally dependent on ATP and GTP, while no 6-phosphofructokinase activity could be demonstrated for a third. Both type I glyceraldehyde 3-phosphate dehydrogenases were found to be NAD^+-dependent, and further, acetate kinase, isocitrate dehydrogenase, and three enzymes predicted to be responsible for the interconversion of phosphoenolpyruvate and pyruvate (i.e. pyruvate kinase; pyruvate, phosphate dikinase; phosphoenolpyruvate synthase), were also assessed.

Introduction

Pseudoclostridium thermosuccinogenes and *Hungateiclostridium thermocellum*, thermophilic bacteria belonging to the *Hungateiclostridiaceae* have been shown to rely on GTP and pyrophosphate (PP_i), as well as the "typical" ATP in their central metabolism [143,331]. Both are being studied for their potential to contribute to the transition towards a more sustainable bio-based economy. *H. thermocellum* for its unrivalled capability to degrade cellulosic biomass [144], and *P. thermosuccinogenes* because it is the only known thermophile to produce succinic acid, a precursor for bioplastics, as one of the main products of fermentation [74,143,279]. The use of thermophiles in industry has the advantage that less energy is required for cooling the large reactors they are grown in, and that simultaneous saccharification and fermentation is possible when the optimal temperature of the commercial fungal cellulases overlaps with the growth temperature of the fermenting microorganism [218,223]. Nevertheless, for either organism to be used successfully in any industrial process, it is crucial to have an in-depth understanding of their physiology. In particular the characteristics of their complex central energy metabolism

should be unravelled, as significant metabolic engineering will be required to improve production yields, rates, and titres [213].

One aspect that is still not well understood is why PP_i and GTP are used in addition to ATP as phosphoryl carriers in the central metabolism, rather than just ATP. PP_i is used for the conversion of fructose 6-phosphate to fructose 1,6-bisphosphate by 6-phosphofructokinase (6-PFK) and for the conversion of phosphoenolpyruvate (PEP) to pyruvate by pyruvate, phosphate dikinase (PPdK). By utilizing PP_i, a "waste" product of many anabolic reactions that would otherwise simply be hydrolysed, ATP-equivalents are being conserved [193]. Analogous to that, using PP_i allows PPdK to form ATP from AMP, instead of ADP as is done by pyruvate kinase (PK). However, it was already calculated that PP_i formation from anabolism by no means accounts for the total PP_i requirement for 6-PFK alone, suggesting that an additional PP_i production mechanism exists [331]. Possible mechanisms include a proton pumping pyrophosphatase, or a cycle involving the simultaneous formation and degradation of glycogen. In such a cycle, glucose 1-phosphate and ATP are converted to ADP-glucose and PP_i. ADP-glucose is used to generate glycogen, releasing the ADP, after which glucose 1-phosphate is regenerated from glycogen combined with orthophosphate, leading to the net formation of ADP and PP_i from ATP and orthophosphate. Much more unclear even is the use of GTP as alternative to ATP. Both *P. thermosuccinogenes* and *H. thermocellum* have a GTP-dependent glucokinase (GK) and PEP carboxykinase (PEPCK), and *P. thermosuccinogenes* also has a GTP-dependent xylulokinase (XK) [143,331]. It was speculated to represent a "simple" regulatory mechanism, via the direct link to protein synthesis, or that a guanylate energy charge could exist that is different from the adenylate energy charge, allowing GTP and ATP to fulfil different roles in the metabolism, analogous to NADH and NADPH having different oxidation states in the cell [143]. The adenylate energy charge is defined as ([ATP] + ½ [ADP]) / ([ATP] + [ADP] + [AMP]) [12].

Furthermore, the finding that GK and XK in these organisms rely on GTP instead of ATP also highlights the fact that it is very often impossible to confer cofactor usage from the amino acid sequence alone. Either because too few (closely related) enzymes of the kind have been experimentally characterized (for cofactor usage) to find a certain consensus sequence or a correlation to phylogenetic groups, or because it is simply not possible to deduce it from the sequence. For this reason it is valuable to conduct basic characterization of metabolic enzymes, in particular from non-model organisms, in order to learn more about cofactor usage.

In this study we cloned and expressed thirteen genes of the central metabolism of *P. thermosuccinogenes* into *Escherichia coli*. Cell-free extracts (CFE) of *E. coli* expressing these enzymes were then used to assess the enzymes' activities and cofactor specificities. Selected enzymes were purified to assess the kinetics in more detail. Furthermore, hypotheses for the use of GTP and PP_i next to ATP are formulated.

Material and methods

Cloning of *P. thermosuccinogenes* genes in *E. coli*.

The primers used to clone the thirteen *P. thermosuccinogenes* genes that were characterized in this study are listed in table 1. The genes were cloned into a pET-28b(+) (Novagen, Madison, Wisconsin) derived backbone, generated using primers ATTGGATTGGAAGTACAGGTTTTCATGGTGATGGTGATGGTGAGAAGAACCCATGGTATATCTCC TTCTTAAAG and ATTGGAAGTGGATAACGGATCCGAATTCGAGCGCCGTCGACAAGCTTGCGG, as described previously [143]. In the final constructs, the cloned enzymes have an N-terminal His_6-tag flanking a TEV protease site. The constructs were initially transformed to *E. coli* DH5α. After verification via pyrosequencing (Macrogen), the plasmids were transformed to *E. coli* Rosetta (Novagen), an *E. coli* BL21 derivative containing the pRARE plasmid encoding tRNAs of rare codons in *E. coli* and a chloramphenicol resistance marker.

Table 1: Primers used to clone the selected *P. thermosuccinogenes* genes into pET-28b(+).

Locus tag	Primers
CDQ83_02810	TACTTCCAATCCAATGCAGATATTAATCAATTAAAGCAAAAATTCATT
	TTATCCACTTCCAATGTTACTTAATCTCCCTGCCT
CDQ83_03295	TACTTCCAATCCAATGCAATGGAGGGTCAAGTAAAAATAC
	TTATCCACTTCCAATGCTATCCTTCAAGCCCC
CDQ83_03625	TACTTCCAATCCAATGCAGAAATTTACGAAAAGGTTAGC
	TTATCCACTTCCAATGCTATTTACATATGAGCTTTTGG
CDQ83_04880	TACTTCCAATCCAATGCAAGTACGAAAGTTGGAATTAAC
	TTATCCACTTCCAATGTCATATGCTTGAAGATACATATG
CDQ83_07070	TACTTCCAATCCAATGCAGTAAAGGTTGGAGTGGC
	TTATCCACTTCCAATGTTACTTCCATTTTCCCATCC
CDQ83_07225	TACTTCCAATCCAATGCACCTGATATAAGAACTATAGGAGTC
	TTATCCACTTCCAATGTTATAAGGCCAGTATCCTG
CDQ83_07295	TACTTCCAATCCAATGCAAAAGTTTTGGTTATCAATGC
	TTATCCACTTCCAATGTTATTTGCTCAATATAGCCACT
CDQ83_07455	TACTTCCAATCCAATGCAACAAAGTATGTTTATCTTTTTAGTGAAG
	TTATCCACTTCCAATGTTATTTATTTTTAATGGCAGCTTGAG
CDQ83_08625	TACTTCCAATCCAATGCAGAAAAAATCAAAATGCGAGTTC
	TTATCCACTTCCAATGTCAAAGGGTTTGCTCC
CDQ83_09600	TACTTCCAATCCAATGCAAGAAAAACAAAAATAATCTGTACAT
	TTATCCACTTCCAATGTTAGTTCTCAGCGTCTG
CDQ83_10590	TACTTCCAATCCAATGCAGCAGTAAAGATAGGTATTAATGG
	TTATCCACTTCCAATGTTATTTAGCGTCAACTTCAG
CDQ83_10650	TACTTCCAATCCAATGCAAAGAAACGTATTGGAGTGTT
	TTATCCACTTCCAATGTTAATCCCCAAAACTTACCC
CDQ83_11320	TACTTCCAATCCAATGCAGCTGAATTAAAAGGCGC
	TTATCCACTTCCAATGTTATTTAGTTGCCAATACTTTCTTAAG

Preparation of cell-free extracts (CFE).

Rosetta strains carrying the expression plasmids, including an empty vector control, were grown overnight in 5 ml LB containing 50 µg/ml kanamycin and 20 µg/ml chloramphenicol at 37 °C. The next day, overnight cultures were added to 50 ml pre-warmed LB with antibiotics, and grown to an OD_{600} of 0.6 to 0.8 at 37 °C, after which they were placed on ice for 20 min. Heterologous gene expression was then induced by the addition of 0.2 mM IPTG (isopropyl-β-D-thiogalactopyranoside). Following an additional incubation step of 3 to 4 h at 37 °C, cells were harvested via centrifugation at 4,800 × g for 10 min. at 4 °C, and were washed twice with cold 50 mM MOPS buffer (pH 7.0 at room temperature). Cells were resuspended in 5 ml MOPS buffer containing cOmplete™, mini, EDTA-free protease inhibitor cocktail, and 1 tablet per ~ 10 mL (Roche). Cells were lysed using a French press at ~120 kPa. Lysate was centrifuged at 20.000 × g for 10 min. at 4 °C. The supernatant (*i.e.* the non-heated CFE) was split in two fractions, of which one was incubated at 60 °C for 30 min. Precipitated proteins were removed by another centrifugation step, leaving the heat-treated CFE. The Bradford assay was used to measure the total protein concentration in the heated and non-heated extracts, which were also run on a SDS-PAGE gel to verify that heterologous expression was successful. Pictures of the gels can be found in the supplementary material (Supplementary Figures 1-3).

Enzyme purification

For affinity chromatography of selected enzymes, lysates were generated in identical fashion as for the CFEs, except that larger cultures were used (0.5 l LB for ribokinase and galactokinase, and 2 l for ATP/GTP-dependent phosphofructokinase), and that the wash/resuspension buffer contained 50 MOPS buffer (pH 7.4 at room temperature) with 20 mM imidazole. A HisTrap™ HP column (GE Healthcare; optimal at pH 7.4) with an ÄKTA pure FPLC system were used for the purification. Elution was done over a gradient with the same buffer containing 500 mM imidazole. The buffer of the eluted protein was then exchanged with 50 mM MOPS (pH 7.0 at room temperature) using an Amicon® ultra centrifugal filter (Merck) with a nominal molecular weight limit of 10.000 Da. SDS-PAGE was used to verify purity.

Enzyme assays.

The enzyme assays in this study are all based on the measurement of NAD(P)H at 340 nm (ε = 6.2 $mM^{-1}cm^{-1}$), which is produced or consumed either directly by the investigated enzyme, or via the coupling to one or more auxiliary enzymes. A Shimadzu U-2010 spectrophotometer in combination with a thermoelectric cell holder was used for the measurements, which were performed at 55 °C. Quartz cuvettes containing 1 ml of the reaction mixture were used with a 1.0-cm path length. Activities are expressed in micromoles of product per minute per mg of CFE protein. The enzymes and biochemicals were obtained from Sigma. 5 to 100 µl CFE was used, that in some cases had to be diluted

first. At least three different concentrations of CFE were used for each assay, to verify that the enzymes in the extract were the limiting factor, and not the auxiliary enzymes.

The ribokinase (EC 2.7.1.15) assay was based on the xylulokinase assay described elsewhere [72,143] and contained 50 mM MOPS (pH 7.0 at room temperature), 10 mM $MgCl_2$, 100 mM KCl, 5 mM D-ribose, 2 mM ATP or GTP, 0.15 mM NADH, 2 mM phosphoenolpyruvate, 4 U/ml pyruvate kinase (rabbit), 4 U/ml lactate dehydrogenase (rabbit). Ribose was added to start the reaction. Since the stock solutions of ATP and in particular GTP contain ADP/GDP impurities, ribose was added only after the OD_{340} had stabilized. The galactokinase (EC 2.7.1.6) and acetate kinase (EC 2.7.2.1) were conducted identically to the ribokinase assay, except that 5 mM D-galactose and 5 mM potassium acetate, respectively, were used instead of D-ribose. Figure 1A shows a graphical scheme of the coupled reactions in the three assays. In the kinetics assays with purified enzymes, ATP or GTP were added at varied concentrations. The Michaelis-Menten equation was fitted to the data by minimizing the sum of the squares of the vertical differences, in order to find K_M and k_{cat}. The data and the fitted model can be found in the supplementary material.

The 6-phosphofructokinase (EC 2.7.1.11; EC 2.7.1.90) assay was adapted from Zhou at al. [331] and contained 50 mM MOPS (pH 7.0 at room temperature), 5 mM $MgCl_2$, 1 mM fructose 6-phosphate, 2 mM ATP, GTP, or pyrophosphate, 0.15 mM NADH, 4 U/ml aldolase (rabbit), 4 U/ml triosephosphate isomerase (rabbit), and 4 U/ml glycerol-3-phosphate dehydrogenase (rabbit). Fructose 6-phosphate was added to start the reaction. Figure 1B shows a graphical scheme of the coupled assays. Since two equivalents of NADH are oxidized per equivalent of fructose 6-phosphate that is phosphorylated, the final rates were adjusted for this. In the kinetics assays with purified enzymes, ATP or GTP were added to start the reaction, at varied concentrations. The Michaelis-Menten equation was fitted to the data by minimizing the sum of the squares of the vertical differences, in order to find K_M and k_{cat}. The data and the fitted model can be found in the supplementary material.

The pyruvate kinase (EC 2.7.1.40) assay was adapted from Zhou et al., 2013 and contained 50 mM MOPS (pH 7.0 at room temperature), 10 mM $MgCl_2$, 100 mM KCl, 2 mM phosphoenolpyruvate, 2 mM ADP, or GDP, 0.15 mM NADH, and 4 U/ml lactate dehydrogenase (rabbit). Phosphoenolpyruvate was added to start the reaction.

The pyruvate, phosphate dikinase (EC 2.7.9.1) assay was adapted from Reeves, 1968 and contained 50 mM MOPS (pH 7.0 at room temperature), 5 mM $MgCl_2$, 10 mM KCl, 20 mM NH_4Cl, 2 mM phosphoenolpyruvate, 2 mM AMP, or GMP, 2 mM pyrophosphate, 0.15 mM NADH, and 4 U/ml lactate dehydrogenase (rabbit). Phosphoenolpyruvate was added to start the reaction.

The phosphoenolpyruvate synthase (EC 2.7.9.2) assay was adapted from Imanaka et al., 2006 and contained 50 mM MOPS (pH 7.0 at room temperature), 5 mM $MgCl_2$, 10 mM KCl, 20 mM NH_4Cl, 2 mM phosphoenolpyruvate, 2 mM AMP, or GMP, 5 mM K_2HPO_4, 0.15 mM NADH, and 4 U/ml lactate dehydrogenase (rabbit). Phosphoenolpyruvate was added to start the reaction.

The glyceraldehyde 3-phosphate dehydrogenase (EC 1.2.1.12) was adapted from Byers, 1982 and contained 50 mM Tris (pH 8.5 at 60 °C), 5 mM $MgCl_2$, 4 mM dihydroxyacetone phosphate, 0.15 mM NAD^+, or $NADP^+$, 5 mM sodium arsenate, and 4 U/ml triosephosphate isomerase (rabbit). Dihydroxyacetone phosphate was added to start the reaction. For our convenience, dihydroxyacetone phosphate and triosephosphate isomerase were used instead of glyceraldehyde 3-phosphate directly. For glyceraldehyde 3-phosphate dehydrogenase assays sodium arsenate is typically used instead of orthophosphate, as the incorporated arsenate is spontaneously hydrolyzed, driving the reaction forward. The elevated pH of 8.5 is also crucial to shift the thermodynamic equilibrium towards 1,3-bisphosphoglycerate-forming direction.

The isocitrate dehydrogenase (EC 1.1.1.42) assay was adapted from Plaut, 1962 and contained 50 mM MOPS (pH 7.0 at room temperature), 5 mM $MgCl_2$, 100 mM NaCl, 0.75 mM NAD^+, or $NADP^+$, and 5 mM isocitrate, which was added to start the reaction.

To test ribokinase and galactokinase activity with pyrophosphate, Malachite Green Phosphate Assay Kit (Sigma) was used to detect to formation of orthophosphate by purified enzymes. The reaction contained 50 mM MOPS (pH 7.0 at room temperature), 1 mM $MgCl_2$, 50 mM KCl, 5 mM D-ribose/galactose, and 2 mM pyrophosphate. Reaction was conducted at 55 °C. Samples were taken every two minutes, and placed on ice until analysis.

Results

Thirteen genes from *P. thermosuccinogenes* involved in the central carbon metabolism were heterologously expressed in *E. coli* in order to investigate the cofactor usage. Most of those were involved in phosphoryl transfer (table 2 and table 3). The three 6-PFK orthologs were tested for ATP, GTP, and PP_i. Ribokinase (RK), galactokinase (GalK) and acetate kinase (AK) were only tested for ATP and GTP, since their assays relied on the coupling with auxiliary pyruvate kinase and lactate dehydrogenase using PEP, to detect NDP formation, which would not work in the case PP_i was used. The assays were carried out using the CFEs from *E. coli*, without any additional purification (e.g. affinity chromatography), except for an *E. coli* protein-denaturing heating step. We previously showed that this method was a quick and simple method for basic characterization of enzymes [143]. For all assays, CFE with an empty vector was used as a control, and in all cases no significant background activity was present.

RK, responsible for the phosphorylation of d-ribose to d-ribose 5-phosphate, and GalK, responsible for the phosphorylation of α-d-galactose to α-d-galactose 1-phosphate represent the entry points for both of these sugars into the metabolism. Phosphorylation prevents them from leaking out of the cell again, due to the increased hydrophilicity [19]. The RK has a modest 50% increased activity with GTP compared to ATP, which is on par with what was observed previously with the XK from *P. thermosuccinogenes*, another C_5-sugar kinase [143]. The difference is significantly higher for GalK, which has over six-fold the activity with GTP. For GK, another C_6-sugar kinase, the difference was shown to be even bigger in *P. thermosuccinogenes*, since it could not use ATP at all.

Table 2: Enzyme assays with *E. coli* cell-free extract containing several heterologously expressed enzymes from *P. thermosuccinogenes*, to determine the cofactors involved in phosphoryl transfer (ATP, GTP, or PP_i). Reaction velocities are given in µmol/mg cell-free extract protein/min ± standard deviation.

Assay	Locus tag	Activity		
		ATP	GTP	PP_i
Ribokinase	CDQ83_03295	36 ± 3	54 ± 2	-
Galactokinase	CDQ83_02810	5.1 ± 0.5	33 ± 1	-
Acetate Kinase**	CDQ83_07295	71 ± 7	10 ± 0	-
6-Phosphofructokinase	CDQ83_07225	13 ± 1	13 ± 5	ND*
	CDQ83_10650	ND	ND	ND
	CDQ83_11320	ND	ND	220 ± 26

* Not detected: value close to zero and not significantly different from empty vector control.
** Non-heated extracts were used, due to the apparent low thermo-stability of the acetate kinase from *P. thermosuccinogenes*.

Table 3: Enzyme assays with *E. coli* cell-free extract containing heterologously expressed enzymes from *P. thermosuccinogenes* involved in the direct conversion of phosphoenolpyruvate to pyruvate, i.e. pyruvate kinase; pyruvate, phosphate dikinase; and phosphoenolpyruvate synthase. Their cofactor usage for those three reactions were assayed. Reaction velocities are given in µmol/mg cell extract protein/min ± standard deviation.

Locus tag	Annotation	Pyruvate kinase activity		PPdK activity		PEP synthase activity	
		ADP	GDP	AMP	GMP	AMP	GMP
CDQ83_03625	pyruvate kinase	ND*	ND	ND	ND	ND	ND
CDQ83_07455	pyruvate, phosphate dikinase	ND	ND	11 ± 1	ND	ND	ND
CDQ83_09600	pyruvate kinase	52 ± 1	34 ± 1	ND	ND	ND	ND

* Not detected: value close to zero and not significantly different from empty vector control.

Following these results, RK and GalK were purified via affinity chromatography, in order to determine the kinetics for ATP and GTP, as that could still vary significantly – and possibly rule out a physiologically function of either ATP or GTP for those two enzymes. Result of the assays to determine the kinetics are shown in table 4. The affinity constants (K_M) of RK for both ATP and GTP were found to be comparably low (i.e. high affinity); 0.028 mM and 0.154 mM, respectively. The turnover number (k_{cat}) was found to be 85% higher for GTP, compared to ATP, corresponding to what was found in the assays with the non-purified enzyme. GalK has a much higher affinity for GTP compared to ATP, with K_M values of 3.98 mM and 0.035 mM for ATP and GTP, respectively. Furthermore, k_{cat} was found to be roughly 2.5 times higher for GTP. Intracellular concentrations of ATP and GTP are not known for *P. thermosuccinogenes*. However, in exponentially growing *E. coli*, yeast, and mammalian cells, ATP concentrations were found to be quite well conserved in the range of 2 – 10 mM. For GTP, it is in the range of 1.6 – 15 mM in *E. coli*, and 0.2 – 0.7 mM for yeast, and mammalian cells [225]. Considering this, it is reasonable to assume that for RK *in vivo*, both ATP and GTP are saturated, with GTP being the moderately preferred substrate – but with both ATP and GTP-dependent activity occurring. For GalK *in vivo*, GTP is certainly saturated, whereas ATP is likely not. Adding to that the big difference in turnover number, it seems that GTP is the physiological relevant cofactor.

Table 4: Affinity constants (K_M) in mM and turnover numbers (k_{cat}) in U/µmol of ribokinase, galactokinase, and the ATP/GTP-dependent 6-phosphofructokinase for ATP and GTP.

Enzyme	Locus tag	ATP		GTP	
		k_{cat}	K_M	k_{cat}	K_M
ribokinase	CDQ83_03295	$8.11 \cdot 10^3$	0.028	$14.4 \cdot 10^3$	0.154
galactokinase	CDQ83_02810	$1.07 \cdot 10^3$	3.98	$2.56 \cdot 10^3$	0.035
6-phosphofructokinase	CDQ83_07225	$3.19 \cdot 10^3$	0.155	$3.58 \cdot 10^3$	0.016

Additionally, the purified RK and GalK were tested with PP_i as a cofactor by using Malachite Green to detect released orthophosphate, but no activity was detected.

AK represents the last step in the fermentation pathway to acetate, where acetyl phosphate is used to convert NDP to NTP, an important mechanism for fermentative organisms to produced extra ATP (equivalents). Conversely, AK can also be the first step in many microorganisms for the production of acetyl-CoA from acetate [118]. Of the thirteen enzymes tested, AK was the only one where the *E. coli* background activity could not be removed with the heating step, since AK denatured as well, suggesting that it is relatively thermolabile. Nevertheless, background activity was negligible in the untreated extracts. In the direction from acetate to acetyl phosphate, the AK of *P. thermosuccinogenes* has a seven-fold higher activity with ATP compared to GTP. The acetate-forming direction is the more physiological relevant direction, since *P. thermosuccinogenes* produces acetate.

However, no simple – real-time – method exists to measure the rate in the acetate-forming direction using different cofactors.

6-PFK catalyses the phosphorylation of β-d-fructose 6-phosphate to β-d-fructose 1,6-bisphosphate and is in many organisms one of the key regulatory steps of the glycolysis. Three orthologous 6-PFKs are present in *P. thermosuccinogenes* that were all assayed for cofactor usage. Previous work only showed PP_i-dependent activity in *P. thermosuccinogenes* CFE [143]. Based on expression data, and the annotation by Prokka, it seemed most likely that CDQ83_11320 is responsible for this activity [143], as is now confirmed by the heterologous expression in *E. coli*. One of the other isoforms, CDQ83_07225, is active with both ATP and GTP at comparable levels. The measured activity is much lower than for CDQ83_11320, but the activities are normalized for CFE protein, and not for the amount of active enzyme, so the activities cannot be compared directly. The SDS-PAGE also shows that expression of CDQ83_11320 was higher compared to CDQ83_07225 (Supplementary Figure 3). For CDQ83_10650 no activity was measured at all, including for the non-heat treated extracts.

CDQ83_07225 – the 6-PFK active with both ATP and GTP – was purified via affinity chromatography, to check whether there are notable differences for the kinetics of ATP versus GTP, as was done with RK and GalK (table 4). The K_M is 0.155 mM for ATP and 0.016 mM for GTP, and the turnover numbers are virtually equal for ATP and GTP, which are both most likely at saturating concentrations *in vivo*, indicating that there is not one preferred cofactor for CDQ83_07225.

Excluding the phosphotransferase system, there are three enzymatic reactions known for the direct interconversion of PEP and pyruvate: PK; PPdK; and PEP synthase (PPS; also called pyruvate, water dikinase). Since these three enzymes of the so-called “PEP-family” share a common evolutionary origin [76], and since the annotations in *P. thermosuccinogenes* are ambiguous (CDQ83_03625 was annotated as PK by NCBI, as PPdK by RAST and as hypothetical by Prokka), the three orthologs/paralogs were each tested for PK, PPdK, and PPS activity, also with different cofactors (ADP/AMP versus GDP/GMP). For CDQ83_03625, no activity was detected in any of the three assays, shown in table 3. CDQ83_07455, annotated as PPdK, also showed PPdK activity with AMP, but not with GMP. CDQ83_09600, annotated as a PK, showed PK activity with both ADP and GDP, accordingly. ADP-dependent activity was approximately 50% higher than GDP-dependent activity.

Table 5 shows the results of the assays with the three glyceraldehyde 3-phosphate dehydrogenase orthologs (GAPDH) and the isocitrate dehydrogenase (IDH), all tested for NAD^+ and $NADP^+$-dependent activity. GAPDH is responsible for the two step reduction and phosphorylation of glyceraldehyde 3-phosphate to d-glycerate 1,3-bisphosphate. The exergonic reduction, typically with NAD^+, drives the endergonic phosphorylation, which

then enables the formation of ATP by PGK. The reverse – gluconeogenic – reaction is also catalyzed by GAPDH, but typically uses NADPH. Organisms often have both a NAD^+ and a $NADP^+$-dependent GAPDH, used in glycolysis and gluconeogenesis, respectively [82]. Of the three GAPDHs *P. thermosuccinogenes* had annotated, only two (CDQ83_04880 and CDQ83_10590) showed any activity in the assays, which was NAD^+-dependent in both cases. CDQ83_10590, which showed the highest activity in the assays, is the ortholog that is also expressed during growth on glucose and xylose [143]. CDQ83_07070, for which no activity was detected, belongs to the class II (archaeal) GAPDHs, for which no functional evidence in bacteria exist. Nevertheless, it does appear to be present in handful of bacterial genomes, according to the InterPro database.

IDH is responsible for the oxidative decarboxylation of isocitrate to form α-ketoglutarate and CO_2, using $NAD(P)^+$. Bacteria most commonly rely on $NADP^+$-dependent IDHs, however, the ones relying on NAD^+-dependent IDH have in common that their TCA-cycle is incomplete, as well as the absence of an isocitrate lyase [315,332]. The IDH from *P. thermosuccinogenes* was found to be dependent on $NADP^+$.

Table 5: Enzyme assays with *E. coli* cell-free extract containing heterologously expressed GAPDH orthologs and isocitrate dehydrogenase from *P. thermosuccinogenes*, to determine the cofactor involved in the oxidation (NAD^+ or $NADP^+$). Reaction velocities are given in µmol/mg cell-free extract protein/min ± standard deviation.

Assay	Locus tag	Annotation	Activity	
			NAD^+	$NADP^+$
Glyceraldehyde 3-phosphate dehydrogenase	CDQ83_04880	type I glyceraldehyde-3-phosphate dehydrogenase	0.20 ± 0.01	ND*
	CDQ83_07070	type II glyceraldehyde-3-phosphate dehydrogenase	ND	ND
	CDQ83_10590	type I glyceraldehyde-3-phosphate dehydrogenase	0.57 ± 0.19	ND
Isocitrate dehydrogenase	CDQ83_08625	isocitrate dehydrogenase (NADP(+))	ND	45 ± 5

* Not detected: value close to zero and not significantly different from empty vector control.

Discussion

Sugar kinases.

It was already known that GK and XK from *P. thermosuccinogenes* prefer GTP over ATP [143]. Adding RK and GalK to that list, it becomes apparent that using GTP could be the prevailing mechanism for the phosphorylation of monosaccharides. There also appears to be a difference between C_6 and C_5 sugars, as GK and GalK greatly prefer GTP over ATP and XK and RK only moderately. At this point, the implications of these observations are not clear, but they might eventually help in understanding the driving factor behind the parallel

use of different phosphoryl carriers in the energy metabolism – some ideas are already discussed below.

Acetate Kinase.

The AK has an apparent preference for ATP over GTP, in the acetyl phosphate forming direction. The reverse, acetate forming direction, however, is the physiological relevant direction, as acetate is one of the main fermentation products. One would easily be tempted to assume that maximum velocities with different substrates scale proportionally to each other in the reverse direction. However, emanating from the complex interactions of enzymes with their substrates, there is really no fundamental reason why the kinetics in one direction could be used to predict the kinetics in the other direction. The thermodynamics of PK restrict it from being used for detection of ATP/GTP formation in the manner it was used for ADP/GDP detection in the acetyl phosphate forming direction. ATP formation could easily be measured via an assay relying on luciferase, of course. However, luciferase is not compatible with GTP, and can therefore not be used to assess preference of ADP versus GDP. Off-line methods that do not rely on the real-time spectrophotometric measurement are still a possibility, but such methods are exceedingly more laborious for studying kinetics and not considered for this study. An attempt was made to use the here described ATP/GTP-dependent 6-PFK for detection of both ATP and GTP production by acetate kinase in a coupled assay with 6-PFK, aldolase, triose-phosphate isomerase, and glycerol-3-phosphate dehydrogenase. However, it was found that the substrate, acetyl-phosphate, inhibited one (or more) of the coupled enzymes (data not shown), rendering the method unreliable.

The relatively low thermo-stability of AK from *P. thermosuccinogenes* was already observed earlier [280], as well as for the AKs from *H. thermocellum*, *Thermoanaerobacter brockii*, and *Moorella thermoaceticum* [154,257,280]. It is fascinating that it appears to be a rather common phenomenon, and it implies there might be an evolutionary pressure for the AK to become unstable at temperatures only slightly above the organisms optimal growth temperature.

6-Phosphofructokinases.

Three only very distantly-related families of 6-PFK are known: The PFKA family; PFKB, belonging to the ribokinase family of sugar kinases; and the archaeal ADP-dependent 6-PFK family [50,192,242]. Best known is the PFKA family, to which most 6-PFK belong, including the three isoenzymes *P. thermosuccinogenes* possesses. The phylogeny is of PFKA is complex, due to highly prevalent lateral gene transfer and phosphoryl donor change within the PFKA family. Originally, three separate phylogenetic clades were recognized (I, II, and III) that are now expanded into seven distinct clades (B1, E, P, LONG, SHORT, X, B2, and III) [18,269]. Each of the three 6-PFKs from *P. thermosuccinogenes* belongs to a separate clade: The PP_i-dependent 6-PFK (CDQ83_11320) to B2, the ATP/GTP-dependent 6-PFK

(CDQ83_07225) to B1, and the 6-PFK without detected activity (CDQ83_10650) to III. CDQ83_10650 did contain the atypical Gly_{117} and Lys_{137} residues in the active site that are associated with ATP-dependent activity [18]. *H. thermocellum* only has homologs to CDQ83_11320 and CDQ83_07225, the isoenzymes for which we were able to detect activity. It is not uncommon for bacteria to have multiple 6-PFKs. For example, *Clostridium perfringens* also has homologs from the B1, B2, and III clades [18], and in the methylotrophic actinomycete *Amycolatopsis methanolica*, PP_i-6-PFK was found to be active during growth on glucose, and ATP-6-PFK during growth on C_1 compounds [5]. The fact that *P. thermosuccinogenes* has isoenzymes for the same reaction using different phosphoryl carriers does, however, again raise the question why *P. thermosuccinogenes* uses several different phosphoryl carriers for it energy metabolism in the first place.

Phosphoenolpyruvate to pyruvate.

Three genes of *P. thermosuccinogenes* were annotated to be either PK, PPdK, or PPS. All three were tested for these three activities. It was clearly shown that CDQ83_09600 represents a PK, an enzyme well known not to be very specific towards nucleoside diphosphates [21,52], and that CDQ83_11320 represents a PPdK, functional with AMP, and not with GMP. Neither is expressed during growth on glucose or xylose at levels comparable to other glycolytic enzymes [143]. It is therefore questionable that they contribute significantly to the conversion of PEP to pyruvate. Instead, pyruvate is likely formed through the malate-shunt, comprised by PEPCK, malate dehydrogenase, and malic enzyme, see Figure 2 [289]. Nevertheless, in *H. thermocellum*, which lacks PK, it was shown that 70% of the flux from PEP to pyruvate runs via PPdK, and 30% via the malate-shunt [219]. This high flux through PPdK poses another interesting question for these organisms, besides the source of all the PP_i, namely that of AMP. Assuming that the majority of sugars taken up are converted to pyruvate, 1.4 moles of AMP need to be formed per mole of hexose consumed in *H. thermocellum*, a sizable flux that cannot be ignored. It is generally assumed that this AMP is formed via adenylate kinase (2 ADP --> ATP + AMP) [183,194], but considering that at physiological relevant adenylate energy charges, the Gibbs free energy of this reaction is close to 0, it would seem to be a very inefficient use of the enzyme [225], even if it was a remarkably fast enzyme, for which there is no reason to believe it is [133]. In fact, for ATP, ADP, and AMP concentrations measured in *H. thermocellum*, the net flux would favour the ADP-forming direction [251]. Considering this, it appears that another mechanism must exist where AMP is formed, at a flux of comparable size to that of PP_i.

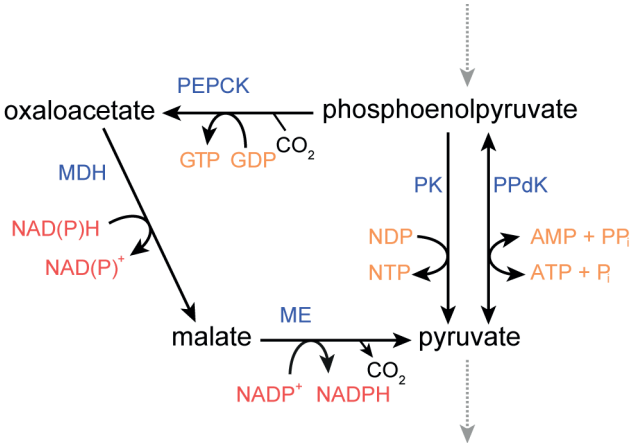

Figure 2: Metabolic routes connecting phosphoenolpyruvate and pyruvate in *P. thermosuccinogenes*, including the malate shunt via oxaloacetate and malate. ME, malic enzyme; MDH, malate dehydrogenase; PEPCK, phosphoenolpyruvate carboxykinase; PK, pyruvate kinase; PPdK, pyruvate, phosphate dikinase.

Pyrophosphate usage.

As explained in the introduction, the use of PP_i is thought to be a mechanism through which energy, or ATP-equivalents are conserved by using PP_i, a by-product of anabolism that is otherwise hydrolysed into orthophosphate in order to maintain the low PP_i levels required for those anabolic reactions to proceed [55]. This anabolic formation of PP_i is only a minor fraction of all the PP_i required for both 6-PFK and PPdK. Hence, there must be another mechanism by which PP_i is formed [331]. There is another way, however, by which the use of PP_i could potentially conserve energy, namely when the proton (or sodium-ion) coupling ratio is lower than that of ATPase, if the extra PP_i would be generated via an H^+/Na^+ translocating pyrophosphatase. For *Syntrophus gentianae*, it was shown that in membrane vesicles, the ratio of ATP formation to PP_i hydrolysis was roughly 1:3 [260]. If such a coupling would exist in thermophilic *Clostridia* as well, and compared to ATP, only one-third of the protons/sodium-ions are required for the formation of PP_i, 2/3 mole of ATP is conserved extra per dissimilated mole of glucose. Nevertheless, even a slightly more efficient coupling ratio would already signify extra energy conservation. It would almost seem obvious for such a mechanism to exist in nature, and might even explain the wide-spread occurrence of PP_i-dependent 6-PFKs. In *Methylococcus capsulatus*, PP_i-6-PFK and a H^+/Na^+ translocating pyrophosphatase were actually found to be present in the same operon [134,240].

Additionally, the use of PP_i also allows 6-PFK as well as PPdK to operate in reverse (i.e. gluconeogenic), whereas the ATP-dependent 6-PFK and PK are strictly catabolic, as the result of the very negative Gibbs free energy for those reactions at physiological conditions [193,194]; the direct consequence of the trade-off between energy conservation and net forward flux (i.e. rate, enzyme usage, and metabolic control). This then raises the question whether the use of PP_i is the result of the need for extra energy conservation, or of the need

for the reaction to be reversible – and the answer is likely different in different organisms. For a strictly anaerobic fermentative carbohydrate degrader such as *P. thermosuccinogenes*, reverse 6-PFK (or fructose 1,6-bisphosphatase, i.e. gluconeogenesis) activity does not seem to be an important requirement.

GTP usage.

It was previously proposed that perhaps GTP could exist next to ATP at different guanylate and adenylate energy charges (GEC and AEC, respectively) [143]. It is generally accepted that the AEC in growing microorganisms is maintained relatively static somewhere between 0.80 and 0.95, which is absolutely crucial for cells to function [13,53,214,232]. Perhaps then, the GEC is allowed to be lower, or more variable. As it appears now, the main source of GTP is the PEPCK reaction, and the main drains are the sugar phosphorylation reactions discussed earlier. Disregarding anabolism, these reactions might in fact comprise a relatively closed circuit for GTP turnover. What would a lower GEC then mean for the thermodynamics for those reactions in comparison to a situation where ATP/ADP was used? The sugar phosphorylation reactions will have a lower driving force, but it is unlikely this will be impacted in any meaningful way, since these reactions generally have very negative standard Gibbs free energy, and if ATP is still used for the import of sugars via a ABC transporters, high transmembrane sugar gradients are still possible. The PEPCK, on the other hand, operates relatively close to the thermodynamic equilibrium [329], so small changes of the product or substrate concentrations might have a relatively big impact on the fluxes. A lower GEC would lower the Gibbs free energy, or in other words, increase the ratio between the forward and reverse fluxes of the reaction, making it more efficient in terms of enzyme usage [225]. Furthermore, and perhaps more significant, a lower GEC would also allow the reaction to proceed at lower environmental CO_2 concentrations, since the PEPCK reaction involves the fixation of a CO_2 molecule. Organisms relying on PEPCK for ATP/GTP production, including natural succinate producers used in industry, are typically considered capnophilic, or "CO_2-loving", as they are absolutely dependent on a minimal CO_2 concentration for growth [190,274]. Therefore, tuning the metabolism such that it would allow growth at lower CO_2 concentrations, with a lower GEC for example, could offer a significant competitive advantage upon CO_2 limitation. A GEC that is higher than the AEC would have the opposite effect, and assuming sugar import is indeed ATP dependent, while sugar phosphorylation is GTP-dependent, it would lower the intracellular concentrations of (non-phosphorylated) sugars. Consequently, higher rates of sugar uptake at lower extracellular sugar concentrations would be possible, potentially offering a competitive advantage under substrate-limiting conditions.

If indeed the GEC and AEC exist at different charges, which is for now purely hypothetical, it will be essential for the cell to carefully regulate the interconversion of ATP and GTP. The two main mechanisms known for balancing the degree of phosphorylation of the different NTP pools are adenylate kinase – in combination with nucleoside-diphosphate kinase – and

PK [52]. Coincidentally, *H. thermocellum* lacks a PK but possesses an adenylate kinase, where *P. thermosuccinogenes* appears to lack an adenylate kinase while possessing a functional PK, suggesting that neither is very relevant, as they seem to be lost without consequence, or that at least only having one or the other is sufficient. Another reaction that could be of importance for balancing the ATP and GTP pools is the phosphoglycerate kinase, which was shown in both thermophilic *Clostridium* species to use both ATP and GTP, but preferring ATP, while carrying a very high flux due to its role in glycolysis [143,331]. The exact kinetics of phosphoglycerate kinase for ADP versus GDP – as well as that of other enzymes that can use both – might then be crucial to maintain the relative pools and energy charges.

The first step to investigate the hypotheses proposed here would be to actually determine whether the AEC and GEC are each maintained at different charges, for which the different nucleoside phosphate pools would need be to accurately measured during different growth conditions. A challenging endeavor, due to the labile nature of ATP and GTP – mostly the result of their high metabolic turnover, rather than actual chemical lability – leading to measured AECs/GECs that are lower than their true values [251]. Perhaps, a recently developed method for real-time metabolome profiling via direct injection of living cells into a high-resolution mass spectrometer could allow the accurate determination of AEC and GEC simultaneously [173].

Glyceraldehyde 3-phosphate dehydrogenase.

As a quintessential example of a multifunctional enzyme, GAPDH has many different functions attributed to it, aside from its catalytic role in glycolysis. For bacteria, these include functions related to virulence and DNA and RNA binding [37,271,321]. Of the three isoforms, only the two type I forms showed activity, dependent on NAD^+, of which CDQ83_10590 belongs to the most highly expressed genes in the genome [143]. CDQ83_04880, only marginally expressed during growth on glucose or xylose might be important during other growth stages instead, such as sporulation or germination. Alternatively, any non-metabolic functions might be the primary role of CDQ83_04880 and the type II GAPDH CDQ83_07070, for which no activity was detected at all. It is uncommon for the 'archaeal' type II GAPDH to be present in bacteria, and it is also not conserved among close relatives of *P. thermosuccinogenes*.

The enzyme assay method.

The method used to assess cofactor usage presents a very simple and robust method to study thermotolerant and thermophilic enzymes, since no chromatography step is involved. This is owed mostly to the higher thermostability of the enzymes studied, which enables the removal of virtually all *E. coli* background activity via a simple heating step. Nevertheless, even omission of the heating step, which was required for the AK, still allowed for collection of sound data required for the identification of the enzyme's activity and the

corresponding cofactor usage, due to the impressive capacity of *E. coli* to overexpress proteins by using the T7 promoter. Of course, the omission of purification steps means that the studied enzyme can only be qualitatively characterized. The simple method used in this study can potentially be taken advantage of for a high-throughput set-up for enzyme characterization. In particular, if it were to be combined with the method published in 2017 by Sévin *et al.* that uses mass spectrometry to identify accumulated or depleted compounds in a supplemented metabolome extract containing hundreds of biologically relevant candidate substrates [266].

In the case several cofactors/substrates are found to be used by an enzyme, further purification is still recommended, in order to determine the enzyme kinetics for the competing cofactors/substrates. The differences in kinetics could rule out any of the found cofactors/substrates from being physiologically relevant.

Conclusion.

To get a better insight in the parallel use of ATP, GTP, and pyrophosphate in the central energy metabolism, and for the inability to predict cofactor usage from the amino acid sequence, thirteen enzymes from *P. thermosuccinogenes* were cloned and heterologous expressed in *Escherichia coli* to assess the cofactor usage via enzyme assays using heat-treated *E. coli* cell-free extract. The thermophilic nature of *P. thermosuccinogenes* allowed for the removal of virtual all background activity of *E. coli* from the heterologously expressed enzyme via a simple heating step, taking away the need for purification via chromatography. Three selected enzymes, ribokinase, galactokinase, and a 6-phosphofructokinase were subsequently purified further by affinity chromatography, to enable the determination of K_M and k_{cat} for ATP versus GTP, as they were found to use both.

As it is now clear that galactokinase and ribokinase prefer GTP over ATP, just like glucokinase and xylulokinase, it seems that this might be the prevalent cofactor for sugar phosphorylation in *P. thermosuccinogenes*, in particularly for hexoses. There might be a more or less closed circuit for GTP-turnover between sugar phosphorylation and phosphoenolpyruvate carboxykinase, that could theoretically allow for different reaction thermodynamics then when ATP were to be used. Further research is needed to corroborate this.

Three 6-phosphofructokinases were tested. In addition to the highly expressed pyrophosphate-dependent 6-phosphofructokinase, another 6-phosphofructokinase was found to be active with both ATP and GTP. No activity was detected for the third. Both type I glyceraldehyde 3-phosphate dehydrogenases were found to be NAD^+-dependent and for the type II “archaeal” glyceraldehyde 3-phosphate dehydrogenase no activity was detected at all. Pyruvate kinase was confirmed to be present and to be active with both ADP and GDP, whereas another enzyme ambiguously annotated as pyruvate kinase did not show any

activity. Pyruvate, phosphate dikinase was active with AMP, but not with GMP. Acetate kinase was found to prefer ATP over GTP in the in the acetyl phosphate-forming direction. Isocitrate dehydrogenase was active with $NADP^+$.

Acknowledgements

This research was funded by Corbion and the European Union Marie Skłodowska-Curie Innovative Training Networks (ITN), contract number 642068.

Supplementary data

Supplementary data for this chapter can be found at: https://www.frontiersin.org/articles/10.3389/fmicb.2019.01162/full#supplementary-material

Chapter 4 - Identification of a Novel Fumarate Reductase Potentially Involved in Electron Bifurcation

Jeroen G. Koendjbiharie[1], Richard van Kranenburg[1,2]

[1] Corbion, Gorinchem, Netherlands
[2] Laboratory of Microbiology, Wageningen University & Research, Netherlands

Part of this chapter has been published as:

Van Kranenburg, R.; Koendjbiharie, J.G. Identification of a Novel Fumarate Reductase Potentially Involved in Electron Bifurcation. Preprints 2019, 2019120288 (doi: 10.20944/preprints201912.0288.v1).

Abstract

In the thermopilic succinic acid producing bacterium *Pseudoclostridium thermosuccinogenes* the fumarate reductase resides in an operon together with a large flavin oxidoreductase-heterodisulfide reductase (FlxABCD-HdrABC) complex. Based on the phylogeny of the putative fumarate reductase and the prevalent co-occurrence with the large electron bifurcating complex that shuttles electrons from NADH to ferredoxin and a disulfide bond, we propose two hypothetical mechanisms via which the fumarate reductase is involved in electron bifurcation: (1) A disulfide bond from a hitherto unknown cofactor is reduced by the electron-bifurcating FlxABCD-HdrABC complex, using NADH, in order to generate two thiol groups, while facilitating the otherwise unfavourable reduction of ferredoxin by NADH. The disulfide bond is subsequently regenerated via the reduction of fumarate to succinate by the fumarate reductase using the previously formed thiol groups. Or (2) the fumarate reductase forms an integral part of the FlxABCD-HdrABC complex, and NADH is used to reduce ferredoxin and fumarate directly, without an intermediate disulfide-forming cofactor. Either way, this would enable the conservation of additional energy by a soluble fumarate reductase, analogous to fumarate respiration via the membrane associated electron transport chain.

Introduction

Pseudoclostridium thermosuccinogenes is the only thermophile known to produce succinic acid as one of its main products of fermentation, together with acetic acid, formic acid and several minor products [74,143,278]. Succinic acid is a versatile molecule that can form one of the core building blocks in a bio-based economy, where it is produced from biomass, as an alternative for petroleum [41,57,320]. From an industrial point of view it can be advantageous to use a thermophilic production organism [328]. Therefore, we set out to identify and characterize the enzymes responsible for succinic acid production in *P. thermosuccinogenes*, as this might facilitate future engineering of thermophilic succinic acid cell-factories.

RNA-seq. data of a previous study led to the identification of set of genes that likely form an operon (Figure 1), starting with the gene encoding a fumarate hydratase, the enzyme responsible for the interconversion of malate and fumarate [143]. This operon further contains a gene homologous to the flavoprotein subunit of fumarate reductase/succinate dehydrogenase (FrdA); the core subunit that is shared between all known fumarate reductases and succinate dehydrogenases [124]. Surprisingly, eight more genes are present in between the fumarate hydratase and the fumarate reductase flavoprotein subunit. The last of those, upstream of *frdA*, encodes a protein that is homologous to ferredoxins and, in all likelihood, represents the iron-sulfur subunit of the suspected fumarate reductase (FrdB). The other seven genes appear to encode a flavin oxidoreductase-heterodisulfide reductase complex (FlxABCD-HdrABC), a large enzyme complex involved in flavin-based

electron bifurcation that appears to be widespread in anaerobic bacteria [237]. Lastly, a small hypothetical membrane protein-encoding gene is present in the operon, directly downstream of *frdA*. The small membrane protein contains a so-called PQ-loop motif, which is found in a specific (newly described) family of membrane transporters, suggesting that it might be a succinic acid transporter [80,164].

Following phylogenetic evidence and the co-occurrence of genes responsible for succinate production with this electron bifurcating FlxABCD-HdrABC complex in one operon, we propose a hypothesis for the mechanisms by which succinic acid is formed in *P. thermosuccinogenes*, which will be presented in the Results section. First, fumarate reductases will be introduced in more detail, as well as flavin-based electron bifurcation, focussing in particularly on the FlxABCD-HdrABC complex.

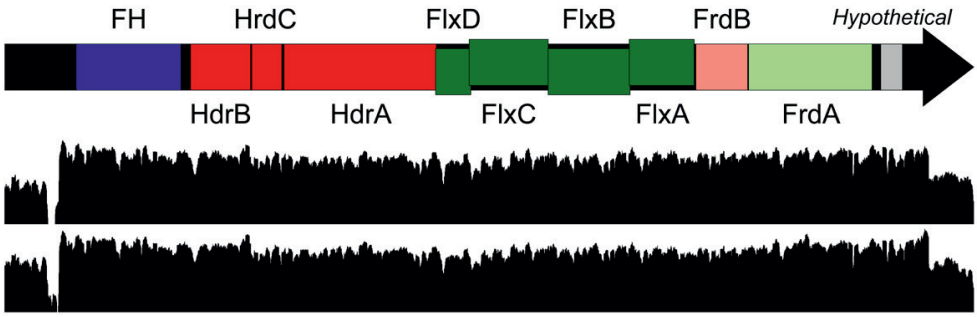

Figure 1. Schematic depiction of the 'succinic acid operon' in *P. thermosuccinogenes*, with below it the (log10) transcription coverage during growth on glucose (upper track) and on xylose (lower track), from data generated previously [143]. Indentations reflect overlap with the preceding open reading frame. FH: fumarate hydratase, Hdr: heterodisulfide reductase, Flx: flavin oxidoreductase, Frd: fumarate reductase. Locus tags of genes are from left to right: CDQ83_03355, CDQ83_03350, CDQ83_03345, CDQ83_03340, CDQ83_03335, CDQ83_03330, CDQ83_03325, CDQ83_03320, CDQ83_03315, CDQ83_03310, CDQ83_03305, CDQ83_03300.

Fumarate reductases

The various enzymes responsible for the interconversion of fumarate and succinate (i.e. fumarate reductases and succinate dehydrogenases, FRD/SDH) are diverse in their subunit configurations, but are all part of a larger protein superfamily based on a homologous flavoprotein, which also includes l-aspartate oxidases, anaerobic glycerol-3-phosphate dehydrogenases, and adenylyl-sulfate reductases [124]. FRD/SDHs can be divided in two main groups: soluble and membrane-bound. The latter are part of the electron transport chain, and thus often linked to proton translocation, and are generally referred to as the succinate:quinone oxidoreductase superfamily (Figure 2) [166]. Five types (i.e. A-E) of the membrane bound succinate:quinone oxidoreductase superfamily are distinguished, containing two anchor domains, FrdC and FrdD (which are fused in type B), together with the flavoprotein subunit (FrdA) and the iron-sulfur subunit (FrdB) [166]. In Type E, which is

only found in archaea, the anchor domains are unrelated to those of the other types, and are therefore referred to as FrdE and FrdF.

Only a handful of soluble FRDs have been described and they are diverse in their function and their electron donor, as well as in the additional subunits associated with FrdA. The soluble FRD in methanogenic archaea is thiol-driven, as it uses the cofactors CoM-SH and CoB-SH to form succinate together with the CoM-S-S-CoB heterodisulfide. It resembles type E of the succinate:quinone oxidoreductase superfamily, and the iron-sulfur subunit (FrdB) is essentially a fusion of FrdB with FrdE from the membrane-bound type E [33,109]. The soluble FRDs described in the eukaryotes *Saccharomyces cerevisiae* and *Trypanosoma brucei* use NADH as electron donor, are monomeric proteins, consisting only of FrdA [61,139,206]. The soluble FRD from *Shewanella* species is also monomeric, and is present in the periplasm, where it accepts electrons from a c-type cytochrome [209,263,264]. Finally, the soluble FRD from *Aquificae*, chemolitoautotrophs that use the reverse TCA-cycle to fix CO_2, has 5 subunits and uses NADH [198]. Its FrdA and FrdB are closely related to those of the membrane bound FRD/SDHs, but the other three subunits are unique. Figure 2 shows an overview of the configurations of the different known FRD/SDHs.

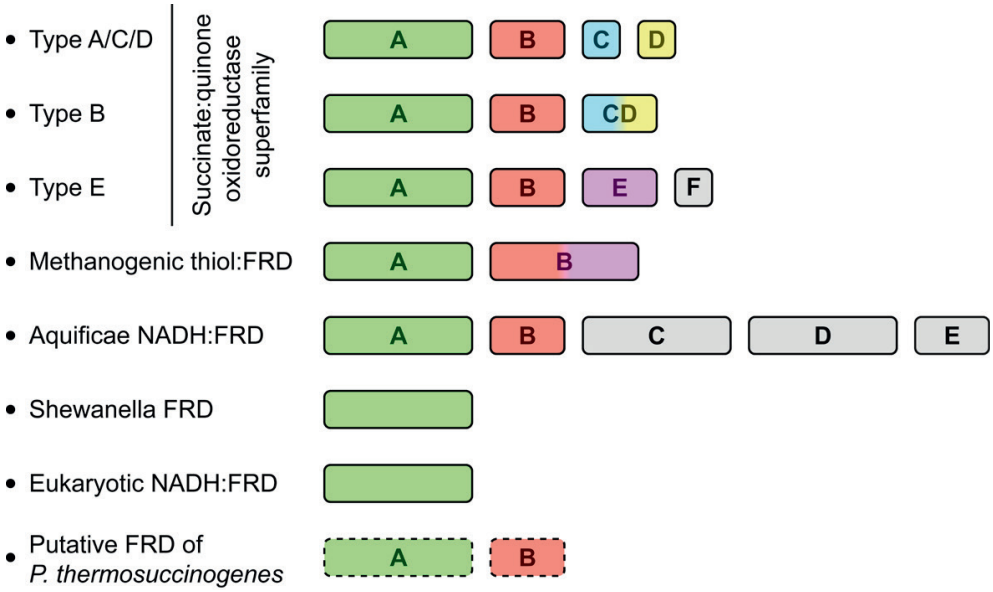

Figure 2. List of the known fumarate reductases, including the putative fumarate reductase of *P. thermosuccinogenes*. A schematic overview of the subunits that are part of each type is shown. The colours indicate homologous proteins or protein domains; the grey subunits are unique to that type of fumarate reductase. Note that the letter annotations used for the *Aquificae* fumarate reductase subunits C, D, and E do not to reflect homology with the corresponding annotations of the succinate:quinone oxidoreductase superfamily. Figure adapted from Jardim-Messeder *et al.* (2017) [124].

Flavin-based electron bifurcation

Electron bifurcation refers to the phenomenon where a hydride electron pair is split into one electron with a more negative reduction potential and another with a more positive reduction potential. As such, the reducing power of one is amplified at the expense of the other [46]. Note that a more negative reduction potential means a higher potential energy.

Two variants of electron bifurcation are known to occur in nature: Quinone-based electron bifurcation (QBEB) and flavin-based electron bifurcation (FBEB). QBEB occurs in complex III of the electron transport chain, where the electron pair of the quinone is split between cytochrome b (low-potential) and cytochrome c (high-potential). FBEB only occurs in strictly anaerobic prokaryotes, and allows them to push the boundaries of what is energetically possible. A flavin (i.e. FAD or FMN) is used as a prosthetic group and the low-potential acceptor is always a ferredoxin or a flavodoxin, but a wide range of different high-potential acceptors and two-electron donors have been described (Figure 3). The low-potential ferredoxin or flavodoxin (generated via FBEB) can subsequently be used in processes where the reduction potential of the two-electron donor (e.g. NADH) is not sufficiently low, such as reduction of N_2 to NH_3 or CO_2 to CO [46,227].

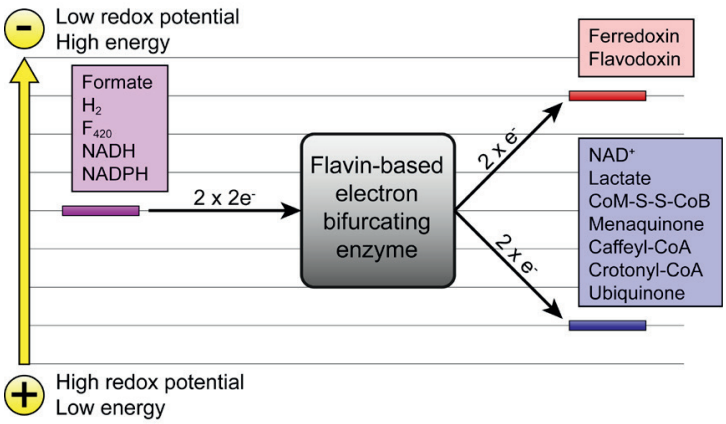

Figure 3. All the currently known electron donors and acceptors involved in flavin-based electron bifurcation (FBEB). Figure was adapted from Buckel and Thauer (2018) [46].

The FlxABCD-HdrABC complex

The predicted seven-subunit flavin oxidoreductase-heterodisulfide reductase (FlxABCD-HdrABC) complex of which the genes are situated in between those of the fumarate hydratase and the FRD in *P. thermosuccinogenes*, is composed of two parts: A three-subunit heterodisulfide reductase part, and a four-subunit flavin oxidoreductase part. *In vitro* evidence regarding the function of the full complex is lacking, but *in vivo* results from *Desulfovibrio vulgaris* strongly support the proposed function as a bifurcation complex coupling the energetically unfavourable reduction of ferredoxin by NADH to the favourable

reduction of a disulfide bond (Figure 4A) [237]. This is analogous to a similar complex in hydrogenotrophic methanogenic archaea, which also contains the three-subunit heterodisulfide reductase part, but then together with a three-subunit [NiFe]-hydrogenase part, i.e. MvhADG-HdrABC [130]. The complex in archaea uses hydrogen to reduce ferredoxin, also by coupling it to a simultaneous reduction of a disulfide bond; namely, that of the CoM-S-S-CoB heterodisulfide (Figure 4B). MvhADG-HdrABC has been studied *in vitro* and recently a crystal structure was published [314]. In *Desulfovibrio vulgaris*, a small protein, DsrC presumably acts as the disulfide electron acceptor, via internal disulfide bonds of cysteine residues [237,309]. The FlxABCD-HdrABC complex is widespread in anaerobic bacteria, but DscR is only conserved in organisms with a dissimilatory sulfur metabolism, where it is often located next to the FlxABCD-HdrABC complex, and is used for reduction of sulfite. It is likely that other disulfide bond-containing compounds or proteins acts as the electron acceptor in other bacteria that possess the FlxABCD-HdrABC complex.

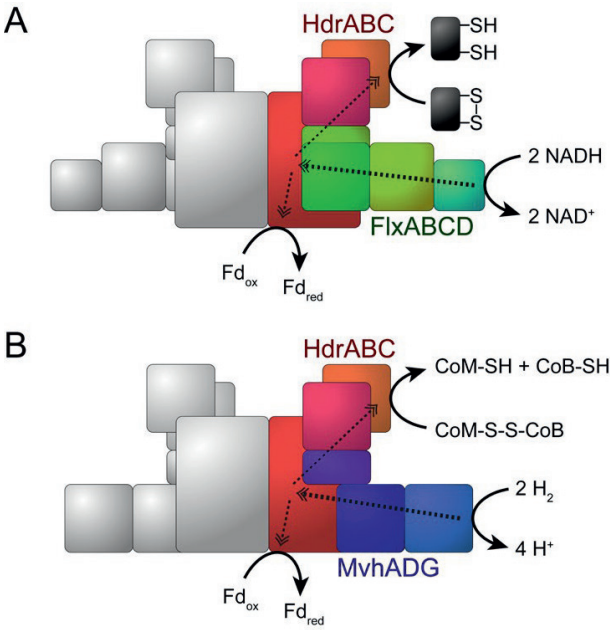

Figure 4. (A) Proposed mechanism of the FlxABCD-HdrABC complex, and (B) the MvhADG-HdrABC complex. Arrangement of the subunits is an interpretation based on the crystal structure of the MvhADG-HdrABC complex, which forms a large dimer of two hetero-hexamers [314]. Dashed arrows indicate the flow of electrons.

Materials and Methods

Phylogenetic trees

The amino acid sequences used for the phylogenetic trees were retrieved from the NCBI database. The following sequences were used for Figure 5A: CAA06780.1, P08065.4, NP_281599.1, AAC77114.1, AAC73817.1, NP_952230.1, WP_000705948.1, BAG70309.1,

CAA04398.1, CAA69872.1, AAB64995.1, AAB59346.1, AAA35026.1, P0C278.1, AAY80343.1, AAN40014.1, AAX20163.1, P17412.3, PNT92608.1, P10902, P13033, O28603. And the following for Figure 5B: CAA06781.1, NP_390721.1, NP_281600.1, AAC77113.1, AAC73818.1, NP_952231.1, AAC46065.1, WP_012963621.1, CAA04399.1, CAA69873.1, AAS56515.1, P17596.1, PNT92609.1, P00195, Q55389. The sequences are all from enzymatically studied SDHs and FRDs, according to the selection made by Miura *et al*. (2008) [198].

Sequences were aligned using ClustalW with the standard settings in MEGA6. The tree was constructed using the neighbor-joining method in MEGA6, using a bootstrap test with 1,000 replicates.

Deletion of IscR in *E. coli*

The transcriptional regulator IscR, which regulates several genes and operons involved in the formation of iron-sulfur clusters an iron-sulfur cluster-containing proteins was deleted in *E. coli* BL21(DE3), to improve the functional overexpression of iron-sulfur cluster-containing proteins [4]. The IscR gene was deleted using Cas9, via the methods by [125]. First, *E. coli* BL21(DE3) was transformed with pCas, containing a kanamycin resistance marker, a temperature sensitive replicon, the λ-Red system, and a constitutively expressed Cas9. Cells harbouring pCas were grown at 30 °C, and made competent in the presence of 10 mM arabinose to induce λ-Red. Cells were then transformed with pTargetF for the IscR deletion. pTargetF-IscR contains a spectinomycin resistance marker, sgRNA targeting IscR, homologous flanks of 250 bp upstream and downstream of IscR, and an IPTG inducible sgRNA targeting pTarget to allow easy curing of the plasmid. pTargetF-IscR was constructed by inserting the homologous flanks, synthesized as a Gblock, into the PCR-amplified backbone using the NEBuilder® HiFi DNA Assembly Master Mix. The backbone was amplified with forward primer TGGTAACCCGGCCTCCCGTTTCGAGTTCATGTGCAGCTCC and reverse primer GCTATTTCTAGCTCTAAAACTTGACGAATCTGTAGATGCCACTAGTATTATACCTAGGACTGAGCTAGC or GCTATTTCTAGCTCTAAAACTTGGCTGATATTTCCGAACGACTAGTATTATACCTAGGACTGAGCTAGC. The reverse primers contained the spacer sequence targeting two different sites in the IscR gene. Cells transformed with pTargetF-IscR and selected on plates containing kanamycin and spectinomycin at 30 °C. For both spacers, 2 out of 24 colonies had a clean knock-out, confirmed by sequencing. pTargetF was cured by growing in liquid LB with kanamycin and IPTG at 30 °C. Then, pCas was cured by growing cells in LB at 37 °C.

The following Gblock sequence was ordered from IDT: GTTTTAGAGCTAGAAATAGCAAGTTAAAATAAGGCTAGTCCGTTATCAACTTGAAAAAGTGGCACCGAGTCGGTGCTTTTTTTGAATTCTCTAGAGTCGACCTGCAGAAGCTTAGATCTATTACCCTGTTATCCCTACGTAATGCGTCTTATCAGGCCTACAGTGTACAGAACCCCAGGGCGGATATGGCGTTCACG

CCGCATCCGACAACAGGTACAAACGCCACGATAAAAAAATGGCACTGAAGGTTAAATACCCGACT
AAATCAGTCAAGTAAATAGTTGACCAATTTACTCGGGAATGTCAGACTTGACCCTGCTATGCAATA
CCCCCACTTTTACAATAAAAAACCCCGGGCAGGGGCGAGTTTGAGGTGAAGTAAGACATGGACGT
TAAGTTACGCGCTTAATAAAAAGAATTCAGAATCAGGCCGGAGTGCTAAATACTCCGTAAACACG
GTCGTACATCCAGCCGGTAGCCTGATTCCTTGCATTGAGTGATGTACGGAGTTTATAGAGCAATGA
AATTACCGATTTATCTCGACTACTCCGCAACCACGCCGGTGGACCCGCGTGTTGCCGAGAAAATGA
TGCAGTTTATGACGATGGACGGAACCTTTGGTAACCCGGCCTCCCGTT.

Cloning of fumarate hydratase and fumarate reductase

The fumarate hydratase gene (CDQ83_03355) from *P. thermosuccinogenes* was amplified via PCR using forward primer TACTTCCAATCCAATGCACAATATCGTGTGGAAAGAGATTCTATG and the reverse primer TTATCCACTTCCAATGTCATACCATCTGCTCAGGCT. The PCR product was inserted via ligase independent cloning into a pET-28b(+) (Novagen, Madison, Wisconsin) derived backbone that was generated using the primers ATTGGATTGGAAGTACAGGTTTTCATGGTGATGGTGATGGTGAGAAGAACCCATGGTATATCTCC TTCTTAAAG and ATTGGAAGTGGATAACGGATCCGAATTCGAGCGCCGTCGACAAGCTTGCGG. The ligase-independent cloning protocol is described elsewhere [11]. In the final construct, the enzyme has an N-terminal His-tag with a TEV protease site in between.

The fumarate reductase subunits FrdA (CDQ83_03310) and FrdB (CDQ83_03315) were cloned in pRSFDuet-1 (Novagen, Madison, Wisconsin) via restriction digestion. FrdB was amplified using forward primer AGAAGTCCATGGAACAAATGGTTAATGTGTTTTTGATG or AGAAGTCCATGGGTCACCATCACCATCACCATGAAAACCTGTACTTCCAATCCAATGCAGAACAAA TGGTTAATGTGTTTTTGATG (to include an N-terminal His-tag with a TEV protease site) and reverse primer TCTTGTGCGGCCGCTATTTCTCAATTTCTCTGTTGTTATATAGTTCC; and then digested with NcoI and NotI, respectively, for cloning site 1. FrdA was amplified using forward primer AGAAGTCATATGTATACACAGGAAATGCTTGATTCTATC or AGAAGTCATATGCACCATCACCATCACCATGAAAACCTGTACTTCCAATCCAATGCATATACACAG GAAATGCTTGATTCTATC (to include an N-terminal His-tag with a TEV protease site) and reverse primer TCTTGTGGTACCTTATTTATCGTGCCTACGAGTATATATCGG; and digested with NdeI and KpnI, respectively, for cloning site 2. The result were eight constructs, encompassing all combinations of FrdA and FrdB, with and without N-terminal His-tag.

The different constructs (with fumarate hydratase and with fumarate reductase) were transformed to *E. coli* DH5α and verified by sequencing. Both pET-28b(+) and pRSFDuet-1 contain a kanamycin resistance marker. *E. coli* Rosetta (Novagen) was subsequently used for heterologous expression; the strain contains an extra plasmid (pRARE) encoding tRNAs of rare codons and a chloramphenicol resistance marker. Fumarate reductase was also expressed in BL21(DE3) ΔIscR + pRARE.

Preparation of *E. coli* cell-free extract with fumarate hydratase

For expression of fumarate hydratase, cells were grown in LB containing 50 µg/ml kanamycin and 20 µg/ml chloramphenicol to an OD_{600} of around 0.6, after which they were placed on ice for 20 min. Heterologous gene expression was then induced by the addition of 0.2 mM IPTG (isopropyl-β-D-thiogalactopyranoside), and the cultures were grown for an additional 3 to 4 h at 37°C.

Cell-free extracts with fumarate hydratase and the empty vector control were prepared by washing the cells twice with 50 mM Tris-HCl buffer (pH 8.0) before being resuspended in 5 ml 50 mM potassium phosphate buffer (pH 7.0). Cells were lysed with a French press, after which the debris was removed by centrifugation (5 min, 20.000 x g), yielding the cell-free extract. Half of the obtained cell-free extract was given a heat treatment at 60 °C for 30 min, after which precipitated protein was removed by repeating the previous centrifugation step. Cell-free extracts stored at 4 °C.

Preparation of anaerobic *E. coli* cell-free extract with fumarate reductase

For anaerobic expression of fumarate reductase the strains were grown in Schott bottles with LB containing 100 mM MOPS buffer (pH 7.0) and 2 mM ammonium ferric citrate (i.e. Fe^{3+}), and a cotton plug. At an OD_{600} of around 0.4 bottles were placed on ice for 20 minutes, and 25 mM KNO_3, 20 µM $ZnCl_2$, 5 g/l glucose, 0.25 mM IPTG, 2 mM L-cysteine, and 1 mM $Fe(II)Cl_2$ were added from concentrated stock solutions, after which the bottle was tightly closed with a lid. The MOPS buffer was added to maintain pH during anaerobic fermentation, glucose as an extra source of energy during fermentation, Fe^{3+} and Fe^{2+} were added to function as an extra supply of iron for the formation of iron-sulfur clusters, and L-cysteine for the extra supply of sulfur, as well as a reducing agent, to create an anaerobic environment. The method for anaerobic protein production was adapted from [151]. The NO_3 was added as an electron acceptor to allow anaerobic respiration, and to repress the native fumarate reductase of *E. coli* [120]. The Zn^{2+} was added as there is evidence that heterodisulfide reductases could contain zinc, although this is not well established [45,314]. After the cold-shock on ice, the cultures were grown at 25 °C for up to 20 hours.

The culture bottles were opened in the anaerobic chamber and poured into plastic centrifugation tubes that had been placed over-night in the anaerobic chamber. Cells were harvested via centrifugation outside of the anaerobic chamber, after which the tubes were directly placed inside. Cells were washed three times using 2 ml tubes that could fit the small centrifuge inside the anaerobic chamber. The washing buffer used contained 50 mM MOPS buffer (pH 7.0 at room temperature). Finally, the cells were resuspended in 1 – 3 ml wash buffer and lysed by sonication; 1 s on followed by 2 s off, for about 5 minutes. The supernatant (i.e. the cell-free extract) was stored at 4 °C in glass vial with a rubber stopper, to keep them without oxygen.

Preparation of anaerobic cell-free extracts of *P. thermosuccinogenes* and separation of the membrane fraction

Up to 2 l of CP medium, separated in serum bottles containing 100 ml was inoculated with 0.5 ml overnight culture per bottle. The cultivation medium and techniques are described previously [143]. After 16 hours, all bottles were place on ice for ~1 hour. Cells were harvested anaerobically, after which tightly closed centrifuge tubes were taken out of the anaerobic chamber for centrifugation at 10,000 x g for 30 minutes. Back in the anaerobic chamber, cells were resuspended in 30 ml cold anaerobic buffer (50 mM sodium phosphate buffer pH7.4, containing 100 mM KCl, 5 mM DTT and 0.5 mg/l resazurin), followed by centrifugation at 4,800 × *g* for 15 min at 4°C. The washing step was repeated once, after which the cells were resuspended in 10 ml of buffer. Cell suspension was incubated at room temperature for 45 minutes with 2.5 ul Ready-Lyse™ Lysozyme Solution (Epicentre, Wisconsin), after which the cells were lysed by sonication for 5 minutes in cycles of 1 second on and 2 seconds off. Lysate was centrifuges in a small benchtop centrifuge placed inside the anaerobic chamber (divided in smaller aliquots) for 7.5 minutes at maximum speed. The supernatant was stored anaerobically in a small glass vial, placed in the fridge. The next day, the supernatant (~11 ml) was centrifuged at 100,000 x g for two hours at 4°C, after which the supernatant was stored anaerobically as the cytoplasmic fraction. The pellet was carefully rinsed twice with 1 ml buffer, after being resuspended in 4 ml buffer; stored anaerobically as the membrane fraction.

Phospholipid extraction and detection with ammonium ferrothiocyanate

As a control for the separation of the membrane fraction from the cytoplasmic fraction, the phospholipid content of the two fractions was checked. Lipid extraction was done according to the protocol by [32]. 1 ml sample was mixed with 3.75 ml of 1:2 chloroform and methanol by vortexing, follwed by the addition of 1.25 ml chloroform and vortexing. Then, 1.25 ml dH_2O was added and the mixture was vortexed again. The mixture was centrifuged, after which the bottom phase was carefully recovered. 1 ml of the bottom phase was dried completely in a vacuum concentrator and then re-dissolved in 2 ml chloroform. Detection of phospholipids was done by adding 1 ml of ammonium ferrothiocyanate solution and vortexing vigorously for 1 minute, according to [283]. Ammonium ferrothiocyanate solution was prepared by dissolving together 27.03 g/l of ferric chloride hexa-hydrate and 30.4 g/l ammonium thiocyanate in dH_2O. Ammonium ferrothiocyanate has a red colour, and is insoluble in chloroform. However, it can form a complex with phospholipids that partitions in chloroform, giving the chloroform a clearly visible pinkish colour that can be quantified at 488 nm, as a measure of phospholipid content.

Enzyme assays

The enzyme assays were based on the detection of reduced methyl viologen (or benzyl viologen) at 578 nm. A Shimadzu U-2010 spectrophotometer in combination with a thermoelectric cell holder was used for the measurements, which were performed at 55°C.

Quartz cuvettes containing approximately 1 ml of the reaction mixture (plus added cell-free extract) were used with a 1.0-cm path length. Cuvettes were closed with small rubber stoppers and flushed with N_2 gas injected with a syringe. All reaction components were added anaerobically with syringes. Reactions were started by the addition of the cell-free extract.

The fumarate reductase assay contained 50 mM MOPS buffer (pH 7.0 at room temperature), 5 mM dithiothreitol, 10 mM sodium fumarate, 2 mM methyl viologen, and cell free extract.

The pyruvate:ferredoxin oxidoreductase assay contained 50 mM MOPS buffer (pH 7.0 at room temperature), 5 mM dithiothreitol, 0.2 mM Coenzyme A, 0.2 mM thiamine pyrophosphate, 2 mM $MgCl_2$, 10 mM sodium pyruvate, 2 mM methyl viologen, and cell free extract.

Results

Genetic evidence for a novel fumarate reductase in *P. thermosuccinogenes*

A phylogenetic tree was constructed from the flavoprotein subunits taken from a range of enzymatically studied FRDs, shown in Figure 5A. Similar to all other soluble FRDs, FrdA of *P. thermosuccinogenes* branches away from the membrane bound FRDs of the succinate:quinone oxidoreductase superfamily (including the soluble FRDs found in Aquificae). Nevertheless, the soluble FRDs also do not seem to form a tight cluster between them. By directly comparing the FrdA of *P. thermosuccinogenes* with those of *Methanothermobacter thermoautotrophicus* and *Shewanella frigidimarina* using BLASTP, it is clear that it is closer related to the former, i.e. the archaeal thiol-driven FRD.

The same seems to be reflected in the phylogenetic tree of the corresponding iron-sulfur subunits (Figure 5B); FrdB of *P. thermosuccinogenes* still branches away from those of the succinate:quinone oxidoreductase superfamily, and that of *M. thermoautotrophicus* is the closest homologue. The other soluble FRDs that branch away (in 5A) do not have an iron-sulfur subunit and are therefore not part of this tree.

The succinic acid operon in *P. thermosuccinogenes* is not conserved within the other *Hungateiclostridiaceae*, with the exception of *Ruminiclostridium josui*, which contains all the genes, save for the class II fumarate hydratase; an unrelated class I fumarate hydratase is present instead. The genes in the operon of *P. thermosuccinogenes* appear to be most homologous to those from the three known *Christensenella* species, suggesting that the operon has been acquired via lateral gene transfer.

The STRING database for protein-protein association networks was consulted to predict functional partners, using FrdA of *R. josui* as the query (*P. thermosuccinogenes* was not

included in the STRING database) [288]. Scoring based on genomic neighborhood and co-occurrence, or both parameters alone led in all three instances to the selection of FrdB together with the seven subunits of the FlxABCD-HdrABC as predicted functional partners with (very) high confidence. The small hypothetical membrane protein is also selected, but with a significantly lower score, suggestive of a less stringent functional relationship. The latter supports the possibility that it represents a novel succinate transporter, as this functionality should be easily replaceable – thus explaining a less stringent co-occurrence. Alternatively, the membrane protein could also be a membrane anchor analogous to succinate:quinone oxidoreductase superfamily, but without any direct enzymatic role in the FRD reaction. However, based on the presence of the PQ-loop, we hypothesise that CDQ83_03300 is a specific succinic acid transporter.

Based on the strong genomic association of the putative FRD in *P. thermosuccinogenes* with the FlxABCD-HdrABC complex, and the distant – but closest – homology of FrdA and FrdB with those of thiol (CoM/CoB) driven FRDs from methanogenic archaea, we propose the following two hypothetical mechanisms by which succinic acid is formed in *P. thermosuccinogenes*:

1) Two thiol groups, either from a specific cofactor (pair) or from a (small) protein are used by FRD to reduce fumarate, forming succinate. The formed disulfide bond is than reduced by the electron-bifurcating FlxABCD-HdrABC complex, using NADH, in order to regenerate the original two thiol groups, while facilitating the otherwise unfavourable reduction of ferredoxin by NADH (Figure 6A).

2) The FRD is an integral part of the electron-bifurcating FlxABCD-HdrABC complex, and NADH is directly used to reduce fumarate and ferredoxin, without an additional disulfide forming cofactor/protein (Figure 6B).

In principle, it should also be possible for NADH to function directly as the cofactor for FRD, without any electron bifurcation, as is the case with many of the other soluble FRDs. However, that would make the strong association with the FlxABCD-HdrABC complex a rather odd coincidence. Furthermore, the known NADH-dependent FRDs are not involved in the central energy metabolism, while *P. thermosuccinogenes*, a strictly anaerobic fermentative organism and likely to be constrained by its ability to produce metabolic energy, produces succinic acid as one of its main products of fermentation. It seems therefore credible that it can couple succinic acid production to additional energy conservation, in the form of reduced ferredoxin, as we hypothesize. Sridhar *et al.* (2000) [280] reported NADH-dependent reduction of fumarate in cell-free extract of *P. thermosuccinogenes*, but did not present their data. We were unable to reproduce this finding.

Experimental evidence should show whether the putative fumarate reductase is indeed involved in electron bifurcation, and whether this proceeds indirectly, via an intermediate thiol/disulfide cofactor (Figure 6A), or whether it perhaps is coupled directly to the reduction of ferredoxin by NADH (Figure 6B), and thus whether fumarate needs to be added to the ever growing list of high-redox-potential acceptors involved in FBEB. Below we present some exploratory, but as of yet inconclusive experimental results.

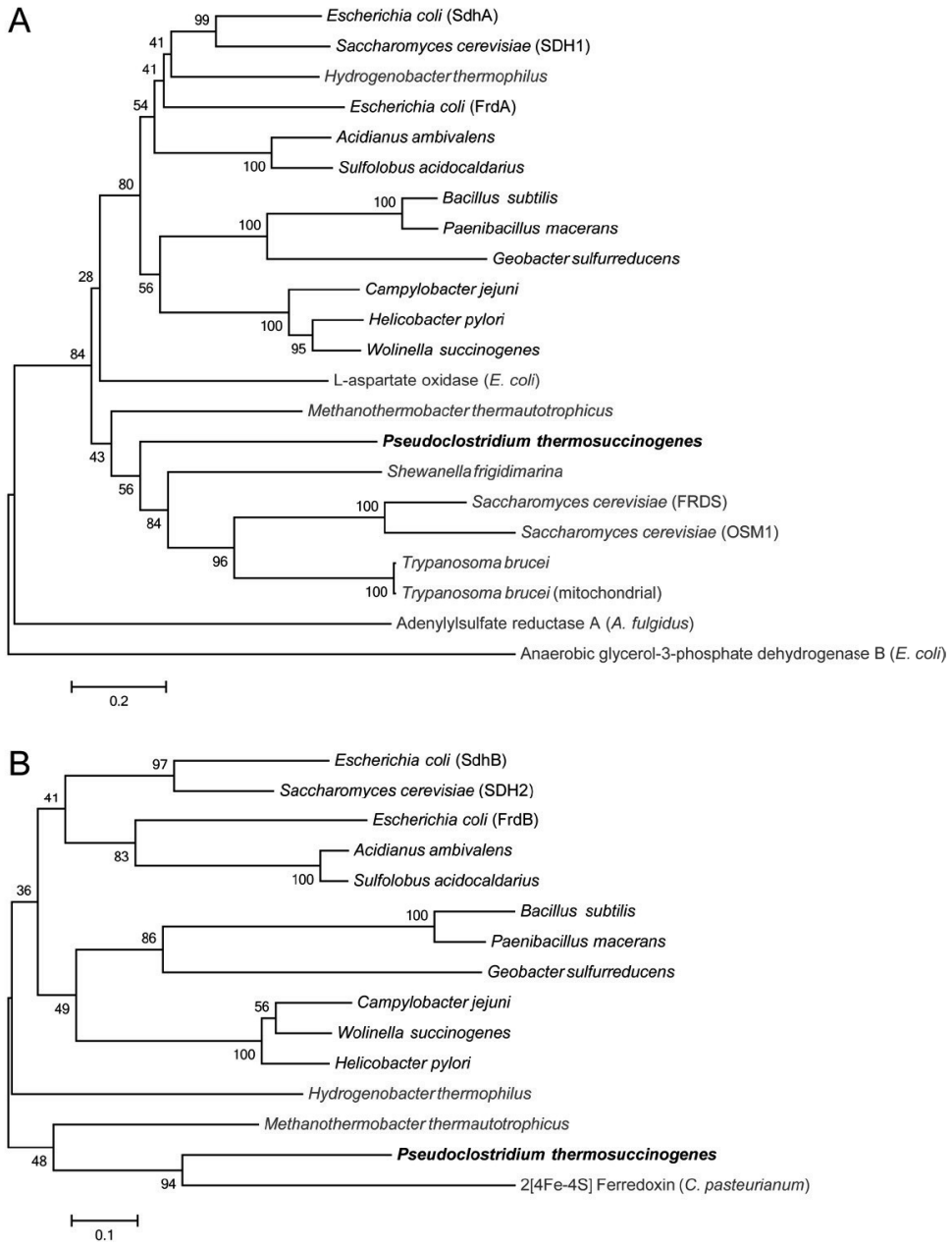

Figure 5. (A) Neighbor joining phylogenetic tree of amino acid sequences from different fumarate reductase flavoprotein subunits. Sequences of the related l-aspartate oxidase, anaerobic glycerol-3-phosphate dehydrogenases, and adenylyl-sulfate reductases are included as well. (B) Neighbor joining phylogenetic tree of amino acid sequences from different fumarate reductase iron-sulfur subunits. Sequence of a ferredoxin that also contains the 4Fe-4S iron-sulfur cluster is included as well. Reference numbers to the used sequences can be found in the material and methods section. Marked in red are the known soluble fumarate reductases, and in grey are different, but evolutionary related enzymes.

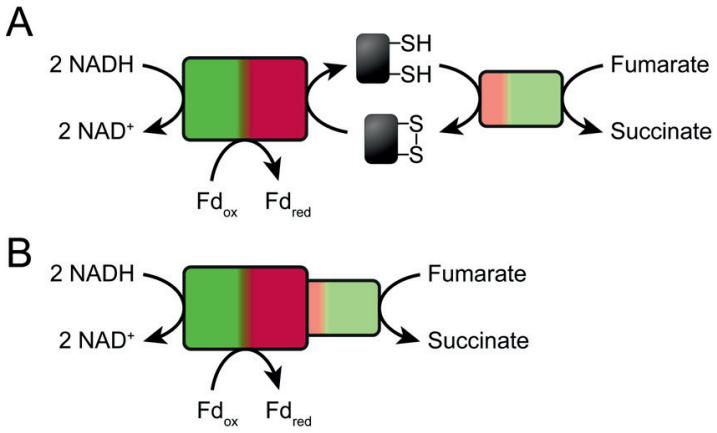

Figure 6. Two proposed hypothetical mechanisms for succinate production in *P. thermosuccinogenes*; (A) either involving an intermediate thiol/disulfide cofactor, which could be both a small molecule (pair) or a peptide, or (B) involving the direct electron transfer from NADH to fumarate, coupled to the simultaneous reduction of ferredoxin.

Experimental evidence for the 'succinic acid operon'

Tools and protocols for genetic engineering of *P. thermosuccinogenes* are currently not available. It is therefore not possible to make a knock-out of any combination of the genes present in the succinic acid operon, in order to verify its connection to succinic acid production. Instead, we attempted to express the fumarate hydratase and the fumarate reductase in *E. coli*, in order to verify their activity. We deemed it unfeasible to try to express the (full) FlxABCD-HdrABC complex for *in vitro* assays.

We were able to convincingly verify the function of CDQ83_03355 as a fumarate hydratase. Without the need for further purification, fumarate hydratase activity was detected in heat-treated cell-free extract (CFE) of *E. coli* expressing the fumarate hydratase (248 ± 11 µmol min^{-1} per mg CFE-protein), whereas heat-treated CFE of an empty vector control only showed 2% of the same activity (6 ± 5 µmol min^{-1} per mg CFE-protein).

The same was attempted by expressing FrdA (CDQ83_03310) and FrdB (CDQ83_03315) together in *E. coli*, in order to try to detect fumarate reductase activity in anaerobically prepared CFE from anaerobically grown cells. Anaerobic enzyme assays with benzyl viologen (BV) and methyl viologen (MV), non-specific electron donors/acceptors, showed slightly higher BV/MV oxidation rates for CFE expressing FrdA and FrdB compared to the empty vector control, in repeated, independent experiments. However, the difference with the empty vector control was very small; in several experiments, no difference was detected at all. Expression of FrdB in *E. coli* was very poor; the vast majority of the protein was present in the insoluble fraction. Attempts to purify the little protein present in the soluble fraction using a histidine-tag did not succeed. The cause of FrdB aggregate formation was thought to be related to the required iron-sulfur clusters, which might not be assembled properly.

A knock-out of the IscR gene in the production strain – known to improve the active expression of iron-sulfur cluster-containing proteins [4] – did also not improve expression or activity in the CFE. So, although the assays hinted at fumarate reductase activity for CDQ83_03310 and CDQ83_03315, the results were not strong enough to draw that conclusion.

To test whether fumarate reductase activity in *P. thermosuccinogenes* is present in the cytoplasm, or whether it might be membrane bound, the two fractions were separated from each other via ultracentrifugation of *P. thermosuccinogenes* CFE. Enzyme assays were done to measure fumarate reductase activity in both fractions, as well as pyruvate:ferredoxin oxidoreductase (PFOR) activity, as a control for cytoplasmic activity. Additionally, phospholipids were extracted from both fractions and detected using ammonium ferrothiocyanate, to verify whether the membrane was indeed separated from the cytoplasm. Fumarate reductase activity was found to be roughly equal between the two fraction, whereas the activity of PFOR was 10-fold enriched in the cytoplasmic fraction, as shown in Figure 7. The ammonium ferrothiocyanate test clearly confirmed the presence of phospholipids in the membrane fraction and their absence in the cytoplasmic fraction (data not shown). It seems therefore that fumarate reductase is roughly 10-fold enriched in the membrane fraction, compared to PFOR. The same experiment was repeated several times, and each time, fumarate reductase activity was enriched in the membrane, relative compared to PFOR activity. However, the degree of enrichment (i.e. the ratio of fumarate reductase activity in the membrane fraction versus the cytoplasmic fraction) seemed to vary significantly. It is possible that fumarate reductase is loosely associated with the membrane. Alternatively, if part of a (very) large protein complex, it might still end up in the pellet after ultracentrifugation (i.e. the membrane fraction), even though it is not associated with the membrane. Both possibilities – that are not mutually exclusive per se – could explain the enrichment in the membrane fraction, as well as the high variability in this degree of enrichment.

The high amount of aggregation of FrdB during the heterologous expression could also suggest that it is part of a bigger complex, as the interaction with the rest of the complex – absent during heterologous expression – is often important for proper folding.

	FRD	PFOR
CYT	0.0168	0.178
MEM	0.0183	0.0191
CYT: MEM	**0.918**	**9.32**

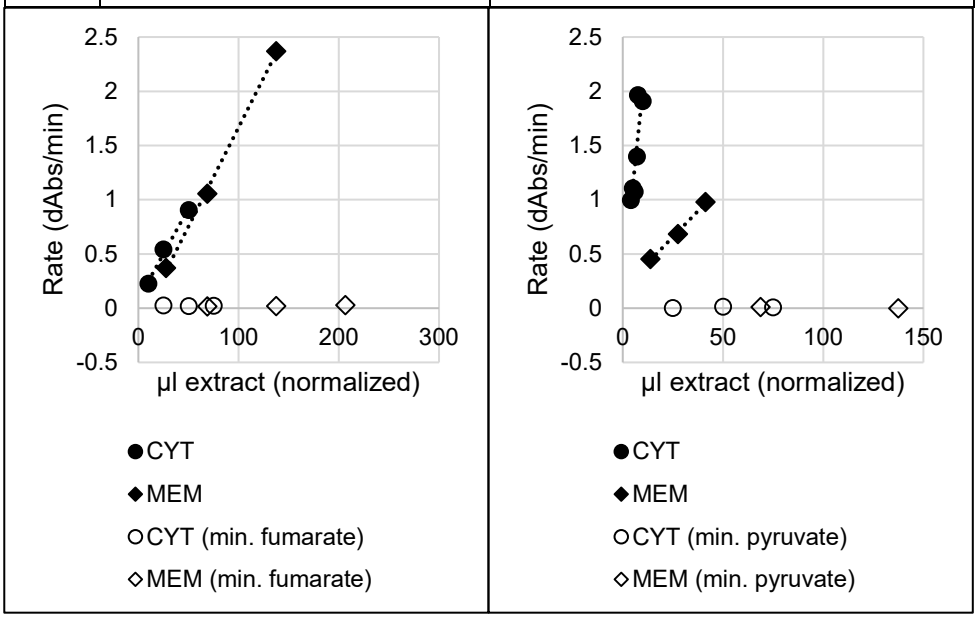

Figure 7: Rate of methyl viologen oxidation/reduction (in dAbs/min) per µl of the respective fractions added to the assay (i.e. cytoplasmic and membrane; CYT and MEM, respectively), calculated as the slope of the fitted lines. The volume of added extract is normalized for the relative concentrations, resulting from the resuspension of the membrane pellet in a smaller volume (i.e. 4 ml versus 11 ml). Assays minus fumarate were used as a control. FRD: fumarate reductase assay, PFOR: pyruvate:ferredoxin oxidoreductase assay.

Discussion

FBEB was discovered little over 10 years ago, when it was shown that electrons from NADH were transferred in parallel to ferredoxin and crotonyl-CoA. Since then, numerous other electron bifurcating reactions have been described (Figure 3) [45]. Here we propose fumarate reduction to be involved with FBEB, either directly, as a novel high-potential electron acceptor, or indirectly, via the regeneration of a disulfide bond.

Something very similar was proposed recently for the reverse TCA-cycle of sulfur-oxidizing bacteria found in symbiosis with tubeworms [245]. In those bacteria, the HdrABC-FlxABCD complex colocalizes on the genome with a FRD (homologous to the methanogenic thiol-driven FRD, TfrAB) as well as a 2-oxoglutarate:ferredoxin oxidoreductase (KorABCD). The authors propose that the electrons from NADH are transferred to fumarate and succinyl-

CoA (forming succinate and 2-oxoglutarate), either directly via the existence of a very large electron bifurcation complex (HdrABC-FlxABCD-KorABCD-TfrAB), or via the mediation of ferredoxin and/or DsrC, formed by HdrABC-FlxABCD.

Unfortunately, no methods for the transformation and genetic engineering of *P. thermosuccinogenes* have been developed yet, which would aid in functional studies into the enzymes encoded by the 'succinic acid operon'. Purification of active FlxABCD-HdrABC proteins has not yet been demonstrated [237], and was beyond the scope of this work. Our attempts for the heterologous expression of FrdA and/or FrdB of *P. thermosuccinogenes* in *E. coli* to determine the activity were inconclusive. We further experienced difficulties with the solubility of FrdB, which could be indicative of it being part of a larger enzyme complex. Ultracentrifugation of *P. thermosuccinogenes* cell-free extract appeared to enrich fumarate-dependent methyl viologen oxidation activity in the pellet/membrane fraction, which could also be indicative of it being part of a large protein complex (if not anchored to the membrane). Nevertheless, the experimental results are very limited, and more research is required to shed light on the proposed mechanisms for fumarate reduction.

If indeed the reduction of fumarate is connected to the reduction of ferredoxin, the net reaction will be: $Fumarate + 2NADH + Fd \rightarrow Succinate + 2NAD^{+} + Fd^{2-}$. Overall, this is similar to the formation of ethanol, where 2 NAD(P)H are oxidized by acetaldehyde dehydrogenase and alcohol dehydrogenase, while a ferredoxin is reduced by the preceding pyruvate:ferredoxin oxidoreductase. The pathway to succinate, however, allows for the reduction of another NADH, by malate dehydrogenase, and therefore allows extra acetate (and ATP) formation, while closing the redox balance [210]. When the reduced ferredoxin is used for proton export, via NAD^{+} reduction in the Rnf complex, the net reaction becomes $Fumarate + NADH \rightarrow Succinate + NAD^{+} + \Delta\mu_{H^{+}}$, quite like anaerobic fumarate respiration [303], except that (I) only two protons (or sodium ions) are pumped by the Rnf complex per reduced fumarate, compared to the four protons pumped by Type 1 NADH dehydrogenase, (II) ferredoxin (vs. quinone) allows for more flexibility, since it can be used in a multitude of processes that are not just membrane associated.

Acknowledgements

This research was funded by Corbion and the European Union Marie Skłodowska-Curie Innovative Training Networks (ITN), contract number 642068.

Chapter 5 – Effects of CO_2 limitation on the metabolism of *Pseudoclostridium thermosuccinogenes*

Jeroen G. Koendjbiharie[1], Willem B. Post[2], Martí Munar Palmer[2], Richard van Kranenburg[1,2]

[1] Corbion, Gorinchem, Netherlands
[2] Laboratory of Microbiology, Wageningen University & Research, Netherlands

Abstract

Bio-based succinic acid holds promise as a sustainable platform chemical. Its production through microbial fermentation concurs with the fixation of CO_2, through the carboxylation of phosphoenolpyruvate. Here, we studied the effect of the available CO_2 on the metabolism of *Pseudoclostridium thermosuccinogenes*, the only known succinate producing thermophile. Batch cultivations in bioreactors sparged with 1% and 20% CO_2 were conducted that allowed us to carefully study the effect of CO_2 limitation. Formate yield was greatly reduced at low CO_2 concentrations, signifying a switch from pyruvate formate lyase (PFL) to pyruvate:ferredoxin oxidoreductase (PFOR) for acetyl-CoA formation. The corresponding increase in endogenous CO_2 production (by PFOR) enabled succinic acid production to be largely maintained as its yield was reduced by only 26%, thus also maintaining the concomitant NADH re-oxidation, essential for regenerating NAD^+ for glycolysis. Acetate yield was slightly reduced as well, while that of lactate was slightly increased. CO_2 limitation also prompted the formation of significant amounts of ethanol, which is only marginally produced during CO_2 excess. Altogether, the changes in fermentation product yields result in increased ferredoxin and NAD^+ reduction, and increased NADPH oxidation during CO_2 limitation, which must be linked to reshuffled (trans)hydrogenation mechanisms of those cofactors, in order to keep them balanced. RNA sequencing, to investigate transcriptional effects of CO_2 limitation, yielded only ambiguous results regarding the known (trans)hydrogenation mechanisms. Those results hinted at a decreased NAD^+/NADH ratio, which could ultimately be responsible for the stress observed during CO_2 limitation. Clear overexpression of an alcohol dehydrogenase (*adhE*) was observed, which may explain the increased ethanol production, while no changes were seen for PFL and PFOR expression that could explain the anticipated switch based on the fermentation results.

Introduction

Succinic acid produced by microbial fermentation is an attractive platform chemical, with the potential to contribute to a bio-based economy. A set of different bio-based platform chemicals, such as succinic acid, allows the sustainable synthesis of the majority of our materials [320]. It is important to produce those chemicals as efficiently as possible, especially as our current market requires them to directly compete with cheap and unsustainable fossil fuel-derived alternatives. The use of thermophilic microorganisms is one of many different ways that could increase the efficiency of industrial fermentations. Primarily through a large reduction in cooling costs, and the possibility of simultaneous saccharification and fermentation, in which (hemi)cellulose-hydrolysing enzymes, functioning optimally around 50 °C, can be used simultaneously with the fermentation process itself [306].

The strictly anaerobic *Pseudoclostridium thermosuccinogenes* is the only known thermophile to produce succinic acid as one of its major fermentation products (along with acetic acid, lactic acid, formic acid, ethanol, and hydrogen gas) [74,143]. It is a close relative of the much better studied *Hungateiclostridium thermocellum* and *Hungateiclostridium cellulolyticum*, both efficient cellulose degraders that produce ethanol; *Pseudoclostridium thermosuccinogenes* is incapable of cellulose degradation, instead it is able to grow rapidly on inulin, a fructose polymer (as well as a range of C5 or C6 monosaccharides).

The metabolic pathway to succinic acid in *P. thermosuccinogenes* involves the fixation of a CO_2 molecule by the GTP-dependent phosphoenolpyruvate carboxykinase (PEPCK), converting phosphoenolpyruvate (PEP) into oxaloacetate, while forming GTP from GDP [143]. Oxaloacetate is then converted into succinate via malate dehydrogenase, fumarate hydratase, and, finally, fumarate reductase (Figure 4). The PEPCK reaction is known to operate close to its thermodynamic equilibrium, so it is likely that CO_2 concentrations can impact the growth of *Pseudoclostridium thermosuccinogenes* and/or its production of succinic acid, as is the case with several other natural succinic acid producers, which are typically considered capnophiles (organisms that thrive in the presence of CO_2) [307]. We previously speculated that the use of GTP, rather than ATP, for PEPCK and sugar phosphorylation might allow growth at lower CO_2 concentrations by modulating the thermodynamics [142]. Other reactions in the central metabolism that could be affected by different CO_2 concentrations include those catalyzed by malic enzyme (ME) and pyruvate ferredoxin oxidoreductase (PFOR), facilitating the oxidative decarboxylation of malate to pyruvate, and that of pyruvate to acetyl-CoA, respectively.

The aim of this study was to investigate how different CO_2 concentrations affect the production of succinic acid and other fermentation products by *P. thermosuccinogenes*. Fermentations were carried out in bioreactors, directly comparing 20% sparged CO_2 (v/v) with 1%, at which CO_2 was found to become limiting. A transcriptome analysis was conducted in order to look further into the mechanisms behind the observed metabolic changes triggered by CO_2 limitation.

Material and methods

Medium composition and bottle cultivations

P. thermosuccinogenes DSM 5809 was routinely cultivated anaerobically in 120-ml serum bottles containing 50 ml medium, incubated at 60 °C.

Adapted bicarbonate-buffered CP medium was used that contained per liter 0.408 g KH_2PO_4, 0.534 g $Na_2HPO_4{\cdot}2H_2O$, 0.3 g NH_4Cl, 0.3 g NaCl, 0.1 g $MgCl_2{\cdot}6H_2O$, 0.11 g $CaCl_2{\cdot}2H_2O$, 4.0 g $NaHCO_3$, 0.1 g Na_2SO_4, 1.0 g L-cysteine, 1.0 g yeast extract (BD Bacto), 0.5 mg resazurin, 1 ml vitamin solution, 1 ml trace elements solution I, and 1 ml trace elements solution II [143,231]. The medium was autoclaved in serum bottles under 80:20 N_2/CO_2 atmosphere

with ~70 kPa overpressure, containing a final volume of 50 ml medium. A solution containing $NaHCO_3$ and L-cysteine was autoclaved separately and added later as well as a solution containing $CaCl_2 \cdot 2H_2O$, to which the vitamin solution was added after it was autoclaved. Glucose was also autoclaved separately and added later to a final concentration of 2 g/l or 5 g/l.

The vitamin solution, which was 1,000× concentrated, contained per liter 20 mg biotin, 20 mg folic acid, 100 mg pyridoxine-HCl, 50 mg thiamine-HCl, 50 mg riboflavin, 50 mg nicotinic acid, 50 mg Ca-D-pantothenate, 1 mg vitamin B_{12}, 50 mg 4-aminobenzoid acid, and 50 mg lipoic acid. Trace elements solution I, which was 1,000× concentrated, contained per liter 50 mM HCl, 61.8 mg H_3BO_4, 99.0 mg $MnCl_2 \cdot 4H_2O$, 1.49 g $FeCl_2 \cdot 4H_2O$, 119 mg $CoCl_2 \cdot 6H_2O$, 23.8 mg $NiCl_2 \cdot 6H_2O$, 68.2 mg $ZnCl_2$, and 17.0 mg $CuCl_2 \cdot 2H_2O$. Trace elements solution II, which was 1,000× concentrated, contained per liter 10 mM NaOH, 17.3 mg Na_2SeO_3, 33.0 mg $Na_2WO_4 \cdot 2H_2O$, and 24.2 mg $Na_2MoO_4 \cdot 2H_2O$.

To test the effect of the different $NaHCO_3$ concentrations in bottle cultivations, the medium was buffered with 10 g/l MOPS instead, and bottles were prepared under a 100% N_2 atmosphere. The pH of the medium placed on ice had been set at 8.0, such that the pH at 60 °C would be ~7.4. $NaHCO_3$ and L-cysteine were added after autoclaving from separate stock solutions, to their desired concentrations.

Batch fermentations

Batch fermentations were carried out in DASGIP® BioBlock reactors (Eppendorf) with 0.5 l medium, that contained 5 g/l yeast extract and 25 g/l glucose. Bioreactors were autoclaved containing 420 ml of CP medium, lacking glucose, L-cysteine, $NaHCO_3$, and $CaCl_2$ with vitamins. After autoclaving, 50 ml glucose (250 g/l), 25 ml L-cysteine (20 g/l) and 5 ml $CaCl_2$ (11 g/l) + vitamins were added. After the medium was fully reduced, inoculation was done using 1 ml overnight culture from a 120-ml serum bottle. The reactors were sparged with varying concentrations of CO_2 in N_2 at a rate of 1 l/h. The pH of the medium was kept at 7.0 by titration with 3M KOH. The temperature was controlled at 60°C and stirring was done at 200 rpm.

Fermentations were carried out over a period of approximately 3 days. Samples were taken over time to measure optical density, cell dry weight, and metabolite concentrations by HPLC.

Chemostat fermentation

The continuous, chemostat fermentation was carried out in the same set-up as the batch fermentations. Glucose was intended to be the limiting component, therefore 5 g/l was used together with 1 g/l yeast extract. Furthermore, the L-cysteine concentration was halved to 0.5 g/l. The reactor was sparged with 50% (v/v) CO_2 in N_2, and the pH of the

medium was kept at 7.0 by titration with 3M KOH. The temperature was controlled at 60 °C and stirring was done at 200 rpm.

After inoculation, the culture was grown under batch conditions up to an OD_{600} of 0.8 – 1, after which the continuous feeding was started. The volume was kept constant by setting the outflow tube at the height corresponding to 0.5 l. The chemostat series at different dilution rates was started from the highest dilution rate, and steady states were assumed after three times the hydraulic retention time. Samples were taken from the outflow to measure optical density, cell dry weight, metabolite concentrations by HPLC and H_2 concentrations by gas chromatography.

HPLC

Glucose and fermentation products were analysed by HPLC using a Unity Lab Services ICS 5000+ system equipped with an Aminex HPX-87H column. The mobile phase contained 8 mM H_2SO_4 and was pumped at 0.8 ml/min through the column, which was kept at 60 °C. Samples and standards were prepared by mixing 160 µl with 40 µl of 10 mM DMSO internal standard in 5 mM H_2SO_4, in a 96-wells plate.

RNA extraction and transcriptomics

15 – 45 ml samples were taken during exponential growth in batch fermentations for transcriptome analysis. Samples were directly placed on ice, after which they were centrifuged for 10 minutes at 4,800 × g at 4 °C. The supernatant was removed and the pellet was resuspended in 10 ml RNA*later* Stabilization Solution (Qiagen) to inactivate RNases and stabilize the RNA. Samples were stored at 4°C overnight and then transferred to -20°C until further processing.

To extract the RNA, 5 ml of the cell suspension was centrifuged for 15 minutes at 4,800 × g at 4 °C. All traces of the RNA*later* were removed and the pellet was resuspended in 0.5 mL of ice-cold TE buffer (pH 8.0). The samples were divided into two 2-ml screw-cap tubes containing 0.5 g zirconium beads, 30 µl 10% SDS, 30 µl 3 M sodium acetate (pH 5.2), and 500 µl water-saturated phenol, chloroform, and isoamyl alcohol at a ratio of 25:24:1 (pH 4.5 to 5) (Roti-Aqua-P/C/I; Carl Roth, Germany). Cells were disrupted in a FastPrep apparatus (MP Biomedicals) at 6,000 rpm for 40 seconds. The tubes were centrifuged for 10 minutes at 10,000 × g at 4 °C and the aqueous phase from both tubes was pooled in a new tube. 400 µL of chloroform was added to the samples, which were then centrifuged for 3 minutes at 21,000 × g at 4 °C. 300 µL of the aqueous phase was finally transferred to a new tube, from which the RNA was purified using High Pure RNA Isolation Kit (Roche). RNA was eluted with 50 µL ultra-pure water and then stored at -80 °C.

RNA integrity was verified using the Qsep100™ capillary gel electrophoresis system (BiOptic, Taiwan). Further quality control, rRNA depletion, library preparation, sequencing,

and data analysis was carried out by BaseClear (The Netherlands). rRNA depletion was done using the MICROB*Express*™ Bacterial mRNA Enrichment Kit. Paired-end reads were generated with the Illumina NovaSeq 6000 system. Tophat2 version 2.1.1 was used to align the reads to the reference genome (NZ_NIOI01000002.1) with short read aligner Bowtie version 2.2.6 [137,157]. Cufflinks version 2.2.1 was used to conduct the differential expression analysis [304].

Results

In order to investigate the effect of the available CO_2 on the formation of succinic acid and other fermentation products by *P. thermosuccinogenes*, a series of bottle cultivations was conducted with medium containing different $NaHCO_3$ concentrations. A range of $NaHCO_3$ concentrations from 0 to 20 mM was tested, although the true concentrations are approximately 1 mM higher, through carry-over from the inoculum. 5 g/l of glucose was used, of which generally only little more than half was consumed, due to the rapid acidification of the medium. The results are presented in Figure 1A and show a stark increase in ethanol yield at lower $NaHCO_3$ concentrations, and a modest decrease in formic acid yield. Surprisingly, succinic acid did not show an apparent change in yield, and neither did acetic acid and lactic acid.

Following the small bottle experiment, a similar, but better-controlled, batch fermentation experiment was carried out using laboratory scale bioreactors, containing 0.5 l medium with 25 g/l glucose. 5 g/l yeast extract was added, instead of 1 g/l, which was otherwise found to be limiting (data not shown). Similar to the bottle experiments, 1 g/l of l-cysteine was used to reduce the medium and remove any traces of oxygen. Instead of $NaHCO_3$ additions, the medium was sparged with different concentrations of CO_2 in N_2 at 1 l/h, while being stirred at 200 rpm. The pH was maintained at 7.0. The results of the batch fermentations are shown in Figure 1B, and are comparable to what was observed for the bottle experiments, with ethanol yield increasing and formic acid yield decreasing at lower CO_2 concentrations. Figure 1C shows the growth rates at the different tested CO_2 concentrations, which are reduced over two fold at 1%, compared to 20%. No growth was observed at all when the reactor was sparged with 100% N_2.

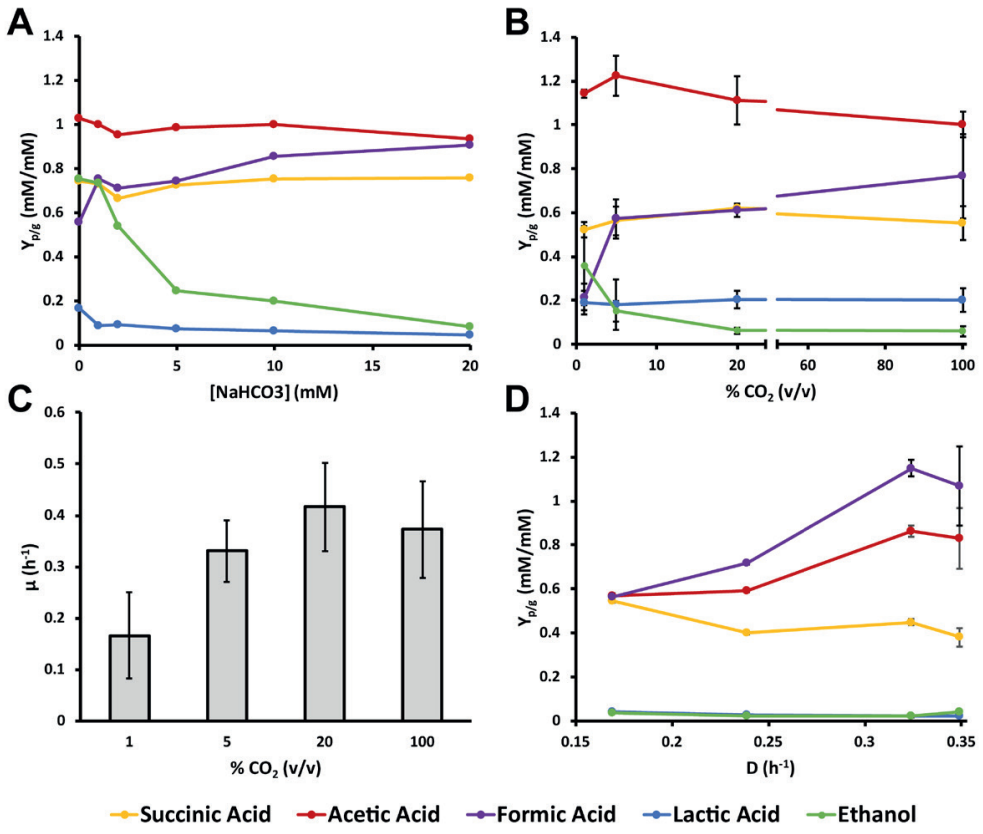

Figure 1: (A) Yield of moles fermentation product produced per consumed mole of glucose (starting concentration of 5 g/l) in serum bottle experiments containing different starting concentrations of $NaHCO_3$. 1 ml of inoculum containing ~50 mM $NaHCO_3$ was used for 50 ml medium, so the true $NaHCO_3$ concentrations are ~1mM higher. (B) Yield of moles fermentation product produced per consumed mole of glucose (starting concentration of 25 g/l) in 0.5 l batch fermentations with different concentrations of CO_2 in N_2 (v/v) sparged at 1 l/h. Every data point is the average of data from at least 3 independent fermentations, with the error bars representing the standard deviation. (C) Growth rates of the fermentations in B. (D) Yield of moles fermentation product produced per consumed mole of glucose (starting concentration of 5 g/l) in a continuous fermentation set a different (step-wise reduced) dilution rates. Every data point is the average of 3 measurements of the same steady state, taken at different time points, with the error bars representing the standard deviation.

To try to discriminate between direct effects of CO_2 concentrations and indirect effects via differences in growth rates, a chemostat fermentation was conducted at different dilution rates and a fixed CO_2 concentration. The chemostat was run similar to the batch fermentations, but medium with 5 g/l of glucose, 1 g/l yeast extract, and 0.5 g/l l-cysteine was used, and the medium was sparged with 50% CO_2. The continuous dilution with fresh medium was initiated at the end of the exponential phase, starting with the highest dilution rate. Figure 1D shows the results of the continuous fermentation. Virtually no ethanol and lactic acid are produced during any of the tested dilution rates, suggesting that the

previously observed increased ethanol yield was not the result of a lower growth rate, but is more directly the result of the lower CO_2 concentration. Formic acid, on the other hand, is produced in large amounts, and its yield also appears to decrease with decreasing growth rate. Acetic acid appears to follow a similar trend, whereas succinic acid yield seems to increase slightly. As such, it seems that the formic acid yield change might indeed be the result of the lower growth rate. Nevertheless, the change in acetic acid (and succinic acid), which was not observed (as strongly) during the batch fermentations could also indicate that another, unaccounted mechanism might be behind the observation.

In order to look more closely at what might be behind the increase in ethanol yield and decrease in formic acid yield, another set of batch fermentations was carried out, directly comparing sparging with 1% versus 20% CO_2. RNA samples were collected for sequencing to investigate transcriptional changes. The data of the fermentations are presented in Figure 2 and Figure 3.

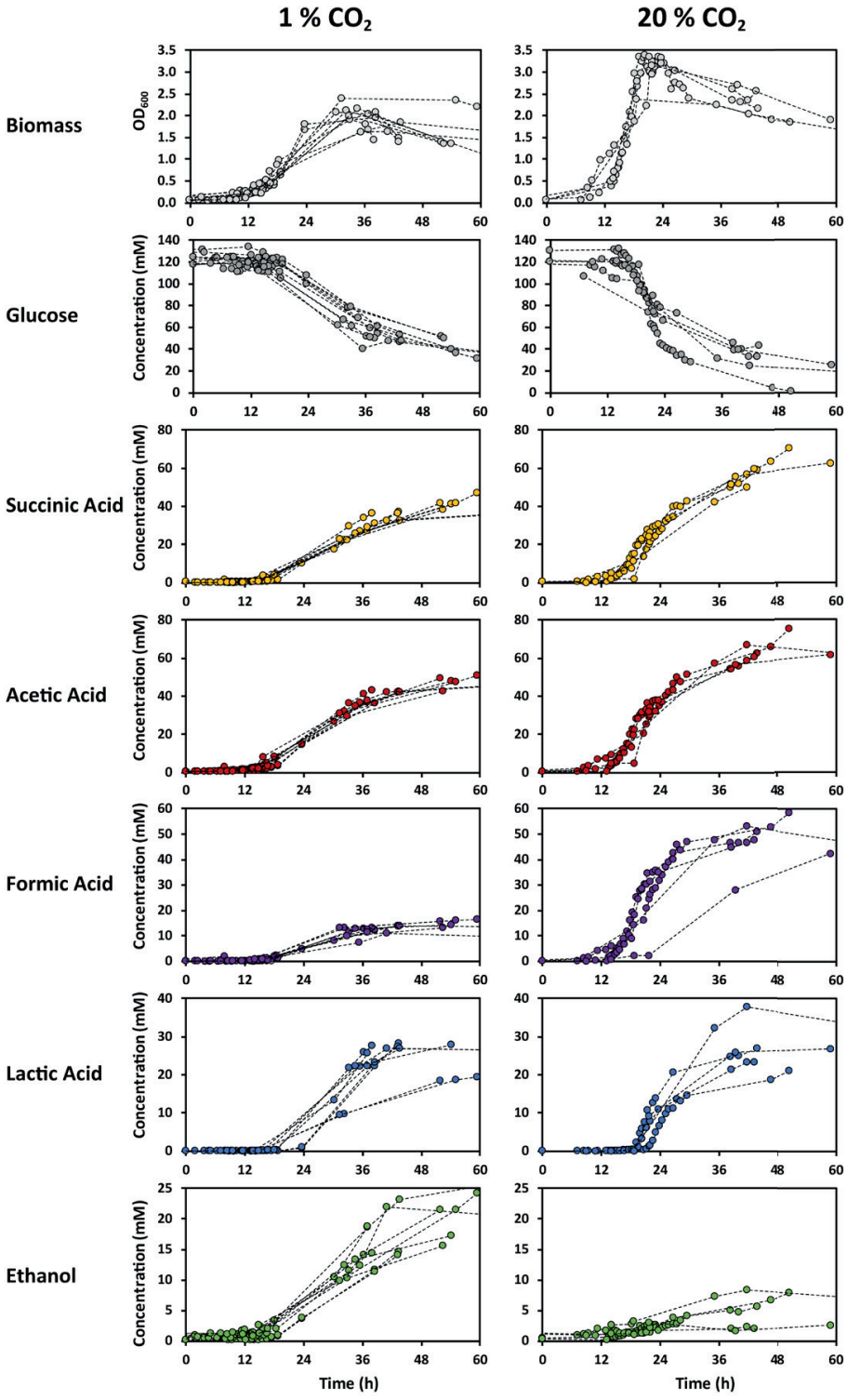
1 % CO2
20 % CO2
Biomass
Glucose
Succinic Acid
Acetic Acid
Formic Acid
Lactic Acid
Ethanol
OD600
Concentration (mM)
Time (h)

Figure 2: Optical density, and concentrations of glucose and fermentation products over-time of a series of batch fermentations (0.5 l) sparged with either 1 % or 20 % CO_2 in N_2 (v/v) at 1 l/h. The dashed lines connect data points from the same run.

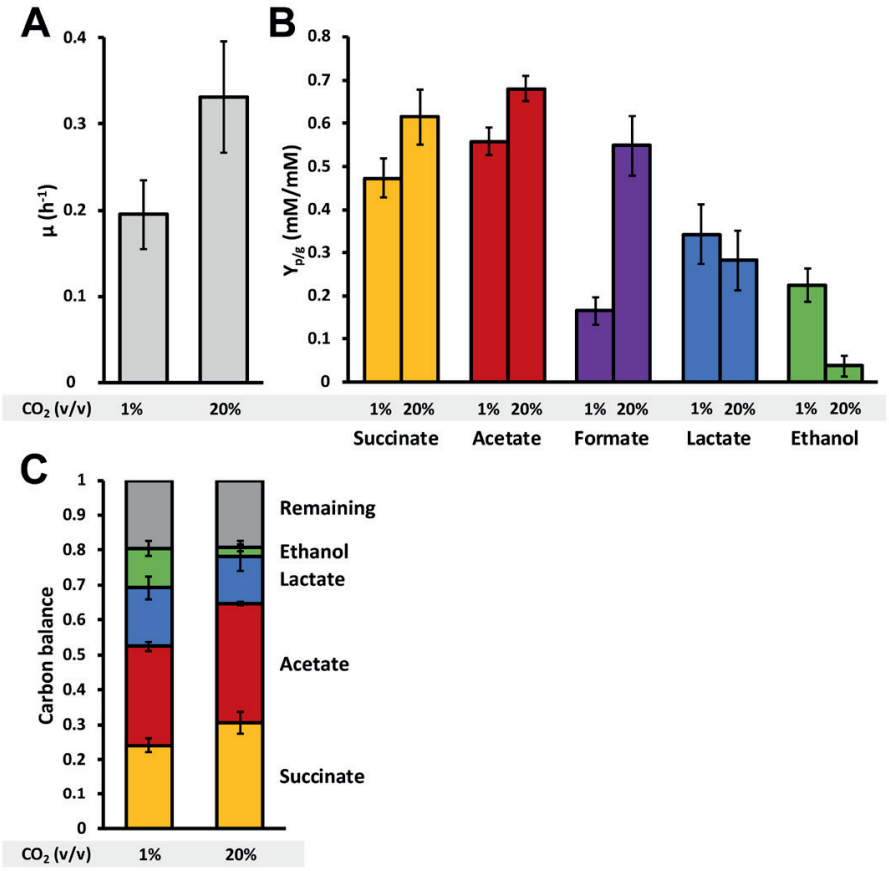

Figure 3: Growth rate (A), fermentation product yields on glucose (B), and carbon balance per mole of glucose (C) of the series of batch fermentations presented in Figure 2. Error bars represent standard deviations. The carbon balance of the consumed glucose is calculated by converting glucose to C-moles (i.e. multiplied by 6) and multiplying succinate, acetate, lactate, and ethanol by 3 (i.e. the number of C-moles from glucose consumed to generate these products, which includes CO_2 or formate formed/consumed).

Figure 2 shows that glucose consumption rates drop near the end of the fermentations, and that not all of the 25 g/l of glucose is consumed. A disparity between 1% and 20% CO_2 is also evident. The OD_{600} stabilizes within 24 hours, after which it also shows a rapid decrease. This suggests that cells are dying and/or sporulating, which would also explain the decrease in glucose consumption, and is presumably caused by salt stress resulting from titration with KOH [182,298]. Lactate production starts at the transition to the stationary phase. It was

further noted that at 1% CO_2 the cells were elongated – a typical stress response [77,127] – and that the cells formed much more sticky or slimy cell-pellets, suggestive of an increased presence of extracellular polysaccharides – another common stress response [51,286].

As before, the results show a stark decrease in formate yield, which dropped from 0.53 to 0.17 mM per mM glucose during CO_2 limitation, while ethanol yield increased from 0.05 to 0.23 mM. Lactate yield also increased slightly (0.29 to 0.34 mM/mM), and succinate and acetate yields decreased slightly (0.64 to 0.47 and 0.69 to 0.56 mM/mM, respectively). Overall, the amount of glucose channelled to succinate, acetate, lactate and ethanol combined remained identical during both conditions, as can be seen in Figure 3C. Approximately 20% of glucose is unaccounted for, and is at least partly represented by the formed biomass.

Figure 4 shows an overview of the pathways towards the different fermentation products. The yields of those products, together with their associated cofactor stoichiometry, starting from PEP, were used to calculate the cofactor (re)generation at 1% and 20% CO_2. The results of the flux balance calculations (Supplementary file 1) are presented in Table 1. During 1% CO_2, 0.42 mole extra ferredoxin per mole glucose was reduced by PFOR, resulting from the decreased pyruvate formate lyase (PFL) flux. Assuming that fumarate reductase is indeed linked to ferredoxin reduction (through NADH dehydrogenase/heterodisulfide reductase complex, as proposed in Chapter 4 [237]), it follows that overall, 0.26 mole extra ferredoxin is reduced during CO_2 limitation. Simultaneously, 0.25 mole fewer NADH and 0.18 mole extra NADPH is oxidized (the latter through the NADPH-dependent alcohol dehydrogenase of *P. thermosuccinogenes* [280]), assuming the transhydrogenase activity of the malate shunt has not changed [289]. In total, this would constitute a relative redox surplus of 0.33 electron pairs during CO_2 limitation. Presumably, this leads to extra H_2 production. Unfortunately, no H_2 data is available from the bioreactor fermentations. Serum bottle experiments, identical to those presented in Figure 1A did show an increase in H_2 production from 0.22 mole H_2 per mole glucose at 20 mM $NaHCO_3$ to 0.44 mole H_2 at 1 mM $NaHCO_3$, suggesting indeed that more H_2 is formed during CO_2 limitation. If we simply assume that 1 ATP-equivalent is generated per PEP to pyruvate conversion, 0.18 mole fewer ATP is generated during CO_2 limitation, of which the majority (0.13 mole) is due to the decrease in acetate yield.

Following these results, it seems that during CO_2 limitation mechanisms must exist for the oxidation of the extra reduced ferredoxin and NADH, as well as for the reduction of the extra $NADP^+$, which strongly suggests that (besides increased hydrogen production) electrons are being transferred from ferredoxin and/or NADH to $NADP^+$. A differential expression analysis was performed through RNA sequencing, in order to find-out what mechanism might be responsible for the change in (redox) metabolism.

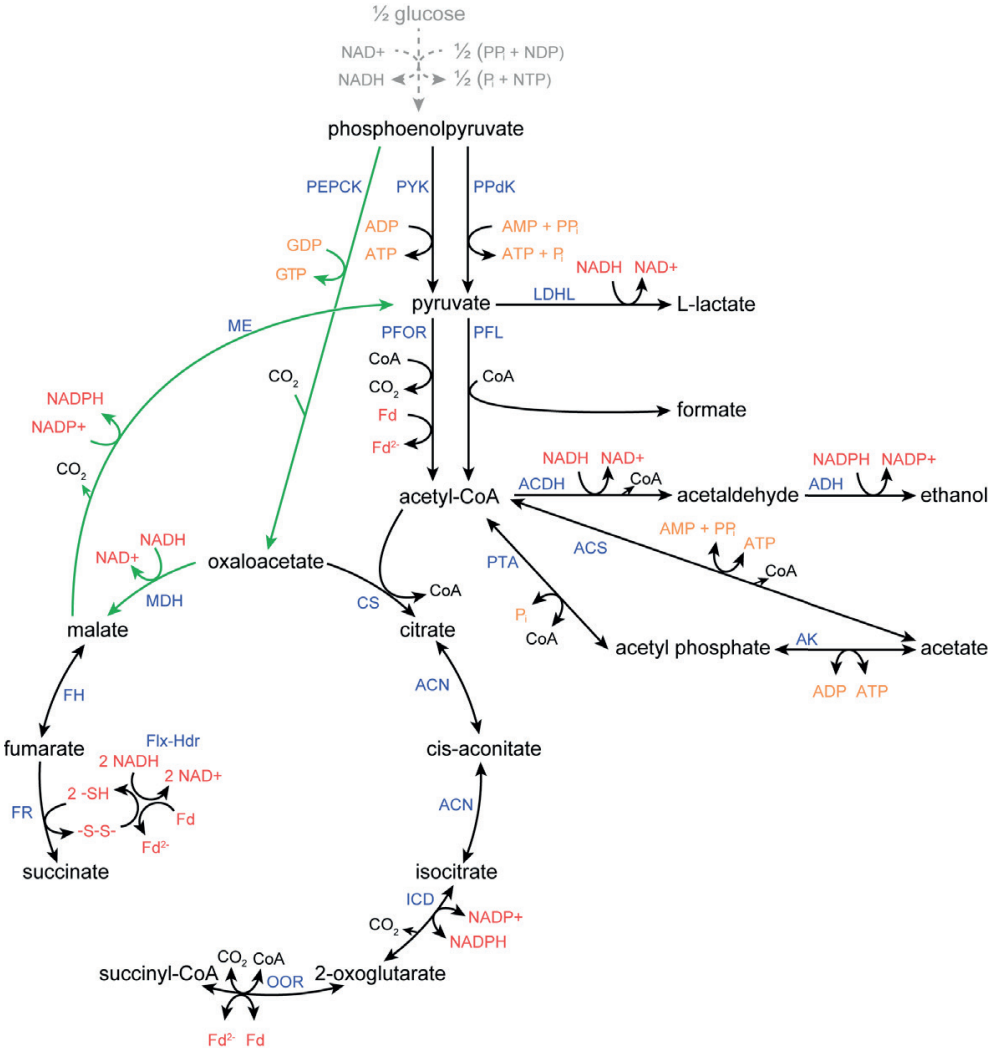

Figure 4: Metabolic pathways from phosphoenolpyruvate (PEP) to the different fermentation products in *P. thermosuccinogenes*. The dashed grey arrow represents the glycolysis, which relies on a PP_i-dependent phosphofructokinase. The green arrows represent the malate shunt for the conversion of PEP to pyruvate. ACDH, acetaldehyde dehydrogenase; ACN, aconitase; ACS, acetyl-CoA synthetase; ADH, alcohol dehydrogenase; AK, acetate kinase; CS, citrate synthase; Flx-Hdr, NADH dehydrogenase/heterodisulfide reductase bifurcation complex; FH, fumarate hydratase; FR, fumarate reductase; ICD, isocitrate dehydrogenase; LDHL, l-lactate dehydrogenase; MDH, malate dehydrogenase; ME, malic enzyme; OOR, 2-oxoglutarate:ferredoxin oxidoreductase; PEPCK, phosphoenolpyruvate carboxykinase; PFL, pyruvate formate lyase; PFOR, pyruvate:ferredoxin oxidoreductase; PPdK, pyruvate, phosphate dikinase; PTA, phosphate acetyltransferase; PYK, pyruvate kinase.

Table 1: Moles of different cofactors or pathway intermediates generated per mole of glucose consumed, calculated using the different product yields as shown in Figure 3 and stoichiometry of the pathways from phosphoenolpyruvate to the different fermentation products (i.e. the NADH/ATP-equivalents consumed/produced in glycolysis are not considered), as depicted in Figure 4. Calculations based on the assumption that there is no difference in transhydrogenation by the malate shunt between 1% and 20% CO_2, and that 1 ATP-equivalent is formed in the conversion from phosphoenolpyruvate to pyruvate.

	1% CO_2	20% CO_2	Difference
Acetyl-CoA	0.79	0.73	0.05
$Fd_{reduced}$ (PFOR only)	0.62	0.20	0.42
$Fd_{reduced}$	1.09	0.84	0.26
NADH	-1.99	-2.25	0.25
NADPH	-0.23	-0.05	-0.18
Total redox cofactors	-1.13	-1.45	0.33
ATP (AK only)	0.56	0.68	-0.13
ATP-equivalents	2.16	2.34	-0.18

Biological triplicates of exponentially growing cells from the batch fermentations were used for RNA sequencing. 5.4 – 10.4 million reads (paired-end, 150 bp) were generated per sample and used to conduct a differential expression analysis between 1% and 20% CO_2 (Supplementary data 2). As can be seen in Figure 5A, one of the seven (putative) alcohol dehydrogenases annotated in *P. thermosuccinogenes* is significantly overexpressed during CO_2 limitation, namely *adhE* (CDQ83_RS17615) – a bifunctional acetaldehyde-CoA/alcohol dehydrogenase that was previously shown to be the relevant isoform for ethanol formation in *H. thermocellum* and *T. saccharolyticum* [179]. Surprisingly, neither of the two annotated PFOR genes were differentially expressed, as shown in Figure 5B, nor were any of the genes coding for other central metabolic enzymes involving CO_2 formation or fixation. None of the genes for PFLs or (putative) PFL-activating enzymes were differentially expressed either (Figure 5B).

The most differentially over-expressed genes during CO_2 limitation include a glutamate synthase (CDQ83_RS06935 and CDQ83_RS06940), glutamine synthetase (CDQ83_RS16740), as well as several other genes related to glutamate/amino acid metabolism, summarized in Figure 7. Furthermore, three genes (CDQ83_RS11600, CDQ83_RS11605, and CDQ83_RS11610) that seem to encode for a putative oxidoreductase complex are highly over-expressed during CO_2 limitation as well. CDQ83_RS11600 encodes a small DUF1667 domain-containing protein; CDQ83_RS11605 an FAD-dependent oxidoreductase related to the small chain of thioredoxin reductase, glutamate synthase, CoA disulfide reductase, and ferredoxin-$NADP^+$ reductase; and CDQ83_RS11610 an NAD(P)/FAD-dependent oxidoreductase related to L-2-hydroxyglutarate dehydrogenase (mitochondrial) and glycerol-3-phosphate dehydrogenase. The three genes are located

downstream of a glycerol-3-phosphate responsive antiterminator protein and upstream of a glycerol kinase.

The 'succinate operon', encoding fumarate hydratase, fumarate reductase and the NADH dehydrogenase/heterodisulfide reductase bifurcation complex showed a statistically significant increase in expression level of approximately 4-fold. Conversely, the ion-translocating reduced ferredoxin:NAD^+ oxidoreductase (RNF) complex showed a decrease of approximately 2-fold. Besides the RNF complex, *P. thermosuccinogenes* possesses several other known enzymes involved in (trans)hydrogenation, summarized in Figure 6; none of these are differentially expressed, except for a cluster of genes related to NADH-quinone oxidoreductase (CDQ83_RS11525-45) that could potentially encode a hydrogenase complex.

Interestingly, a large cluster of genes (CDQ83_RS11365-420 that appear to be organized into three adjacent operons) predicted to be involved in fucose and mannose metabolism is overexpressed during CO_2 limitation. It is plausible that this relates to the sticky phenotype that was observed for the cells grown at 1% CO_2.

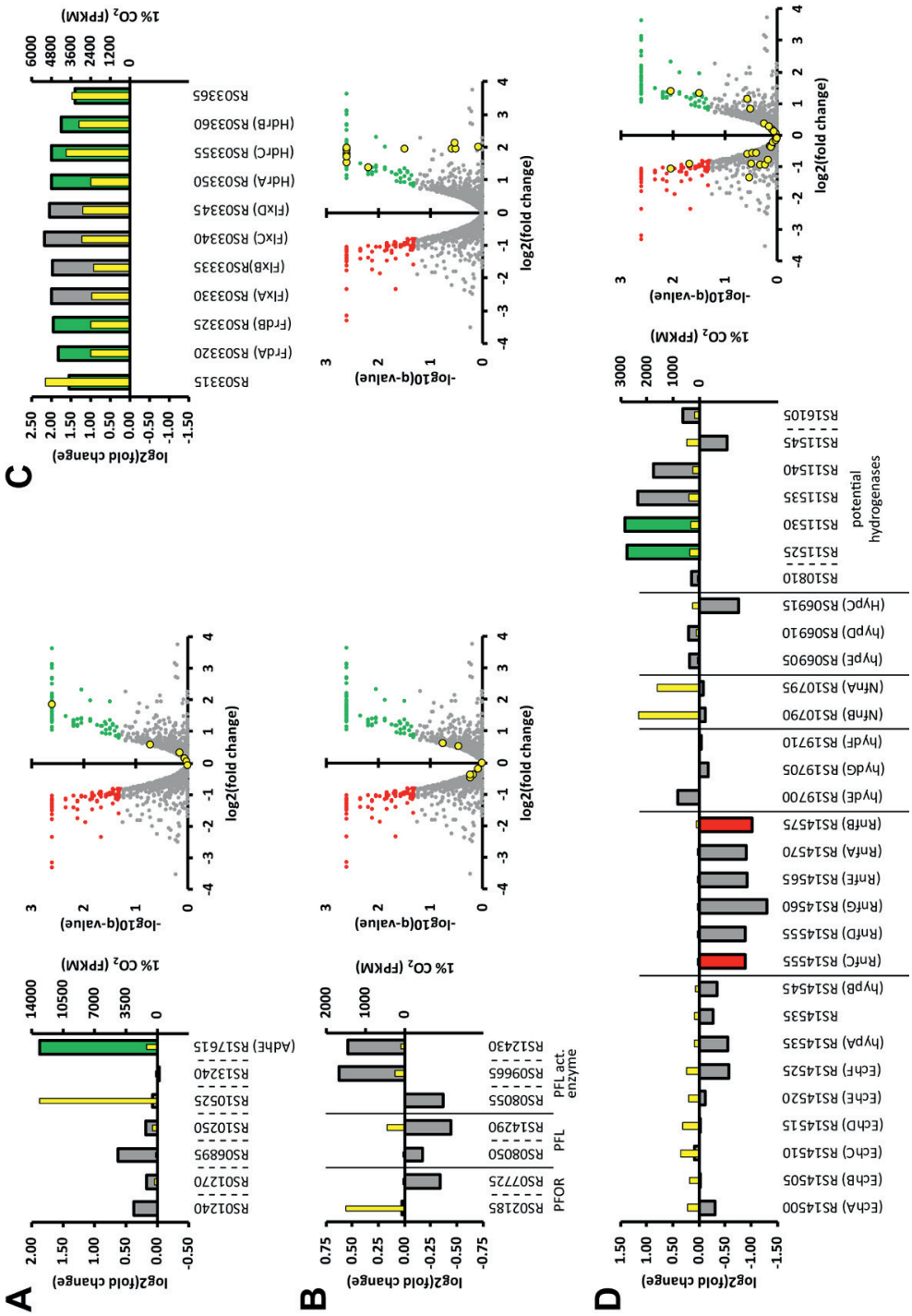
A
log2(fold change)
2.00
1.50
1.00
0.50
0.00
-0.50
1% CO2 (FPKM)
14000
10500
7000
3500
0
RS01240
RS01270
RS06895
RS10250
RS10525
RS13240
(AdhE) RS17615
-log10(q-value)
log2(fold change)
B
log2(fold change)
0.75
0.50
0.25
0.00
-0.25
-0.50
-0.75
1% CO2 (FPKM)
2000
1000
0
RS02185
RS07725
RS08050
RS14290
RS08055
RS09665
RS12430
PFOR
PFL
PFL act. enzyme
-log10(q-value)
log2(fold change)
C
log2(fold change)
2.50
2.00
1.50
1.00
0.50
0.00
-0.50
-1.00
-1.50
1% CO2 (FPKM)
6000
4800
3600
2400
1200
0
RS03315
(FrdA) RS03320
(FrdB) RS03325
(FlxA) RS03330
(FlxB)RS03335
(FlxC) RS03340
(FlxD) RS03345
(HdrA) RS03350
(HdrC) RS03355
(HdrB) RS03360
RS03365
-log10(q-value)
log2(fold change)
D
log2(fold change)
1.50
1.00
0.50
0.00
-0.50
-1.00
-1.50
1% CO2 (FPKM)
3000
2000
1000
0
(EchA) RS14500
(EchB) RS14505
(EchC) RS14510
(EchD) RS14515
(EchE) RS14520
(EchF) RS14525
(HypA) RS14535
RS14535
(HypB) RS14545
(RnfC) RS14555
(RnfD) RS14555
(RnfG) RS14560
(RnfE) RS14565
(RnfA) RS14570
(RnfB) RS14575
(HydE) RS19700
(HydG) RS19705
(HydF) RS19710
(NfnB) RS10790
(NfnA) RS10795
(HypE) RS06905
(HypD) RS06910
(HypC) RS06915
RS10810
RS11525
RS11530
RS11535
RS11540
RS11545
RS16105
potential hydrogenases
-log10(q-value)
log2(fold change)

Figure 5: Selected results from differential expression analysis. Positive fold change represents an increase of mRNA coverage during CO_2 limitation (i.e. 1% versus 20% CO_2). In the volcano plots, green data points depict genes with a statistically significant increase (i.e. q-value < 0.05) during CO_2 limitation and red data points those with a statistically significant decrease in coverage during CO_2 limitation. Yellow data points correspond to the genes presented in the accompanying bar graph. In the bar graphs, the wide bars display the log2(fold change) and the narrow (yellow) bars display the mean coverage in FPKM during 1% CO_2. (A) Results for potential alcohol dehydrogenases (including AdhE). (B) Results for two annotated pyruvate:ferredoxin oxidoreductases (PFOR), two annotated pyruvate formate lyases (PFL), and three (potential) PFL-activating enzymes. (C) Results for the 'succinate operon', harbouring fumarate hydratase (CDQ83_RS03365), an electron bifurcating NADH dehydrogenase/heterodisulfide reductase complex (CDQ83_RS03360-30), fumarate reductase (CDQ83_RS03325-20), and a hypothetical protein (CDQ83_RS03315; potentially a succinic acid transporter). (D) Results for the energy-converting [NiFe] hydrogenase with hydrogenase maturation factors (Ech; CDQ83_RS14500-45); the ion-translocating reduced ferredoxin:NAD^+ oxidoreductase (Rnf; CDQ83_RS14555-75); HydEFG [FeFe] hydrogenase maturation factors; electron bifurcating ferredoxin:$NADP^+$ reductase (Nfn; CDQ83_RS10790-95); HypCDE [NiFe] hydrogenase maturation factors (CDQ83_RS06905-15); and three potential hydrogenases (CDQ83_RS10810, CDQ83_RS11525-45, and CDQ83_RS16105).

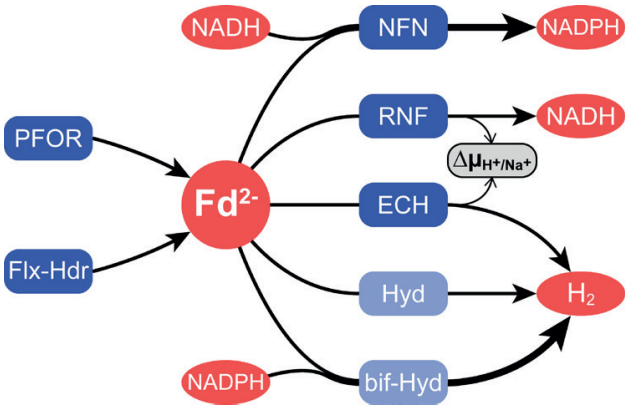

Figure 6: Overview of major (trans)hydrogenase reactions involving ferredoxin in *P. thermosuccinogenes*. Arrow represent the flow of electrons. PFOR: pyruve:ferredoxin oxidoreductase; Flx-Hdr: NADH dehydrogenase/heterodisulfide reductase bifurcation complex; NFN: NADH-dependent reduced ferredoxin:$NADP^+$ oxidoreductase; RNF: ion-translocating reduced ferredoxin:NAD^+ oxidoreductase; ECH: energy-converting [NiFe] hydrogenase; Hyd: hydrogenase; bif-Hyd: bifurcating hydrogenase. It is not entirely clear what hydrogenases are present besides ECH. The presence of several genes potentially encoding hydrogenases, and of [FeFe] hydrogenase maturation factors does suggest *P. thermosuccinogenes* possesses additional hydrogenases.

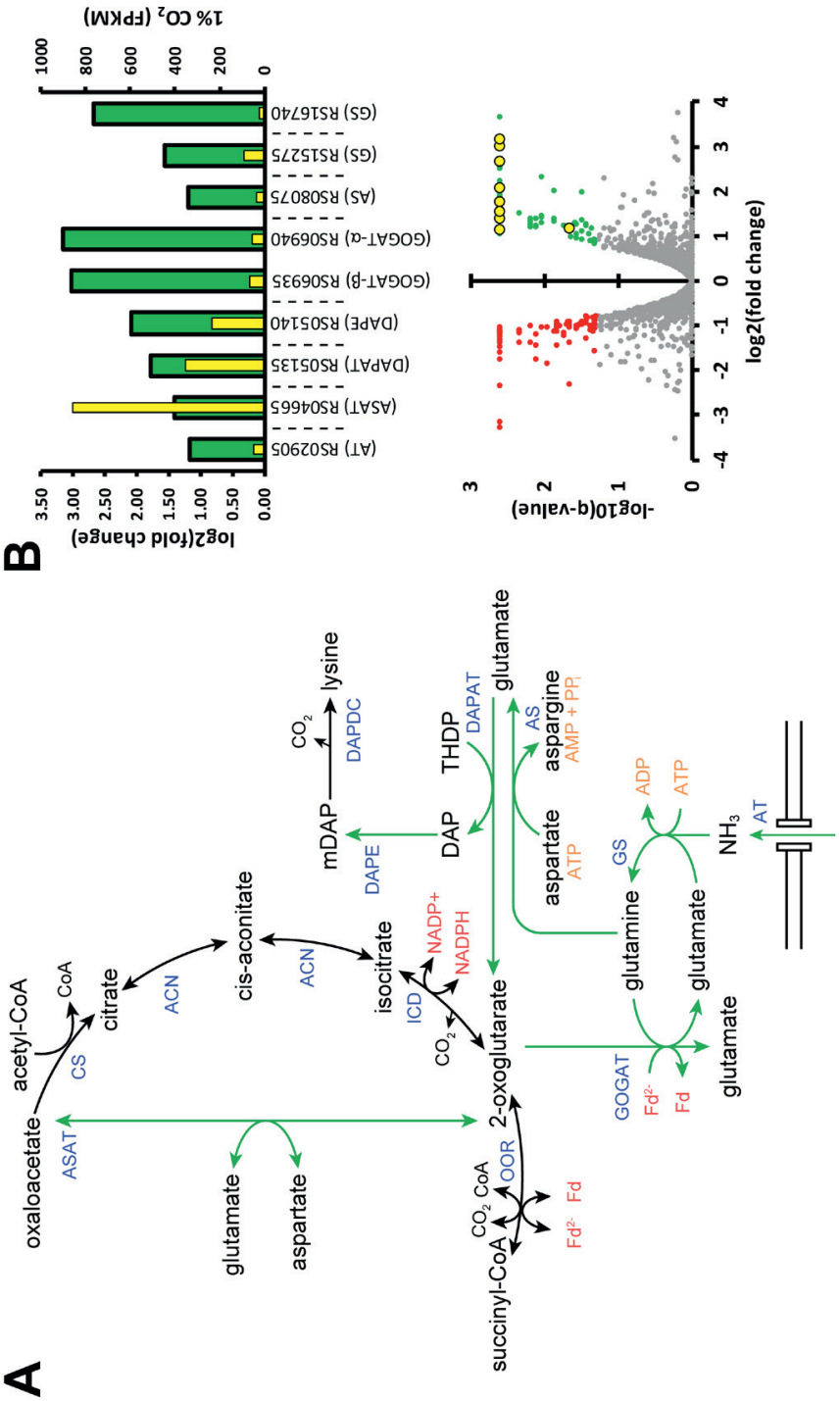
A
oxaloacetate
acetyl-CoA
CoA
CS
citrate
ACN
cis-aconitate
ACN
isocitrate
ICD
NADP+
NADPH
CO2
2-oxoglutarate
CO2 CoA
OOR
succinyl-CoA
Fd2- Fd
ASAT
glutamate
aspartate
mDAP
CO2
lysine
DAPDC
DAPE
DAP
THDP
DAPAT
glutamate
AS
asparagine
AMP + PPi
aspartate
ATP
GS
ADP
ATP
glutamine
glutamate
NH3
AT
GOGAT
Fd2-
Fd
glutamate
B
log2(fold change)
1% CO2 (FPKM)
(AT) RS02905
(ASAT) RS04665
(DAPAT) RS05135
(DAPE) RS05140
(GOGAT-β) RS06935
(GOGAT-α) RS06940
(AS) RS08075
(GS) RS15275
(GS) RS16740
-log10(q-value)
log2(fold change)

Figure 7: (A) Overview of the statistically significantly overexpressed reaction (green) involved in glutamate metabolism during CO_2 limitation. ACN, aconitase; AS, asparagine synthase (CDQ83_RS08075); ASAT, aspartate transaminase (CDQ83_RS04665); AT, ammonium transporter (CDQ83_RS02905); CS, citrate synthase; DAPAT, l,l-diaminopimelate aminotransferase (CDQ83_RS05135); DAPDC, diaminopimelate decarboxylase; DAPE, diaminopimelate epimerase (CDQ83_RS05140); GOGAT, ferredoxin-dependent glutamate synthase (CDQ83_RS06935-40); GS, glutamine synthethase (CDQ83_RS15275 & CDQ83_RS16740); ICD, isocitrate dehydrogenase; OOR, 2-oxoglutarate:ferredoxin oxidoreductase. (B) Results from differential expression analysis for the genes involved in the highlighted reactions in A. Positive fold change represents an increase of mRNA coverage during CO_2 limitation (i.e. 1% versus 20% CO_2). In the volcano plots, green data points depict genes with a statistically significant increase (i.e. q-value < 0.05) during CO_2 limitation and red data points those with a statistically significant decrease in coverage during CO_2 limitation. Yellow data points correspond to the genes presented in the accompanying bar graph. In the bar graphs, the wide bars display the log2(fold change) and the narrow (yellow) bars display the mean coverage in FPKM during 1% CO_2.

Discussion

PFOR versus PFL

Upon CO_2 limitation, decarboxylation reactions (where a carboxyl group is removed) become thermodynamically more favourable, whereas the reverse (i.e. carboxylation) becomes less favourable [20]. A large number of metabolic pathways, both catabolic and anabolic, involve (de)carboxylation reactions and it is therefore likely that the observed effects during CO_2 limitation are either directly or indirectly related to the thermodynamic changes. In general, a certain amount of CO_2 is required for many microorganisms to thrive [69,239], as was also demonstrated by the complete lack of growth of *P. thermosuccinogenes* during fermentations sparged with pure N_2. The predominant catabolic (de)carboxylation reactions of *P. thermosuccinogenes* are PEPCK, malic enzyme, and PFOR. Phosphogluconate dehydrogenase in the oxidative pentose phosphate pathway is only marginally expressed, while isocitrate dehydrogenase and 2-oxoglutarate:ferredoxin oxidoreductase only fulfil an anabolic role (due to the incomplete TCA-cycle).

Of the three major catabolic (de)carboxylases, only PEPCK operated in the CO_2-fixing direction, through which the production of succinic acid leads to net CO_2 fixation, while the malate shunt does not lead to net CO_2 fixation (or generation), because of subsequent decarboxylation by malic enzyme. In fact, the amount of CO_2 required by PEPCK for the observed succinic acid production at 1% CO_2 (~20 mmol in a 24 hours window) is higher than the CO_2 provided (0.01 l/h * 24 h * 22.4^{-1} mol/l = ~11 mmol), which can only mean that endogenous CO_2 is being used to facilitate succinic acid formation. The source of endogenous CO_2 is PFOR (being the only anabolic net-CO_2-forming reaction), which produces 0.62 mole CO_2 per mole glucose, compared to the 0.47 mole required for succinic acid production. During 20% CO_2, only 0.20 mole CO_2 is produced by PFOR versus 0.64 mole required for succinic acid. Therefore, it seems that the switch from PFL to PFOR (i.e. from formate production to that of CO_2 and reduced ferredoxin) allows succinic acid formation and its concomitant NADH sink to proceed in the absence of the required exogenous CO_2.

The re-oxidation of more than one NADH through succinate production allows the subsequent generation of extra ATP via the (redox neutral) pathway to acetate.

Whether the switch from PFL to PFOR is intentional (i.e. regulated) is not clear. It does not appear to be regulated on a transcriptional level. (Post)-Translational or allosteric regulation is still possible, but it could simply be a thermodynamic effect, since PFOR becomes more favourable relative to PFL during CO_2 limitation. Recent data from Dash *et al*. (2019) show that the free energy change of PFOR in *H. thermocellum* (a close relative of *P. thermosuccinogenes*) changes quite drastically during the course of a batch fermentation, being close to 0 in the beginning of the fermentation [66]. With a ΔG allowed close to 0, at which its rate is very sensitive to changes in reactant concentrations, it is fully plausible that the switch from PFL to PFOR in *P. thermosuccinogenes* upon CO_2 limitation is a thermodynamic effect.

Changes in redox metabolism

The overall consequence of the observed metabolic changes is an increased need for ferredoxin and NADH oxidation, and $NADP^+$ reduction. It is credible then to assume that part of the ferredoxin and NADH are used for the reduction of $NADP^+$, which could occur through the electron bifurcating ferredoxin:NADP+ reductase (NFN; Figure 6) [316]. Again, no transcriptional changes occur that could indicate increased NFN activity. Of course, it is still wholly plausible that there is an increase in NFN-flux. The flux through the malate shunt might also change, increasing NADH to NADPH transhydrogenase activity. Alternatively, the putative oxidoreductase complex that is most differentially upregulated might encode a novel protein complex involved in the transfer of electrons from ferredoxin (and NAHD) to $NADP^+$. Further research into this putative oxidoreductase complex is required, however. Its genomic association with glycerol kinase would in fact suggest a relation to membrane lipid synthesis.

Unlike NFN, the ion-translocating reduced ferredoxin:NAD^+ oxidoreductase (RNF) seems to be transcriptionally downregulated, albeit statistically significant for only two of the six subunits. Conversely, the succinic acid operon, harbouring the bifurcating NADH dehydrogenase/heterodisulfide reductase complex (Flx-Hdr), is upregulated, albeit also not statistically significant for all subunits. RNF transfers electrons from ferredoxin to NAD^+, whereas Flx-Hdr transfers electrons from NADH to ferredoxin (and thiols) [237] (Chapter 4). The transcriptional effects could therefore indicate that the excess of NADH is more pressing than the excess of ferredoxin, as they would result in reduced transfer of electrons from ferredoxin to NADH. This is conceivable, considering the fact that ferredoxin can be re-oxidized relatively easily through the formation of hydrogen. The observed stress could therefore be the result of a decreased NAD^+/NADH ratio, which is (for example) known to inhibit glyceraldehyde-3-phosphate dehydrogenase, decreasing glucose consumption and growth [90,95,96].

Sridhar & Eiteman (2001) attempted to decrease the NAD^+/NADH ratio of *P. thermosuccinogenes* throught the addition of 85% H_2 to the headspace, which resulted in almost completely abolished succinate and formate production and greatly reduced lactic acid production, with their fluxes completely diverted to ethanol [279]. This is surprising, as in most natural succinate producers, H_2 addition enhances succinate production [116,161,319]. Nevertheless, it fits the notion that *P. thermosuccinogenes* has a unique fumarate reductase, coupling succinate formation to ferredoxin reduction (Chapter 4), since inhibition of hydrogenases by high H_2 partial pressure would impair ferredoxin reducing reactions [155,296]. In the same study, confusingly, decreased culture redox potential (CRP; assumed to increase NADH availability) by addition of Na_2S resulted in the complete opposite effect as H_2 addition. Overall, there seems to be a very complex interplay between pH, CRP, as well as H_2 and CO_2 on the fermentation profile of *P. thermosuccinogenes*.

CO_2 limitation in succinic acid producers

The premise of this investigation was the idea that succinic acid formation would be strongly impacted by the concentration of CO_2, asserted from the CO_2-fixing PEPCK reaction, which is believed to operate close to equilibrium [329], as well as from evidence from other succinic acid producers. A decrease of 26% in succinate yield was observed, which albeit significant is smaller than the 65% decrease seen for *Anaerobiospirillum succiniciproducens*, and 72% for *Actinobacillus succinogenes*, summarized in Table 2 with results from literature. *Mannheimia succiniciproducens* shows a decrease of 14%. However, the lowest amount of CO_2 tolerated by *M. succiniciproducens* was many times higher than that for *P. thermosuccinogenes*. Beyond the general observed decrease in succinic acid yield upon CO_2 limitation, the response in terms of the other fermentation products varies widely between different succinic acid producers (Table 2). E.g. where *P. thermosuccinogenes* shows a stark decrease in formate yield, *A. succinogenes* shows an increase, while the formate yield of *A. succiniproducens* is unaffected, but was already low to begin with. In more recent work into CO_2 limitation in *A. succinogenes*, two specific CO_2 threshold concentrations were found. Below 8.4 mM dissolved CO_2 (or 37% saturation), the glucose consumption rate decreased while the flux distribution (i.e. yields) between succinate, acetate and formate remained constant. Below 3.9 mM dissolved CO_2 (or 17% saturation), the yield of succinate also decreased, as flux was diverted towards other products [113].

Like *P. thermosuccinogenes*, *A. succiniciproducens* has a PFOR and a PFL [250], while *A. succinogenes* and *M. succiniciproducens* have a pyruvate dehydrogenase (PDH) instead of a PFOR [42,140], forming NADH instead of reduced ferredoxin. Additionally, *P. thermosuccinogenes* has a GTP-dependent PEPCK, whereas the other three have ATP-dependent versions. We previously speculated that GTP-dependent PEPCK might allow growth at lower CO_2 concentrations [142]. However, the data from literature presented in Table 2 are not sufficient to support that, as not enough other succinate producers relying

on GTP-dependent PEPCK (e.g. *Fibrobacter succinogenes* [97]) have been studied during CO_2 limitation and the tested limiting CO_2 concentrations cannot be adequately compared.

Conclusion

Through bioreactor cultivations of *Pseudoclostridium thermosuccinogenes* sparged with 1% and 20% CO_2 we studied the effect of CO_2 limitation on its metabolism. Formate yield is greatly reduced as the pyruvate to acetyl-CoA flux shifts from pyruvate formate lyase (PFL) to pyruvate:ferredoxin oxidoreductase (PFOR). This shift is presumably caused by more favourable decarboxylase thermodynamics of PFOR upon CO_2 limitation, but might also be actively regulated, as the resulting endogenous CO_2 formation is able to compensate the CO_2 required to sustain the succinate flux. Succinate yield is (only) reduced by 26%. Acetate yield is slightly reduced as well, while that of lactate is slightly increased. CO_2 limitation also prompts the formation of significant amounts of ethanol, which is only marginally produced during CO_2 excess. Overall, the changes in those product yields are associated with increased ferredoxin and NAD+ reduction, and increased NADPH oxidation during CO_2 limitation, which must result in altered (trans)hydrogenation mechanisms of those cofactors, in order to keep them balanced. Transcriptional changes show a clear overexpression of an alcohol dehydrogenase (*adhE*), while no change in PFL and PFOR expression is observed. Transcription results are more ambiguous regarding the altered (trans)hydrogenation mechanisms, but they hint at a decreased NAD^+/NADH ratio, which might ultimately be responsible for the stress observed during CO_2 limitation.

Table 2: Comparison with other studies looking into the effects of CO_2 limitation on succinic acid producers grown on glucose. SA: succinate, AA: acetate, FA: formate, LA: lactate, EtOH: ethanol, PA: pyruvate. Biomass and product yields are given in mol/mol glucose. Growth rate in h^{-1}.

Organism	SA	AA	FA	LA (PA)	EtOH	Biomass	Growth rate	CO_2 provided	Ref.
Anaerobiospirillum succiniciproducens[a]	1.21	0.67	0.12	0.00	0.00	1.13	?[f]	0.98 mol $MgCO_3$ / mol glucose	[250]
	0.43	0.16	0.12	0.87	0.09	0.44	?	0.065 mol $MgCO_3$ / mol glucose	
Actinobacillus succinogenes	0.69	0.84	0.88	?	0.18	1.07	?	1.00 mol $MgCO_3$ / mol glucose	[319]
	0.19	0.81	1.20	?	0.71	1.08	?	0.10 mol $MgCO_3$ / mol glucose	
Mannheimia succiniciproducens[b]	0.70	?	?	?	?	0.18 g/g	1.12	100% CO_2 at 0.25 vvm (23 mM)	[274]
	0.60	?	?	?	?	0.13 g/g	0.78	37% CO_2 at 0.25 vvm (8.7 mM)	
Escherichia coli AFP111[c]	1.10	0.12	?	(0.20)	0.12	?	?	50% CO_2 at 0.42 vvm	[181]
	0.79	0.09	?	(0.39)	0.08	?	?	3% CO_2 at 0.42 vvm	
Escherichia coli BA207[d]	1.46	0.48	?	(0.04)	?	1.72 g/l	?	100% CO_2 at 0.13 vvm	[177]
	1.07	0.27	?	(0.12)	?	0.42 g/l	?	0% CO_2 at 0.13 vvm	
Corynebacterium glutamicum[e]	0.87	0.28	?	0.42	?	-	0	100% CO_2	[236]
	0.29	0.13	?	1.22	?	-	0	0% CO_2	
Pseudoclostridium thermosuccinogenes	0.64	0.69	0.53	0.29	0.05	?	0.33	20% CO_2 at 0.033 vvm	This study
	0.47	0.56	0.17	0.35	0.23	?	0.20	1% CO_2 at 0.033 vvm	

[a] Growth rate decreased by almost 50% during CO_2 limitation.
[b] *M. succiniproducens* shows severely suppressed growth at CO_2 concentrations below 8.7 mM
[c] *Escherichia coli* AFP111 has mutations in pfl, ldhA, ptsG. During 0% CO_2 succinic acid yield dropped to 0.06.
[d] *Escherichia coli* BA207: *E. coli* K12, ΔpflB, ΔldhA, Δppc, pTrc-pncB-pyc.
[e] Non-growing high-density cell suspensions.
[F] Not known (?)

Acknowledgements

This research was funded by Corbion and the European Union Marie Skłodowska-Curie Innovative Training Networks (ITN), contract number 642068.

Supplementary data

Supplementary file 1

Yields (mol/mol glucose)

	1%	St dev	20%	St dev
Acetate	0.560019	0.032931	0.686697	0.029221
Succinate	0.474664	0.046133	0.637693	0.054757
Lactate	0.344226	0.069586	0.285975	0.066152
Formate	0.166577	0.031695	0.533579	0.056401
Ethanol	0.225331	0.039411	0.046433	0.024449

Analysed system

Assumed that:

- 1 ATP (equivalent) is generated per PEP to pyruvate conversion, regardless if pyruvate kinase; pyruvate, phosphate dikinase; or the malate shunt is used.
- There is no difference in the transhydrogenase activity of the malate shunt.
- Fumarate reductase is linked to the electron bifurcating NADH dehydrogenase/heterodisulfide reductase complex.

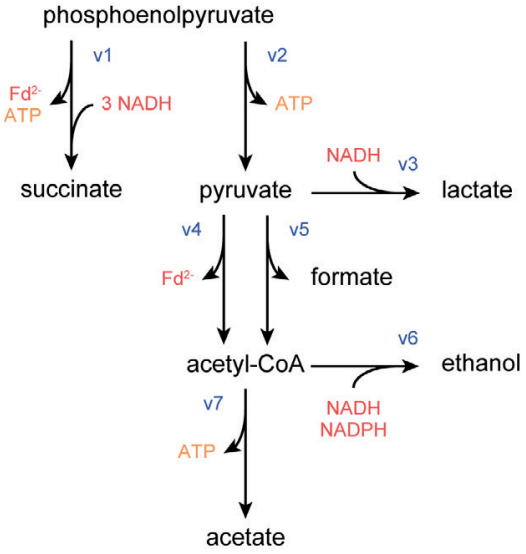

v1 = $Y_{SA/G}$

v2 = v3 + v6 + v7 = $Y_{LA/G} + Y_{EtOH/G} + Y_{AC/G}$

v3 = $Y_{LA/G}$

v4 = v6 + v7 – v5 = $Y_{EtOH/G} + Y_{AC/G} - Y_{FA/G}$

v5 = $Y_{FA/G}$

v6 = $Y_{EtOH/G}$

v7 = $Y_{AC/G}$

Cofactors/pathway intermediates generated (mol/mol glucose)

		1% CO_2	20% CO_2
NADH	(-3 * v1) + (-1 * v3) + (-1 * v6)	-1.993549664	-2.24548692
NADPH	(-1 * v6)	-0.225330504	-0.046433034
Fd^{2-}	(1 * v1) + (1 * v4)	1.093437725	0.837244389
Fd^{2-} (v4 only)	(1 * v4)	0.618773324	0.199551296
Total redox	NADH + NADPH + Fd^{2-}	-1.125442443	-1.454675566
ATP	(1 * v1) + (1 * v2) + (1 * v7)	2.164259833	2.343495278
ATP (v7 only)	(1 * v7)	0.560019485	0.686697271
Acetyl-CoA	(1 * v6) + (1 * v7)	0.785349989	0.733130305

Supplementary file 2

Supplementary_data_Chapter5_file2.txt

Chapter 6 - The pentose phosphate pathway of cellulolytic clostridia relies on 6-phosphofructokinase instead of transaldolase

Jeroen G. Koendjbiharie[1*], Shuen Hon[2,3*], Martin Pabst[4], Robert Hooftman[5], David M. Stevenson[6], Jingxuan Cui[3,7], Daniel Amador-Noguez[3,6], Lee R. Lynd[2,3,7], Daniel Olson[2,3], Richard van Kranenburg[1,5]

[1] Corbion, Netherlands
[2] Thayer School of Engineering, Dartmouth College, NH, USA
[3] Center for Bioenergy Innovation, Oak Ridge National Laboratories, TN, USA
[4] Cell Systems Engineering, Delft University of Technology, Netherlands
[5] Laboratory of Microbiology, Wageningen University & Research, Netherlands
[6] Department of Bacteriology, University of Wisconsin-Madison, WI, USA
[7] Department of Biological Sciences, Dartmouth College, NH, USA
[*] Contributed equally

Chapter has been published as:

Koendjbiharie, Jeroen G., et al. "The pentose phosphate pathway of cellulolytic clostridia relies on 6-phosphofructokinase instead of transaldolase." *Journal of Biological Chemistry* (2019): jbc-RA119.

Abstract

Most cellulolytic clostridia species are not annotated to contain a transaldolase gene. Therefore, they must possess a pathway that is able to connect pentose metabolism with the rest of the metabolism, for assimilating pentose sugars, and/or for generating C_5 precursors (such as ribose) during growth on other (non-C_5) substrates. Here we provide evidence that for this connection cellulolytic clostridia rely on the sedoheptulose 1,7-bisphosphate (SBP) pathway, using pyrophosphate-dependent phosphofructokinase (PP_i-PFK) instead of transaldolase. In this reversible pathway, sedoheptulose 7-phosphate (S7P) is converted to SBP, by PFK, after which fructose bisphosphate aldolase cleaves SBP into dihydroxyacetone phosphate and erythrose 4-phosphate. We show that PP_i-PFK of *Clostridium thermosuccinogenes* and C*lostridium thermocellum* indeed is able to convert S7P to SBP, and that they have similar affinity for S7P and fructose 6-phosphate (F6P), the canonical substrate. By contrast, (ATP-dependent) PfkA of *Escherichia coli* (which does rely on transaldolase) has a very poor affinity for S7P. This is indicative of the fact that the PP_i-PFK of the cellulolytic clostridia has evolved for the use of S7P. We further show that *C. thermosuccinogenes* contains a significant SBP pool, an otherwise unusual metabolite, which is elevated during growth on xylose, demonstrating its relevance for pentose assimilation. Lastly, we demonstrate that a second PFK of *C. thermosuccinogenes* that operates with ATP and GTP shows unusual kinetics towards F6P, as it appears to have an extremely high degree of cooperative binding, resulting in a virtual on/off switch for substrate concentrations near its $K_{1/2}$ value.

Introduction

Transaldolase plays a key role in the non-oxidative pentose phosphate pathway (PPP). Together with transketolase it is responsible for the interconversion of C_5 and C_3/C_6 metabolites, as depicted in Figure 1. Specifically, transaldolase transfers a three-carbon ketol unit from sedoheptulose 7-phosphate (S7P) to glyceraldehyde 3-phosphate (G3P), forming erythrose 4-phosphate (E4P) and fructose 6-phosphate (F6P). Transketolase is responsible for the transfer of a two-carbon ketol unit from xylulose 5-phoshate, either to ribose 5-phosphate, yielding the S7P and G3P used by transaldolase, or to E4P – one of the products of transaldolase – yielding G3P and F6P. In contrast to the oxidative part, the non-oxidative PPP is reversible and essential both for catabolism of pentoses (e.g. xylose) and for the production of the C_5 metabolites required for anabolism during growth on other substrates. The latter can also be facilitated by the oxidative PPP, but is then accompanied with the formation of NADPH, another important role of the PPP in many organisms.

Several cellulolytic Clostridia[1] have been reported to lack an annotated transaldolase gene, while at least a few of those are able to grow very efficiently on pentose sugars, including *Clostridium thermosuccinogenes* and *Clostridium cellobioparum* subsp. *termitidis*, and *Clostridium stercorarium* [143,208,259]. This implies that an alternative route to link C5 to the rest glycolysis must be present in those organisms. In *C. thermosuccinogenes* only the genes in the PPP responsible for the conversions of C5 sugars to xylulose 5-phosphate (i.e. xylose transporters, xylose isomerase, and xylulokinase) were upregulated during growth on xylose versus glucose [143]. In *C. termitidis*, a transketolase was found to be upregulated as well, during growth on xylose or xylan versus cellobiose [208]. Yet, neither of those transcriptome studies resulted in an obvious candidate for an alternative pathway. *Clostridium thermocellum* also lacks an annotated transaldolase, but in contrast to the other cellulolytic Clostridia, it cannot grow on xylose [184]. However, it lacks the oxidative PPP as well (present in *C. thermosuccinogenes*) [154], so *C. thermocellum* would still be expected to have an alternative route, in order to produce the C_5 metabolites required for anabolism.

While most organisms use transketolase/transaldolase, several alternative pathways to convert C_5 to C_3/C_6 intermediates are known to exist (Figure 2):

The phosphoketolase pathway (PKP). In the PKP, xylulose 5-phosphate is directly cleaved with orthophosphate into acetyl-P and G3P by phosphoketolase [287]. The PKP is responsible for the degradation of pentose sugars in lactic acid bacteria, but more recently, it was shown that PKP is also, at least partly, responsible for pentose utilization in a variety of other bacteria, including *Clostridium acetobutylicum* and cyanobacteria [93,176,324].

The Weimberg pathway & Dahms pathway. The Weimberg pathway is a 5-step, oxidative, non-phosphorylating pathway that converts pentoses into 2-oxoglutarate, an intermediate in the TCA-cycle [44,318]. In the Dahms pathway 2-keto-3-deoxy-D-xylonate or 2-keto-3-deoxy-L-arabinonate, intermediates in the Weimberg pathway, are cleaved by an aldolase

[1] 'Cellulolytic Clostridia' refers to a large group of mesophilic and thermophilic bacteria of which most are able to grow on (hemi)cellulosic substrates, and of which *Clostridium thermocellum* and *Clostridium cellulolyticum* are probably the most well-studied. Recently, they have been placed within a newly named family called *Hungateiclostridiaceae*, containing genus names such as *Hungateiclostridium* and *Pseudoclostridium* [330], and for a brief while some also referred to cellulolytic clostridia as the *Ruminiclostridium* genus [141,326]. However, even more recently, the family name *Hungateiclostridiaceae* and the corresponding genus names were suggested to be illegitimate and placement within the *Acetivibrio* genus was proposed [300]. In light of this ongoing discussion, we have decided to refer to them as 'cellulolytic Clostridia', and use the commonly used names *Clostridium thermocellum* and *Clostridium thermosuccinogenes* for the organisms of interest in this study (instead of *Hungateiclostridium thermocellum* and *Pseudoclostridium thermosuccinogenes*). Note that *C. thermosuccinogenes* ferments a wide range of C5 and C6 sugars, and sugar polymers, but not crystalline cellulose.

into pyruvate and glycolaldehyde [44,63]. Both variants of the pathway occur in prokaryotes.

The sedoheptulose 1,7-bisphosphate pathway. In the amoebozoan *Entamoeba histolytica*, which lacks both glucose 6-phosphate dehydrogenase and transaldolase, S7P was shown to be the substrate of a pyrophosphate (PP_i)-dependent 6-phosphofructokinase (PFK). The resulting sedoheptulose 1,7-bisphosphate (SBP) is subsequently cleaved into dihydroxyacetone phosphate (DHAP) and E4P by fructose bisphosphate aldolase, effectively replacing the function of transaldolase, shown in Figure 2 [285]. PP_i-PFK is physiologically reversible, in contrast to ATP-dependent PFK, allowing it to function in the PPP. Although, a number of reports exists where S7P kinase activity with high affinity is documented for PPi-PFKs from methanotrophs [129,135,240,244], the study discussed above is the only one where the SBP-pathway was shown to exist in a wild-type metabolism. A double transaldolase knock-out in *Escherichia coli* (Δ*talAB*) resulted in xylose degradation via the SBP-pathway, in conjunction with its native ATP-PFK and fructose bisphosphate aldolase enzymes. In addition, S7P and SBP were observed to accumulate [211].

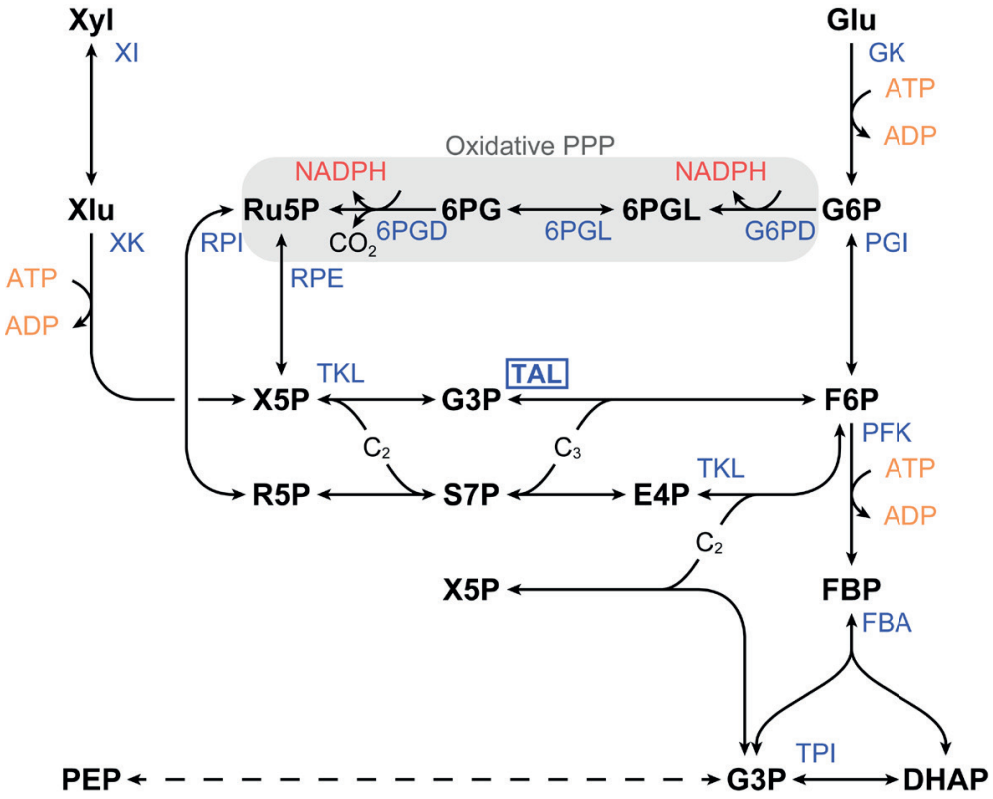

Figure 1: The reactions of the pentose phosphate pathway and its connection to the C3/C6 metabolites of the *Embden–Meyerhof–Parnas* (EMP) pathway. PFK: 6-phosphofructokinase; 6PG: 6-phosphogluconate; 6PGD: 6-

phosphogluconate dehydrogenase; 6PGL: 6-phosphogluconolactone; DHAP: dihydroxyacetone phosphate; E4P: erythrose 4-phosphate; FBP: fructose 1,6-bisphosphate; F6P: fructose 6-phosphate; FBA: fructose bisphosphate aldolase; GK: glucokinase; Glu: glucose; G6P: glucose 6-phosphate; G6PD: glucose-6-phosphate dehydrogenase; G3P: glyceraldehyde 3-phosphate; Pi: orthophosphate; PEP: phosphoenolpyruvate; PGI: phosphoglucoisomerase; PPi: pyrophosphate; R5P: ribose 5-phosphate; RPI: ribose 5-phosphate isomerase; Ru5P: ribulose 5-phosphate; RPE: ribulose 5-phosphate 3-epimerase; S7P: sedoheptulose 7-phosphate; TAL: transaldolase; TKL: transketolase; TPI: triosephosphate isomerase; Xyl: xylose; XI: xylose isomerase; XK: xylulokinase; Xlu: xylulose; X5P: xylulose 5-phosphate. The dashed arrow represents the trunk or lower part of the glycolysis, which consist of several reactions. X5P is shown in two different locations in the diagram for clarity. The grey box indicates reactions in the oxidative PPP.

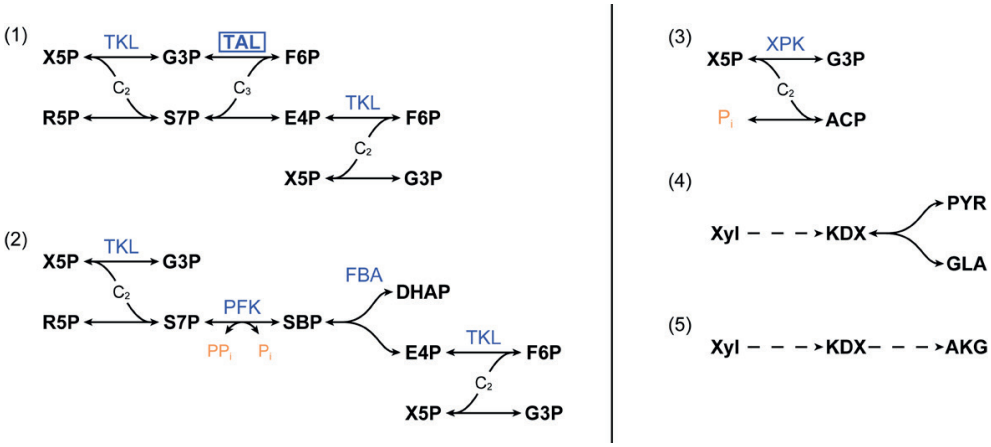

Figure 2: Overview of the different pathways known for the interconversion of C_5 and C_3/C_6 metabolites. (1) Typical pentose phosphate pathway involving transketolase and transaldolase. (2) Sedoheptulose 1,7-bisphosphate pathway. (3) Phosphoketolase pathway. (4) Dahms pathway. (5) Weimberg pathway. ACP: acetyl phosphate; AKG: α-ketoglutarate; DHAP: dihydroxyacetone phosphate; E4P: erythrose 4-phosphate; F6P: fructose 6-phosphate; FBA: fructose bisphosphate aldolase; G3P: glyceraldehyde 3-phosphate; GLA: glycolaldehyde; KDX: 2-keto-3-deoxy-d-xylonate; PFK: 6-phosphofructokinase; P_i: orthophosphate; PP_i: pyrophosphate; PYR: pyruvate; R5P: ribose 5-phosphate; SBP: sedoheptulose 1,7-bisphosphate; S7P: sedoheptulose 7-phosphate; TAL: transaldolase; TKL: transketolase; X5P: xylulose 5-phosphate; XPK: xylulose 5-phosphate phosphoketolase; Xyl: xylose. Dashed arrows represent more than one reaction.

There is no real indication (genomic or physiological) for any of the routes other than the SBP-pathway, which follows on the reliance of cellulolytic clostridia on PP_i-PFKs, analogous to *E. histolytica*. Hence, the SBP-pathway is generally assumed to be the responsible pathway [65,247], but this has never been experimentally verified. This is not a trivial exercise, as metabolites required for enzyme assays are difficult to acquire and stable isotopic labelling studies are complicated by the recursive nature of the PPP and the typically low thermodynamic driving force in anaerobic metabolism, leading to relative high reverse fluxes [66,121].

SBP should be a rather uncommon metabolite in bacteria without the Calvin-cycle, the only known pathway with SBP as intermediate. In this cycle, SBP is formed from E4P and DHAP by aldolase and cleaved by sedoheptulose bisphosphatase. Besides algae and plants, some non-photosynthetic eukaryotes have also been reported to possess this enzyme [220], but it has not been annotated in any of the cellulolytic Clostridia. Therefore, presence of an SBP pool alone in *C. thermosuccinogenes* would already be a strong, albeit indirect, indication for the presence of the SBP-pathway. The first aim of this study was therefore to investigate the possible presence of SBP in *C. thermosuccinogenes*, using high mass-resolution Orbitrap mass spectrometry. Unfortunately, an SBP reference standard was not commercially available, due to poor chemical stability. Instead, we constructed an *E. coli* Δ*talAB* strain with a double transaldolase knock-out, which accumulated SBP [211]. We were able to use metabolite extracts from this strain as an SBP reference.

The accumulation of S7P in addition to SBP in *E. coli* Δ*talAB* suggests that *E. coli* PFK has a low affinity for S7P. However, this is expected, since activity towards SBP is not necessary in *E. coli* because of the presence of transaldolase. If the PP_i-PFKs of cellulolytic clostridia are indeed natively responsible for the conversion of S7P in the PPP, one would expect a much higher affinity for S7P. Therefore, the second aim of the study was to confirm *in vitro*, the ability of PFKs of to phosphorylate S7P and to compare their affinity for S7P vs. F6P.

Material and methods

Growth medium and cultivation

For strain construction, plasmid construction, and protein purification, *E. coli* strains were grown on LB medium containing per liter 10 g tryptone, 5 g yeast extract, 10 g NaCl.

For metabolome extraction, *E. coli* BW25113 was grown on M9 minimal medium, made with M9 Minimal Salts (5X) from Sigma, containing additionally 0.4% xylose, 1 mM $MgSO_4$, 0.3 mM $CaCl_2$, 1 mg/l biotin, and 1 mg/l thiamine hydrochloride, that were all separately sterilized. Cells were grown at 37 °C in shake flasks containing 50 ml medium, inoculated with 0.5 ml overnight culture grown in LB.

C. thermosuccinogenes was grown anaerobically in adapted CP medium [231], as described previously [143], which contained per liter 0.408 g KH_2PO_4, 0.534 g $Na_2HPO_4{\cdot}2H_2O$, 0.3 g NH_4Cl, 0.3 g NaCl, 0.1 g $MgCl_2{\cdot}6H_2O$, 0.11 g $CaCl_2{\cdot}2H_2O$, 4.0 g $NaHCO_3$, 0.1 g Na_2SO_4, 1.0 g l-cysteine, 1.0 g yeast extract (BD Bacto), 1 ml vitamin solution, 1 ml trace elements solution I, and 1 ml trace elements solution II. No resazurin was added to eliminate the possibility of it interfering with the metabolomics, as it appeared to adsorb to the nylon filter used for making the metabolome extracts.

The vitamin solution, which was 1,000× concentrated, contained per liter 20 mg biotin, 20 mg folic acid, 100 mg pyridoxine-HCl, 50 mg thiamine-HCl, 50 mg riboflavin, 50 mg nicotinic

acid, 50 mg Ca-d-pantothenate, 1 mg vitamin B_{12}, 50 mg 4-aminobenzoid acid, and 50 mg lipoic acid.

Trace elements solution I, which was 1,000× concentrated, contained per liter 50 mM HCl, 61.8 mg H_3BO_4, 99.0 mg $MnCl_2{\cdot}4H_2O$, 1.49 g $FeCl_2{\cdot}4H_2O$, 119 mg $CoCl_2{\cdot}6H_2O$, 23.8 mg $NiCl_2{\cdot}6H_2O$, 68.2 mg $ZnCl_2$, and 17.0 mg $CuCl_2{\cdot}2H_2O$.

Trace elements solution II, which was 1,000× concentrated, contained per liter 10 mM NaOH, 17.3 mg Na_2SeO_3, 33.0 mg $Na_2WO_4{\cdot}2H_2O$, and 24.2 mg $Na_2MoO_4{\cdot}2H_2O$.

Construction of *E. coli* Δ*talAB* double knock-out strain

E. coli BW25113, a K-12 derivative, which has been used for the Keio collection, was used to make the double transaldolase knock-out, as was done by Nakahigashi *et al*. First, the strain was transformed with pKD46, a temperature sensitive plasmid containing the Lambda Red recombination system and an ampicillin resistance marker. Cells were then grown at 30 °C and transformed with a linear knock-out cassette derived from pKD3, containing a kanamycin resistance marker flanked by *FRT* sites and 50 base-pair arms homologous to the chromosome, such that *talB* would be removed, save for the start codon, and the last seven codons. The knock-out cassette was generated from pKD4 with primers AGACCGGTTACATCCCCCTAACAAGCTGTTTAAAGAGAAATACTATCATGGTGTAGGCTGGAGCT GCTTC and GACCGACTTCCCGGTCACGCTAAGAATGATTACAGCAGATCGCCGATCATCATATGAATATCCTCC TTAGTTCCTATTCC. Transformed cells were grown on LB + kanamycin, at 37 °C, to select mutants and simultaneously cure pKD46. Following the selection of a correct mutant, pCP20, a temperature sensitive plasmid containing the yeast flippase (flp) recombinase gene was transformed to remove the kanamycin marker from the genome by recombining the *FRT* sites. pCP20 was cured by growing the cells at 37 °C. The whole process was repeated to remove the *talA* gene as well. Primers GAATTAACGCACTCATCTAACACTTTACTTTTCAAGGAGTATTTCCTATGGTGTAGGCTGGAGCTGC TTC and TTCGGGACATATAACACTCCGTGGCTGGTTTATAGTTTGGCGGCAAGAAGCATATGAATATCCTCC TTAGTTCCTATTCC were used to generate the linear knock-out cassette for *talA*, using pKD4 as a template.

Plasmid construction and heterologous expression of 6-phosphofructokinases

The two 6-phosphofructokinases of *C. thermosuccinogenes* (CDQ83_11320 & CDQ83_07225) were cloned previously into pET-28b(+) [142]. The 6-phosphofructokinase of *E. coli* (BW25113_3916) was cloned in identical fashion using primers TACTTCCAATCCAATGCAATTAAGAAAATCGGTGTGTTGACAAGC and TTATCCACTTCCAATGTTAATACAGTTTTTTCGCGCAGTCC. The pET-28b(+)-based vectors were

constructed in *E. coli* DH5α and then then transformed to *E. coli* Rosetta for heterologous expression.

The pyrophosphate-dependent 6-phosphofructokinase of *C. thermocellum* strain DSM 1313 (locus_tag *Clo1313_1876*) was amplified using primers XSH0718 (sequence 5'-CATCACCACCACCACCATATGAGCCGTTTAGAAGGTG-3') and XSH0719 (sequence 5'-GCGGCCGCGAGACCCTAACCTTATTTTCTTGCAAGAACC-3'), and then cloned into the pD861-NT expression vector (DNA 2.0 Inc, Menlo Park, CA, USA) using isothermal assembly [94], to create plasmid pSH157. The assembled plasmid pSH157 was then cloned into T7 Express *lysY*/*Iq* Competent *E. coli* (New England Biolabs catalog number C3013I), using 50 µg/ml kanamycin for selection of transformants.

Expression of the 6-phosphofructokinases was done by growing the *E. coli* strains in 0.5 – 2 l LB medium containing the appropriate antibiotics up to an OD_{600} of around 0.6, after which the cultures were place on ice for 20 minutes and expression was induced with 0.2 mM IPTG for the pET-28b(+)-based vectors and with 4 mM rhamnose for the pD861-NT-based vector. Cells were grown for another 3 – 4 hours at 37 °C, after which the cells were harvested for protein purification.

Metabolite extraction for mass spectrometry

Biomass was isolated by rapid vacuum filtration of 5 – 20 ml of culture broth, adapted from the method by Sander *et al*. 2017 [251]. For this, 0.2 µm nylon filters (Whatman®) were used. After filtration, the filter was immediately placed upside down in 3 to 10 ml solvent which was kept in a polystyrene petri dish (50 mm diameter, Falcon®) placed on an aluminium block precooled at -80 °C. The extraction solvent consisted of a mixture of acetonitrile, methanol and water, mixed at a ratio of 2:2:1 (v/v). The filter was kept in the extraction solvent for 5 minutes, after which the extract was kept on dry ice until transferred to a freezer for storage at -80 °C. All Aliquots were stored until further processed in low protein binding collection tubes (Thermo Scientific™). The entire process was carried out aerobically.

20 ml of the *E. coli* cultures grown in M9 medium at OD_{600} of 0.5 – 0.8 was used, in combination of 5 ml extraction solvent. For *C. thermosuccinogenes*, up to 10 ml culture was used, depending on the OD_{600}, in combination with 3 ml extraction solvent. The higher the OD_{600}, the smaller the culture that could be filtered without clogging the filter. It is not clear why cellulolytic clostridia cultures tend to clog the filters so quickly.

HILIC Mass spectrometry for detection of sedoheptulose 7-phosphate and sedoheptulose 1,7-bisphosphate in metabolite cell extracts

Identification of sedoheptulose 7-phosphate and sedoheptulose 1,7-bisphosphate was performed using a LC-MS setup as described by Schatschneider *et al*. [256]. Briefly, LC-

Orbitrap-MS analysis was performed using an ACQUITY UPLC M-Class chromatography system coupled to a high-resolution Orbitrap mass spectrometer (Q-Exactive plus, Thermo Fisher Scientific). For chromatographic separation, a ZIC-HILIC column (1.0 mm × 150 mm, 5 µm particle size, Merck KGaA, Germany) was operated at room temperature using a 20 mM ammonium carbonate in water (pH 9.1) as mobile phase A and 100% acetonitrile as mobile phase B. A gradient was maintained at 40 µL/min from 25% A to 55% A over 15 minutes and further to 30% A over 2.5 minutes. Samples were taken from -80°C immediately before injection, brought to 4-8°C on ice and mixed with injection buffer (85% solvent B in solvent A, including 20 mM sodium citrate) at a ratio of 1:1 (v/v). The reaction mixture was centrifuged at 14.000 rpm for 3 minutes at 4-8°C and 2.5 µL were subsequently injected onto the separation column. The mass spectrometer was operated alternating in full scan and PRM mode. Full scan was acquired from 260-700 m/z in ESI negative mode (-2.5 kV), at a resolution of 70.000. Parallel reaction monitoring was performed for m/z 289.03 ($[M-H]^-$, S7P) and 368.99 ($[M-H]^-$, S1,7BP) precursor ions at an isolation window of 2.0 m/z. HCD fragmentation was performed using a NCE of 27 which fragment ions were measured at a resolution of 17.000. Raw data were analysed using XCalibur 4.1 (Thermo) and areas were integrated using Skyline 4.1.0. The fragmentation pattern and elution time for sedoheptulose 7-phosphate was compared to a commercial standard (Sigma, Aldrich) and the peak obtained from the *E. coli* double transaldolase mutant and wild type metabolite extracts, used as control. The fragmentation pattern and elution position for sedoheptulose 1,7-bisphosphate was compared to the metabolite extract *E. coli* Δ*talAB* (see above).

In vitro phosphofructokinase assays with analysis by mass-spectrometry

Protein purification

50 ml LB cultures of *E. coli* strains overexpressing the *C. thermocellum* or *C. thermosuccinogenes* PP_i-Pfks were grown, induced, and harvested as described above.

Protein purification for the purposes of demonstrating in-vitro conversion of sedoheptulose-7-phosphate to sedoheptuoloase-1,7-bisphosphate by the purified PP_i-Pfks in the presence of PP_i was performed as previously described [297]. To obtain purified PP_i-Pfk protein, the induced *E. coli* cells were resuspended in 100 mM Tris-HCl buffer (pH 7 at 55 °C). Approximately 70,000 U of Readylyse enzyme (Lucigen catalog number R1802) was added to the cell suspension, and the mixture was incubated for 10 minutes at room temperature. 5 units of DNase I (Thermo Fisher Scientific catalog number 90083) were then added to reduce the viscosity of the cell lysate; the sample was incubated for another 10 minutes at room temperature. The resulting solution was at >20,000 g for 5 minutes, and the cell extract supernatant was used in future steps. *E. coli* proteins in the cell extract were denatured by incubating the cell extract at 55 °C for 30 minutes; the denatured proteins were removed by centrifugation at > 20,000 g for 5 minutes. His-Tag purification of the PP_i-Pfks from the heat-treated cell extracts was done using the HisSpinTrap kit (GE Healthcare

catalog number 28-4013-53). Eluted PP_i-Pfk proteins were desalted using a 10 kD molecular weight cutoff filter (Millipore catalog number UFC501024) and 100 mM Tris-HCl buffer, to reduce the imidazole concentration to < 1 mM.

Assay conditions

Enzyme assays were performed in an anaerobic chamber, with an atmospheric composition of 85% nitrogen, 10% carbon dioxide, and 5% hydrogen. Assay chemicals were purchased from Sigma Aldrich. All samples were incubated at 55 °C in a heat block for the entirety of the experiment. Assay reaction composition was based off previously described assay conditions, and comprised 100 mM Tris-HCl (pH7 at 55 °C), 5 mM $MgCl_2$, 5 mM sodium PP_i, 1 mM of either sedoheptulose-7-phosphate or fructose-6-phosphate, 4 U of rabbit aldolase where used (Sigma catalog number A8811), and purified PP_i-Pfk protein (see next paragraph for more information on enzyme loading). In all cases, the reactions were started upon addition of sodium PP_i, or an equivalent volume of buffer for assay reactions that did not contain PP_i. The initial assay volume was 400 µL.

The specific PP_i-PFK activity was first determined for each of the purified PP_i-Pfks on the day of the experiment. The amount of purified PP_i-Pfk used for the assay was then adjusted for each sample and replicate, such that each assay reaction would contain an enzyme loading corresponding to ~0.01 µmol/min of PP_i-PFK activity.

Samples from the enzyme reactions were collected in the following manner: the tube containing a given assay mixture was removed from the heat block and briefly vortexed to mix the contents. 20 µL of assay mixture was then collected and then quickly added to 80 µL of very cold (≤ -30 °C) 1:1 acetonitrile:methanol mixture to quench enzyme activity, and then vortexed briefly to mix; quenching solution was kept at ≤ -30 °C by putting them in contact with a metal heat block sitting atop a 4-inch thick aluminium block, both of which had been pre-chilled at -80 °C for at least 48 h prior to use [219]. The quenched sample was then stored at -80 °C until analysis. Standards of S7P, F6P, FBP, E4P, and DHAP at three different concentrations each were also prepared to allow for quantification of these compounds in the assay samples.

Mass spectrometry analyses of assay samples

Assay samples were analyzed as previously described [297], using an LC-MS/MS system a Thermo Scientific Vanquish UHPLC coupled by heated electrospray ionization(HESI) to a hybrid quadrupole-high resolution mass spectrometer (Q exactive orbitrap, Thermo Scientific).. Liquid chromatography separation was performend using an ACQUITY UPLC BEH C18 (2.1 x 100 mm column, 1.7-µm particle size), with a flow rate of 0.2 ml/min For the instrument run, Solvent A was 97:3 water:methanol with 10 mM tributylamine (TBA) and approximately 9.8 mM acetic acid, pH ~ 8.2; solvent B was 100% methanol. Total run time was 24.5 min with the following gradient: 0 min, 5% B; 2.5 min, ramp from 5% B to

95% B over 14.5 min; hold at 95% B for 2.5 min; return to 5% B over 0.5 min; hold at 5% B for 5 min. MS scans consisted of full negative mode MS scanning for m/z between 70 and 1000 from time 0 to 18.5 min. Sample preparation involved first evaporating the solvents with a nitrogen blowdown evaporator, and then resuspending the dried samples in Solvent A.

Metabolite peaks were identified using the open source software, El-MAVEN (URL: https://elucidatainc.github.io/ElMaven/). Response factors for S7P, F6P, FBP, E4P, and DHAP standards were used to determine the concentrations of these five compounds in the assay samples.

Phosphofructokinase kinetics assays

The harvested cells were washed with cold 50 mM MOPS buffer (pH 7.4 at room temperature) containing 20 mM imidazole and resuspended in the same buffer with cOmplete™, mini, EDTA-free protease inhibitor cocktail (Roche) added; 1 tablet per ~10 ml. Cells were lysed using a French press at ~120 kPa. Lysate was centrifuged at 20.000 × g for 10 min. at 4 °C. A HisTrap™ HP column (GE Healthcare, optimal at pH 7.4) with an ÄKTA pure FPLC system were used for the purification. Elution was done over a gradient with 50 mM MOPS buffer (pH 7.4 at room temperature) containing 500 mM imidazole. The buffer of the eluted protein was then exchanged with 50 mM MOPS (pH 7.0 at room temperature) using an Amicon® ultra centrifugal filter (Merck) with a nominal molecular weight limit of 10.000 Da. SDS-PAGE was used to verify purity.

The 6-phosphofructokinase assay was adapted from Zhou at al. [331] and contained 50 mM MOPS (pH 7.0 at room temperature), 5 mM $MgCl_2$, 2 mM ATP or 1 mM pyrophosphate, 0.15 mM NADH, 4 U/ml aldolase (lyophilized, rabbit), and 2 U/ml glycerol-3-phosphate dehydrogenase (lyophilized, rabbit). Fructose 6-phosphate or sedoheptulose 7-phosphate (Ba-salt, Carbosynth) was added to start the reaction, at varied concentrations. For the PfkA of *E. coli*, 0.25 mM ADP was added to the assay, as it is known to be an allosteric activator [31]. For the ATP/GTP-dependent 6-phosphofructokinases of *C. thermosuccinogenes* 20 mM NH_4Cl_2 was added to the reaction, as it was found to be an absolute requirement for its activity. Previously, auxiliary enzymes from as ammonium sulfate suspension were used [142], but with sedoheptulose 7-phosphate as a Ba-salt, this was not possible due to precipitation of $BaSO_4$, which is how we found out that the enzyme requires ammonium.

The Michaelis-Menten equation and the Hill equation were fitted to the data by minimizing the sum of the squares of the vertical differences, in order to find $K_M/K_{1/2}$, k_{cat}, and n. The data and the fitted models can be found in the supporting information (File S1).

Results

Metabolomics

Presence of SBP in metabolite extracts of cellulolytic clostridia would give a preliminary indication of the presence of the SBP-pathway. To unambiguously confirm the presence of SBP it is crucial to have a reference standard, which is not currently available from commercial sources, due to the very low stability of SBP. Nakahigashi *et al*. (2009) showed the accumulation of S7P and a molecular ion conform with SBP (m/z 369.0) in extracts of an *E. coli* harbouring a double transaldolase knock-out (Δ*talAB*). We decided to use the above mentioned strain, which presumably accumulated SBP as well as S7P, to subsequently function as a molecular reference for SBP. The strain used by Nakahigashi *et al*. (2009) was recreated as described in the material and methods. The growth rate of the Δ*talAB* derivative on a minimal medium with xylose was only marginally lower compared to that of the wild type: 0.33 ± 0.00 h^{-1} versus 0.39 ± 0.01 h^{-1}, when grown in shake flasks with 50 ml M9 medium (in triplicate), in line with the findings of Nakahigashi *et al*. (2009). Further, the growth rate on minimal medium with glucose was in fact slightly higher for the mutant: 0.52 ± 0.00 h^{-1} versus 0.49 ± 0.01 h^{-1}.

Mass spectrometry of metabolome extracts from *E. coli* Δ*talAB* and wild type grown on xylose showed the accumulation of S7P and a compound with a m/z 369.0 for the Δ*talAB* strain. Accurate mass, retention behaviour as well as higher-energy collisional dissociation (HCD) fragments exactly matched those expected for SBP, as shown in Figure 3, concluding that SBP was produced and could successfully be used as a reference. Nevertheless, we could only successfully detect SBP at a relatively strong signal comparable to S7P when the metabolic extract was analysed while avoiding further purification/enrichment steps, further illustrating its very low stability.

corresponding to SBP, confirmed by indicative fragment peaks at m/z 199 and m/z 271, which are further absent in the blank (B). The red arrow indicate the bonds that, when broken, result in the fragment at m/z 199 and m/z 271.

Traces of SBP were also detected in the cell extract of wild type *E. coli*, suggesting that even in the wild type metabolism a small fraction of the S7P is converted to SBP by PFK. This flux is amplified after the double transaldolase deletion, causing S7P to accumulate. This provides further support for our assumption that the *E. coli* PFKs have a low affinity for S7P.

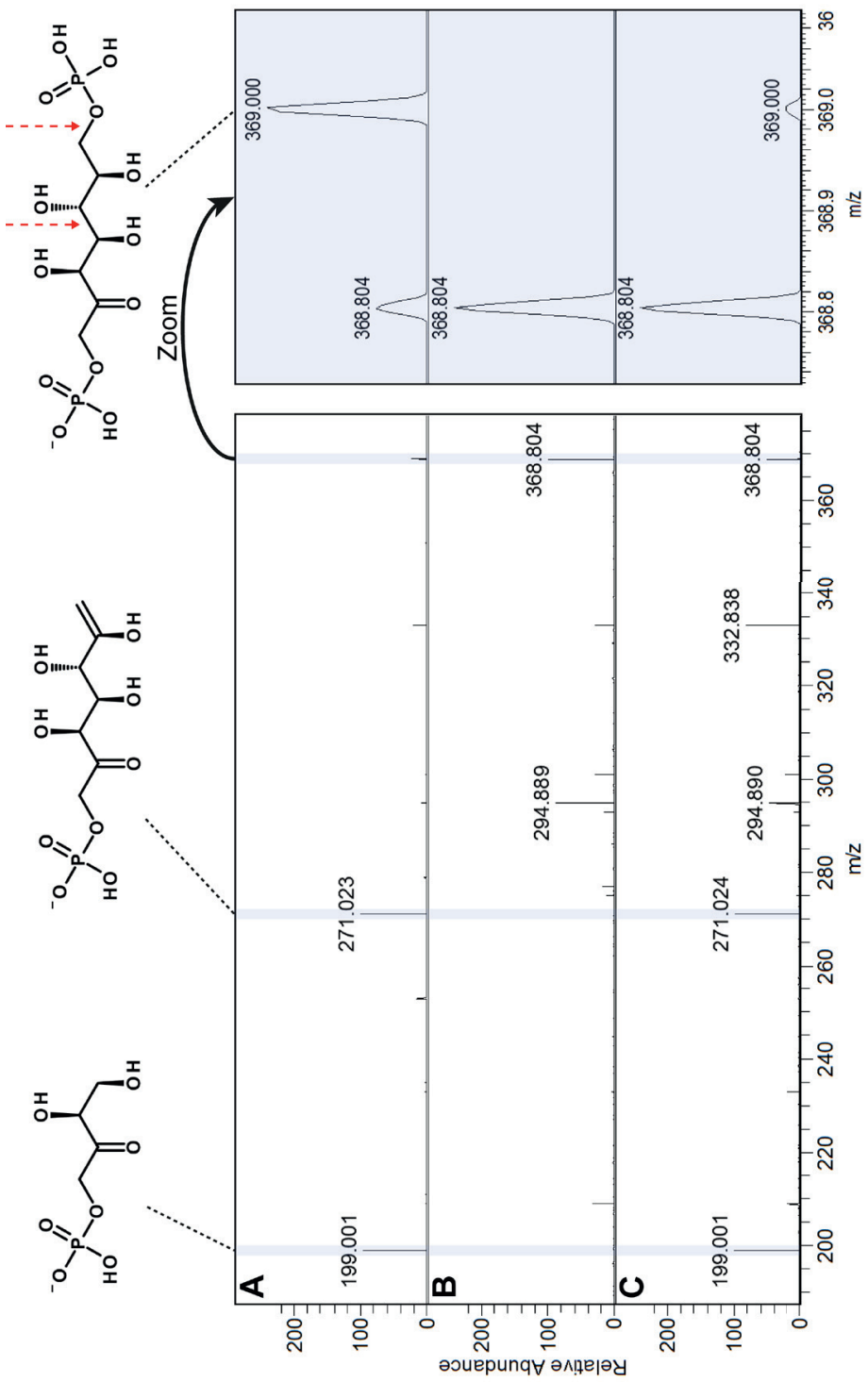
A
B
C
Zoom
Relative Abundance
m/z
199.001
271.023
294.889
368.804
271.024
294.890
332.838
368.804
369.000
368.804

Figure 3: Identification of sedoheptulose 1,7-bisphosphate (SBP; m/z 368.99) via targeted monitoring of fragments for the precursor ion at m/z 368-370 from: (A) *E. coli* Δ*talAB* extract; (B) blank run; (C) xylose grown *C. thermosuccinogenes* extract. A clear peak is present in A and C at m/z 369

Next, *C. thermosuccinogenes* was grown on xylose versus glucose, in order to try to detect SBP, and to see if the SBP pool increases during growth on xylose, as would be expected, since virtually the entire flux of carbon will have to be channelled through SBP into glycolysis. The results of the metabolome extract analysis are shown in Figure 3. SBP was found to be present in significant quantities (i.e. much higher than compared to wildtype *E. coli*), and was several times higher in cells grown on xylose. Normalized to the optical density of the cultures at 600 nm (OD_{600}), the SBP concentration increased 4-fold. Similarly, the S7P concentration increased 2.5-fold during growth on xylose.

In *E. coli* Δ*talAB* grown on xylose, the S7Pconcentration was roughly 6-fold higher compared to that of *C. thermosuccinogenes* grown on xylose. For SBP this difference was roughly 20-fold. Although many factors could explain the difference in concentrations between the two organisms, the higher accumulation in *E. coli* suggests that the PFK and the fructose bisphosphate aldolase enzymes of *C. thermosuccinogenes* have higher affinities for S7P and SBP, respectively, compared to those of *E. coli*. A higher affinity, in turn, suggests evolutionary pressure towards the use of those substrates. For this reason, we studied the *in vitro* affinities of the cellulolytic clostridia PFKs towards F6P and S7P.

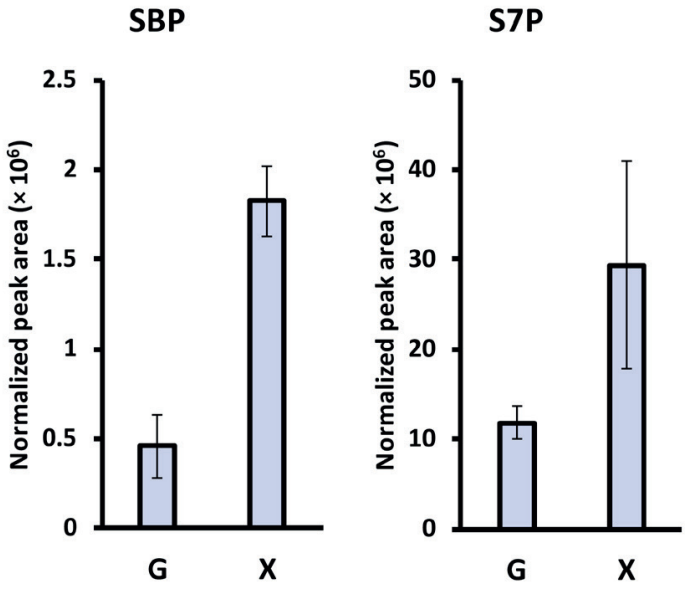

Figure 4: Relative pools of sedoheptulose 1,7-bisphosphate (SBP) and sedoheptulose 7-phosphate (S7P) in *C. thermosuccinogenes* grown on xylose (X), compared to glucose (G). Mass spectrometry peak area is normalized to OD_{600} of the culture.

In vitro phosphofructokinase assays

C. thermosuccinogenes and *C. thermocellum* contain two PFKs; the PPi-dependent PFK and another one that was shown to function with both ATP and GTP in *C. thermosuccinogenes* [142]. A third PFK has been annotated in the genome of *C. thermosuccinogenes* for which no activity had been detected, and which is absent in *C. thermocellum*. From assays with cell-free extract, it was already clear that PP_i-dependent PFK is the dominant isoform [143,331]. We repeated the aforementioned assays with *C. thermosuccinogenes* cell-free extract in the presence of NH_4 – which we had serendipitously found to activate ATP/GTP-PFK – but were still unable to detect ATP-dependent activity (data not shown), confirming that PP_i-dependent PFK is the dominant isoform in this organism as well.

To determine whether the PP_i-Pfk proteins participated in the non-oxidative pentose phosphate pathways of their respective organisms, we investigated whether the PP_i-Pfks were in fact capable of interconversion of S7P and SBP. *In vitro* time course experiments showed that S7P concentrations decreased over time in an assay mixture where both a PP_i-Pfk and PP_i were also present (Figure 5); this decrease in S7P concentrations was concomitant with an increase in signal intensity at the m/z 369, which corresponds to the presence of SBP (Figure 3). In the absence of PP_i, S7P concentrations remained relatively stable, and no increase in signal intensity at m/z 369 was observed (Figure 5), providing further evidence that the PP_i-Pfk proteins were using PP_i as a cofactor to phosphorylate of S7P. As expected, assay reactions containing S7P and PPi, but no PPi-Pfk protein, did not show any decrease in S7P, nor increase in peak intensity at m/z 369 (supporting information Figure S1).

Further confirmation of the identity of the m/z 369 compound as SBP was obtained, by repeating the assay with the inclusion of fructose bisphosphate aldolase. The SBP pathway would result in the formation of E4P and DHAP (both commercially available compounds) from SBP via the action of the aldolase (Figure 2). In this additional set of assays, a similar pattern of decreasing S7P concentration coupled to an increased in peak intensity at m/z 369 was observed; in addition, it was also observed that E4P and DHAP concentrations increased over time as well, where accumulation of these compounds was not detected in the reactions without the added aldolase. Notably, the peak intensities at m/z 369 in the aldolase-containing reactions were lower than that observed in the corresponding assay reactions that did not contain aldolase, in line with the conversion of SBP to E4P and DHAP. It was observed that the DHAP concentrations tended to be lower than those of E4P, despite the fact that they should be produced in equimolar amounts, as the stoichiometry in Figure 2 would suggest; one explanation is that the added rabbit aldolase contains triose-phosphate isomerase as a trace contaminant, which would catalyze the interconversion of DHAP to G3P. Nonetheless, the results support the proposed SBP pathway.

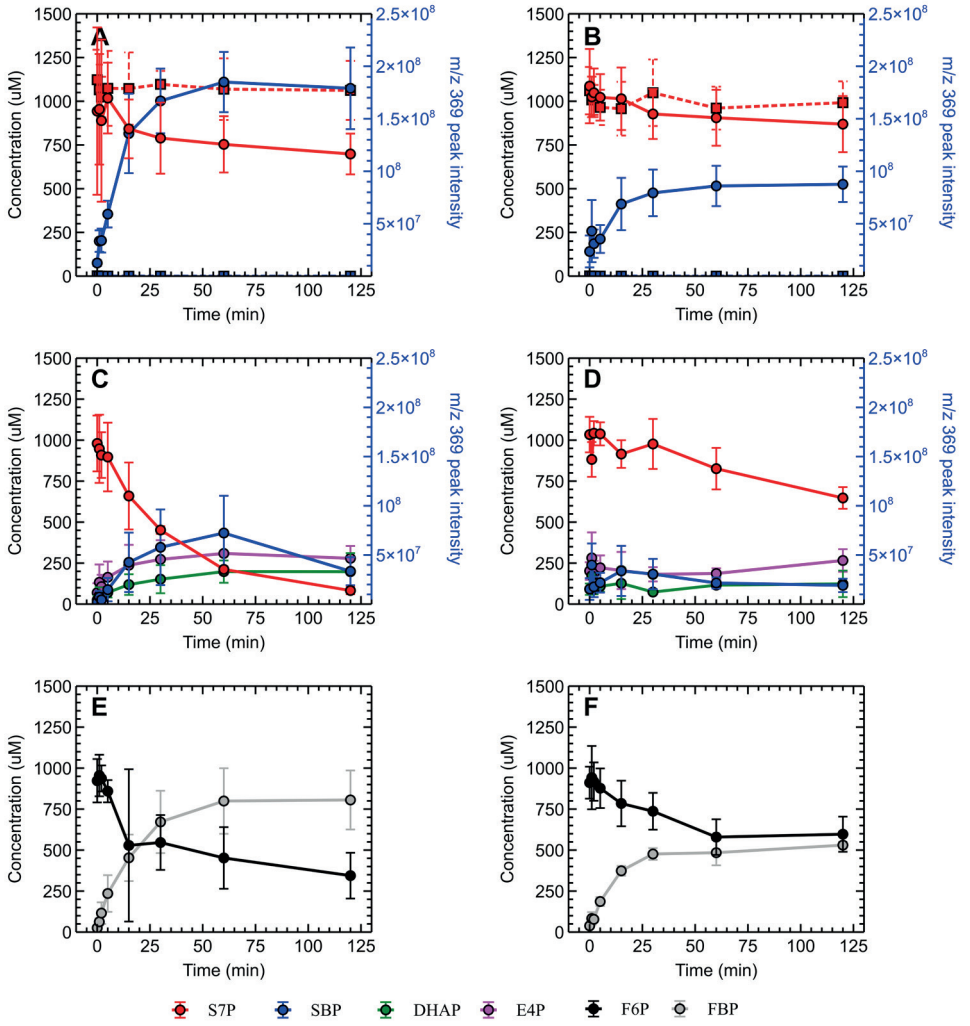

Figure 5: *In vitro* time-course assay of *C. thermocellum* (left panels **A, C, E**) and *C. thermosuccinogenes* (right panels **B**, **D, F**) PP_i-Pfk proteins' abilities to convert sedoheptulose-7-phosphate (S7P) to sedoheptulose-1,7,-bisphosphate (SBP). **A** and **B.** Conversion of S7P (red) in the presence (circle datapoints on solid lines) or absence (square datapoints on dotted lines) of 5 mM pyrophosphate, with corresponding increase in a compound (SBP) with a m/z of 369 (blue). SBP peak intensities in assays lacking PP_i were, in general, between the range of 10,000-20,000 arbitrary units throughout the assay. **C** and **D.** Conversion of S7P (red) to SBP (blue), and SBP's subsequent conversion to DHAP (green) and E4P (pink). **E** and **F.** Control reactions for the purified PP_i-Pfk proteins, demonstrating their ability to function as 6-PFKs and convert F6P (black) to FBP (grey). Error bars represent one standard deviation ($n \geq 2$).

For the determination of the enzyme kinetics for F6P and S7P, analysis via mass-spectrometry is impractical, as the response is not obtained in real-time. Instead, the formation of FBP and SBP can be coupled to oxidation of NADH via auxiliary fructose

bisphosphate aldolase and glycerol-3-phosphate dehydrogenase (both from rabbit), as illustrated in Figure 5. We confirmed that rabbit aldolase was able to convert the formed SBP to E4P and DHAP – validating the coupled assay method – as shown in Figure 6 . Note that commonly, triose-phosphate isomerase is used additionally for such assays (to convert glyceraldehyde 3-phosphate to DHAP, increasing the signal and the driving force), which we excluded, as this would not function with E4P, making it easier to directly compare the two different substrates.

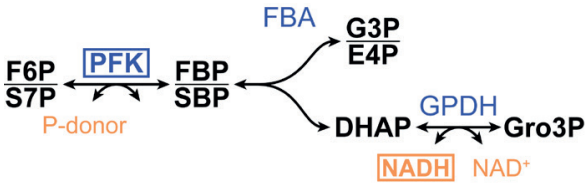

Figure 6: Enzyme assay to couple FBP/SBP formation by PFK to NADH oxidation, allowing the study of the PFK enzyme kinetics. PFK: 6-phosphofructokinase; FBA: fructose bisphosphate aldolase; GPDH: glycerol 3-phosphate dehydrogenase; F6P: fructose 6-phosphate; S7P: sedoheptulose 7-phosphate; FBP: fructose 1,6-bisphosphate; SBP: sedoheptulose 1,7-phosphate; G3P: glyceraldehyde 3-phosphate; E4P: erythrose 4-phosphate; DHAP: dihydroxyacetone phosphate; Gro3P: glycerol 3-phosphate. Boxes highlight the investigated enzyme (i.e. PFK) and detected metabolite (i.e. NADH).

Table 1: Kinetics of the PFKs tested. Parameters of both Michaelis-Menten and Hill kinetics were approximated by minimizing the sum of the squared vertical difference. The plots with the data-points can be found in the supporting information (File S1). ATP/GTP-PFK did not show any activity with S7P, and due to the high cooperativity (n = 24) with F6P, it was not possible to fit the Michaelis-Menten equation.

			Hill kinetics				Michaelis-Menten kinetics		
			$K_{1/2}$ (mM)	k_{cat} (s^{-1})	n	$k_{cat}/K_{1/2}$ ($s^{-1}M^{-1}$)	K_M (mM)	k_{cat} (s^{-1})	k_{cat}/K_M ($s^{-1}M^{-1}$)
CDQ83_11320 **P.ts PP_i-PFK**	PP_i	F6P	0.080	172	1.5	2.1 *10^6	0.070	182	2.6 *10^6
		S7P	0.10	47	1.2	0.46 *10^6	0.11	49	0.46 *10^6
Clo1313_1876 **H.tc PP_i-PFK**		F6P	0.044	134	0.74	2.8 *10^6	0.046	127	2.8 *10^6
		S7P	0.098	75	1.5	0.80 *10^6	0.10	80	0.80 *10^6
CDQ83_07225 **P.ts A/GTP-PFK**	ATP	F6P	0.688	41	24	59 *10^3	*No fit*	*No fit*	*No fit*
		S7P	-	-	-	-	-	-	-
PfkA **E.co PFK**		F6P	0.074	1.1	1.7	15 *10^3	0.065	1.2	19 *10^3
		S7P	1.2	0.25	1.6	0.20 *10^3	2.5	0.25	0.15 *10^3

The results of the kinetics assays are presented in Table 1. Although the two tested PP_i-dependent PFKs showed 2-3 fold lower maximal activity (k_{cat}) with S7P versus F6P, the affinity (K_M or $K_{1/2}$) for both substrates was comparably high (K_M or $K_{1/2}$ of ~0.1 mM). This is in stark contrast with the PfkA from *E. coli*, for which the affinity constant for S7P is almost two orders of magnitude larger (i.e. lower affinity; K_M of 2.5 mM or $K_{1/2}$ of 1.2 mM,

depending on the model) than that for F6P; the latter being on par with the affinities of the other tested PFKs. In exponentially growing *E. coli* cells on glucose, the concentration of F6P and S7P are 2.2 and 0.9 mM respectively [225], which means that *in vivo* PfkA is highly saturated with F6P, but not with S7P. The intracellular concentrations of those metabolites are not known in any of the the cellulolytic Clostridia, but with the equally high affinities for both F6P and S7P it is reasonable to assume that both metabolites are saturating, and thus physiologically relevant substrates for the PP_i-dependent PFKs. These results strongly suggest that the PP_i-dependent PFKs of cellulolytic clostridia – lacking a transaldolase – evolved for the use of S7P as a substrate, whereas the (ATP-dependent) PfkA of *E. coli*, which does possess a transaldolase, did not; although PfkA is still able to use S7P as a substrate at higher, non-physiological concentrations. The latter can explain why traces of SBP were found in WT *E. coli* grown on xylose, and why S7P accumulates in the Δ*talAB* strain. The data of the assays and the fitted kinetic models can be found in the supporting information (File S1).

The ATP/GTP-dependent PFK of *C. thermosuccinogenes* was able to use F6P, but did not show any activity with S7P – at least, not in the range of tested S7P concentrations, up to 4 mM. Interestingly, it showed an extreme degree of cooperativity with F6P, reflected by a Hill-coefficient (n) of 24. The high degree of cooperativity results in a virtual on/off switch of the enzyme, activating it at F6P concentrations above the $K_{1/2}$ of 0.7 mM.

Discussion

The SBP pathway in cellulolytic Clostridia

A considerable pool of SBP is shown to be present in *C. thermosuccinogenes*, which, together with the S7P pool, increases several-fold when *C. thermosuccinogenes* is grown on xylose versus glucose. This increase demonstrates the role for SBP in the pentose metabolism, and agrees with the hypothesis that the SBP-pathway is present instead of transaldolase. In the SBP-pathway, PFK and fructose bisphosphate aldolase together convert S7P to E4P and DHAP (via SBP, as shown in Figure 2). These two enzymes are known to convert F6P to glyceraldehyde 3-phosphate and DHAP (via fructose 1,6-bisphosphate as intermediate). *In E. coli*, it was already shown that these enzymes could take over the role of transaldolase after a double transaldolase knock-out, and in *E. histolytica* it was shown that the SBP-pathway likely exists in the wild type metabolism [211,285].

If in *C. thermosuccinogenes* and other cellulolytic Clostridia, in the absence of a transaldolase, the SBP-pathway is really the native pathway to connect pentose with hexose metabolism, their affinities for these “alternative” substrates should reflect that. Indeed, here we show that the PP_i-PFKs of both *C. thermosuccinogenes* and *C. thermocellum* can use S7P, and have an affinity similar to that for F6P. The same was previously found for *E. histolytica* PP_i-PFK, where the K_M for S7P is 0.064 mM and 0.038 mM for F6P [285]. On the contrary, here we show that the affinity of *E. coli* PfkA for S7P is almost two orders of

magnitude lower compared to its affinity for F6P, such that the affinity constant for S7P is much higher than its typical intracellular concentration.

Considering the fact that *E. coli* has a transaldolase to facilitate the interconversion of pentoses and hexoses, it makes sense that the affinity of PfkA for S7P is such that *in vivo* this reaction does not proceed; there is no need for S7P kinase activity and the resultant SBP-pathway.

The SBP pathway versus transaldolase

A question that remains is whether there is an advantage to having either the transaldolase or the SBP-pathway? A crucial aspect of the SBP-pathway is the physiological reversibility of the PP_i-PFK in contrast to the ATP-dependent variant [193], since the non-oxidative PPP should be able to operate in both directions. It therefore seems a prerequisite to rely on PP_i-PFK, and the associated PP_i-generating metabolism in order to use the SBP-pathway. If this is not the case and PFK is ATP-dependent, transaldolase would still be required to facilitate the reverse (anabolic) direction in the PPP. As such, it seems that transaldolase might simply be or become obsolete in the case PP_i-PFK is used in glycolysis. The underlying question therefore is why a PP_i-dependent PFK is used at all, instead of an ATP-dependent one?

The irreversibility (i.e. large decrease in Gibbs free energy) of ATP-dependent PFK grants it a lot of control over the metabolism, but comes at the cost of about half available free energy [225]. The trade-off between control and energy conservation could perhaps be the main factor behind the use of a PP_i-dependent PFK versus an ATP-dependent one.

Organisms that almost exclusively rely on substrate level phosphorylation for ATP generation, such as the strictly anaerobic cellulose fermenting cellulolytic Clostridia, might prioritize energy conservation over control, while respiring organisms might have done the opposite.

PP_i generation

PP_i is a by-product of many anabolic reactions, often operating close to equilibrium. Many organisms hydrolyse PP_i to orthophosphate using inorganic pyrophosphatase, in order to drive these anabolic reactions forward, releasing heat [302]. Using the otherwise “wasted” PP_i instead of ATP for the phosphorylation of F6P should therefore allow the conservation of metabolic energy. It was already calculated for *C. thermocellum*, however, that the formation of PP_i as by-product of anabolism alone is not enough to sustain the PFK reaction in glycolysis as it accounted for less than 10% of the flux [331], meaning that there must be another, dedicated source of PP_i.

One potential source that could also further increase the energy conservation via the use of PP_i by PFK relies on a membrane-bound proton or sodium ion-translocating

pyrophosphatase (M-PPase). Both ATPases and M-PPases have a certain coupling ratios of number of H^+/Na^+ translocated per phosphate-phosphate bond hydrolysed/formed. A lower coupling ratio for PPase compared to ATPase means that more than one PP_i can be formed per consumed ATP through this chemiosmotic coupling, decreasing the stoichiometric ATP requirement for PP_i driven reactions [28,87,134,142,248,260]. PP_i can also be formed through the simultaneous formation and breakdown of glycogen, with the net conversion of ATP (or UTP) and orthophosphate to ADP (or UDP) and pyrophosphate [143,248,290,331]. From the point of view of energy (i.e. ATP) conservation, there is no advantage to using the glycogen cycle, as one PP_i would be generated per ATP to ADP conversion; except that it would allow for the anabolic PP_i-"waste" to be utilized via PP_i-PFK, conserving somewhat fewer than 0.1 ATP per dissimilated glucose, as discussed above. Alternatively, glycogen cycling could represent a buffering system for PP_i-flow rather than for the carbon-flow [71,91], working in conjunction with a dedicated PP_i-generating system (e.g. M-PPase), in order to maintain an adequate PP_i to P_i ratio.

Unusual kinetics for ATP/GTP-PFK

ATP/GTP-PFK was previously found to have similar affinities for ATP versus GTP [142], and here we show that it has an extreme degree of cooperativity for F6P. The extreme cooperativity effectively means that below ~0.7 mM F6P there is no activity, while above this concentration the enzyme operates at maximum activity. At this point we can only speculate on the function behind this peculiar characteristic, and doing so it seems wholly plausible that it could function as a kind of relief valve that prevents the intracellular concentration of F6P from rising above 0.7 mM.

It might in fact be detrimental for organisms relying on the SBP-pathway to accumulate a large intracellular concentration of F6P (relative to S7P/SBP), due to the competition between S7P/SBP and F6P/fructose 1,6-bisphosphate for PP_i-PFK. For example, a ten-fold higher F6P concentration compared to S7P, means that only ~9% of the PP_i-PFK enzyme pool is available for S7P-depdendent activity. Of course, the opposite is also true, in case S7P accumulates, relative to F6P. Here too, ATP/GTP-PFK could aid, by allowing F6P phosphorylation to occur regardless (but with ATP or GTP).

In the case one enzyme is responsible for two separate (metabolic) reactions (via the same active site), it becomes crucial for the cell to regulate those relative pools, in order for both reactions to be able to occur. Our hypothesis is that the ATP/GTP-dependent PFK is responsible for a fail-safe mechanisms relieving the negative effects caused by the perturbation of the S7P and F6P pools. How and if the enzyme's activation by NH_4^+ relates to this hypothesized function is not clear.

Widespread occurrence of the SBP-pathway?

It is common for both PP_i-dependent and ATP-dependent PFKs to coexist in one organism. In such cases, it was previously thought that PP_i-PFK might have an alternative, unknown function [18]. Here we show that the PP_i-PFK has a dual function in glycolysis and the PPP, while the ATP-dependent PFK might have an alternative function. Similarly, in *Amycolatopsis methanolica* PP_i-PFK is used in glycolysis during growth on glucose, whereas its ATP-PFK is used in the ribulose monophosphate cycle, during growth on one-carbon compounds [5]. The widespread occurrence of PP_i-PFK could therefore suggest that the SBP-pathway is also more widespread than is currently recognized, particularly when the presence of PP_i-PFK coincides with the absence of a transaldolase. The latter might also be underestimated due to F6P aldolases being wrongly annotated as transaldolase, resulting from their high similarity [254,262].

Of all the 45 cellulolytic clostridia genomes in the JGI database, only the two *Clostridium papyrosolvens* genomes contain annotated transaldolases; two per genome, of which one contains the characteristic Glu and Tyr residues associated with transaldolase activity, rather than F6P aldolase activity [254]. Except for the *C. thermosuccinogenes* genomes, none of the genomes harbours a complete oxidative PPP, and besides the *C. thermocellum* genomes almost all harbour xylose isomerase and xylulokinase (required for growth on pentoses), meaning that cellulolytic clostridia in general rely on the SBP-pathway for the PPP, with the possible exception of *Clostridium papyrosolvens*.

How widespread the SBP-pathway is outside the cellulolytic clostridia would require further research, which is outside the scope of this study. The spread of PP_i-PFKs in a wide variety of organisms, the proved existence of the SBP-pathway in cellulolytic clostridia as well as the eukaryotic *E. histolytica*, and the high affinity of methylotrophic PFKs for S7P does hint at a much more widespread occurrence of the this pathway.

SBP identification

In some metabolomics studies, the identification of SBP is simply omitted, because the standard reagent was not available [252]. In others, SBP was synthesized *in vitro* using purified enzymes [59], which is laborious and expensive; and due to the low stability the product cannot be stored for longer periods. The method described here for the identification of SBP, relying on the *E. coli* Δ*talAB* strain is simple and cheap, and might therefore benefit other researchers studying pentose metabolism.

Furthermore, we noticed that commonly used practices for metabolomics studies, such as prolonged storage, and enrichment of extracts (e.g. via vacuum evaporation) will decrease the chance of detecting SBP in the extracts enormously.

Conclusion

An *E. coli* double transaldolase mutant was shown here to accumulate sedoheptulose 1,7-bisphosphate (SBP), verified by orbitrap mass-spectrometry. A metabolite extract from this *E. coli* mutant was used as an SBP reference for analysis (since SBP is not commercially available), and enabled us to show that a significant pool of sedoheptulose 1,7-bisphosphate (SBP) is present in *C. thermosuccinogenes*, an uncommon metabolite in organisms without the Calvin cycle. Moreover, the SBP pool was elevated during growth on xylose, confirming its relevance in pentose assimilation.

In vitro assays showed that PP_i-PFK of *C. thermosuccinogenes* and *C. thermocellum* is able to convert sedoheptulose 7-phosphate (S7P) to SBP, and that they have similar affinity for S7P and fructose 6-phosphate (F6P), the canonical substrate. In contrast, PfkA of *E. coli* showed a very poor affinity for S7P, which explains the high accumulation of S7P and SBP in the *E. coli* mutant. Furthermore, the enzyme kinetics suggest that the PP_i-PFK enzymes of cellulolytic clostridia may have evolved for the use of S7P.

Additionally, we found that the ATP/GTP-dependent PFK of *C. thermosuccinogenes* shows an extremely high degree of cooperative binding towards F6P, resulting in a virtual on/off switch for substrate concentrations near its $K_{1/2}$ value. We hypothesize that this PFK might represent a fail-safe mechanism that regulates the relative pools of F6P and S7P, in order to prevent competition for the active site of PP_i-PFK between the two parallel substrate pools causing one substrate to dominate the other.

Overall, these results verify the existence of the SBP-pathway in cellulolytic clostridia instead of the canonical transaldolase, connecting pentose metabolism with the rest of the metabolism.

Acknowledgements

The Center for Bioenergy Innovation is a US Department of Energy Bioenergy Research Center supported by the Office of Biological and Environmental Research in the DOE Office of Science.

JGK was funded by Corbion and the European Union Marie Skłodowska-Curie Innovative Training Networks (ITN), contract number 642068.

Conflicts of interest

Lee R. Lynd is a founder of Enchi Corporation, which has a financial interest in *C. thermocellum*.

Supporting information

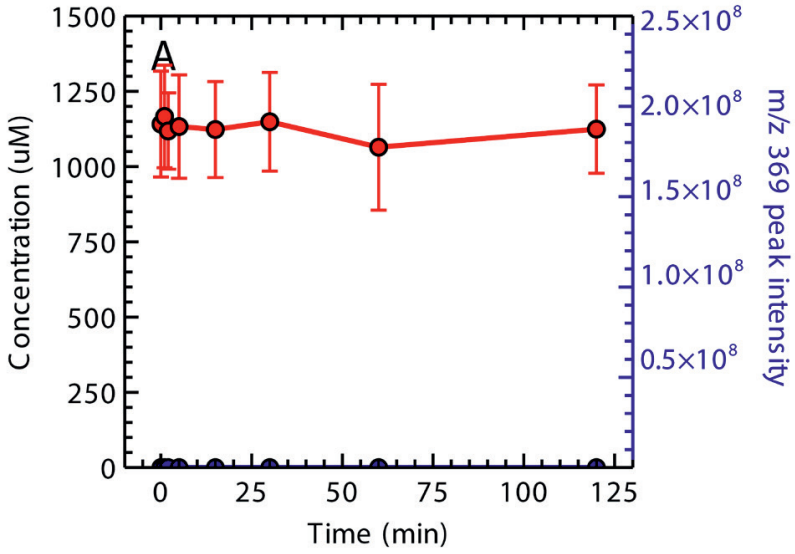

Figure S1: Negative control of the In vitro time-course assays using sedoheptulose-7-phosphate (red), lacking added enzyme. In blue the peak intensity at a m/z of 369, corresponding to sedoheptulose-1,7-bisphosphate. Error bars represent one standard deviation (n ≥ 2).

Clostridium thermosuccinogenes PPi-PFK

Michaelis-Menten kinetics

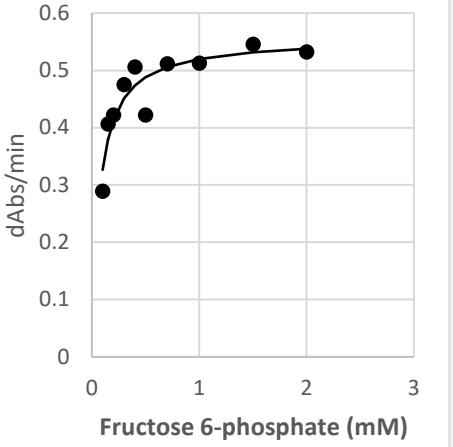

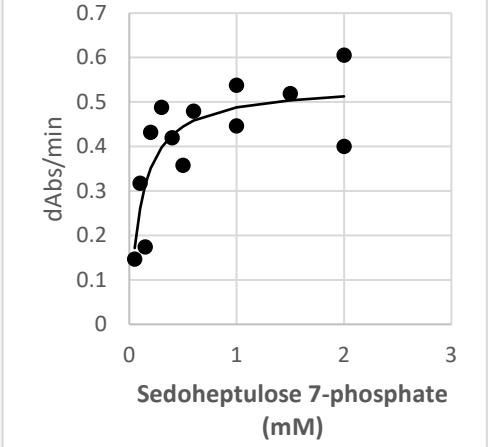

F6P: K_M = 0.07045054 mM, V_{max} = 0.556745262 dAbs/min

S7P: K_M = 0.107440985 mM, V_{max} = 0.540231693 dAbs/min

Hill kinetics

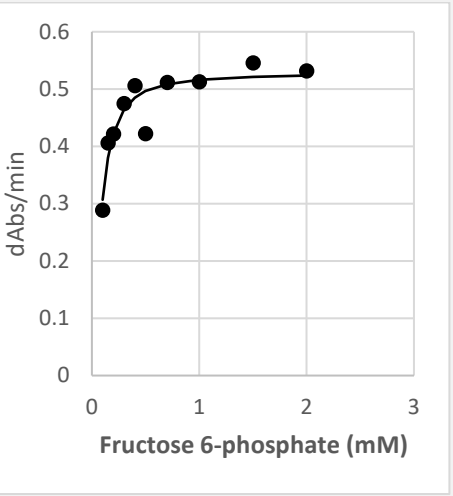

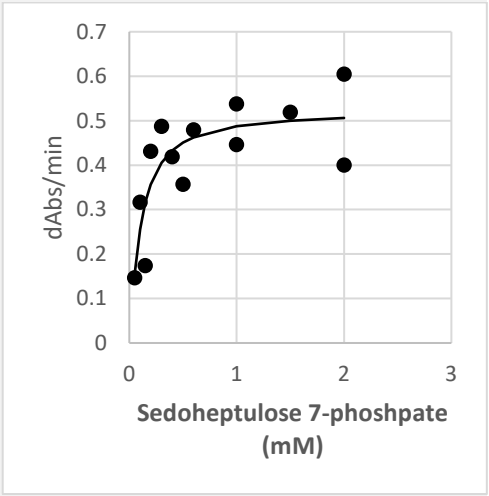

F6P: $K_{1/2}$ = 0.080468265 mM, V_{max} = 0.527619413 dAbs/min, n = 1.51508789

S7P: $K_{1/2}$ = 0.103684272 mM, V_{max} = 0.521954034 dAbs/min, n = 1.170962878

Figure S2: Data of the kinetics assays using *Clostridium thermosuccinogenes* PPi-6-phosphofructokinase (PFK) for the conversion of fructose 6-phosphate (F6P) and sedoheptulose 7-phosphate (S7P). Including fitted models of both Michealis-Menten kinetics and Hill kinetics.

Clostridium thermocellum PPi-PFK

Michaelis-Menten kinetics

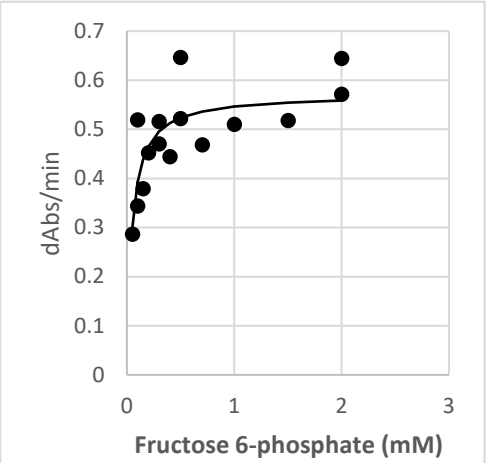

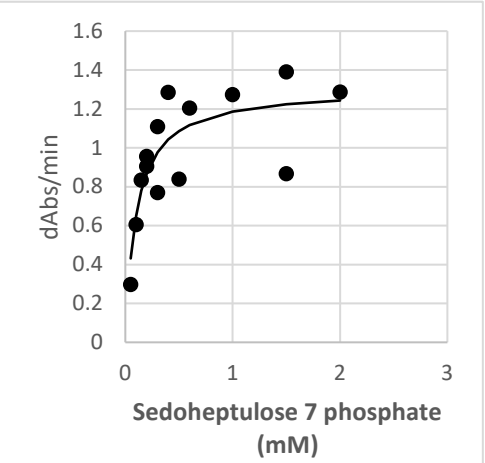

F6P: K_M = 0.046004018 mM, V_{max} = 0.571547641 dAbs/min

S7P: K_M = 0.10131141 mM, V_{max} = 1.306125685 dAbs/min

Hill kinetics

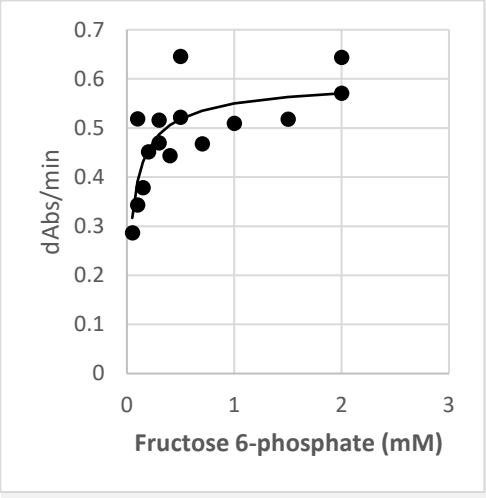

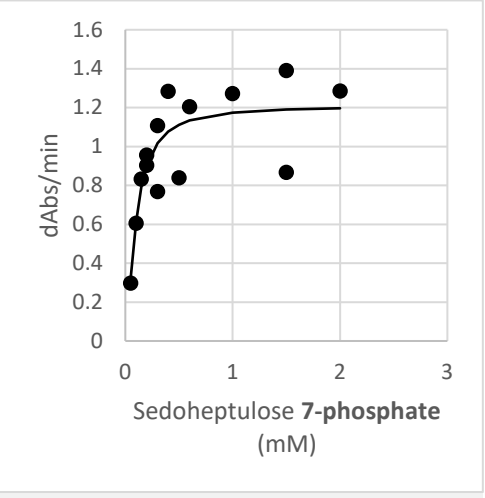

F6P: $K_{1/2}$ = 0.04393566 mM, V_{max} = 0.605090926 dAbs/min, n = 0.735169235

S7P: $K_{1/2}$ = 0.098186063 mM, V_{max} = 1.20981373 dAbs/min, n = 1.491188053

Figure S3: Data of the kinetics assays using *Clostridium thermocellum* PPi-6-phosphofructokinase (PFK) for the conversion of fructose 6-phosphate (F6P) and sedoheptulose 7-phosphate (S7P). Including fitted models of both Michealis-Menten kinetics and Hill kinetics.

E. coli PfkA

Michaelis-Menten kinetics

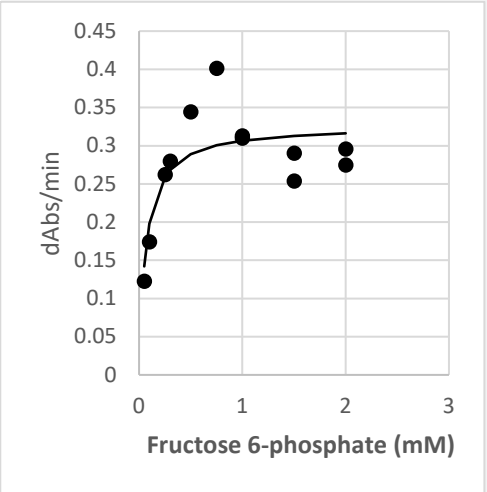

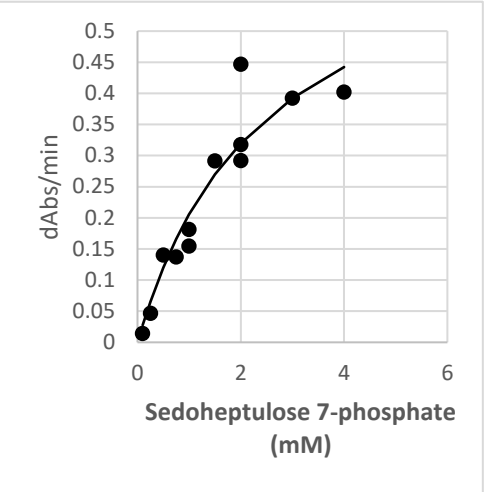

F6P: K_M = 0.064895717 mM, V_{max} = 0.326490009 dAbs/min

S7P: K_M = 2.489181822 mM, V_{max} = 0.717467989 dAbs/min

Hill kinetics

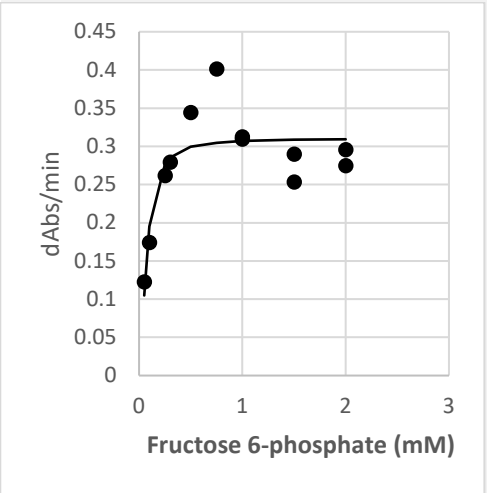

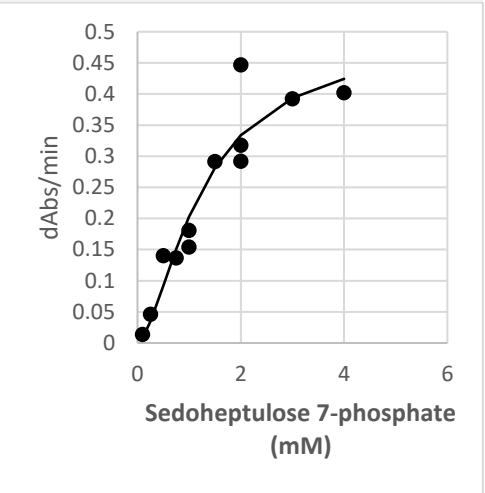

F6P: $K_{1/2}$ = 0.073763326 mM, V_{max} = 0.310312305 dAbs/min, n = 1.729659661

S7P: $K_{1/2}$ = 1.24179394 mM, V_{max} = 0.48943044 dAbs/min, n = 1.603138135

Figure S4: Data of the kinetics assays using *E. coli* 6-phosphofructokinase (PfkA) for the conversion of fructose 6-phosphate (F6P) and sedoheptulose 7-phosphate (S7P). Including fitted models of both Michealis-Menten kinetics and Hill kinetics.

P. thermosuccinogenes ATP/GTP-PFK

Michaelis-Menten kinetics

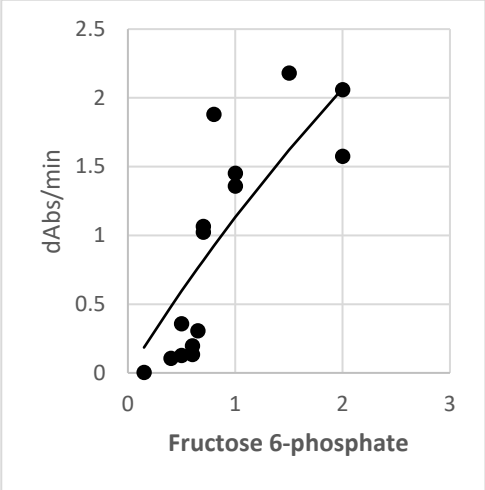

F6P: K_M = 9.550905907 mM, V_{max} = 11.94361907 dAbs/min

S7P: No activity

Hill kinetics

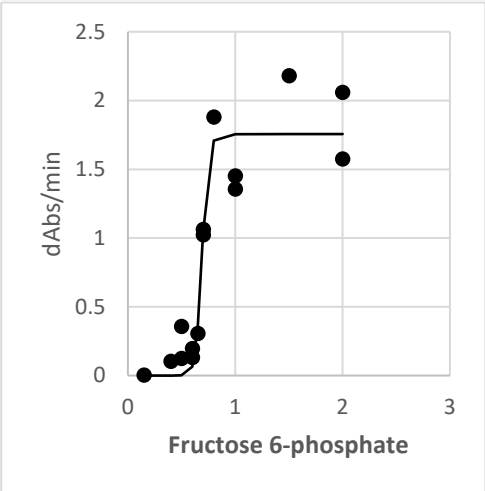

F6P: $K_{1/2}$ = 0.68836161 mM, V_{max} = 1.756115449 dAbs/min, n = 23.87224309

S7P: No activity

Figure S5: Data of the kinetics assays using *Clostridium thermosuccinogenes* ATP/GTP-6-phosphofructokinase (PFK) for the conversion of fructose 6-phosphate (F6P) and sedoheptulose 7-phosphate (S7P). Including fitted models of both Michealis-Menten kinetics and Hill kinetics.

Chapter 7 – Thesis summary

English summary

Pseudoclostridium thermosuccinogenes is the only known thermophile that produces succinic acid as one of its main fermentations products, together with acetic acid and formic acid, as well as ethanol, lactic acid, and hydrogen in smaller quantities. Thermophilic cell-factories, and succinic acid are both of interest for industrial biotechnology, and it is therefore that we set out to try to understand the metabolism of *P. thermosuccinogenes*.

In **Chapter 2** we published the genome sequences of the four available *P. thermosuccinogenes* strains (at that point still called *Clostridium thermosuccinogenes*). The genome of the type strain (DSM 5807) was fully closed. Using these annotated genomes, we were able to reconstruct its central metabolism. The genes for the pathways towards all the fermentation products were identified, as well as the complete Embden-Meyerhof-Parnas pathway for glycolysis. All genes for the pentose phosphate pathway (including those for xylose assimilation) were identified except for a transaldolase. Transcriptomics during growth on xylose versus glucose did not provide any leads to potential transaldolase genes or alternative pathways connecting the C_5 with the C_3/C_6 metabolism. Enzyme assays with cell-free extract were conducted to study cofactor usage of various glycolytic reactions. We were able to show that glucokinase was GTP-dependent and that 6-phosphofructokinase was PP_i-dependent, verifying what was previously shown in *Hungateiclostridium thermocellum*, a close relative of *P. thermosuccinogenes*. Furthermore, xylulokinase (absent in *Hungateiclostridium thermocellum*) was shown to use GTP as well.

In **Chapter 3** we looked further at the cofactor usage of *P. thermosuccinogenes*. Thirteen genes were cloned and heterologously expressed in *Escherichia coli* (encoding ribokinase, galactokinase, acetate kinase, isocitrate dehydrogenase, three 6-phosphofructokinase (PFK) orthologs, three glyceraldehyde 3-phosphate dehydrogenase (GAPDH) orthologs, and three genes encoding either pyruvate kinase, pyruvate, phosphate dikinase, or phosphoenolpyruvate synthase). Via enzyme assays we showed that besides glucokinase and xylulokinase, galactokinase and ribokinase are also GTP-dependent, suggesting that sugar phosphorylation by and large is GTP-dependent in *P. thermosuccinogenes*. Of the three PFKs, we confirmed which was PP_i-dependent, and we found that another was active with both ATP and GTP; no activity was found for the third. Two GAPDHs were found to be NAD^+-dependent, while no activity was detected for the third. Further, the use of PP_i and GTP as phosphoryl carriers was extensively discussed; we hypothesize that the use of GTP allows for different (or more flexible) reaction thermodynamics compared to reactions relying on ATP.

In **Chapter 4** the pathway to succinic acid in *P. thermosuccinogenes* was investigated in more detail. The fumarate hydratase and fumarate reductase (FRD) genes reside in an

operon together with the genes for a large electron bifurcating NADH-reductase-heterodisulfide reductase complex (Flx-Hdr) that takes electrons from NADH, reducing ferredoxin and a disulfide bond simultaneously. The FRD differs significantly from studied isoforms, but is closest related to methanogenic FRDs that use thiols to reduce fumarate, forming succinate and a disulphide compound. Based on this genomic context and comparative genomics, we propose two hypothetical mechanisms through which the FRD associates with the electron bifurcating Flx-Hdr complex: (1) A disulfide bond from a hitherto unknown cofactor is reduced by the Flx-Hdr complex, using NADH to generate two thiol groups, while facilitating the unfavourable reduction of ferredoxin by NADH. The disulfide bond is subsequently regenerated via the reduction of fumarate to succinate by the FRD using the previously formed thiol groups. Or, (2) the FRD forms an integral part of the FlxABCD-HdrABC complex, and NADH is used to reduce ferredoxin and fumarate directly, without an intermediate disulfide-forming cofactor. Either way enables the conservation of additional energy (in the form of reduced ferredoxin) by a soluble FRD, analogous to fumarate respiration. Some preliminary, inconclusive experimental data are presented as well.

In **Chapter 5** the effect of CO_2 limitation on succinate yield and on the metabolism of *P. thermosuccinogenes* in general was studied. Succinate production is connected to net fixation of CO_2 (by PEP carboxykinase) and was, therefore, expected to be impacted significantly. Batch cultivations in bioreactors sparged with 1% and 20% CO_2 were conducted that allowed us to carefully study the effect of CO_2 limitation. Formate yield was greatly reduced at low CO_2 concentrations, signifying a switch from pyruvate formate lyase (PFL) to pyruvate:ferredoxin oxidoreductase (PFOR) for acetyl-CoA formation. The corresponding increase in endogenous CO_2 production (by PFOR) enabled succinic acid production to be largely maintained as its yield was reduced by only 26%. Acetate yield was slightly reduced as well, while that of lactate was slightly increased. CO_2 limitation also prompted the formation of significant amounts of ethanol, which is only marginally produced during CO_2 excess. Altogether, the changes in fermentation product yields result in increased ferredoxin and NAD^+ reduction, and increased NADPH oxidation during CO_2 limitation, which must be linked to reshuffled (trans)hydrogenation mechanisms of those cofactors, in order to keep them balanced. RNA sequencing, to investigate transcriptional effects of CO_2 limitation, yielded only ambiguous results regarding the known (trans)hydrogenation mechanisms. Those results hinted at a decreased NAD^+/NADH ratio, which could ultimately be responsible for the stress observed during CO_2 limitation. Clear overexpression of an alcohol dehydrogenase (*adhE*) was observed, which may explain the increased ethanol production, while no changes were seen for PFL and PFOR expression that could explain the anticipated switch based on the fermentation results.

In **Chapter 6** the pentose phosphate pathway of *Hungateiclostridiaceae* was investigated in order to find out how they are able to interconvert C_5 and C_3/C_6 metabolites in the absence

of a transaldolase. We were able to confirm that *Hungateiclostridiaceae* rely on the sedoheptulose 1,7-bisphosphate (SBP) pathway, using pyrophosphate-dependent phosphofructokinase (PP_i-PFK) instead of transaldolase, as was proposed previously. In the SBP pathway, sedoheptulose 7-phosphate (the dead-end without transaldolase) is converted to SBP by PP_i-PFK after which fructose bisphosphate aldolase cleaves SBP into dihydroxyacetone phosphate and erythrose 4-phosphate. We showed that PP_i-PFK of *P. thermosuccinogenes* and of *H. thermocellum* indeed are able to convert S7P to SBP, and that they have similar affinities for S7P and fructose 6-phosphate (F6P), the canonical substrate. By contrast, (ATP-dependent) PfkA of *Escherichia coli* (which does rely on transaldolase) has a very poor affinity for S7P. This is indicative of the fact that the PP_i-PFK of the *Hungateiclostridiaceae* has evolved for the use of S7P. We further show that *P. thermosuccinogenes* contains a significant SBP pool, an otherwise unusual metabolite, which is elevated during growth on xylose, demonstrating its relevance for pentose assimilation. Lastly, we demonstrate that the other PFK of *P. thermosuccinogenes* that operates with ATP and GTP shows unusual kinetics towards F6P, as it appears to have an extremely high degree of cooperative binding, resulting in a virtual on/off switch for substrate concentrations near its $K_{1/2}$ value.

Chapter 8 – General Discussion

Natural succinic acid production

Many microorganisms have been isolated that naturally produce succinic acid as one of their fermentation products. Yet, little is generally written about the biological and ecological roles behind this phenomenon, as the focus is usually on the industrial production of succinic acid.

Microbial *fermentation* refers to specific mode of energy-conservation where the majority of ATP equivalents are generated via substrate level phosphorylation, in contrast to respiration, where the majority of ATP equivalents is produced by ATPase, through the formation of a membrane potential via electron transport. In fermentation, the electrons generated by the oxidation of a substrate are used for to the reduction of another substrate, or – usually – a pathway intermediate, without the immediate formation of a membrane potential [210].

Ethanol, lactic acid, and acetic acid are the typical fermentation products, but many more exists, such as butyric acid, acetone, and succinic acid. Different fermentation products have different chemical properties, and are associated with different metabolic pathways, that may have different cofactors associated with it, at different stoichiometry. As such, the type of fermentation product is intricately linked to the organism's physiology.

To give a few examples [185,210]: Ethanol fermentation and homolactic acid fermentation both yield 2 ATP per glucose, but lactic acid lowers the pH of the environment, and needs a dedicated membrane transporter. Ethanol, on the other hand, is linked with CO_2 formation, and requires several metabolic steps from pyruvate (compared to simply lactate dehydrogenase), which includes the formation of the toxic intermediate acetaldehyde. Furthermore, butyrate fermentation yields 3 ATP per glucose, whereas heterolactic fermentation (generating equal amounts of lactic acid, ethanol, and CO_2) only yields 1 ATP per glucose.

Succinic acid is produced during mixed acid fermentation, where it is produced in a variable mix with acetic acid, formic acid (and/or H_2), lactic acid, and ethanol [58,210]. The formation of succinic acid, or that of ethanol with formic acid (and/or H_2), allows the redox neutral production of acetic acid from pyruvate, and the concomitant formation of extra ATP. The substrate level ATP yield of mixed acid fermentation can therefore vary, depending on the distribution of the different fermentation products, but also due to variations in the specific pathways towards those products.

For the pathway to succinic acid, two different reactions are possible for the formation of oxaloacetate from phosphoenolpyruvate (PEP) and inorganic carbon: PEP carboxylase or PEP carboxykinase [138,196,292]. In the latter, CO_2 is used, and one ATP equivalent is

formed, whereas in the former, HCO_3^- is used, but no ATP equivalents are formed. Moreover, the fumarate reductase reaction can be linked to different cofactors in different organisms [124], which can also have further implications (**Chapter 4**). In the case quinol:fumarate reductase is used, four protons can be pumped out by a Type 1 NADH dehydrogenase, allowing the generation of up to 1 ATP, per succinic acid molecule formed. For the thiol:fumarate reductase coupled to the NADH dehydrogenase-heterodisulfide reductase complex (as is believed to be the case for *P. thermosuccinogenes*) the reduced ferredoxin allows up to two protons to be translocated via the RNF complex per succinic acid molecule formed, yielding up to 0.5 extra ATP.

Similarly, the formation of pyruvate from PEP can occur via three different pathways in *P. thermosuccinogenes* (i.e. pyruvate kinase; pyruvate, phosphate dikinase; and the malate shunt, as discussed in **Chapter 2 and 3**) that each have different cofactors associated with it [143,289,290]. The subsequent conversion from pyruvate to acetyl CoA can also occur via two different pathways in *P. thermosuccinogenes*, namely pyruvate:ferredoxin oxidoreductase or pyruvate formate lyase, while other organisms might use pyruvate dehydrogenase (**Chapter 5**) [147]. Such situations, with conversions involving electron bifurcation and/or ferredoxin reduction or involving parallel pathways, make that it is not always trivial to determine precise ATP yields of fermentation.

Besides mixed acid fermentation, succinate can also be formed through anaerobic fumarate respiration, where fumarate is used as final electron acceptor by quinol:fumarate reductase. Fumarate is the only known metabolic intermediate that can serve as acceptor in anaerobic respiration, and simultaneously represents the most widespread type of anaerobic respiration, likely because fumarate is readily formed from both carbohydrates and proteins [149]; other known acceptors include nitrate, sulphate, and sulphur, as well as many metals [241]. Fumarate respiration is best studied in *Wolinella succinogenes*, which uses hydrogen or formate as electron donor [148].

Beyond the energetics, different fermentation products also affect the organism's ecology in different ways. Accumulation of acids and alcohol can become toxic [112,172], and might prevent competitors from thriving. For example, one hypothesis for aerobic fermentation, a situation where some facultative anaerobes ferment in the presence of oxygen before switching to respiration (such as the Crabtree effect in yeast), is that it could be a tactic to stay ahead of the competition [107,228]. At high enough concentrations, fermentation products will eventually also become toxic to the producer, as is often the case in laboratory settings, where fermenting organisms are grown in isolation. In reality, however, fermentation products will form the substrates for other organisms, leading to a complex ecological network of cross-feeding. The guts of animals, in particular the rumen, are known to harbour complex trophic interactions [145,323].

In some cases, the producer is dependent on the consumption of a fermentation product by another organism, in order for its metabolism to proceed. This is referred to as *syntrophy* [202]. The best example is that of interspecies hydrogen transfer, where hydrogen formation is only feasible at low partial pressures, requiring its simultaneous consumption, i.e. by a methanogen or a sulphate-reducer [79,210]. In fact, in absence of a syntrophic hydrogen-consuming partner – again, typical for laboratory settings – many sugar-fermenting microorganisms shift to other fermentation products, in order to maintain a redox balance [202].

It is interesting to note that most natural succinic acid producing organisms have been isolated from animal guts (or from dung, as is the case for *P. thermosuccinogenes*). The likely explanation for this is that animal guts, and especially the rumen, have high partial pressures of CO_2, which makes PEP carboxykinase reaction more feasible in the ATP/GTP-forming direction (towards succinic acid, **Chapter 5**) [275]. Relatively little is known regarding the trophic interactions of succinic acid producers with other organisms. It is expected that they vary between various succinic acid producers; some produce succinic acid through the oxidation of hydrogen gas, while others might actually decrease the formation of succinic acid with increasing partial pressures of hydrogen (as observed for *P. thermosuccinogenes*) [116,161,279]. Several reports show that succinate conversion by propionate producers, such as *Selenomonas ruminantium* synergistically enhances rumen fibre digestion by succinate producing cellulolytic bacteria, such as *Ruminococcus flavefaciens* and *Fibrobacter succinogenes* [88,255]. In any case, the actual extracellular concentrations of succinic acid are very low in the rumen, as it is decarboxylated to form propionate as fast as it is produced [30,323]. In mouse models, the accumulation of succinic acid upon antibiotic use has been associated with *Clostridium difficile* infection, through the conversion of succinate to butyrate by the pathogen [81]. Furthermore, succinic acid producing *Bacteroides* excrete succinic acid when CO_2 is abundant, but convert it further to propionate to regenerate CO_2 when that becomes limiting [84]. This allows the pathway to keep operating as an electron sink, similar to what seems to happen in *P. thermosuccinogenes*, where the endogenous CO_2 is formed through PFOR, while lowering the PFL flux (**Chapter 5**).

Open questions regarding *Pseudoclostridium thermosuccinogenes*

In this thesis, we probed the central metabolism of *P. thermosuccinogenes* and were able to uncover several characteristic features that include: Cofactor usage (**Chapter 2 and 3**), a novel fumarate reductase (**Chapter 4**), the metabolic and transcriptional response upon CO_2-limitation (**Chapter 5**), and the sedoheptulose 1,7-bisphosphate (SBP) pathway (**Chapter 6**). Many open questions, still remain, however. Some of the pressing ones will be discussed below, and possible ways to tackle them will be proposed. A recurring problem is

the current lack of genetic systems for *P. thermosuccinogenes* that would otherwise allow us to make knock-outs or express heterologous proteins; this will be ignored for the moment.

What is the role of GTP as cofactor?

As was shown in **Chapter 3**, the sugar kinase reactions of *P. thermosuccinogenes* by and large appear to be GTP-dependent. With PEP carboxykinase seemingly the main GTP-generating reaction, this would create a relative closed loop for GTP turnover, ignoring the GTP used for anabolism. Our presented hypothesis states that GTP might exist at a different energy charge in parallel to that of ATP, and that this might improve CO_2 uptake rates under limiting concentrations. Accurate quantification via mass spectrometry or equivalent technology would provide an answer – at least to the first part of the hypothesis. Unfortunately, quantification of the different nucleotide pools can be very challenging [308], and might not be accurate enough.

Another approach could be the replacement of GTP-dependent glucokinase or xylulokinase as well as the GTP-dependent PEP carboxykinase with ATP-dependent variants to investigate how this would affect its physiology (in particular with regard to CO_2 limitation). Alternatively, ATP-dependent and GTP-dependent xylulose degrading pathways could be engineered in *H. thermocellum*, as this would remove the inherent bias created by comparing a native versus a heterologous pathway. Or, simpler maybe, the heterologous overexpression of nucleoside-diphosphate kinase (absent in *P. thermosuccinogenes*) could be attempted. By equalizing the energy charges of the different nucleotide pools, it will nullify any effects that a difference in energy charge would have, if indeed there is a difference. Worthwhile as well might be to accurately determine the concentration at which CO_2 becomes limiting, as was done by Herselman *et al*. (2017) [113], for a wide range of succinate producers that either rely on ATP, or GTP-dependent PEP carboxykinases, in order to see if there is a difference.

What is the role of PP_i as cofactor?

And additionally, what is the source of PP_i and AMP? The use of a PP_i–dependent phosphofructokinase (PFK), instead of ATP-PFK is believed to be a mechanism to conserve energy. PP_i is generated as a waste product of anabolism, which would otherwise simply be hydrolysed to maintain low enough PP_i concentrations (required to drive those anabolic reactions forward) and as such, ATP is being conserved by using PP_i. A similar thing happens with the conversion of PEP to pyruvate by pyruvate, phosphate dikinase (PPdK), where the use of PP_i allows the conversion of AMP to ATP, conserving two high energy phosphate bonds (instead of one, by pyruvate kinase). As calculated by Zhou *et al*. (2013), however, the flux of PP_i-generation by anabolism alone would not be enough to sustain the PP_i-PFK flux, suggesting that another PP_i generating mechanisms exists [331]. The current hypothesis is that a proton (or Na^+) translocating pyrophosphatase is responsible for the

formation of additional pyrophosphate through the proton gradient; and/or that a cycle exist around glycogen, which should lead to a net conversion of ATP and P_i to ADP and PP_i. The use of a translocating pyrophosphatase would lead to extra energy (i.e. ATP) conservation in the case that the proton/PP_i ratio is lower than the proton/ATP ratio.

Unclear also is the source of AMP, required for PPdK, as the thermodynamics of the adenylate kinase reaction (in *H. thermocellum*) appear restrictive for AMP formation (**Chapter 3**). Following the calculations of the PP_i fluxes, the flux of AMP generated through anabolism should also not be enough to sustain the PPdK flux. Possibly, a cycle between acetyl-CoA and acetate, via phosphate acetyltransferase, acetate kinase, and acetyl-CoA synthetase could exist, that would lead to the net conversion of ADP and P_i to AMP and PP_i, but for now that would be pure speculation.

The PP_i generating flux, resulting from anabolism, as calculated by Zhou *et al*. (2013) is based purely on the biomass composition, which represents the minimum requirement [331]. The continuous turnover of different biomass components, such as mRNA and proteins is only captured as part of the maintenance ATP-requirement, as it very hard to quantify, but likely represents a major part of it [132]. Such turn-over would correspond to additional PP_i (and AMP) formation. Therefore, the gap between PP_i required for PFK flux and PP_i formed by anabolism might not be as big as presumed.

In order to study the role of PP_i as cofactor, and pinpoint its source (beyond anabolism) it would be a good step to create knock-out/knock-down strains of genes involved in the proposed PP_i-sources (i.e. pyrophosphatases, glycogen metabolism, and acetyl-CoA synthetase), as well as to try to replace PP_i-PFK with an ATP-PFK, and assess the impact on the growth-rate and biomass yield, since a lower ATP yield should translate in a lower biomass yield. (Inside-out) Membrane vesicle preparations could provide insight whether there is indeed an energy conserving coupling between ATP hydrolysis and PP_i synthesis that would lead to more PP_i formed per ATP consumed [260].

How widespread is the SBP-pathway?

In **Chapter 6** we presented evidence for the existence of the SBP-pathway in *Hungateiclostridiaceae*, as an alternative to the typical transaldolase in the pentose phosphate pathway. Likely, there is no real advantage for relying on either of the two mechanism for connecting pentose metabolism with the rest of glycolysis. Glycolysis using PP_i-PFK, which is reversible (in contrast to ATP-PFK) would likely simply allow the loss of transaldolase, as it is no longer essential.

Unclear is how widespread the SBP-pathway really is. A reasonable assumption is that it is intricately linked to the use of PP_i-PFK in glycolysis, of which the occurrence across the tree of life is possibly also not fully recognized. A wide range of organisms appear to harbour the

PP_i-dependent variant [18,207], of which many also harbour the ATP-dependent variant (including *P. thermosuccinogenes*) making it hard to draw any conclusions. Perhaps the absence of a transaldolase, in the presence of a PP_i-PFK is a strong indicator for the reliance on PP_i as a cofactor for PFK in glycolysis (as well as the presence of the SBP-pathway). A detailed phylogenetic study into the occurrence of transaldolase and PP_i-PFK might therefore shed light on the prevalence of "atypical" PP_i-dependent metabolism as well as the SBP-pathway.

What is the essential component in yeast extract required for growth?

It has not been mentioned explicitly, except briefly in **Chapter 5**, but *P. thermosuccinogenes* requires yeast extract to grow. From experiments we know that 1 g/l of yeast extract allows the consumption of 5 g/l of glucose, but not of 25 g/l (data not shown). It is therefore that for the batch fermentations in **Chapter 5** 5 g/l yeast extract was used. For quantitative studies, you would want to use a medium that is as defined as possible, and therefore minimize the use of yeast extract, as well as similar complex medium components. For *H. thermocellum* a defined medium has been developed [126]. Yeast extract was effectively replaced by biotin, vitamin B12, *p*-aminobenzoic acid, and pyridoxamine (or pyridoxal, but not pyridoxine), but for *P. thermosuccinogenes* this was not sufficient. We have tested many different compounds for *P. thermosuccinogenes* (including vitamins, amino acids, nucleobases, and fatty acids). Unfortunately, we were unable to find out what compound in yeast extract was essential for growth. Other complex medium additives tested (such as tryptone, bacto casitone, and bacto beef extract) only allowed limited growth and were all inferior to yeast extract (data not shown). As yeast extract is known to be especially rich in B-vitamins, this would hint at a B-vitamin being limiting, but all of them were added separately as well, without the growth promoting effect of yeast extract. Possibly, more specific vitamin derivatives (e.g. thiamine pyrophosphate, pyridoxal 5-phosphate, or tetrahydrofolic acid) should be tested as well.

Several examples exists where the use of a genome scale metabolic model (GEM) was able to assist in finding specific auxotrophies, by finding reactions missing from the GEM that prevent *in silico* growth [10,78,273]. This approach could also assist in finding what essential nutrients present in yeast extract *P. thermosuccinogenes* requires.

Why is not all glucose consumed during batch fermentations?

Even in the presence of sufficient yeast extract, not all glucose is consumed during batch fermentations with 25 g/l glucose, as cells reach a stationary phase and the OD_{600} even decreases. The pH is maintained at 7. Acidification, which blocks growth after consumption of approximately 2 g/l glucose during bicarbonate buffered serum bottle cultivation, can therefore not be causing the incomplete consumption of the glucose. Nevertheless, even at neutral pH, the accumulation of fermentation products as salts (through titration with KOH) can become toxic. Serum bottle tests (data not shown) with added fermentation products

present at typical concentrations found at the end of batch fermentations (i.e. succinate, 70 mM; acetate, 50 mM; formate, 50 mM; lactate, 25 mM; and ethanol, 8.5 mM) did indeed show a reduction in growth rate from 0.43 μ^{-1} to 0.11-0.22 μ^{-1}. The presence of KCl alone at equal concentration (200 mM) also reduced the growth rate to 0.24 μ^{-1}, which strongly suggest that salt addition for pH titration is inhibiting growth of *P. thermosuccinogenes*, especially since additional KOH will be added to neutralize the acidifying effect of CO_2 present in the sparged gas. Surprisingly, an equivalent concentration of NaCl did not allow any growth at all.

Besides toxicity alone, additional mechanisms that could explain the incomplete glucose consumption still remain. For example, quorum sensing could limit the maximum cell-density, as well as trigger sporulation, which would also decrease glucose consumption [197]. More fermentations would be required to test this, for example by using supernatant of a finished fermentation run for the medium of new batch fermentation, or by having different starting concentrations of KCl, and check whether this correlates to the residual glucose.

What is the interaction between the novel fumarate reductase and the large NADH dehydrogenase-heterodisulfide reductase complex?

In **Chapter 4** we propose a mechanism by which fumarate is reduced to succinate in *P. thermosuccinogenes* by a novel fumarate reductase involved in electron bifurcation. Two hypothetical mechanisms are presented (**Chapter 4**, Fig. 6): (1) A disulfide bond from a hitherto unknown cofactor is reduced by the electron-bifurcating NADH dehydrogenase-heterodisulfide (Flx-Hdr) reductase complex, using NADH, in order to generate two thiol groups, while facilitating the otherwise unfavourable reduction of ferredoxin by NADH. The disulfide bond is subsequently regenerated via the reduction of fumarate to succinate by the fumarate reductase using the previously formed thiol groups. Or (2) the fumarate reductase forms an integral part of the Flx-Hdr complex, and NADH is used to reduce ferredoxin and fumarate directly, without an intermediate disulfide-forming cofactor.

The first step in (dis)proving the hypothetical mechanisms would be to (dis)prove that the Flx-Hdr complex is indeed essential for succinic acid formation, which could be achieved by creating Flx-Hdr knock-out strain, without interrupting the upstream fumarate hydratase or the downstream fumarate reductase. If succinic acid is still being formed, Flx-Hdr is not required for fumarate reductase activity.

Further, many approaches are imaginable to investigate whether the fumarate reductase and the Flx-Hdr complex indeed form a larger protein complex for electron bifurcation from NADH to ferredoxin and fumarate, without the mediation of a disulfide cofactor. For example, native gel electrophoresis combined with proteomics could allow the identification of macromolecular protein complexes containing Flx-Hdr proteins and

fumarate reductase. If antibodies are available, the same can be achieved without mass spectrometry. Another possibility is the use affinity tags, which should be inserted in the genome, followed by the identification of co-eluting proteins via proteomics. The use of a protein crosslinking reagent could further assist co-elution, or could possibly even eliminate the need of affinity tags altogether [270].

If no complex is formed between Flx-Hdr and fumarate reductase (but Flx-Hdr is required for succinic acid formation), it is likely that an intermediate disulfide cofactor is used. This cofactor could either be a (small) protein forming inter/intrachain disulfide bonds (through cysteine residues), or a set of two small molecules with thiol groups, such as glutathione, CoA, L-cysteine, or CoB & CoB used by methanogenic archaea. A small protein as cofactor could also be identified through co-elution/crosslinking. The identification of a small molecule could be a bit trickier. Mass-spectrometry of (reduced) metabolite extract supplemented with fumarate pre and post incubation with purified fumarate reductase might reveal what small metabolites are used, through the formation of larger disulfide molecules, according to a method described by Sévin *et al*. (2017) [266].

Future perspectives for industrial biobased succinic acid

Succinic acid is one of the first biobased platform chemicals that has been successfully commercialized, and the current industrial processes for bio-based succinic acid, and the entities behind them, have been presented in the thesis introduction. The market for bio-based polybutylene succinate (PBS) and other bio-based and biodegradable polymers is still lagging, however, and further improvements in process costs are desired for succinic acid to become a more ubiquitous bulk chemical [29,294]. Here we outline some of the prospects of different processes that might improve the efficiency of succinic acid production.

Production by *P. thermosuccinogenes*

P. thermosuccinogenes was the topic of this thesis for its ability to produce succinic acid as a major fermentation product, and for being the only thermophile known to do so. Aspects that are both of interest to biotechnology, as succinic acid has the potential to be used as a bio-based platform chemical, and because elevated temperatures can improve process economics.

We started off with the aim to understand the central metabolism of this scarcely studied anaerobic bacterium, which would form the basis for us to subsequently engineer the metabolism for improved succinic acid production. A parallel research project was initiated to set-up the genetic tools that would enable this to be done. The latter proved to be a more lengthy task than anticipated, and, therefore, this thesis only deals with understanding the metabolism of *P. thermosuccinogenes*. Nevertheless, progress has been made regarding the set-up genetic tools that deserves mentioning, as Joyshree Ganguly together with several

students developed a protocol for the electro-transformation of *P. thermosuccinogenes* strain DSM 5809 and the first steps have been made towards the use of a recently developed thermophilic Cas9 nuclease [204].

Following these developments it might soon become possible for the metabolic engineering of *P. thermosuccinogenes*, in order to improve succinic acid production. Currently, there are several problems that would prevent the organism from being used in industry, which could be addressed by metabolic engineering: Most importantly, the formation of large amounts of by-products, but also the requirement for added yeast extract. For polymer grade succinic acid, its purity typically needs to be high enough to reach weight-average molecular weights of 40.000 to 1.000.000 (i.e. 350~8.500 monomers). Molecules such as acetic acid and ethanol will terminate the chain elongation. Large amounts of by-products will therefore greatly impact the down-stream processing costs to reach such purities. Thus, having a homo-succinate producing strain is crucial.

Possible engineering targets:
In order to increase succinic acid production in *P. thermosuccinogenes* and turn it into a homo-succinate producer, the following engineering targets are proposed (Figure 1):

- Heterologous expression of a succinyl-CoA ligase, converting succinyl-CoA, P_i, and NDP to succinate, CoA, and NTP, while closing the TCA cycle. This way, succinate can also be formed through the oxidative branch of the TCA cycle (besides the reductive branch), which was shown to occur natively in *Clostridium acetobutylicum*, albeit with very low total succinic acid formation rates [6]. In theory, this would enable succinate to be produced in a redox neutral manner. Such a redox neutral pathway is important for homo-succinate production and something that is otherwise only possible through the co-production of other metabolites (e.g. acetate) or by providing an additional electron source (e.g. electricity or H_2).
- Deletion of pathways to other fermentation products: pyruvate formate lyase, acetaldehyde dehydrogenase and/or alcohol dehydrogenase, phosphate acetyltransferase and/or acetate kinase, and lactate dehydrogenase. This is the most obvious tactic to improve succinate production, but it can only work if enough ATP is generated in the absence of acetate kinase activity, and if the redox cofactors (NAD(P)H and ferredoxin) are properly balanced.
- Overexpression of the energy-converting ferredoxin:NAD^+ reductase complex (RNF) and/or the energy-converting ferredoxin-dependent hydrogenase complex (ECH) might enable proper balancing of the redox cofactors, while providing metabolic energy through the generation of a membrane potential. Over-expression of other transhydrogenase enzymes could also be attempted to achieve proper redox balancing.

- Knock-out or knock-down of malic enzyme, to reduce competition with fumarate hydratase for malic acid. The reduction in NADPH generation can be compensated by isocitrate dehydrogenase activity if the oxidative branch of the TCA cycle is active (by succinyl-CoA ligase expression).
- Overexpression of the succinate exporter. Currently, the encoding gene is unknown, but in **Chapter 4** we provide a likely candidate.

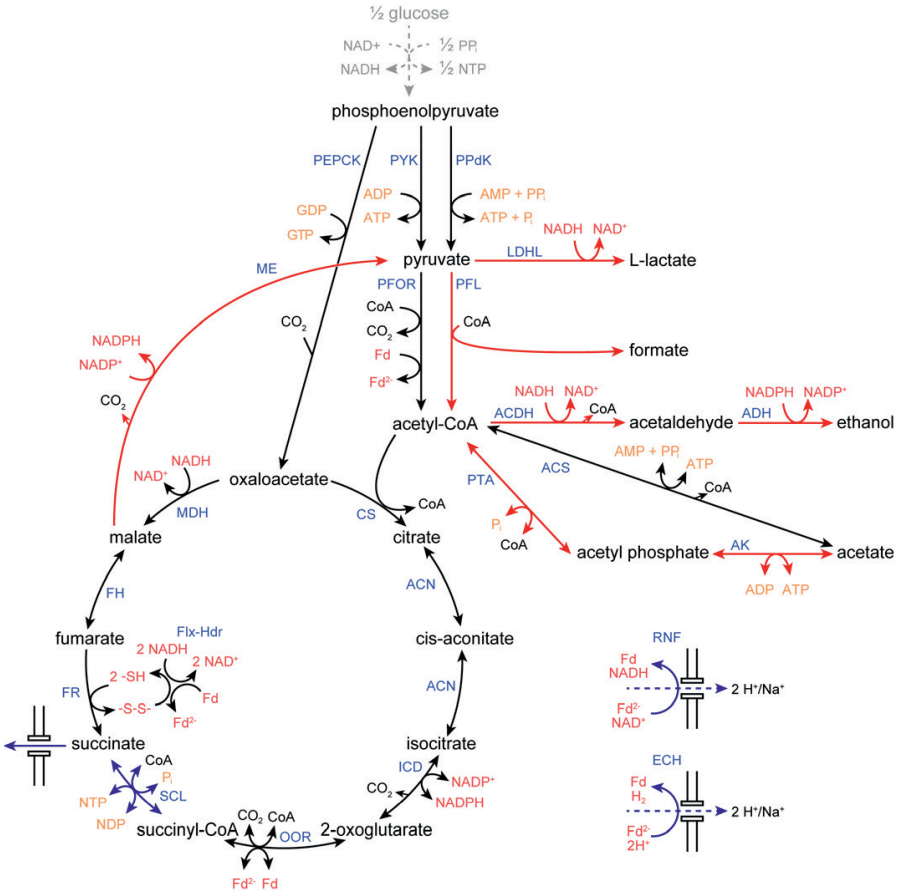

Figure 1: Metabolic pathways from phosphoenolpyruvate (PEP) to the different fermentation products in *P. thermosuccinogenes*, with proposed metabolic engineering targets; red arrow for knock-out/knock-down targets, blue arrow for (heterologous) over-expression targets. The dashed grey arrow represents the glycolysis, which relies on a PP_i-dependent phosphofructokinase. ACDH, acetaldehyde dehydrogenase; ACN, aconitase; ACS, acetyl-CoA synthetase; ADH, alcohol dehydrogenase; AK, acetate kinase; CS, citrate synthase; ECH. Energy-converting hydrogenase; Flx-Hdr, NADH dehydrogenase/heterodisulfide reductase bifurcation complex; FH, fumarate hydratase; FR, fumarate reductase; ICD, isocitrate dehydrogenase; LDHL, l-lactate dehydrogenase; MDH, malate dehydrogenase; ME, malic enzyme; OOR, 2-oxoglutarate:ferredoxin oxidoreductase; PEPCK, phosphoenolpyruvate carboxykinase; PFL, pyruvate formate lyase; PFOR, pyruvate:ferredoxin oxidoreductase; PPdK, pyruvate, phosphate dikinase; PTA, phosphate acetyltransferase; PYK, pyruvate kinase; RNF, energy-converting ferredoxin:NAD^+ reductase; SCL, succinyl-CoA ligase.

Production by other thermophiles

Even if *P. thermosuccinogenes* were to be engineered to produce succinic acid as the only major fermentation product, it still needs to be able to withstand the harsh conditions of industrial fermenters. Considering the relatively low tolerance to salts observed during lab-scale bioreactor experiments, this might also be problematic. Adaptive evolution might improve this. Otherwise, other thermophiles that are better suited for industrial fermentations might be engineered to produce succinic acid, using the (thermophilic) succinic acid pathway of *P. thermosuccinogenes*.

To engineer another organism with the succinate pathway of *P. thermosuccinogenes*, it is imperative to further study its fumarate reductase, to fully understand what cofactor(s) are used, and how it interacts with the NADH dehydrogenase-heterodisulfide reductase (Flx-Hdr) complex. If it requires a specific (disulfide) cofactor, this needs to be known, and it needs be present or introduced into the host as well. Moreover, ferredoxin reduced by the (Flx-Hdr) complex needs a way to be re-oxidized. Overall, this would make it seem rather complicated to use the *P. thermosuccinogenes* fumarate reductase. It might be easier to use a NADH or quinol-dependent fumarate reductase from a thermophile, even if this would not be a natural succinate producer. Nevertheless, the connection with the Flx-Hdr complex might also be an advantage, as the conserved energy, in the form of a low-potential ferredoxin might enable the formation of extra ATP (through ECH or RNF), which might otherwise be the limiting factor in an anaerobic homo-succinate producer.

Regardless of the type of fumarate reductase used, for engineering a microorganism to produce a novel product, it is important that is possesses the means to export the product out of the cell, if it is not able to diffuse through the membrane, as is the case for succinate (at neutral pH). Since *P. thermosuccinogenes* is the only known thermophile to produce succinic acid, it is likely also the only known thermophile to possess an efficient succinic acid exporter protein. Identifying that protein in *P. thermosuccinogenes* should therefore be a top priority for further research into thermophilic succinic acid production.

Potential hosts for the succinic acid pathway of *P. thermosuccinogenes* include the close relative *Hungateiclostridium thermocellum,* or *Thermoanaerobacterium saccharolyticum*, which have both been studied extensively for their possible application in industry [16,268]. Or *Bacillus smithii*, which already has efficient genome editing tools available, thanks to the work in the Laboratory of Microbiology here at Wageningen University [38–40,203,204]. However, none of the aforementioned strains, have yet been applied successfully in industry. As such, industrial succinic acid production by an engineered thermophile is not likely to happen soon.

Production from C_1 compounds

The use of C_1 compounds, such as CO_2 (plus H_2), CO, methanol, and formate as substrates is a different biotechnological process that has been gaining a lot of attention in recent years. Its main advantage is that it does not rely on biomass (i.e. agriculture or forestry), but can simply be based on CO_2 and electricity. In particular the research into the use of acetogenic bacteria growing on syngas has been increasing tremendously [26], albeit specific research into succinic acid production by acetogens is lacking. A computational study estimated that microbial CO_2 to succinate conversion could be feasible, assuming substantial strain optimization is achieved [170].

Finally, the fact that sugar based (i.e. heterotrophic) succinic acid fermentation also co-occurs with net CO_2 fixation offers further opportunities; in particular if governments increase taxation on CO_2 emissions. It could be applied as a mechanism for CO_2 scrubbing. In order to remove the bulk of the CO_2 that is present in biogas, for example [104].

Downstream processing

The downstream processing (DSP) procedures for succinic acid remain costly, even if it is the only fermentation product formed by the production organism; the costs are typically estimated to be more than half of the total production cost [22,114]. Substantial research efforts are therefore also put into DSP as well as other aspects of the bioreactor designs.

The current commercial succinic acid plants rely either direct crystallization or on ammonia precipitation methods for the DSP of succinic acid. Both processes are relatively simple, but require significant energy inputs [56]. Moreover, direct crystallization yield can be poor, while the ammonia precipitation process is less selective for succinic acid and results in formation of large amounts of $(NH4)_2SO_4$ [122,153]. Alternative DSP methods being investigated include membrane filtration (including electrodialysis), liquid-liquid extraction, as well as reactive extraction, and resin adsorption [68,136,233,276].

Conclusion

In order for the chemical industry to decrease its dependency on fossil fuels as feedstock, significant research is still required, including into the use of microorganisms as cell-factories, which facilitates the use of biomass or CO_2 as raw material. Much is already possible, but it is often hard or even impossible to compete with those fossil feedstocks. It is therefore important that fundamental research into microbial metabolism, such as that presented in this thesis, is conducted and is funded. New insights, in particular in extremophilic (e.g. thermophilic) non-model organisms may well enable future processes to be more efficient – and even if biobased processes did not need to compete with the dinosaurs of the fossil fuel industry, that is of course favoured.

Appendices

References

[1] B.M.A. Abdel-Banat, H. Hoshida, A. Ano, S. Nonklang, R. Akada, High-temperature fermentation: how can processes for ethanol production at high temperatures become superior to the traditional process using mesophilic yeast?, Appl. Microbiol. Biotechnol. 85 (2010) 861–867.

[2] F. Adom, J.B. Dunn, J. Han, N. Sather, Life-Cycle Fossil Energy Consumption and Greenhouse Gas Emissions of Bioderived Chemicals and Their Conventional Counterparts, Environ. Sci. Technol. 48 (2014) 14624–14631.

[3] J.H. Ahn, Y.-S. Jang, S.Y. Lee, Production of succinic acid by metabolically engineered microorganisms, Curr. Opin. Biotechnol. 42 (2016) 54–66.

[4] M.K. Akhtar, P.R. Jones, Deletion of iscR stimulates recombinant clostridial Fe–Fe hydrogenase activity and H2-accumulation in Escherichia coli BL21(DE3), Appl. Microbiol. Biotechnol. 78 (2008) 853–862.

[5] A.M.C.R. Alves, G.J.W. Euverink, H. Santos, L. Dijkhuizen, Different Physiological Roles of ATP- and PPi-Dependent Phosphofructokinase Isoenzymes in the Methylotrophic Actinomycete Amycolatopsis methanolica, J. Bacteriol. 183 (2001) 7231–7240.

[6] D. Amador-Noguez, X.J. Feng, J. Fan, N. Roquet, H. Rabitz, J.D. Rabinowitz, Systems-level metabolic flux profiling elucidates a complete, bifurcated tricarboxylic acid cycle in Clostridium acetobutylicum, J. Bacteriol. 192 (2010) 4452–4461.

[7] C. Ampelli, S. Perathoner, G. Centi, CO2 utilization: an enabling element to move to a resource- and energy-efficient chemical and fuel production, Philos. Trans. R. Soc. A Math. Phys. Eng. Sci. 373 (2015) 20140177–20140177.

[8] S. Andrews, FastQC: a quality control tool for high throughput sequence data, (2010).

[9] A. Argyos, T. Barrett, N. Caiazza, D. Hogsett, GENETICALLY MODIFIED CLOSTRIDIUM THERMOCELLUM ENGINEERED TO FERMENT XYLOSE, WO2012088467 (A2), 2012.

[10] K.C.H. van der Ark, S. Aalvink, M. Suarez-Diez, P.J. Schaap, W.M. de Vos, C. Belzer, Model-driven design of a minimal medium for Akkermansia muciniphila confirms mucus adaptation, Microb. Biotechnol. 11 (2018) 476–485.

[11] C. Aslanidis, P.J. de Jong, Ligation-independent cloning of PCR products (LIC-PCR), Nucleic Acids Res. 18 (1990) 6069–6074.

[12] D.E. Atkinson, The energy charge of the adenylate pool as a regulatory parameter. Interaction with feedback modifiers., Biochemistry. 7 (1968) 4030–4.

[13] D.E. Atkinson, Energy charge of the adenylate pool as a regulatory parameter. Interaction with feedback modifiers, Biochemistry. 7 (1968) 4030–4034.

[14] A.F. Auch, M. von Jan, H.-P. Klenk, M. Göker, Digital DNA-DNA hybridization for microbial species delineation by means of genome-to-genome sequence comparison, Stand. Genomic Sci. 2 (2010) 117–134.

[15] R.K. Aziz, D. Bartels, A.A. Best, M. DeJongh, T. Disz, R.A. Edwards, K. Formsma, S. Gerdes, E.M. Glass, M. Kubal, F. Meyer, G.J. Olsen, R. Olson, A.L. Osterman, R.A. Overbeek, L.K. McNeil, D. Paarmann, T. Paczian, B. Parrello, G.D. Pusch, C. Reich, R. Stevens, O. Vassieva, V. Vonstein, A. Wilke, O. Zagnitko, The RAST Server: Rapid Annotations using Subsystems Technology, BMC Genomics. 9 (2008) 75.

[16] M.L. Balch, E.K. Holwerda, M.F. Davis, R.W. Sykes, R.M. Happs, R. Kumar, C.E. Wyman, L.R. Lynd, Lignocellulose fermentation and residual solids characterization for senescent switchgrass fermentation

by Clostridium thermocellum in the presence and absence of continuous in situ ball-milling, Energy Environ. Sci. 10 (2017) 1252–1261.

[17] A. Bankevich, S. Nurk, D. Antipov, A.A. Gurevich, M. Dvorkin, A.S. Kulikov, V.M. Lesin, S.I. Nikolenko, S. Pham, A.D. Prjibelski, A. V. Pyshkin, A. V. Sirotkin, N. Vyahhi, G. Tesler, M.A. Alekseyev, P.A. Pevzner, SPAdes: A New Genome Assembly Algorithm and Its Applications to Single-Cell Sequencing, J. Comput. Biol. 19 (2012) 455–477.

[18] E. Bapteste, D. Moreira, H. Philippe, Rampant horizontal gene transfer and phospho-donor change in the evolution of the phosphofructokinase, Gene. 318 (2003) 185–191.

[19] A. Bar-Even, A. Flamholz, E. Noor, R. Milo, Rethinking glycolysis: on the biochemical logic of metabolic pathways, Nat. Chem. Biol. 8 (2012) 509–517.

[20] A. Bar-Even, A. Flamholz, E. Noor, R. Milo, Thermodynamic constraints shape the structure of carbon fixation pathways, Biochim. Biophys. Acta - Bioenerg. 1817 (2012) 1646–1659.

[21] O. Bârzu, I. Abrudan, I. Proinov, L. Kiss, N.G. Ty, G. Jebeleanu, I. Goia, M. Kezdi, H.H. Mantsch, Nucleotide specificity of pyruvate kinase and phosphoenolpyruvate carboxykinase, Biochim. Biophys. Acta - Enzymol. 452 (1976) 406–412.

[22] I. Bechthold, K. Bretz, S. Kabasci, R. Kopitzky, A. Springer, Succinic Acid: A New Platform Chemical for Biobased Polymers from Renewable Resources, Chem. Eng. Technol. 31 (2008) 647–654.

[23] J. Becker, A. Lange, J. Fabarius, C. Wittmann, Top value platform chemicals: bio-based production of organic acids, Curr. Opin. Biotechnol. 36 (2015) 168–175.

[24] J. Becker, J. Reinefeld, R. Stellmacher, R. Schäfer, A. Lange, H. Meyer, M. Lalk, O. Zelder, G. von Abendroth, H. Schröder, S. Haefner, C. Wittmann, Systems-wide analysis and engineering of metabolic pathway fluxes in bio-succinate producing *Basfia succiniciproducens*, Biotechnol. Bioeng. 110 (2013) 3013–3023.

[25] J. Becker, C. Wittmann, Advanced Biotechnology: Metabolically Engineered Cells for the Bio-Based Production of Chemicals and Fuels, Materials, and Health-Care Products, Angew. Chemie Int. Ed. 54 (2015) 3328–3350.

[26] F.R. Bengelsdorf, M. Straub, P. Dürre, Bacterial synthesis gas (syngas) fermentation, Environ. Technol. 34 (2013) 1639–1651.

[27] B.K. Bhuyan, F.J. Simpson, SOME PROPERTIES OF THE D -YLULOKINASE OF AEROBACTER AEROGENES, Can. J. Microbiol. 8 (1962) 737–745.

[28] A.A.M. Bielen, K. Willquist, J. Engman, J. Van Der Oost, E.W.J. Van Niel, S.W.M. Kengen, Pyrophosphate as a central energy carrier in the hydrogen-producing extremely thermophilic Caldicellulosiruptor saccharolyticus, FEMS Microbiol. Lett. 307 (2010) 48–54.

[29] Bioplasticsmagazine.com, Showa Denko abandons production of Bionolle biodegradable polyester, (2016).

[30] T.H. BLACKBURN, R.E. HUNGATE, Succinic acid turnover and propionate production in the bovine rumen., Appl. Microbiol. 11 (1963) 132–5.

[31] D. Blangy, H. Buc, J. Monod, Kinetics of the allosteric interactions of phosphofructokinase from Escherichia coli, J. Mol. Biol. 31 (1968) 13–35.

[32] E.G. Bligh, W.J. Dyer, A RAPID METHOD OF TOTAL LIPID EXTRACTION AND PURIFICATION, Can. J. Biochem. Physiol. 37 (1959) 911–917.

[33] T.A. Bobik, R.S. Wolfe, An unusual thiol-driven fumarate reductase in Methanobacterium with the production of the heterodisulfide of coenzyme M and N-(7-mercaptoheptanoyl)threonine-O3-phosphate., J. Biol. Chem. 264 (1989) 18714–8.

[34] M. Boetzer, W. Pirovano, Toward almost closed genomes with GapFiller, Genome Biol. 13 (2012) R56.

[35] M. Boetzer, W. Pirovano, SSPACE-LongRead: scaffolding bacterial draft genomes using long read sequence information, BMC Bioinformatics. 15 (2014) 211.

[36] F.C. Boogerd, P. Bos, J.G. Kuenen, J.J. Heijnen, R.G.J.M. van der Lans, Oxygen and carbon dioxide mass transfer and the aerobic, autotrophic cultivation of moderate and extreme thermophiles: A case study related to the microbial desulfurization of coal, Biotechnol. Bioeng. 35 (1990) 1111–1119.

[37] V.M. Boradia, M. Raje, C.I. Raje, Protein moonlighting in iron metabolism: glyceraldehyde-3-phosphate dehydrogenase (GAPDH), Biochem. Soc. Trans. 42 (2014) 1796–1801.

[38] E.F. Bosma, J.J. Koehorst, S.A.F.T. van Hijum, B. Renckens, B. Vriesendorp, A.H.P. van de Weijer, P.J. Schaap, W.M. de Vos, J. van der Oost, R. van Kranenburg, Complete genome sequence of thermophilic Bacillus smithii type strain DSM 4216T, Stand. Genomic Sci. 11 (2016) 52.

[39] E.F. Bosma, A.H.P. van de Weijer, M.J.A. Daas, J. van der Oost, W.M. de Vos, R. van Kranenburg, Isolation and Screening of Thermophilic Bacilli from Compost for Electrotransformation and Fermentation: Characterization of Bacillus smithii ET 138 as a New Biocatalyst, Appl. Environ. Microbiol. 81 (2015) 1874–1883.

[40] E.F. Bosma, A.H.P. van de Weijer, L. van der Vlist, W.M. de Vos, J. van der Oost, R. van Kranenburg, Establishment of markerless gene deletion tools in thermophilic Bacillus smithii and construction of multiple mutant strains., Microb. Cell Fact. 14 (2015) 99.

[41] J.J. Bozell, G.R. Petersen, Technology development for the production of biobased products from biorefinery carbohydrates—the US Department of Energy's "Top 10" revisited, Green Chem. 12 (2010) 539.

[42] M.F.A. Bradfield, W. Nicol, Continuous succinic acid production by Actinobacillus succinogenes in a biofilm reactor: Steady-state metabolic flux variation, Biochem. Eng. J. 85 (2014) 1–7.

[43] K. Bretz, Succinic Acid Production in Fed-Batch Fermentation of Anaerobiospirillum succiniciproducens Using Glycerol as Carbon Source, Chem. Eng. Technol. 38 (2015) 1659–1664.

[44] S.J.J. Brouns, J. Walther, A.P.L. Snijders, H.J.G. van de Werken, H.L.D.M. Willemen, P. Worm, M.G.J. de Vos, A. Andersson, M. Lundgren, H.F.M. Mazon, R.H.H. van den Heuvel, P. Nilsson, L. Salmon, W.M. de Vos, P.C. Wright, R. Bernander, J. van der Oost, Identification of the Missing Links in Prokaryotic Pentose Oxidation Pathways, J. Biol. Chem. 281 (2006) 27378–27388.

[45] W. Buckel, R.K. Thauer, Flavin-Based Electron Bifurcation, Ferredoxin, Flavodoxin, and Anaerobic Respiration With Protons (Ech) or NAD+ (Rnf) as Electron Acceptors: A Historical Review, Front. Microbiol. 9 (2018) 401.

[46] W. Buckel, R.K. Thauer, Flavin-Based Electron Bifurcation, A New Mechanism of Biological Energy Coupling, Chem. Rev. 118 (2018) 3862–3886.

[47] B. van den Burg, Extremophiles as a source for novel enzymes, Curr. Opin. Microbiol. 6 (2003) 213–218.

[48] Business Wire, Global Polypropylene (PP) Market Size, Demand Forecasts, Industry Trends & Updates (2018-2025) - ResearchAndMarkets.com, (2018).

[49] L.D. Byers, [57] Glyceraldehyde-3-phosphate dehydrogenase from yeast, in: Methods Enzymol.,

Academic Press, 1982: pp. 326–335.

[50] R. Cabrera, J. Babul, V. Guixé, Ribokinase family evolution and the role of conserved residues at the active site of the PfkB subfamily representative, Pfk-2 from Escherichia coli, Arch. Biochem. Biophys. 502 (2010) 23–30.

[51] G. Caggianiello, M. Kleerebezem, G. Spano, Exopolysaccharides produced by lactic acid bacteria: from health-promoting benefits to stress tolerance mechanisms, Appl. Microbiol. Biotechnol. 100 (2016) 3877–3886.

[52] A.M. Chakrabarty, Nucleoside diphosphate kinase: role in bacterial growth, virulence, cell signalling and polysaccharide synthesis, Mol. Microbiol. 28 (1998) 875–882.

[53] A.G. Chapman, L. Fall, D.E. Atkinson, Adenylate energy charge in Escherichia coli during growth and starvation., J. Bacteriol. 108 (1971) 1072–86.

[54] H. Chen, J. Liu, X. Chang, D. Chen, Y. Xue, P. Liu, H. Lin, S. Han, A review on the pretreatment of lignocellulose for high-value chemicals, Fuel Process. Technol. 160 (2017) 196–206.

[55] J. Chen, A. Brevet, M. Fromant, F. Leveque, J.-M. Schmitter, S. Blanquet, P. Plateau, Pyrophosphatase Is Essential for Growth of Escherichia coli, 1990.

[56] K.-K. Cheng, X.-B. Zhao, J. Zeng, R.-C. Wu, Y.-Z. Xu, D.-H. Liu, J.-A. Zhang, Downstream processing of biotechnological produced succinic acid, Appl. Microbiol. Biotechnol. 95 (2012) 841–850.

[57] F. Cherubini, The biorefinery concept: Using biomass instead of oil for producing energy and chemicals, Energy Convers. Manag. 51 (2010) 1412–1421.

[58] D. CLARK, The fermentation pathways of Escherichia coli, FEMS Microbiol. Rev. 63 (1989) 223–234.

[59] M.F. Clasquin, E. Melamud, A. Singer, J.R. Gooding, X. Xu, A. Dong, H. Cui, S.R. Campagna, A. Savchenko, A.F. Yakunin, J.D. Rabinowitz, A.A. Caudy, Riboneogenesis in Yeast, Cell. 145 (2011) 969–980.

[60] B. Cok, I. Tsiropoulos, A.L. Roes, M.K. Patel, Succinic acid production derived from carbohydrates: An energy and greenhouse gas assessment of a platform chemical toward a bio-based economy, Biofuels, Bioprod. Biorefining. 8 (2014) 16–29.

[61] V. Coustou, S. Besteiro, L. Rivière, M. Biran, N. Biteau, J.-M. Franconi, M. Boshart, T. Baltz, F. Bringaud, A Mitochondrial NADH-dependent Fumarate Reductase Involved in the Production of Succinate Excreted by Procyclic Trypanosoma brucei, J. Biol. Chem. 280 (2005) 16559–16570.

[62] Dachema, Hard Times for Bio-based Products | chemanager-online.com, (2018).

[63] A.S. Dahms, R.L. Anderson, 2-Keto-3-deoxy-L-arabonate aldolase and its role in A new pathway of L-arabinose degradation, Biochem. Biophys. Res. Commun. 36 (1969) 809–814.

[64] B. Damen, A. Pollet, E. Dornez, W.F. Broekaert, I. Van Haesendonck, I. Trogh, F. Arnaut, J. a. Delcour, C.M. Courtin, Xylanase-mediated in situ production of arabinoxylan oligosaccharides with prebiotic potential in whole meal breads and breads enriched with arabinoxylan rich materials, Food Chem. 131 (2012) 111–118.

[65] S. Dash, A. Khodayari, J. Zhou, E.K. Holwerda, D.G. Olson, L.R. Lynd, C.D. Maranas, Development of a core Clostridium thermocellum kinetic metabolic model consistent with multiple genetic perturbations, Biotechnol. Biofuels. 10 (2017) 108.

[66] S. Dash, D.G. Olson, S.H. Joshua Chan, D. Amador-Noguez, L.R. Lynd, C.D. Maranas, Thermodynamic analysis of the pathway for ethanol production from cellobiose in Clostridium thermocellum, Metab.

Eng. 55 (2019) 161–169.

[67] C.P. DAVIS, D. CLEVEN, J. BROWN, E. BALISH, Anaerobiospirillum, a New Genus of Spiral-Shaped Bacteria, Int. J. Syst. Bacteriol. 26 (1976) 498–504.

[68] B.H. Davison, N.P. Nghiem, G.L. Richardson, Succinic Acid Adsorption from Fermentation Broth and Regeneration, in: Proc. Twenty-Fifth Symp. Biotechnol. Fuels Chem. Held May 4–7, 2003, Breckenridge, CO, Humana Press, Totowa, NJ, 2004: pp. 653–669.

[69] B.A. Dehority, Carbon dioxide requirement of various species of rumen bacteria., J. Bacteriol. 105 (1971) 70–6.

[70] Y. Deng, D.G. Olson, J. Zhou, C.D. Herring, A. Joe Shaw, L.R. Lynd, Redirecting carbon flux through exogenous pyruvate kinase to achieve high ethanol yields in Clostridium thermocellum, Metab. Eng. 15 (2013) 151–158.

[71] M. Desvaux, Clostridium cellulolyticum : model organism of mesophilic cellulolytic clostridia, FEMS Microbiol. Rev. 29 (2005) 741–764.

[72] W.L. Dills, P.D. Parsons, C.L. Westgate, N.J.A. Komplin, Assay, Purification, and Properties of Bovine Liver D-Xylulokinase, Protein Expr. Purif. 5 (1994) 259–265.

[73] P. Dimroth, P. Jockel, M. Schmid, Coupling mechanism of the oxaloacetate decarboxylase Na+ pump, Biochim. Biophys. Acta - Bioenerg. 1505 (2001) 1–14.

[74] W.J. Drent, G. a Lahpor, W.M. Wiegant, J.C. Gottschal, Fermentation of Inulin by Clostridium thermosuccinogenes sp. nov., a Thermophilic Anaerobic Bacterium Isolated from Various Habitats., Appl. Environ. Microbiol. 57 (1991) 455–462.

[75] D. Dunuwila, M. Cockrem, Methods and systems of producing dicarboxylic acids, CA2774341A1, 2012.

[76] M. Enriqueta Muñoz, E. Ponce, Pyruvate kinase: current status of regulatory and functional properties, Comp. Biochem. Physiol. Part B Biochem. Mol. Biol. 135 (2003) 197–218.

[77] L. Everis, G. Betts, pH stress can cause cell elongation in Bacillus and Clostridium species: a research note, Food Control. 12 (2001) 53–56.

[78] S. Fan, Z. Zhang, W. Zou, Z. Huang, J. Liu, L. Liu, Development of a minimal chemically defined medium for Ketogulonicigenium vulgare WSH001 based on its genome-scale metabolic model, J. Biotechnol. 169 (2014) 15–22.

[79] T. Fenchel, Bacterial Ecology, in: ELS, John Wiley & Sons, Ltd, Chichester, UK, 2011.

[80] L. Feng, W.B. Frommer, Evolution of Transporters: The Relationship of SWEETs, PQ-loop, and PnuC Transporters, Trends Biochem. Sci. 41 (2016) 118–119.

[81] J.A. Ferreyra, K.J. Wu, A.J. Hryckowian, D.M. Bouley, B.C. Weimer, J.L. Sonnenburg, Gut Microbiota-Produced Succinate Promotes C. difficile Infection after Antibiotic Treatment or Motility Disturbance, Cell Host Microbe. 16 (2014) 770–777.

[82] S. Fillinger, S. Boschi-Muller, S. Azza, E. Dervyn, G. Branlant, S. Aymerich, Two Glyceraldehyde-3-phosphate Dehydrogenases with Opposite Physiological Roles in a Nonphotosynthetic Bacterium, J. Biol. Chem. 275 (2000) 14031–14037.

[83] K.R. Finley, J.M. Huryta, B.M. Mastel, T.W. McMullin, G.M. Poynter, B.J. Rush, K.T. Watts, A.M. Fosmer, V.L. McIntosh, K.M. Brady, Compositions and Methods for Succinate Production, 2012.

[84] M.A. Fischbach, J.L. Sonnenburg, Eating For Two: How Metabolism Establishes Interspecies Interactions in the Gut, Cell Host Microbe. 10 (2011) 336–347.

[85] B. Flach, S. Lieberz, J. Lappin, S. Bolla, S. Phillips, EU-28: Biofuels Annual - U.S. Department of Agriculture (USDA), 2018.

[86] M. Francis, About 7% of fossil fuels are consumed for non-combustion use in the United States - Today in Energy - U.S. Energy Information Administration (EIA), (2018).

[87] A.T. Fuglsang, J. Paez-Valencia, R.A. Gaxiola, Plant Proton Pumps: Regulatory Circuits Involving H+-ATPase and H+-PPase, in: Springer, Berlin, Heidelberg, 2010: pp. 39–64.

[88] N.M. Fukuma, S. Koike, Y. Kobayashi, Monitoring of gene expression in Fibrobacter succinogenes S85 under the co-culture with non-fibrolytic ruminal bacteria, Arch. Microbiol. 197 (2015) 269–276.

[89] L.M. Fulton, L.R. Lynd, A. Körner, N. Greene, L.R. Tonachel, The need for biofuels as part of a low carbon energy future, Biofuels, Bioprod. Biorefining. 9 (2015) 476–483.

[90] C. Garrigues, M. Mercade, M. Cocaign-Bousquet, N.D. Lindley, P. Loubiere, Regulation of pyruvate metabolism inLactococcus lactis depends on the imbalance between catabolism and anabolism, Biotechnol. Bioeng. 74 (2001) 108–115.

[91] G. Gaudet, E. Forano, G. Dauphin, A.M. Delort, Futile cycling of glycogen in Fibrobacter succinogenes as shown by in situ 1H-NMR and 13C-NMR investigation., Eur. J. Biochem. 207 (1992) 155–62.

[92] S.J. Gerberding, R. Singh, PURIFICATION OF SUCCINIC ACID FROM THE FERMENTATION BROTH CONTAINING AMMONIUM SUCCINATE, WO/2011/082378, 2011.

[93] E.S. Gerlach, C.J. Sund, M.M. Hurley, S. Liu, M.D. Servinsky, K.L. Germane, Phosphoketolase flux in Clostridium acetobutylicum during growth on l-arabinose, Microbiology. 161 (2015) 430–440.

[94] D.G. Gibson, Enzymatic assembly of overlapping DNA fragments, in: Methods Enzymol., Academic Press Inc., 2011: pp. 349–361.

[95] L. Girbal, C. Croux, I. Vasconcelos, P. Soucaille, Regulation of metabolic shifts in Clostridium acetobutylicum ATCC 824, FEMS Microbiol. Rev. 17 (1995) 287–297.

[96] L. Girbal, P. Soucaille, Regulation of Clostridium acetobutylicum metabolism as revealed by mixed-substrate steady-state continuous cultures: role of NADH/NAD ratio and ATP pool., J. Bacteriol. 176 (1994) 6433–6438.

[97] T.L. Glass, J.S. Sherwood, Phosphorylation of glucose by a guanosine-5'-triphosphate (GTP)-dependent glucokinase in Fibrobacter succinogenes subsp. succinogenes S85, Arch. Microbiol. 162 (1994) 180–186.

[98] R.R. Gokarn, M.A. Eiteman, S.A. Martin, K.-E.L. Eriksson, Production of succinate from glucose, cellobiose, and various cellulosic materials by the ruminai anaerobic bacteriaFibrobacter succinogenes andRuminococcus flavefaciens, Appl. Biochem. Biotechnol. 68 (1997) 69–80.

[99] W. Gong, S. Dole, T. Grabar, A.C. Collard, J.G. Pero, R.R. Yocum, ENGINEERING MICROBES FOR EFFICIENT PRODUCTION OF CHEMICALS, (2011).

[100] R. Gonzalez, H. Tao, K.T. Shanmugam, S.W. York, L.O. Ingram, Global Gene Expression Differences Associated with Changes in Glycolytic Flux and Growth Rate in Escherichia coli during the Fermentation of Glucose and Xylose, Biotechnol. Prog. 18 (2002) 6–20.

[101] T. Grabar, W. Gong, R. Yocum, Metabolic Evolution of Escherichia Coli Strains That Produce Organic Acids, US8871489B2, 2010.

[102] M.T. Guarnieri, Y.-C. Chou, D. Salvachúa, A. Mohagheghi, P.C. St. John, D.J. Peterson, Y.J. Bomble, G.T. Beckham, Metabolic Engineering of Actinobacillus succinogenes Provides Insights into Succinic Acid Biosynthesis, Appl. Environ. Microbiol. 83 (2017) e00996-17.

[103] M. V. Guettler, D. Rumler, M.K. Jain, Actinobacillus succinogenes sp. nov., a novel succinic-acid-producing strain from the bovine rumen, Int. J. Syst. Bacteriol. 49 (1999) 207–216.

[104] I.B. Gunnarsson, M. Alvarado-Morales, I. Angelidaki, Utilization of CO 2 Fixating Bacterium Actinobacillus succinogenes 130Z for Simultaneous Biogas Upgrading and Biosuccinic Acid Production, Environ. Sci. Technol. 48 (2014) 12464–12468.

[105] P.L. Gupta, S.-M. Lee, H.-J. Choi, A mini review: photobioreactors for large scale algal cultivation, World J. Microbiol. Biotechnol. 31 (2015) 1409–1417.

[106] A.B. De Haan, J. Van Breugel, P.L.J. Van Der Weide, P.P. Jansen, J.M.V. Lancis, A.C. Baró, Acid/salt separation, 2017.

[107] A. Hagman, J. Piškur, A Study on the Fundamental Mechanism and the Evolutionary Driving Forces behind Aerobic Fermentation in Yeast, PLoS One. 10 (2015) e0116942.

[108] T. Hahn, F. Figge, J. Pinkse, L. Preuss, A Paradox Perspective on Corporate Sustainability: Descriptive, Instrumental, and Normative Aspects, J. Bus. Ethics. 148 (2018) 235–248.

[109] S. Heim, A. Kunkel, R.K. Thauer, R. Hedderich, Thiol : fumarate reductase (Tfr) from Methanobacterium thermoautotrophicum . Identification of the catalytic sites for fumarate reduction and thiol oxidation, Eur. J. Biochem. 253 (1998) 292–299.

[110] R.J. Henry, Evaluation of plant biomass resources available for replacement of fossil oil., Plant Biotechnol. J. 8 (2010) 288–93.

[111] B.G. Hermann, K. Blok, M.K. Patel, Producing Bio-Based Bulk Chemicals Using Industrial Biotechnology Saves Energy and Combats Climate Change, Environ. Sci. Technol. 41 (2007) 7915–7921.

[112] A.A. Herrero, End-product inhibition in anaerobic fermentations, Trends Biotechnol. 1 (1983) 49–53.

[113] J. Herselman, M.F.A. Bradfield, U. Vijayan, W. Nicol, The effect of carbon dioxide availability on succinic acid production with biofilms of Actinobacillus succinogenes, Biochem. Eng. J. 117 (2017) 218–225.

[114] J.H. Hulse, Biotechnologies: past history, present state and future prospects, Trends Food Sci. Technol. 15 (2004) 3–18.

[115] D. Humbird, R. Davis, J.D. McMillan, Aeration costs in stirred-tank and bubble column bioreactors, Biochem. Eng. J. 127 (2017) 161–166.

[116] E.L. Iannotti, D. Kafkewitz, M.J. Wolin, M.P. Bryant, Glucose fermentation products in Ruminococcus albus grown in continuous culture with Vibrio succinogenes: changes caused by interspecies transfer of H 2 ., J. Bacteriol. 114 (1973) 1231–40.

[117] H. Imanaka, A. Yamatsu, T. Fukui, H. Atomi, T. Imanaka, Phosphoenolpyruvate synthase plays an essential role for glycolysis in the modified Embden-Meyerhof pathway in Thermococcus kodakarensis, Mol. Microbiol. 61 (2006) 898–909.

[118] C. Ingram-Smith, S.R. Martin, K.S. Smith, Acetate kinase: not just a bacterial enzyme, Trends Microbiol. 14 (2006) 249–253.

[119] IPCC, Summary for Policymakers of IPCC Special Report on Global Warming of 1.5°C approved by governments, 2018.

[120] S. Iuchi, E.C. Lin, The narL gene product activates the nitrate reductase operon and represses the fumarate reductase and trimethylamine N-oxide reductase operons in Escherichia coli., Proc. Natl. Acad. Sci. 84 (1987) 3901–3905.

[121] B.E. Jackson, M.J. McInerney, Anaerobic microbial metabolism can proceed close to thermodynamic limits, Nature. 415 (2002) 454–456.

[122] M. LA Jansen, W.M. van Gulik, Towards large scale fermentative production of succinic acid, Curr. Opin. Biotechnol. 30 (2014) 190–197.

[123] M.L. JANSEN, R. VERWAAL, DICARBOXYLIC ACID PRODUCTION BY FERMENTATION AT LOW PH, EP3176265A1, 2009.

[124] D. Jardim-Messeder, C. Cabreira-Cagliari, R. Rauber, A.C. Turchetto-Zolet, R. Margis, M. Margis-Pinheiro, Fumarate reductase superfamily: A diverse group of enzymes whose evolution is correlated to the establishment of different metabolic pathways, Mitochondrion. 34 (2017) 56–66.

[125] Y. Jiang, B. Chen, C. Duan, B. Sun, J. Yang, S. Yang, Multigene Editing in the Escherichia coli Genome via the CRISPR-Cas9 System, Appl. Environ. Microbiol. 81 (2015) 2506–2514.

[126] E.A. Johnson, A. Madia, A.L. Demain, Chemically defined minimal medium for growth of the anaerobic cellulolytic thermophile Clostridium thermocellum, Appl. Environ. Microbiol. 41 (1981) 1060–1062.

[127] A.E.I. de Jong, F.M. Rombouts, R.R. Beumer, Behavior of Clostridium perfringens at low temperatures, Int. J. Food Microbiol. 97 (2004) 71–80.

[128] Z. Kádár, Z. Szengyel, K. Réczey, Simultaneous saccharification and fermentation (SSF) of industrial wastes for the production of ethanol, Ind. Crops Prod. 20 (2004) 103–110.

[129] N.S. Karadsheh, G.A. Tejwani, A. Ramaiah, Sedoheptulose-7-phosphate kinase activity of phosphofructokinase from the different tissues of rabbit, Biochim. Biophys. Acta - Enzymol. 327 (1973) 66–81.

[130] A.-K. Kaster, J. Moll, K. Parey, R.K. Thauer, Coupling of ferredoxin and heterodisulfide reduction via electron bifurcation in hydrogenotrophic methanogenic archaea, Proc. Natl. Acad. Sci. 108 (2011) 2981–2986.

[131] T. Kelesidis, Bloodstream Infection with Anaerobiospirillum succiniciproducens: A Potentially Lethal Infection, South. Med. J. 104 (2011) 205–214.

[132] C.P. Kempes, P.M. van Bodegom, D. Wolpert, E. Libby, J. Amend, T. Hoehler, Drivers of Bacterial Maintenance and Minimal Energy Requirements, Front. Microbiol. 8 (2017).

[133] S.J. Kerns, R. V Agafonov, Y.-J. Cho, F. Pontiggia, R. Otten, D. V Pachov, S. Kutter, L.A. Phung, P.N. Murphy, V. Thai, T. Alber, M.F. Hagan, D. Kern, The energy landscape of adenylate kinase during catalysis., Nat. Struct. Mol. Biol. 22 (2015) 124–31.

[134] V.N. Khmelenina, O.N. Rozova, I.R. Akberdin, M.G. Kalyuzhnaya, Y.A. Trotsenko, Pyrophosphate-Dependent Enzymes in Methanotrophs: New Findings and Views, in: Methane Biocatal. Paving W. to Sustain., Springer International Publishing, Cham, 2018: pp. 83–98.

[135] V.N. Khmelenina, O.N. Rozova, Y.A. Trotsenko, Characterization of the Recombinant Pyrophosphate-Dependent 6-Phosphofructokinases from Methylomicrobium alcaliphilum 20Z and Methylococcus capsulatus Bath, in: Methods Enzymol., Academic Press, 2011: pp. 1–14.

[136] B.S. Kim, Y.K. Hong, W.H. Hong, Effect of salts on the extraction characteristics of succinic acid by predispersed solvent extraction, Biotechnol. Bioprocess Eng. 9 (2004) 207–211.

[137] D. Kim, G. Pertea, C. Trapnell, H. Pimentel, R. Kelley, S.L. Salzberg, TopHat2: accurate alignment of transcriptomes in the presence of insertions, deletions and gene fusions, Genome Biol. 14 (2013) R36.

[138] P. Kim, M. Laivenieks, C. Vieille, J.G. Zeikus, Effect of Overexpression of Actinobacillus succinogenes Phosphoenolpyruvate Carboxykinase on Succinate Production in Escherichia coli, Appl. Environ. Microbiol. 70 (2004) 1238–1241.

[139] S. Kim, C.M. Kim, Y.-J. Son, J.Y. Choi, R.K. Siegenthaler, Y. Lee, T.-H. Jang, J. Song, H. Kang, C.A. Kaiser, H.H. Park, Molecular basis of maintaining an oxidizing environment under anaerobiosis by soluble fumarate reductase, Nat. Commun. 9 (2018) 4867.

[140] T.Y. Kim, H.U. Kim, J.M. Park, H. Song, J.S. Kim, S.Y. Lee, Genome-scale analysis of Mannheimia succiniciproducens metabolism, Biotechnol. Bioeng. 97 (2007) 657–671.

[141] D.E. Koeck, D. Wibberg, I. Maus, A. Winkler, A. Albersmeier, V. V. Zverlov, W. Liebl, A. Pühler, W.H. Schwarz, A. Schlüter, Corrigendum to "Complete genome sequence of the cellulolytic thermophile Ruminoclostridium cellulosi wild-type strain DG5 isolated from a thermophilic biogas plant" [J. Biotechnol. 188 (2014) 136–137], J. Biotechnol. 237 (2016) 35.

[142] J.G. Koendjbiharie, K. Wevers, R. van Kranenburg, Assessing Cofactor Usage in Pseudoclostridium thermosuccinogenes via Heterologous Expression of Central Metabolic Enzymes, Front. Microbiol. 10 (2019) 1162.

[143] J.G. Koendjbiharie, K. Wiersma, R. van Kranenburg, Investigating the Central Metabolism of Clostridium thermosuccinogenes, Appl. Environ. Microbiol. 84 (2018) e00363-18.

[144] N. Kothari, E.K. Holwerda, C.M. Cai, R. Kumar, C.E. Wyman, Biomass augmentation through thermochemical pretreatments greatly enhances digestion of switchgrass by Clostridium thermocellum, Biotechnol. Biofuels. 11 (2018) 219.

[145] D.O. Krause, T.G. Nagaraja, A.D.G. Wright, T.R. Callaway, Board-invited review: Rumen microbiology: Leading the way in microbial ecology1,2, J. Anim. Sci. 91 (2013) 331–341.

[146] J.M. KRAWCZYK, S. HAEFNER, H. SCHRÖDER, E. DANTAS COSTA, O. ZELDER, G. VON ABENDROTH, C. WITTMANN, R. STELLMACHER, J. BECKER, A. LANGE, Improved microorganisms for succinic acid production, EP3102675B1, 2015.

[147] A. Krivoruchko, Y. Zhang, V. Siewers, Y. Chen, J. Nielsen, Microbial acetyl-CoA metabolism and metabolic engineering, Metab. Eng. 28 (2015) 28–42.

[148] A. Kröger, S. Biel, J. Simon, R. Gross, G. Unden, C.R.D. Lancaster, Fumarate respiration of Wolinella succinogenes: enzymology, energetics and coupling mechanism, Biochim. Biophys. Acta - Bioenerg. 1553 (2002) 23–38.

[149] A. Kröger, V. Geisler, E. Lemma, F. Theis, R. Lenger, Bacterial fumarate respiration, Arch. Microbiol. 158 (1992) 311–314.

[150] A. Krogh, B. Larsson, G. von Heijne, E.L.. Sonnhammer, Predicting transmembrane protein topology with a hidden markov model: application to complete genomes11Edited by F. Cohen, J. Mol. Biol. 305 (2001) 567–580.

[151] J.M. Kuchenreuther, C.S. Grady-Smith, A.S. Bingham, S.J. George, S.P. Cramer, J.R. Swartz, High-Yield Expression of Heterologous [FeFe] Hydrogenases in Escherichia coli, PLoS One. 5 (2010) e15491.

[152] P. Kuhnert, E. Scholten, S. Haefner, D. Mayor, J. Frey, Basfia succiniciproducens gen. nov., sp. nov., a new member of the family Pasteurellaceae isolated from bovine rumen, Int. J. Syst. Evol. Microbiol. 60 (2010) 44–50.

[153] T. Kurzrock, D. Weuster-Botz, Recovery of succinic acid from fermentation broth, Biotechnol. Lett. 32 (2010) 331–339.

[154] R. Lamed, J.G. Zeikus, Ethanol production by thermophilic bacteria: relationship between fermentation product yields of and catabolic enzyme activities in Clostridium thermocellum and Thermoanaerobium brockii., J. Bacteriol. 144 (1980) 569–78.

[155] R.J. Lamed, J.H. Lobos, T.M. Su, Effects of Stirring and Hydrogen on Fermentation Products of Clostridium thermocellum., Appl. Environ. Microbiol. 54 (1988) 1216–21.

[156] A. Lange, J. Becker, D. Schulze, E. Cahoreau, J.-C. Portais, S. Haefner, H. Schröder, J. Krawczyk, O. Zelder, C. Wittmann, Bio-based succinate from sucrose: High-resolution 13C metabolic flux analysis and metabolic engineering of the rumen bacterium Basfia succiniciproducens, Metab. Eng. 44 (2017) 198–212.

[157] B. Langmead, S.L. Salzberg, Fast gapped-read alignment with Bowtie 2, Nat. Methods. 9 (2012) 357–359.

[158] J. Lee, Development of a model to determine mass transfer coefficient and oxygen solubility in bioreactors, Heliyon. 3 (2017) e00248.

[159] J.W. Lee, J. Yi, T.Y. Kim, S. Choi, J.H. Ahn, H. Song, M.-H. Lee, S.Y. Lee, Homo-succinic acid production by metabolically engineered Mannheimia succiniciproducens, Metab. Eng. 38 (2016) 409–417.

[160] P.C. Lee, S.Y. Lee, H.N. Chang, Kinetic study on succinic acid and acetic acid formation during continuous cultures of Anaerobiospirillum succiniciproducens grown on glycerol, Bioprocess Biosyst. Eng. 33 (2010) 465–471.

[161] P.C. Lee, W.G. Lee, S. Kwon, S.Y. Lee, H.N. Chang, Succinic acid production by Anaerobiospirillum succiniciproducens: Effects of the H2/CO2 supply and glucose concentration, Enzyme Microb. Technol. 24 (1999) 549–554.

[162] R.A. Lee, J.-M. Lavoie, From first- to third-generation biofuels: Challenges of producing a commodity from a biomass of increasing complexity, Anim. Front. 3 (2013) 6–11.

[163] S.J.Y. Lee, H. Song, S.J.Y. Lee, Genome-Based Metabolic Engineering of Mannheimia succiniciproducens for Succinic Acid Production, Appl. Environ. Microbiol. 72 (2006) 1939–1948.

[164] Y. Lee, T. Nishizawa, K. Yamashita, R. Ishitani, O. Nureki, Structural basis for the facilitative diffusion mechanism by SemiSWEET transporter, Nat. Commun. 6 (2015) 6112.

[165] I.A. Leenson, Old Rule of Thumb and the Arrhenius Equation, J. Chem. Educ. 76 (1999) 1459.

[166] R.S. Lemos, A.S. Fernandes, M.M. Pereira, C.M. Gomes, M. Teixeira, Quinol:fumarate oxidoreductases and succinate:quinone oxidoreductases: phylogenetic relationships, metal centres and membrane attachment, Biochim. Biophys. Acta - Bioenerg. 1553 (2002) 158–170.

[167] L. Li, OrthoMCL: Identification of Ortholog Groups for Eukaryotic Genomes, Genome Res. 13 (2003) 2178–2189.

[168] Q. Li, J.A. Siles, I.P. Thompson, Succinic acid production from orange peel and wheat straw by batch fermentations of Fibrobacter succinogenes S85, Appl. Microbiol. Biotechnol. 88 (2010) 671–678.

[169] Q. Li, D. Wang, Y. Wu, W. Li, Y. Zhang, J. Xing, Z. Su, One step recovery of succinic acid from fermentation broths by crystallization, Sep. Purif. Technol. 72 (2010) 294–300.

[170] U.W. Liebal, L.M. Blank, B.E. Ebert, CO 2 to succinic acid – Estimating the potential of biocatalytic routes, Metab. Eng. Commun. 7 (2018).

[171] H.D. Lightfoot, W. Manheimer, D.A. Meneley, D. Pendergast, G.S. Stanford, D.P. Computare, G.S. Stanford, Nuclear Fission Fuel is Inexhaustible, IEEE, 2006.

[172] S.K.C. Lin, C. Du, A. Koutinas, R. Wang, C. Webb, Substrate and product inhibition kinetics in succinic acid production by Actinobacillus succinogenes, Biochem. Eng. J. 41 (2008) 128–135.

[173] H. Link, T. Fuhrer, L. Gerosa, N. Zamboni, U. Sauer, Real-time metabolome profiling of the metabolic switch between starvation and growth, Nat. Methods. 12 (2015) 1091–1097.

[174] A.J. Liska, H. Yang, M. Milner, S. Goddard, H. Blanco-Canqui, M.P. Pelton, X.X. Fang, H. Zhu, A.E. Suyker, Biofuels from crop residue can reduce soil carbon and increase CO 2 emissions, Nat. Clim. Chang. 4 (2014) 398–401.

[175] B. Litsanov, M. Brocker, M. Bott, Toward Homosuccinate Fermentation: Metabolic Engineering of Corynebacterium glutamicum for Anaerobic Production of Succinate from Glucose and Formate, Appl. Environ. Microbiol. 78 (2012) 3325–3337.

[176] L. Liu, L. Zhang, W. Tang, Y. Gu, Q. Hua, S. Yang, W. Jiang, C. Yang, Phosphoketolase pathway for xylose catabolism in Clostridium acetobutylicum revealed by 13C metabolic flux analysis., J. Bacteriol. 194 (2012) 5413–22.

[177] R. Liu, L. Liang, M. Wu, K. Chen, M. Jiang, J. Ma, P. Wei, P. Ouyang, CO2 fixation for succinic acid production by engineered Escherichia coli co-expressing pyruvate carboxylase and nicotinic acid phosphoribosyltransferase, Biochem. Eng. J. 79 (2013) 77–83.

[178] Y.-P. Liu, P. Zheng, Z.-H. Sun, Y. Ni, J.-J. Dong, L.-L. Zhu, Economical succinic acid production from cane molasses by Actinobacillus succinogenes, Bioresour. Technol. 99 (2008) 1736–1742.

[179] J. Lo, T. Zheng, S. Hon, D.G. Olson, L.R. Lynd, The Bifunctional Alcohol and Aldehyde Dehydrogenase Gene, adhE , Is Necessary for Ethanol Production in Clostridium thermocellum and Thermoanaerobacterium saccharolyticum, J. Bacteriol. 197 (2015) 1386–1393.

[180] J. Lou, K.A. Dawson, H.J. Strobel, Cellobiose and Cellodextrin Metabolism by the Ruminal Bacterium Ruminococcus albus, Curr. Microbiol. 35 (1997) 221–227.

[181] S. Lu, M.A. Eiteman, E. Altman, Effect of CO2 on succinate production in dual-phase Escherichia coli fermentations, J. Biotechnol. 143 (2009) 213–223.

[182] L.R. Lynd, S. Baskaran, S. Casten, Salt Accumulation Resulting from Base Added for pH Control, and Not Ethanol, Limits Growth of Thermoanaerobacterium thermosaccharolyticum HG-8 at Elevated Feed Xylose Concentrations in Continuous Culture, Biotechnol. Prog. 17 (2001) 118–125.

[183] L.R. Lynd, A.M. Guss, M.E. Himmel, D. Beri, C. Herring, E.K. Holwerda, S.J. Murphy, D.G. Olson, J. Paye, T. Rydzak, X. Shao, L. Tian, R. Worthen, Advances in Consolidated Bioprocessing Using Clostridium thermocellum and Thermoanaerobacter saccharolyticum, in: Ind. Biotechnol., Wiley-VCH Verlag GmbH & Co. KGaA, Weinheim, Germany, 2016: pp. 365–394.

[184] L.R. Lynd, P.J. Weimer, W.H. van Zyl, I.S. Pretorius, Microbial Cellulose Utilization: Fundamentals and Biotechnology, Microbiol. Mol. Biol. Rev. 66 (2002) 506–577.

[185] M.T. Madigan, K.S. Bender, D.H. Buckley, W.M. Sattley, D.A. Stahl, Brock Biology of Microorganisms, 15th Global Edition, (2018).

[186] J.S. Martín del Campo, Y. Chun, J.-E. Kim, R. Patiño, Y.-H.P. Zhang, Discovery and characterization of a novel ATP/polyphosphate xylulokinase from a hyperthermophilic bacterium Thermotoga maritima, J. Ind. Microbiol. Biotechnol. 40 (2013) 661–669.

[187] T.M. Mata, A.A. Martins, N.S. Caetano, Microalgae for biodiesel production and other applications: A review, Renew. Sustain. Energy Rev. 14 (2010) 217–232.

[188] C. Matheron, A.-M. Delort, G. Gaudet, E. Forano, Re-investigation of glucose metabolism in Fibrobacter succinogenes, using NMR spectroscopy and enzymatic assays.: Evidence for pentose phosphates phosphoketolase and pyruvate formate lyase activities, Biochim. Biophys. Acta - Mol. Cell Res. 1355 (1997) 50–60.

[189] H.D. Matthews, K. Zickfeld, R. Knutti, M.R. Allen, Focus on cumulative emissions, global carbon budgets and the implications for climate mitigation targets, Environ. Res. Lett. 13 (2018) 010201.

[190] J.B. McKinlay, J.G. Zeikus, C. Vieille, Insights into Actinobacillus succinogenes Fermentative Metabolism in a Chemically Defined Growth Medium, Appl. Environ. Microbiol. 71 (2005) 6651–6656.

[191] J.P. Meier-Kolthoff, R.L. Hahnke, J. Petersen, C. Scheuner, V. Michael, A. Fiebig, C. Rohde, M. Rohde, B. Fartmann, L.A. Goodwin, O. Chertkov, T. Reddy, A. Pati, N.N. Ivanova, V. Markowitz, N.C. Kyrpides, T. Woyke, M. Göker, H.-P. Klenk, Complete genome sequence of DSM 30083T, the type strain (U5/41T) of Escherichia coli, and a proposal for delineating subspecies in microbial taxonomy, Stand. Genomic Sci. 9 (2014) 2.

[192] F. Merino, V. Guixé, Specificity evolution of the ADP-dependent sugar kinase family -in silico studies of the glucokinase/phosphofructokinase bifunctional enzyme from Methanocaldococcus jannaschii, FEBS J. 275 (2008) 4033–4044.

[193] E. Mertens, Pyrophosphate-dependent phosphofructokinase, an anaerobic glycolytic enzyme?, FEBS Lett. 285 (1991) 1–5.

[194] E. Mertens, ATP versus pyrophosphate: glycolysis revisited in parasitic protists, Parasitol. Today. 9 (1993) 122–126.

[195] H.-P. Meyer, W. Minas, D. Schmidhalter, Industrial-Scale Fermentation, Wiley-VCH Verlag GmbH & Co. KGaA, 2017.

[196] C.S. Millard, Y.P. Chao, J.C. Liao, M.I. Donnelly, Enhanced production of succinic acid by overexpression of phosphoenolpyruvate carboxylase in Escherichia coli., Appl. Environ. Microbiol. 62 (1996) 1808–10.

[197] M.B. Miller, B.L. Bassler, Quorum Sensing in Bacteria, Annu. Rev. Microbiol. 55 (2001) 165–199.

[198] A. Miura, M. Kameya, H. Arai, M. Ishii, Y. Igarashi, A soluble NADH-dependent fumarate reductase in the reductive tricarboxylic acid cycle of Hydrogenobacter thermophilus TK-6., J. Bacteriol. 190 (2008) 7170–7.

[199] P.W. MOHR, S. KRAWIEC, Temperature Characteristics and Arrhenius Plots for Nominal Psychrophiles, Mesophiles and Thermophiles, Microbiology. 121 (1980) 311–317.

[200] M. Morales, M. Ataman, S. Badr, S. Linster, I. Kourlimpinis, S. Papadokonstantakis, V. Hatzimanikatis, K. Hungerbü Hler, Sustainability assessment of succinic acid production technologies from biomass using metabolic engineering Sustainability assessment of succinic acid production technologies from biomass using metabolic engineering †, 2794 | Energy Environ. Sci. 9 (2016) 2794.

[201] J. Morelli, Environmental Sustainability: A Definition for Environmental Professionals, J. Environ. Sustain. 1 (2011) 1–10.

[202] B.E.L. Morris, R. Henneberger, H. Huber, C. Moissl-Eichinger, Microbial syntrophy: interaction for the common good, FEMS Microbiol. Rev. 37 (2013) 384–406.

[203] I. Mougiakos, E.F. Bosma, K. Weenink, E. Vossen, K. Goijvaerts, J. van der Oost, R. van Kranenburg,

Efficient Genome Editing of a Facultative Thermophile Using Mesophilic spCas9, ACS Synth. Biol. 6 (2017) 849–861.

[204] I. Mougiakos, P. Mohanraju, E.F. Bosma, V. Vrouwe, M. Finger Bou, M.I.S. Naduthodi, A. Gussak, R.B.L. Brinkman, R. van Kranenburg, J. van der Oost, Characterizing a thermostable Cas9 for bacterial genome editing and silencing, Nat. Commun. 8 (2017) 1647.

[205] H.I. Moussa, A. Elkamel, S.B. Young, Assessing energy performance of bio-based succinic acid production using LCA, J. Clean. Prod. 139 (2016) 761–769.

[206] J. MRACEK, S.J. SNYDER, U.B. CHAVEZ, J.F. TURRENS, A Soluble Fumarate Reductase in Trypanosoma brucei Procyclic Trypomastigotes, J. Protozool. 38 (1991) 554–558.

[207] M. Muller, J.A. Lee, P. Gordon, T. Gaasterland, C.W. Sensen, Presence of Prokaryotic and Eukaryotic Species in All Subgroups of the PPi-Dependent Group II Phosphofructokinase Protein Family, J. Bacteriol. 183 (2001) 6714–6716.

[208] R.I. Munir, V. Spicer, O. V. Krokhin, D. Shamshurin, X. Zhang, M. Taillefer, W. Blunt, N. Cicek, R. Sparling, D.B. Levin, Transcriptomic and proteomic analyses of core metabolism in Clostridium termitidis CT1112 during growth on α-cellulose, xylan, cellobiose and xylose, BMC Microbiol. 16 (2016) 91.

[209] C.R. Myers, J.M. Myers, Fumarate reductase is a soluble enzyme in anaerobically grown Shewanella putrefaciens MR-1, FEMS Microbiol. Lett. 98 (1992) 13–19.

[210] V. Müller, Bacterial Fermentation, in: Encycl. Life Sci., John Wiley & Sons, Ltd, Chichester, UK, 2008.

[211] K. Nakahigashi, Y. Toya, N. Ishii, T. Soga, M. Hasegawa, H. Watanabe, Y. Takai, M. Honma, H. Mori, M. Tomita, Systematic phenome analysis of Escherichia coli multiple-knockout mutants reveals hidden reactions in central carbon metabolism., Mol. Syst. Biol. 5 (2009) 306.

[212] B. Niebel, S. Leupold, M. Heinemann, An upper limit on Gibbs energy dissipation governs cellular metabolism, Nat. Metab. 1 (2019) 125–132.

[213] J. Nielsen, J.D. Keasling, Engineering Cellular Metabolism, Cell. 164 (2016) 1185–1197.

[214] J.S. Oakhill, R. Steel, Z.-P. Chen, J.W. Scott, N. Ling, S. Tam, B.E. Kemp, AMPK is a direct adenylate charge-regulated protein kinase., Science. 332 (2011) 1433–5.

[215] H.S. Oberoi, N. Babbar, S.K. Sandhu, S.S. Dhaliwal, U. Kaur, B.S. Chadha, V.K. Bhargav, Ethanol production from alkali-treated rice straw via simultaneous saccharification and fermentation using newly isolated thermotolerant Pichia kudriavzevii HOP-1, J. Ind. Microbiol. Biotechnol. 39 (2012) 557–566.

[216] S. Okino, R. Noburyu, M. Suda, T. Jojima, M. Inui, H. Yukawa, An efficient succinic acid production process in a metabolically engineered Corynebacterium glutamicum strain, Appl. Microbiol. Biotechnol. 81 (2008) 459–464.

[217] Olan S. Fruchey, B.T. Keen, B.A. Albin, B.D. Dombek, N.A. Clinton, P.R. Zitzelsberger, M.B. Brumley, Processes for producing carboxylic acids from fermentation broths containing their ammonium salts, US20120021473A1, 2011.

[218] K. Olofsson, M. Bertilsson, G. Lidén, A short review on SSF – an interesting process option for ethanol production from lignocellulosic feedstocks, Biotechnol. Biofuels. 1 (2008) 7.

[219] D.G. Olson, M. Hörl, T. Fuhrer, J. Cui, J. Zhou, M.I. Maloney, D. Amador-Noguez, L. Tian, U. Sauer, L.R. Lynd, Glycolysis without pyruvate kinase in Clostridium thermocellum, Metab. Eng. 39 (2016) 169–180.

[220] W.J. Olson, D. Stevenson, D. Amador-Noguez, L.J. Knoll, Dual metabolomic profiling uncovers

Toxoplasma manipulation of the host metabolome and the discovery of a novel parasite metabolic capability, BioRxiv. (2018) 463075.

[221] G. Van Oost, J. Ongena, Energy for future centuries-Will fusion be an inexhaustible, safe and clean energy source?, Fusion Technol. 29 (1996).

[222] S. Ostergaard, L. Olsson, J. Nielsen, Metabolic Engineering of Saccharomyces cerevisiae, Microbiol. Mol. Biol. Rev. 64 (2000) 34–50.

[223] M.S. Ou, N. Mohammed, L.O. Ingram, K.T. Shanmugam, Thermophilic Bacillus coagulans Requires Less Cellulases for Simultaneous Saccharification and Fermentation of Cellulose to Products than Mesophilic Microbial Biocatalysts, Appl. Biochem. Biotechnol. 155 (2009) 76–82.

[224] M. Özkan, E.I. Yllmaz, L.R. Lynd, G. Özcengiz, Cloning and expression of the Clostridium thermocellum L-lactate dehydrogenase gene in Escherichia coli and enzyme characterization, Can. J. Microbiol. 50 (2004) 845–851.

[225] J.O. Park, S.A. Rubin, Y.-F. Xu, D. Amador-Noguez, J. Fan, T. Shlomi, J.D. Rabinowitz, Metabolite concentrations, fluxes and free energies imply efficient enzyme usage, Nat. Chem. Biol. 12 (2016) 482–489.

[226] M.K. Patel, M. Crank, V. Dornburg, B.G. Hermann, A.L. Roes, B. Hüsing, L. Overbeek, F. Terragni, E. Recchia, Medium and Long-term Opportunities and Risks of the Biotechnological Production of Bulk Chemicals from Renewable Resources, UU CHEM NW&S (Copernicus), 2006.

[227] J.W. Peters, D.N. Beratan, B. Bothner, R.B. Dyer, C.S. Harwood, Z.M. Heiden, R. Hille, A.K. Jones, P.W. King, Y. Lu, C.E. Lubner, S.D. Minteer, D.W. Mulder, S. Raugei, G.J. Schut, L.C. Seefeldt, M. Tokmina-Lukaszewska, O.A. Zadvornyy, P. Zhang, M.W. Adams, A new era for electron bifurcation, Curr. Opin. Chem. Biol. 47 (2018) 32–38.

[228] T. Pfeiffer, A. Morley, An evolutionary perspective on the Crabtree effect, Front. Mol. Biosci. 1 (2014).

[229] J.M. Pinazo, M.E. Domine, V. Parvulescu, F. Petru, Sustainability metrics for succinic acid production: A comparison between biomass-based and petrochemical routes, Catal. Today. 239 (2015) 17–24.

[230] G.W.E. Plaut, [89] Isocitric dehydrogenase (TPN-linked) from pig heart (revised procedure), in: Methods Enzymol., Academic Press, 1962: pp. 645–651.

[231] C.M. Plugge, Anoxic Media Design, Preparation, and Considerations, Methods Enzymol. 397 (2005) 3–16.

[232] A. Pradet, P. Raymond, Adenine Nucleotide Ratios and Adenylate Energy Charge in Energy Metabolism, Annu. Rev. Plant Physiol. 34 (1983) 199–224.

[233] K. Prochaska, J. Antczak, M. Regel-Rosocka, M. Szczygiełda, Removal of succinic acid from fermentation broth by multistage process (membrane separation and reactive extraction), Sep. Purif. Technol. 192 (2018) 360–368.

[234] Z. Qin, C.E. Canter, J.B. Dunn, S. Mueller, H. Kwon, J. Han, M.M. Wander, M. Wang, Land management change greatly impacts biofuels' greenhouse gas emissions, GCB Bioenergy. 10 (2018) 370–381.

[235] Z. Qin, J.B. Dunn, H. Kwon, S. Mueller, M.M. Wander, Soil carbon sequestration and land use change associated with biofuel production: empirical evidence, GCB Bioenergy. 8 (2016) 66–80.

[236] D. Radoš, D.L. Turner, L.L. Fonseca, A.L. Carvalho, B. Blombach, B.J. Eikmanns, A.R. Neves, H. Santos, Carbon Flux Analysis by 13 C Nuclear Magnetic Resonance To Determine the Effect of CO 2 on Anaerobic Succinate Production by Corynebacterium glutamicum, Appl. Environ. Microbiol. 80 (2014) 3015–3024.

[237] A.R. Ramos, F. Grein, G.P. Oliveira, S.S. Venceslau, K.L. Keller, J.D. Wall, I.A.C. Pereira, The FlxABCD-HdrABC proteins correspond to a novel NADH dehydrogenase/heterodisulfide reductase widespread in anaerobic bacteria and involved in ethanol metabolism in D esulfovibrio vulgaris Hildenborough, Environ. Microbiol. 17 (2015) 2288–2305.

[238] R.E. Reeves, A new enzyme with the glycolytic function of pyruvate kinase., J. Biol. Chem. 243 (1968) 3202–4.

[239] R. Repaske, M.A. Clayton, Control of Escherichia coli growth by CO2., J. Bacteriol. 135 (1978) 1162–4.

[240] A.S. Reshetnikov, O.N. Rozova, V.N. Khmelenina, I.I. Mustakhimov, A.P. Beschastny, J.C. Murrell, Y.A. Trotsenko, Characterization of the pyrophosphate-dependent 6-phosphofructokinase from Methylococcus capsulatus Bath, FEMS Microbiol. Lett. 288 (2008) 202–210.

[241] K. Richter, M. Schicklberger, J. Gescher, Dissimilatory Reduction of Extracellular Electron Acceptors in Anaerobic Respiration, Appl. Environ. Microbiol. 78 (2012) 913–921.

[242] R.S. Ronimus, E. de Heus, H.W. Morgan, Sequencing, expression, characterisation and phylogeny of the ADP-dependent phosphofructokinase from the hyperthermophilic, euryarchaeal Thermococcus zilligii, Biochim. Biophys. Acta - Gene Struct. Expr. 1517 (2001) 384–391.

[243] L. Rosso, J.R. Lobry, J.P. Flandrois, An Unexpected Correlation between Cardinal Temperatures of Microbial Growth Highlighted by a New Model, J. Theor. Biol. 162 (1993) 447–463.

[244] O.N. Rozova, V.N. Khmelenina, Y.A. Trotsenko, Characterization of recombinant PPi-dependent 6-phosphofructokinases from Methylosinus trichosporium OB3b and Methylobacterium nodulans ORS 2060, Biochem. 77 (2012) 288–295.

[245] M. Rubin-Blum, N. Dubilier, M. Kleiner, Genetic Evidence for Two Carbon Fixation Pathways (the Calvin-Benson-Bassham Cycle and the Reverse Tricarboxylic Acid Cycle) in Symbiotic and Free-Living Bacteria, MSphere. 4 (2019).

[246] B.J. Rush, A.M. Fosmer, Methods for Succinate Production, 2013.

[247] T. Rydzak, P.D. McQueen, O. V Krokhin, V. Spicer, P. Ezzati, R.C. Dwivedi, D. Shamshurin, D.B. Levin, J.A. Wilkins, R. Sparling, Proteomic analysis of Clostridium thermocellum core metabolism: relative protein expression profiles and growth phase-dependent changes in protein expression, BMC Microbiol. 12 (2012) 214.

[248] E. Saavedra, R. Encalada, C. Vázquez, A. Olivos-García, P.A.M. Michels, R. Moreno-Sánchez, Control and regulation of the pyrophosphate-dependent glucose metabolism in Entamoeba histolytica., Mol. Biochem. Parasitol. 229 (2019) 75–87.

[249] D. Salvachúa, A. Mohagheghi, H. Smith, M.F.A. Bradfield, W. Nicol, B.A. Black, M.J. Biddy, N. Dowe, G.T. Beckham, Succinic acid production on xylose-enriched biorefinery streams by Actinobacillus succinogenes in batch fermentation, Biotechnol. Biofuels. 9 (2016) 28.

[250] N.S. Samuelov, R. Lamed, S. Lowe, J.G. Zeikus, Influence of CO(2)-HCO(3) Levels and pH on Growth, Succinate Production, and Enzyme Activities of Anaerobiospirillum succiniciproducens., Appl. Environ. Microbiol. 57 (1991) 3013–9.

[251] K. Sander, K.G. Asano, D. Bhandari, G.J. Van Berkel, S.D. Brown, B. Davison, T.J. Tschaplinski, Targeted redox and energy cofactor metabolomics in Clostridium thermocellum and Thermoanaerobacterium saccharolyticum, Biotechnol. Biofuels. 10 (2017) 270.

[252] S. Sato, M. Arita, T. Soga, T. Nishioka, M. Tomita, Time-resolved metabolomics reveals metabolic modulation in rice foliage, BMC Syst. Biol. 2 (2008) 51.

[253] U. Sauer, B.J. Eikmanns, The PEP—pyruvate—oxaloacetate node as the switch point for carbon flux distribution in bacteria: We dedicate this paper to Rudolf K. Thauer, Director of the Max-Planck-Institute for Terrestrial Microbiology in Marburg, Germany, on the occasion of his 65th, FEMS Microbiol. Rev. 29 (2005) 765–794.

[254] V. Sautner, M.M. Friedrich, A. Lehwess-Litzmann, K. Tittmann, Converting Transaldolase into Aldolase through Swapping of the Multifunctional Acid-Base Catalyst: Common and Divergent Catalytic Principles in F6P Aldolase and Transaldolase., Biochemistry. 54 (2015) 4475–86.

[255] S. SAWANON, Y. KOBAYASHI, Synergistic fibrolysis in the rumen by cellulolytic Ruminococcus flavefaciens and non-cellulolytic Selenomonas ruminantium: Evidence in defined cultures, Anim. Sci. J. 77 (2006) 208–214.

[256] S. Schatschneider, S. Abdelrazig, L. Safo, A.M. Henstra, T. Millat, D.-H. Kim, K. Winzer, N.P. Minton, D.A. Barrett, Quantitative Isotope-Dilution High-Resolution-Mass-Spectrometry Analysis of Multiple Intracellular Metabolites in *Clostridium autoethanogenum* with Uniformly ^{13} C-Labeled Standards Derived from Spirulina, Anal. Chem. 90 (2018) 4470–4477.

[257] A. Schaupp, L.G. Ljungdahl, Purification and properties of acetate kinase from Clostridium thermoaceticum, Arch. Microbiol. 100 (1974) 121–129.

[258] J.J. Schellenberg, T.J. Verbeke, P. McQueen, O. V Krokhin, X. Zhang, G. Alvare, B. Fristensky, G.G. Thallinger, B. Henrissat, J.A. Wilkins, D.B. Levin, R. Sparling, Enhanced whole genome sequence and annotation of Clostridium stercorarium DSM8532T using RNA-seq transcriptomics and high-throughput proteomics, BMC Genomics. 15 (2014) 567.

[259] J.J. Schellenberg, T.J. Verbeke, P. McQueen, O. V Krokhin, X. Zhang, G. Alvare, B. Fristensky, G.G. Thallinger, B. Henrissat, J.A. Wilkins, D.B. Levin, R. Sparling, Enhanced whole genome sequence and annotation of Clostridium stercorarium DSM8532T using RNA-seq transcriptomics and high-throughput proteomics, BMC Genomics. 15 (2014) 567.

[260] L. Schöcke, B. Schink, Membrane-bound proton-translocating pyrophosphatase of Syntrophus gentianae, a syntrophically benzoate-degrading fermenting bacterium., Eur. J. Biochem. 256 (1998) 589–94.

[261] E. Scholten, T. Renz, J. Thomas, Continuous cultivation approach for fermentative succinic acid production from crude glycerol by Basfia succiniciproducens DD1, Biotechnol. Lett. 31 (2009) 1947–1951.

[262] M. Schurmann, G.A. Sprenger, Fructose-6-phosphate aldolase is a novel class I aldolase from Escherichia coli and is related to a novel group of bacterial transaldolases., J. Biol. Chem. 276 (2001) 11055–61.

[263] C. Schwalb, S.K. Chapman, G.A. Reid, The membrane-bound tetrahaem c-type cytochrome CymA interacts directly with the soluble fumarate reductase in Shewanella., Biochem. Soc. Trans. 30 (2002) 658–62.

[264] C. Schwalb, S.K. Chapman, G.A. Reid, The Tetraheme Cytochrome CymA Is Required for Anaerobic Respiration with Dimethyl Sulfoxide and Nitrite in Shewanella oneidensis †, Biochemistry. 42 (2003) 9491–9497.

[265] T. Seemann, Prokka: rapid prokaryotic genome annotation, Bioinformatics. 30 (2014) 2068–2069.

[266] D.C. Sévin, T. Fuhrer, N. Zamboni, U. Sauer, Nontargeted in vitro metabolomics for high-throughput identification of novel enzymes in Escherichia coli, Nat. Methods. 14 (2017) 187–194.

[267] A.J. Shaw, F.H. Lam, M. Hamilton, A. Consiglio, K. MacEwen, E.E. Brevnova, E. Greenhagen, W.G. LaTouf, C.R. South, H. van Dijken, G. Stephanopoulos, Metabolic engineering of microbial competitive advantage for industrial fermentation processes., Science. 353 (2016) 583–6.

[268] A.J. Shaw, K.K. Podkaminer, S.G. Desai, J.S. Bardsley, S.R. Rogers, P.G. Thorne, D.A. Hogsett, L.R. Lynd, Metabolic engineering of a thermophilic bacterium to produce ethanol at high yield, Proc. Natl. Acad. Sci. 105 (2008) 13769–13774.

[269] B. Siebers, H.P. Klenk, R. Hensel, PPi-dependent phosphofructokinase from Thermoproteus tenax, an archaeal descendant of an ancient line in phosphofructokinase evolution., J. Bacteriol. 180 (1998) 2137–43.

[270] A. Sinz, Chemical cross-linking and mass spectrometry to map three-dimensional protein structures and protein–protein interactions, Mass Spectrom. Rev. 25 (2006) 663–682.

[271] M.A. Sirover, Structural analysis of glyceraldehyde-3-phosphate dehydrogenase functional diversity, Int. J. Biochem. Cell Biol. 57 (2014) 20–26.

[272] V. Smil, Energy transitions : global and national perspectives, 2016.

[273] H. Song, T.Y. Kim, B.-K. Choi, S.J. Choi, L.K. Nielsen, H.N. Chang, S.Y. Lee, Development of chemically defined medium for Mannheimia succiniciproducens based on its genome sequence, Appl. Microbiol. Biotechnol. 79 (2008) 263–272.

[274] H. Song, J.W. Lee, S. Choi, J.K. You, W.H. Hong, S.Y. Lee, Effects of dissolved CO2 levels on the growth ofMannheimia succiniciproducens and succinic acid production, Biotechnol. Bioeng. 98 (2007) 1296–1304.

[275] H. Song, S.Y. Lee, Production of succinic acid by bacterial fermentation, Enzyme Microb. Technol. 39 (2006) 352–361.

[276] P.A. Sosa, C. Roca, S. Velizarov, Membrane assisted recovery and purification of bio-based succinic acid for improved process sustainability, J. Memb. Sci. 501 (2016) 236–247.

[277] J.H. Spangenberg, J. Settele, Value pluralism and economic valuation – defendable if well done, Ecosyst. Serv. 18 (2016) 100–109.

[278] J. Sridhar, M. a. Eiteman, Influence of Redox Potential on Product Distribution in *Clostridium thermosuccinogenes*, Appl. Biochem. Biotechnol. 82 (1999) 91–102.

[279] J. Sridhar, M. a Eiteman, Metabolic flux analysis of *Clostridium thermosuccinogenes*: effects of pH and culture redox potential., Appl. Biochem. Biotechnol. 94 (2001) 51–69.

[280] J. Sridhar, M.A. Eiteman, J.W. Wiegel, Elucidation of Enzymes in Fermentation Pathways Used by Clostridium thermosuccinogenes Growing on Inulin, Appl. Environ. Microbiol. 66 (2000) 246–251.

[281] J.D. Stephen, W.E. Mabee, J.N. Saddler, Will second-generation ethanol be able to compete with first-generation ethanol? Opportunities for cost reduction, Biofuels, Bioprod. Biorefining. 6 (2012) 159–176.

[282] C. Stewart, H. Flint, Bacteroides (Fibrobacter) succinogenes, a cellulolytic anaerobic bacterium from the gastrointestinal tract, Appl. Microbiol. Biotechnol. 30 (1989) 433–439.

[283] J.C.M. Stewart, Colorimetric determination of phospholipids with ammonium ferrothiocyanate, Anal. Biochem. 104 (1980) 10–14.

[284] G. Suen, P.J. Weimer, D.M. Stevenson, F.O. Aylward, J. Boyum, J. Deneke, C. Drinkwater, N.N. Ivanova, N. Mikhailova, O. Chertkov, L.A. Goodwin, C.R. Currie, D. Mead, P.J. Brumm, The Complete Genome Sequence of Fibrobacter succinogenes S85 Reveals a Cellulolytic and Metabolic Specialist, PLoS One. 6 (2011) e18814.

[285] B.M. Susskind, L.G. Warren, R.E. Reeves, A pathway for the interconversion of hexose and pentose in the

parasitic amoeba Entamoeba histolytica, Biochem. J. 204 (1982) 191–199.

[286] I.W. Sutherland, Biofilm exopolysaccharides: a strong and sticky framework, Microbiology. 147 (2001) 3–9.

[287] R. Suzuki, T. Katayama, B.-J. Kim, T. Wakagi, H. Shoun, H. Ashida, K. Yamamoto, S. Fushinobu, Crystal Structures of Phosphoketolase, J. Biol. Chem. 285 (2010) 34279–34287.

[288] D. Szklarczyk, A.L. Gable, D. Lyon, A. Junge, S. Wyder, J. Huerta-Cepas, M. Simonovic, N.T. Doncheva, J.H. Morris, P. Bork, L.J. Jensen, C. von Mering, STRING v11: protein–protein association networks with increased coverage, supporting functional discovery in genome-wide experimental datasets, Nucleic Acids Res. 47 (2019) D607–D613.

[289] M. Taillefer, T. Rydzak, D.B. Levin, I.J. Oresnik, R. Sparling, Reassessment of the Transhydrogenase/Malate Shunt Pathway in Clostridium thermocellum ATCC 27405 through Kinetic Characterization of Malic Enzyme and Malate Dehydrogenase, Appl. Environ. Microbiol. 81 (2015) 2423–2432.

[290] M. Taillefer, R. Sparling, Glycolysis as the Central Core of Fermentation, Springer, Cham, 2016.

[291] K. Tamura, G. Stecher, D. Peterson, A. Filipski, S. Kumar, MEGA6: Molecular Evolutionary Genetics Analysis Version 6.0, Mol. Biol. Evol. 30 (2013) 2725–2729.

[292] Z. Tan, X. Zhu, J. Chen, Q. Li, X. Zhang, Activating Phosphoenolpyruvate Carboxylase and Phosphoenolpyruvate Carboxykinase in Combination for Improvement of Succinate Production, Appl. Environ. Microbiol. 79 (2013) 4838–4844.

[293] T. Tatusova, M. DiCuccio, A. Badretdin, V. Chetvernin, E.P. Nawrocki, L. Zaslavsky, A. Lomsadze, K.D. Pruitt, M. Borodovsky, J. Ostell, NCBI prokaryotic genome annotation pipeline, Nucleic Acids Res. 44 (2016) 6614–6624.

[294] R. Taylor, L. Nattrass, G. Alberts, P. Robson, C. Chudziak, A. Bauen, I.M. Libelli, G. Lotti, M. Prussi, R. Nistri, others, From the sugar platform to biofuels and biochemicals: final report for the European Commission Directorate-General Energy, 2015.

[295] M. Theisen, J.C. Liao, Industrial Biotechnology: Escherichia coli as a Host, in: Ind. Biotechnol., Wiley-VCH Verlag GmbH & Co. KGaA, Weinheim, Germany, 2016: pp. 149–181.

[296] R.A. Thompson, C.T. Trinh, Overflow metabolism and growth cessation in Clostridium thermocellum DSM1313 during high cellulose loading fermentations, Biotechnol. Bioeng. 114 (2017) 2592–2604.

[297] L. Tian, J. Lo, X. Shao, T. Zheng, D.G. Olson, L.R. Lynd, Ferredoxin:NAD + Oxidoreductase of Thermoanaerobacterium saccharolyticum and Its Role in Ethanol Formation, Appl. Environ. Microbiol. 82 (2016) 7134–7141.

[298] L. Tian, S.J. Perot, D. Stevenson, T. Jacobson, A.A. Lanahan, D. Amador-Noguez, D.G. Olson, L.R. Lynd, Metabolome analysis reveals a role for glyceraldehyde 3-phosphate dehydrogenase in the inhibition of C. thermocellum by ethanol, Biotechnol. Biofuels. 10 (2017) 276.

[299] D. Tilman, R. Socolow, J.A. Foley, J. Hill, E. Larson, L. Lynd, S. Pacala, J. Reilly, T. Searchinger, C. Somerville, R. Williams, Beneficial Biofuels--The Food, Energy, and Environment Trilemma, Science (80-.). 325 (2009) 270–271.

[300] B.J. Tindall, The names Hungateiclostridium Zhang et al. 2018, Hungateiclostridium thermocellum (Viljoen et al. 1926) Zhang et al. 2018, Hungateiclostridium cellulolyticum (Patel et al. 1980) Zhang et al. 2018, Hungateiclostridium aldrichii (Yang et al. 1990) Zhang et , Int. J. Syst. Evol. Microbiol. (2019) ijsem003685.

[301] M. Toivari, M.-L. Vehkomäki, Y. Nygård, M. Penttilä, L. Ruohonen, M.G. Wiebe, Low pH d-xylonate production with Pichia kudriavzevii, Bioresour. Technol. 133 (2013) 555–562.

[302] K. Tommi, K. Juho, G. Adrian, A. Gabibov, V. Skulachev, F. Wieland, W. Just, Inorganic pyrophosphatases: One substrate, three mechanisms, (2013).

[303] Q.H. Tran, J. Bongaerts, D. Vlad, G. Unden, Requirement for the proton-pumping NADH dehydrogenase I of Escherichia coli in respiration of NADH to fumarate and its bioenergetic implications., Eur. J. Biochem. 244 (1997) 155–60.

[304] C. Trapnell, A. Roberts, L. Goff, G. Pertea, D. Kim, D.R. Kelley, H. Pimentel, S.L. Salzberg, J.L. Rinn, L. Pachter, Differential gene and transcript expression analysis of RNA-seq experiments with TopHat and Cufflinks, Nat. Protoc. 7 (2012) 562–578.

[305] L. Tretter, A. Patocs, C. Chinopoulos, Succinate, an intermediate in metabolism, signal transduction, ROS, hypoxia, and tumorigenesis, Biochim. Biophys. Acta - Bioenerg. 1857 (2016) 1086–1101.

[306] P. Turner, G. Mamo, E. Karlsson, Potential and utilization of thermophiles and thermostable enzymes in biorefining, Microb. Cell Fact. 6 (2007) 9.

[307] K. Ueda, Y. Tagami, Y. Kamihara, H. Shiratori, H. Takano, T. Beppu, Isolation of bacteria whose growth is dependent on high levels of CO 2 and implications of their potential diversity, Appl. Environ. Microbiol. 74 (2008) 4535–4538.

[308] V. Varik, S.R.A. Oliveira, V. Hauryliuk, T. Tenson, HPLC-based quantification of bacterial housekeeping nucleotides and alarmone messengers ppGpp and pppGpp, Sci. Rep. 7 (2017) 11022.

[309] S.S. Venceslau, Y. Stockdreher, C. Dahl, I.A.C. Pereira, The “bacterial heterodisulfide” DsrC is a key protein in dissimilatory sulfur metabolism, Biochim. Biophys. Acta - Bioenerg. 1837 (2014) 1148–1164.

[310] A.A. Vertes, M. Inui, H. Yukawa, Manipulating Corynebacteria, from Individual Genes to Chromosomes, Appl. Environ. Microbiol. 71 (2005) 7633–7642.

[311] K. Vijayaraghavan, D. Yamini, V. Ambika, N. Sravya Sowdamini, Trends in inulinase production – a review, Crit. Rev. Biotechnol. 29 (2009) 67–77.

[312] J.C.T. Vogelaar, Temperature effects on the oxygen transfer rate between 20 and 55°C, Water Res. 34 (2000) 1037–1041.

[313] T. de Vrije, M. Budde, H. van der Wal, P.A.M. Claassen, A.M. López-Contreras, “In situ” removal of isopropanol, butanol and ethanol from fermentation broth by gas stripping, Bioresour. Technol. 137 (2013) 153–159.

[314] T. Wagner, J. Koch, U. Ermler, S. Shima, Methanogenic heterodisulfide reductase (HdrABC-MvhAGD) uses two noncubane [4Fe-4S] clusters for reduction, Science (80-.). 357 (2017) 699–703.

[315] P. Wang, M. Jin, G. Zhu, Biochemical and molecular characterization of NAD+-dependent isocitrate dehydrogenase from the ethanologenic bacterium Zymomonas mobilis, FEMS Microbiol. Lett. 327 (2012) 134–141.

[316] S. Wang, H. Huang, J. Moll, R.K. Thauer, NADP+ Reduction with Reduced Ferredoxin and NADP+ Reduction with NADH Are Coupled via an Electron-Bifurcating Enzyme Complex in Clostridium kluyveri, J. Bacteriol. 192 (2010) 5115–5123.

[317] A.D. Warth, Relationship between the heat resistance of spores and the optimum and maximum growth temperatures of Bacillus species., J. Bacteriol. 134 (1978) 699–705.

[318] R. Weimberg, Pentose Oxidation by Pseudomonas fragi*, 1961.

[319] M.J. Van der Werf, M. V. Guettler, M.K. Jain, J.G. Zeikus, Environmental and physiological factors affecting the succinate product ratio during carbohydrate fermentation by Actinobacillus sp. 130Z, Arch. Microbiol. 167 (1997) 332–342.

[320] T. Werpy, G. Petersen, A. Aden, J. Bozell, J. Holladay, J. White, A. Manheim, D. Eliot, L. Lasure, S. Jones, Top Value Added Chemicals From Biomass. Volume 1 - Results of Screening for Potential Candidates From Sugars and Synthesis Gas, (2004).

[321] M.R. White, E.D. Garcin, D-Glyceraldehyde-3-Phosphate Dehydrogenase Structure and Function, in: Springer, Cham, 2017: pp. 413–453.

[322] H.M. Wilks, K.W. Hart, R. Feeney, C.R. Dunn, H. Muirhead, W.N. Chia, D.A. Barstow, T. Atkinson, A.R. Clarke, J.J. Holbrook, A specific, highly active malate dehydrogenase by redesign of a lactate dehydrogenase framework, Science (80-.). 242 (1988) 1541–1545.

[323] M.J. Wolin, The Rumen Fermentation: A Model for Microbial Interactions in Anaerobic Ecosystems, in: 1979: pp. 49–77.

[324] W. Xiong, T.-C. Lee, S. Rommelfanger, E. Gjersing, M. Cano, P.-C. Maness, M. Ghirardi, J. Yu, Phosphoketolase pathway contributes to carbon metabolism in cyanobacteria, Nat. Plants. 2 (2015) 15187.

[325] Y. Yin, J.F. Kirsch, Identification of functional paralog shift mutations: Conversion of Escherichia coli malate dehydrogenase to a lactate dehydrogenase, Proc. Natl. Acad. Sci. 104 (2007) 17353–17357.

[326] N. Yutin, M.Y. Galperin, A genomic update on clostridial phylogeny: Gram-negative spore formers and other misplaced clostridia, Environ. Microbiol. 15 (2013) n/a-n/a.

[327] J.G. Zeikus, M.K. Jain, P. Elankovan, Biotechnology of succinic acid production and markets for derived industrial products, Appl. Microbiol. Biotechnol. 51 (1999) 545–552.

[328] B.M. Zeldes, M.W. Keller, A.J. Loder, C.T. Straub, M.W.W. Adams, R.M. Kelly, Extremely thermophilic microorganisms as metabolic engineering platforms for production of fuels and industrial chemicals, Front. Microbiol. 6 (2015) 1209.

[329] R.M. Zelle, J. Trueheart, J.C. Harrison, J.T. Pronk, A.J.A. van Maris, Phosphoenolpyruvate carboxykinase as the sole anaplerotic enzyme in Saccharomyces cerevisiae., Appl. Environ. Microbiol. 76 (2010) 5383–9.

[330] X. Zhang, B. Tu, L. Dai, P.A. Lawson, Z. Zheng, L.-Y. Liu, Y. Deng, H. Zhang, L. Cheng, Petroclostridium xylanilyticum gen. nov., sp. nov., a xylan-degrading bacterium isolated from an oilfield, and reclassification of clostridial cluster III members into four novel genera in a new Hungateiclostridiaceae fam. nov., Int. J. Syst. Evol. Microbiol. 68 (2018) 3197–3211.

[331] J. Zhou, D.G. Olson, D. a. Argyros, Y. Deng, W.M. van Gulik, J.P. van Dijken, L.R. Lynd, Atypical Glycolysis in Clostridium thermocellum, Appl. Environ. Microbiol. 79 (2013) 3000–3008.

[332] G. Zhu, G.B. Golding, A.M. Dean, The selective cause of an ancient adaptation., Science. 307 (2005) 1279–82.

Acknowledgments

Although it is only my name on the front of this thesis, I could have done none of it on my own. I have a great deal of people to thank for it, and I will use this opportunity to express my gratitude to as many of those as I can.

Richard, behalve als begeleider of leidinggevende heb ik je toch vooral als mentor beschouwd. Al vanaf het begin merkte ik dat we goed matchte en besefte ik hoeveel geluk ik daarmee had. Tijdens ons eerste gesprek waarschuwde je me dat het een project betrof voor iemand die goed met tegenslagen om kan gaan. Die tegenslagen ben ik dan ook wel tegengekomen, maar ik ben zeer tevreden met wat we ervan hebben gemaakt. Ik wil je daarom uit de grond van mijn hart bedanken voor de afgelopen vier jaar, waarin je altijd meteen voor mij en je andere studenten klaarstond en waarin ik zo veel van jou heb geleerd. Jou pragmatische kijk en de vrijheid die je me gaf waren precies wat ik nodig had.

John, ik was officieel dan misschien geen medewerker van Microbiologie of BacGen, toch heb ik dit voor geen moment als nadelig ervaren. Ik wil je zeer bedanken hoe je mij en Joyshree bij al het reilen en zeilen van het lab hebt betrokken. Het was werkelijk een geweldige plek om een promotieonderzoek uit te mogen voeren en ik was dan ook zeer verheugd dat je me aanbood om als Postdoc bij BacGen verder te gaan; lang heb ik daar dan ook niet over getwijfeld.

Serve, hoewel je op papier geen begeleider van mij was, wil ik je wel expliciet bedanken voor de begeleiding die je me hebt gegeven. Jouw ervaring met enzyme assays en op het gebied van “ongewone” metabolismen hebben me veel geholpen. Met mijn nieuwe baan als PostDoc bij BacGen zullen we nog veel meer samenwerken, en daar kijk ik erg naar uit.

Without all the great technicians and other supporting staff of Microbiology, as well as Systems and Synthetic Biology, very little research would be possible indeed. Thank you for all the help and support, **Anja**, **Guus**, **Heidi**, **Iame**, **Ineke**, **Merlijn**, **Monika**, **Philippe**, **Rob**, **Sjon**, **Steven**, **Tom**, **Tom**, **Ton**, and **Wim**. **Tom v/d W**, de snelheid waarmee je mij en anderen – zonder uitzondering – altijd te hulp stond was ongekent. Bedankt voor de jaren dat we samen bij BacGen hebben gewerkt.

To my fantastic paranymphs, Wen and Rob: Thank you so much for your support. **Wen**, I am so lucky to have started my PhD around the same time as you and to have had you as a colleague and friend throughout the entirety of it. **Rob**, hoewel je pas in de eindfase van mijn promotieonderzoek bij BacGen bent komen werken, klikte het meteen als tussen ons. I feel honored to have you both as my paranymphs and I hope we have many years of working together ahead of us.

Joyshree, I hope you will look back on our time of working with *C. thermosuccinogenes* here in Wageningen with the same sense of accomplishment and relief as I probably will. Thanks for working together, and I wish you all the best.

Kilian, I was very privileged to have had you as my first student to supervise. I thoroughly enjoyed it, and you set the bar very high for the students that followed. Nevertheless, **Kimberly**, **Robert**, **Martí**, and **Wilbert**, you all managed to raise the bar a little higher. Thank you for your dedication; I'm proud to have you all as co-authors on my chapters. It was a pleasure supervising you, and I wish you all the best in your careers.

I would also like to thank my colleagues from Corbion. **Judith**, **Koendert**, **Mariska**, **Miranda**, **Rudy**, and **Zhen** from the strain development team, **Bastienne** for all her help with my bioinformatics analyses, as well as everyone else for their support. Even though my time spent in Gorinchem was limited, it was great to be part of Corbion, and I am grateful that they support scientific research such as mine.

Thanks to **Martin**, **Shuen**, and **Dan**, as well as the other collaborators, for the great teamwork on the transaldolase paper.

Aleksandr, **Erika**, **Hugo**, **Ioannis**, **Johanna**, **Joyshree**, **Prarthana**, and **Wen**, it was a great organizing the unforgettable MIB SSB PhD trip of 2017 with you. **Adriano**, **Amaury**, **Ana**, **Carolina**, **Daphne**, **Eleonora**, **Elodie**, **Inês**, **Isabelle**, **Joyshree**, **Kristian**, **Liz**, **Mamou**, **Maria**, **Marjon**, **Matt**, **Miia**, **Nigel**, **Raquel**, **Richard**, **Rubab**, and **Sasha**, it was always a lot of fun hanging out with you during the many CLOSPORE meetings we had. **Costas**, **Gerben**, **Ioannis**, **Joyshree**, **Mamou**, **Mihris**, **Romy**, **Tijn**, and **Tom**, thanks for the fun times we shared in our offices at De Dreijen and Helix. **Daan**, **Ismael**, **Max**, **Nico**, **Peter**, **Rob**, **Thijs**, and **Wen**, thanks for all the adventures down in the MIB dungeons. Thanks also to **Alex**, **Becca**, **Belen**, **Brenda**, **Carina**, **Catarina**, **Despoina**, **Elleke**, **Enrico**, **Eric**, **Franklin**, **Hanne**, **James**, **Janneke**, **Jochem**, **Joep**, **Jorrit**, **Jurre**, **Lione**, **Lorenzo**, **Mark**, **Marnix**, **Melvin**, **Nico**, **Patrick**, **Prarthana**, **Raymond**, **Sjoerd**, **Sebastian**, **Stan**, **Teunke**, **Thomas**, **Tim**, **Yifan**, and all other past and present BacGen colleagues, for creating such a great working environment; as well as **Bastian**, **Benoit**, **Catalina**, **Emma**, **Emmy**, **Irene**, **Ivette**, **Lot**, **Maarten**, **Martijn**, **Nikolas**, **Peer**, **Rob**, **Ruben**, **Yuan**, and everybody else from MIB and SSB. Special thanks to the "Dutch lunch table" for all the great lunchtime conversations.

I would also like to thank **Dolf**, **Elvira**, **Gerlinde**, **Jelle**, **Jochem**, **Julia**, **Karin**, **Margo**, **Marina**, **Mirelle**, **Neli**, **Nico**, **Pim**, **Pina**, **Raul**, **Simon**, and **Tessa**. Organizing the Science Café with you has always been (and still is) a pleasant and inspiring change from the work on my thesis.

Matt, thanks for cooking.

Pilar, turns out that meeting you was the high-impact result that every starting PhD student dreams of. Te amo.

Sita, zusje, op niemand ben ik trotser dan op jou. Bedankt voor alle inspiratie die je mij biedt.

Papa, bedankt voor alle steun, en misschien wel het allerbelangrijkste: oneindig veel vertrouwen. Het moet niet makkelijk zijn om een zoon te hebben die alles, maar dan ook echt alles beter denkt te weten; of het afronden van mijn proefschrift daar verandering in zal brengen durf ik niet te zeggen.

And finally, I would like to thank **my mother**, the wisest person I have ever known, and to whom I have dedicated this work. I have no doubt that her 16 years of tireless support of my young curiosity has made me the person I am today.

List of publications

J.G. Koendjbiharie, K. Wiersma, R. van Kranenburg. Investigating the Central Metabolism of *Clostridium thermosuccinogenes*, Appl. Environ. Microbiol. 84 (2018) e00363-18.

J.G. Koendjbiharie, K. Wevers, R. van Kranenburg. Assessing Cofactor usage in *Pseudoclostridium thermosuccinogenes* via Heterologous Expression of Central Metabolic Enzymes, Front. Microbiol. 10 (2019) 1162.

J.G. Koendjbiharie, R. van Kranenburg. Identification of a Novel Fumarate Reductase Potentially Involved in Electron Bifurcation. Preprints 2019, 2019120288

J.G. Koendjbiharie*, S. Hon*, M. Pabst, R. Hooftman, D.M. Stevenson, J. Cui, D. Amador-Noguez, L.R. Lynd, D.G. Olson, R. van Kranenburg. The pentose phosphate pathway of cellulolytic clostridia relies on 6-phosphofructokinase instead of transaldolase, Journal of Biological Chemistry (2019): jbc-RA119.

* Authors contributed equally

Overview of completed training activities

Discipline specific activities

Courses

- Gene Road Map Training, University of Nottingham, Nottingham, UK (2015)
- Insight into Biofuel Production, Green Biologics Ltd., Oxford, UK (2015)
- Advanced course Microbial Physiology and Fermentation technology, TU Delft, Delft, NL (2016)
- RNA seq. workshop, Institut Pasteur, Paris, FR (2016)
- CLOSPORE workshop, Corbion, Gorinchem, NL (2016)
- Workshop on Cell and Developmental Biology of the Clostridia, NOVA University Lisbon, Lisbon, PT (2017)**
- Workshop on Biorefineries, WUR-FBR, Wageningen, NL (2018)
- Training in Translational Skills, NIZO, Ede, NL (2018)

Meetings & Conferences

- Clostridium XIV conference, Dartmouth College, Hanover (NH), USA (2016)
- Microbiology Centennial Symposium, WUR-Laboratory of Microbiology, Wageningen, NL (2017)*
- Netherlands Biotechnology Congress 18, Nederlandse Biotechnologie Vereniging, Ede, NL (2018)**
- Metabolic Engineering 12, AiChE, Munich, DE (2018)*
- Clostridium XV conference, Technical University of Munich, Freising, DE (2018)**
- FEMS 2019, FEMS, Glasgow, UK (2019)*

* Poster presentation, ** Oral presentation

General courses

- VLAG PhD week, VLAG, Baarlo, NL (2019)
- Basic IP workshop, Corbion, Gorinchem, NL (2016)
- Mid-term progress review, European Commission, Brussels, BE (2016)
- Scientific Publishin, WGS, Wageningen, NL (2016)
- 7 Habits course, Corbion, Gorinchem, NL (2017)
- Efficient Writing Strategies, WGS, Wageningen, NL (2018)
- Writing Grant Proposals, WGS, Wageningen, NL (2018)

Optionals

- Research proposal, WUR, Wageningen, NL (2015)
- Bacterial Genetics group meetings (weekly)
- Microbiology PhD meetings (monthly)
- PhD study trip to Hamburg & Copenhagen + organization

About the author

Jeroen Girwar Koendjbiharie was born on the 13th of April 1992 in 's-Hertogenbosch, The Netherlands. After finishing gymnasium at the Jeroen Bosch College in 2010, he started the BSc Life Science & Technology at Leiden University and TU Delft. His BSc thesis was performed in the Industrial Microbiology group at the TU Delft, under the supervision of Nick Milne, where he looked into heterologous nitrogen assimilation pathways in *Saccharomyces cerevisiae* for the production of amino acids.

In 2013, after completion of his BSc studies, Jeroen moved to Lund, Sweden to study Biotechnology (MSc) at Lund University. His MSc thesis was performed in the Systems and Synthetic Biology group at Chalmers University in Gothenburg, under the supervision of Yun Chen. For his MSc thesis, Jeroen worked on modulating the activity of acetyl-CoA carboxylase 1 in *S. cerevisiae* for increased production of malonyl-CoA derived products.

In 2010, he started with his PhD project at Corbion under the supervision of Richard van Kranenburg. The project was part of the EU funded Marie Skłodowska-Curie Innovative Training Network called CLOSPORE. The research was conducted in the Bacterial Genetics group of John van der Oost, at the laboratory of Microbiology at Wageningen University. During this four-year project, Jeroen investigated the central metabolism of *Clostridium thermosuccinogenes*, of which the results are described in this thesis.

Currently, Jeroen is employed as Post-Doc in the Bacterial Genetics group at the laboratory of Microbiology at Wageningen University. His work focusses on the hyperthermophilic archaeon *Pyrococcus furiosus*.

The research described in this thesis was financially supported by the European Union Marie Skłodowska-Curie Innovative Training Networks (ITN), contract number 642068; and by Corbion.

Financial support from Wageningen University for printing this thesis is gratefully acknowledged

Cover design: Photo by Ervins Strauhmanis, Amber, https://flic.kr/p/omYxja, CC BY 2.0

Printed: ProefschriftMaken | www.proefschriftmaken.nl on recycled, FSC certified paper

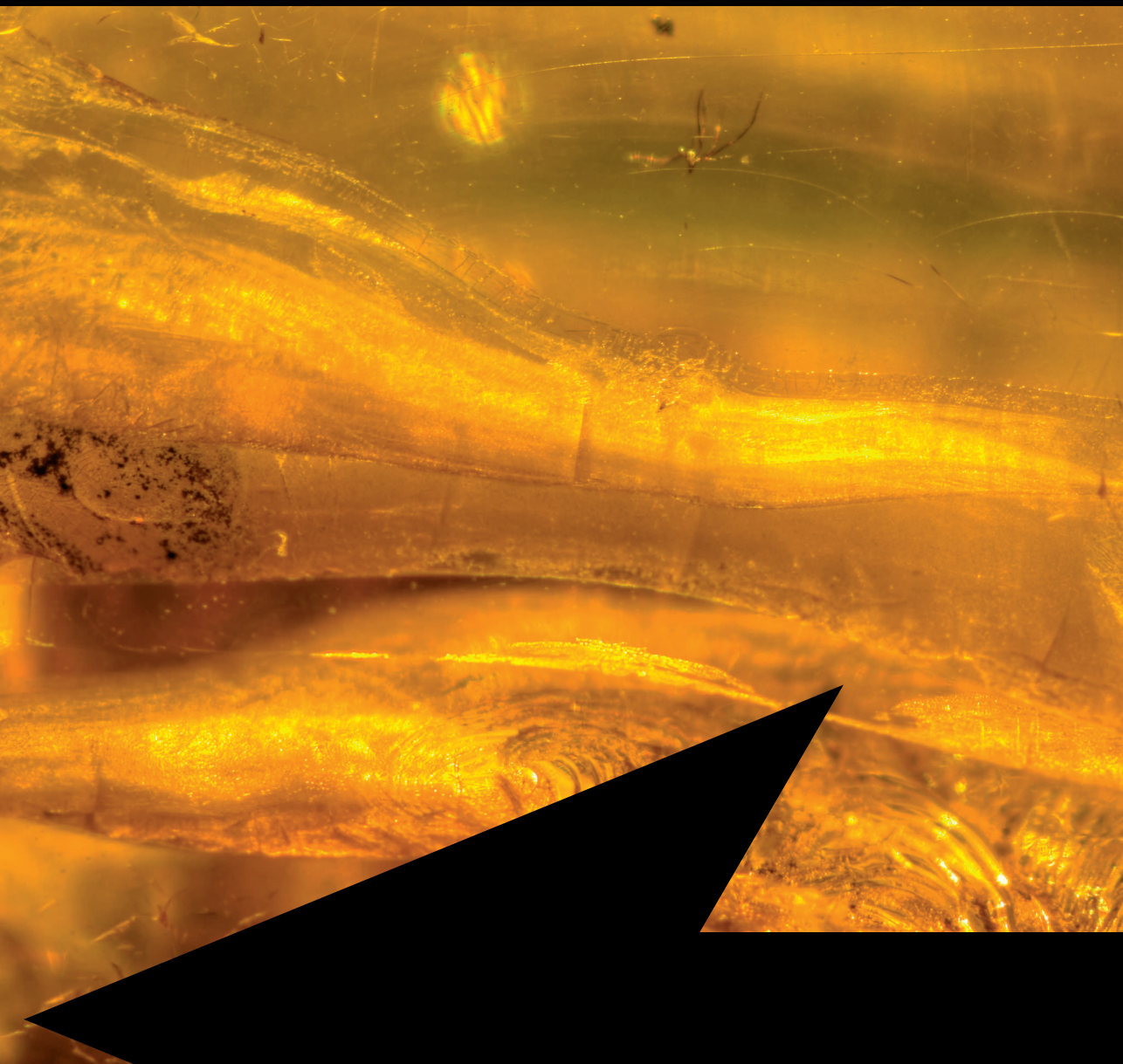

Propositions

1. Prokaryotic taxonomy is a necessary evil.
   (this thesis)

2. Understanding anaerobic redox metabolism requires classical biochemistry.
   (this thesis)

3. Biotechnology will eventually turn out to be a stepping stone to nanotechnology.

4. Publicly funded research conducted at a public university ought not to be patented.

5. The tendency to not publish hypotheses anymore is detrimental to the scientific process.

6. Present-day academic publishing is archaic, capitalistic, and discriminatory.

7. Pointing out the problem of population growth without pointing out the problem of western consumption habits is unethical.

8. Many services by the likes of Google, Facebook, and Amazon could be considered natural monopolies, and should therefore be regulated by a democratic institution.

Propositions belonging to the thesis entitled:
"The Thermophilic Route to Succinic Acid"

Jeroen G. Koendjbiharie
Wageningen, March 4th 2020